DISSERTATION

submitted to the
Combined Faculties for the Natural Sciences and for Mathematics
of the Ruperto-Carola University of Heidelberg, Germany
for the degree of
Doctor of Natural Sciences

Identification and functional characterization of candidate genes in recurrently gained genomic regions of mantle cell lymphoma and chronic lymphocytic leukemia

presented by
Diplom-Biologin Alexandra Farfsing
born in Iserlohn

Heidelberg 2009

Accepted by the Combined Faculties for the Natural Sciences and for Mathematics
of the Ruperto-Carola University of Heidelberg, Germany: May 12, 2009

Referees:
Prof. Dr. Werner Buselmaier
Prof. Dr. Peter Lichter

Day of the oral examination: July 02, 2009

The investigations of the following dissertation were performed from February 2006 till January 2009 under the supervision of Prof. Dr. Peter Lichter and Dr. Armin Pscherer in the division of molecular genetics at the German Cancer Research Center (DKFZ), Heidelberg, Germany.

Publication

Farfsing A, Engel F, Seiffert M, Hartmann E, Ott G, Rosenwald A, Stilgenbauer S, Döhner H, Boutros M, Lichter P, Pscherer A

Gene knockdown studies identified CCDC50 as candidate gene in mantle cell lymphoma and chronic lymphocytic leukemia

In preparation.

Declarations

I hereby declare that I have written the submitted dissertation 'Identification and functional characterization of candidate genes in recurrently gained genomic regions of mantle cell lymphoma and chronic lymphocytic leukemia' myself and in this process have used no other sources or materials than those expressly indicated. I hereby declare that I have not applied to be examined at any other institution, nor have I used the dissertation in this or any other form at any other institution as an examination paper, nor submitted it to any other faculty as a dissertation.

_____ _____

(Place, Date) Alexandra Farfsing

To Jan
& my family

Contents

Abbreviations

A	Adenine
AB	Antibody
Array CGH	Array comparative genomic hybridization
BAC	Bacterial artificial chromosome
B-CLL	B-cell chronic lymphocytic leukemia
bp	Base pairs
BSA	Bovine serum albumine
C	Cytosine
CCDC50	Coiled-coil domain-containing protein 50
CD19+	CD19 positive cells
cDNA	Complementary DNA
Chr	Chromosome
DAPI	4’,6-Diamidino-2’-phenyllindol-dihydrochloride
DLBCL	Diffuse large B-cell lymphoma
DNA	Desoxy-ribonucleic acid
DIG	Digoxygenine
dNTP	Desoxy-nucleotide triphosphate
ds	Double stranded
E. coli	*Escherichia coli*
esiRNA	Endoribonuclease-prepared siRNA
FCS	Fetal cow serum
FACS	Fluorescence-activated cell sorting
FISH	Fluorescence in situ hybridization
G	Guanine
GFP	Green fluorescent protein
HRP	Horse radish peroxidase
kb	Kilo base pairs
lg	Immunoglobulin
LB	Lysogeny Broth / Luria Broth
LOF	Loss-of-function
MCL	Mantle cell lymphoma
mRNA	Messenger RNA
NFκB	Nuclear factor kappa B
NHL	Non-Hodgkin lymphoma
PBS	Phosphate buffered saline
PCR	Polymerase chain reaction

PI	Propidium iodide
p.t.	Post transfection
PVDF	Polyvinylidene fluoride
qRT-PCR	Quantitative real-time polymerase chain reaction
RNA	Ribonucleic acid
RNAi	RNA interference
rpm	Rounds per minute
RT	Room temperature
SDS	Sodium dodecyl sulfate
SDS-PAGE	Sodium dodecyl sulfate polyacrylamide gel electrophoresis
sh	Short hairpin
siRNA	Small interfering RNA
ssRNA	Single stranded RNA
T	Thymidine
TBE	Tris-borate buffer
TSG	Tumor suppressor gene
TNFα	Tumor necrosis factor alpha
U	Uracil
UV	Ultraviolet
V	Variable
V(H)	Variable heavy chain
v/v	Volume per volume
w/v	Weight per volume

Summary

The two B-cell non-Hodgkin lymphoma entities chronic lymphocytic leukemia (CLL) and mantle cell lymphoma (MCL) are lymphoproliferative neoplasms characterized by different aggressive clinical courses. However, they show striking geneotypic similarities like recurrent chromosomal gains of 3q25-q29, 12q13-q14 and 18q21-q22. The genetic pathomechanisms affected by these aberrations are mainly not understood. Several studies reported the high resolution detection of chromosomal imbalances in MCL and CLL using array CGH, accurately defining the gained regions. These imbalances, however, still contain too many genes in order to enable a reasonable selection of candidates. The aim of the present study was to identify genes with oncogenic potential in recurrently gained chromosomal regions of MCL and CLL using high resolution expression arrays, followed by studying the effect of gene silencing on cell proliferation. First, the expression of 24 primary CLL and 6 primary MCL patients, as well as 6 cell lines was profiled, and the identified genes in the three gained regions (3q, 12q, and 18q) were compared to published data. Second, the 72 candidate genes derived from this analysis were functionaly investigated by the use of an RNA interference screen in a multiwell format. Third, the changes in cell viability were validated in primary CLL cells and downstream effects of the identified candidate genes were analyzed. The three genes *CCDC50*, *SERPINI2* and *SMARCC2* emerged as candidates mediating a reduction in cell viability in cell lines and in primary CLL cells. *CCDC50* was identified as a candidate gene with a 3.5-fold mean overexpression in primary cells of MCL and CLL patients. Gene knockdown and reporter gene assays revealed a role of *CCDC50* in promoting cell survival. MCL and CLL cell lines with stable *CCDC50* knockdown revealed 75% less proliferation than the parental cells. Interestingly, and in contrast to results shown in Hela cells, the data of this study gave rise to a survival stimulating effect of *CCDC50*. TNFα induced NFκB activation revealed a direct correlation of inducibility and *CCDC50* expression. Genome wide expression profiling studies identified several target genes of p53 signaling pathways as upregulated in accordance with low *CCDC50* transcript levels. Overexpression of pro-apoptotic genes like *TP53I3* and *BAX* and downregulation of apoptosis-protecting genes like *BNIP3L and GADD45A* were a plausible cause for the reduction in cell viability in primary CLL cells and cell lines after *CCDC50* silencing. In conclusion, *CCDC50* was identified as activated candidate gene in MCL and CLL that is responsible for cell survival and plays a role in NFκB and p53 signaling pathways.

Zusammenfassung

Die beiden B-Zell Non-Hodgkin Lymphome, chronisch lymphatische Leukämie (CLL) und Mantelzell-Lymphom (MCL), sind als lymphoproliferative Neoplasien durch unterschiedlich aggressive Krankheitsverläufe charakterisiert. Dennoch zeigen sie ausgeprägte Gemeinsamkeiten genetischer Natur. Häufig auftretende Veränderungen sind zum Beispiel genetische Zugewinne auf den Chromosomen 3q25-q29, 12q13-q14 und 18q21-q22. Die Pathomechanismen, die durch diese Aberrationen ausgelöst werden, sind größtenteils noch nicht aufgeklärt. Die Methode „array CGH“ (vergleichende genomische Hybridisierung auf Biochips) ermöglicht es, genomweite Veränderungen der DNA-Kopienzahl, die durch den Zugewinn oder den Verlust bestimmter Chromosomenregionen entstanden sind, sehr sensitiv zu erkennen. Amplifizierte Regionen in MCL und CLL enthalten oftmals Onkogene, die bei der Tumorentstehung und -entwicklung eine entscheidende Rolle spielen. Viele Publikationen, in denen die array CGH Methode benutzt wurde, konnten die veränderten Chromosomenregionen in MCL und CLL auf so genannte “minimal veränderte Regionen“ eingrenzen. Trotzdem enthalten diese noch zu viele Gene, um eine geeignete Auswahl an Kandidaten für weitere funktionelle Studien treffen zu können. Das Ziel dieser Studie war es, Kandidatengene mit onkogenem Potential zu identifizieren, die in häufig amplifizierten chromosomalen Regionen von MCL und CLL liegen. Dazu wurden umfassende Expressionsprofile von primären Zellen aus 24 CLL und 6 MCL Patienten sowie von 6 Zelllinien beider Entitäten erstellt. Die 72 identifizierten und überexprimierten Kandidatengene, die in den häufigen Zugewinnregionen 3q25-q29, 12q13-q14 und 18q21-q22 lokalisiert sind, wurden mittels der RNA Interferenz-Methode antagonisiert. Abschließend wurden die beobachteten Verluste in der Zellviabilität in Zelllinien und in primären CLL-Zellen durch den Einsatz von vier einzelnen siRNA-Sequenzen pro Gen validiert. Die Gene *CCDC50*, *SERPINI2* und *SMARCC2* wurden dabei als Kandidatengene bestätigt, deren mRNA Knock-down sowohl den Verlust der Zellviabilität in primären Zellen als auch in Zelllinien induzierte. *CCDC50* konnte schon in früheren Studien als überexperimiertes Gen in MCL im Vergleich zu anderen Leukämien und zu gutartigen Lymphknotengeweben identifiziert werden. In dieser Arbeit zeigten quantitative PCR Messungen eine mittlere 3.5-fache Überexpression in primären Zellen der Lymphome MCL und CLL. Reportergenanalysen belegten darüber hinaus, dass *CCDC50* im NFκB-Signalweg beteiligt ist, der u.a. die Viabilität von MCL- und CLL- Zellen reguliert. Weiterhin wurden Zelllinien mit stabilem *CCDC50* Knock-down generiert. Diese zeigten eine bis zu 75% verminderte Zellproliferation im Vergleich zu parentalen Zellen mit unveränderter *CCDC50*-Expression. Im Gegensatz zu Experimenten, die in früheren Studien in Hela-Zellen durchgeführt wurden, belegten die Ergebnisse in diesen Untersuchungen einen

stimulierenden Effekt von *CCDC50* auf das Überleben und die Proliferation von MCL und CLL Zellen. Die TNFα-induzierte NFκB-Aktivität konnte in HEK-293T-Zellen direkt mit dem *CCDC50*-Expressionslevel korreliert werden. Durch genomweite Expressionsstudien, die nach der Modifikation der *CCDC50*-Expression durchgeführt wurden, konnte eine Mehrzahl von Genen aus dem p53-Signalweg als dereguliert identifiziert werden. Die Überexpression der Apoptose-induzierenden Gene *TP53I3* und *BAX*, sowie eine Herunterregulierung von Genen, die vor Apoptoseinduktion schützen (z.B. *BNIP3L* und *GADD45A*), sind eine plausible Erklärung für die Reduktion der Zellviabilität nach *CCDC50* Knock-down in primären CLL-Zellen sowie in Zelllinien. Zusammenfassend konnte in dieser Arbeit *CCDC50* als hochreguliertes Gen identifiziert werden, das in MCL und CLL die Zellproliferation fördert und an den NFκB- und p53-Signalwegen maßgeblich beteiligt ist.

1 Introduction

1.1 Cancer

Cancer is the second most common cause of death in Germany and the Western world after cardio-vascular diseases. According to estimations by the World Health Organization (WHO), cancer causes around 25% of all deaths worldwide. The development of cancer is the result of microevolution of an initial cell clone towards malignancy. Such aberrant development is suppressed in healthy organisms by multiple defense systems (Klein *et al.*, 2007).

1.1.1 The hallmarks of cancer

Hanahan and Weinberg reviewed in 2000 six crucial steps in the transformation process of a normal to a malignant cell (Hanahan and Weinberg, 2000). The 'hallmarks of cancer' are alterations in cell physiology that constitutively influence malignant cell growth (Figure 1). All of these physiological changes are novel capabilities acquired during tumor development. They represent the successful suppression of an anticancer defense mechanism tightly connected to cells and tissues. The mechanistic pathways vary from cell to cell and not all six hallmarks have to be fulfilled in each malignant cellular transformation.

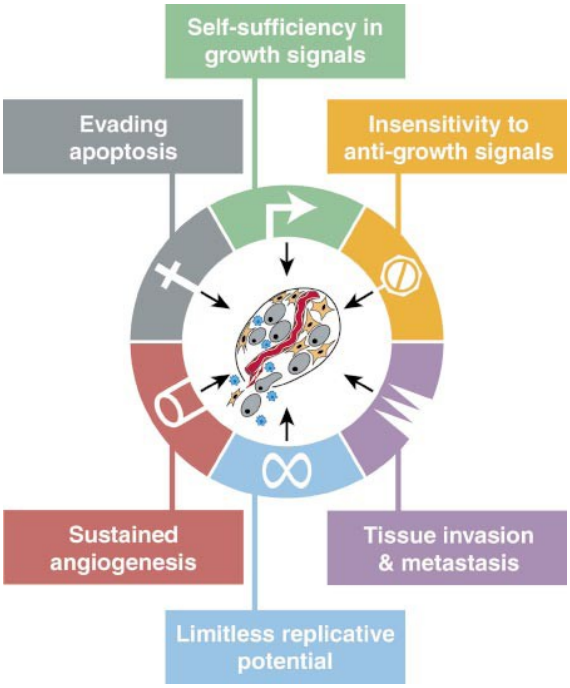

Figure 1: Acquired capabilities of cancer (Hanahan and Weinberg, 2000).

Tumor cells generate many of their own growth signals, thereby reducing their dependence on stimulation from their normal tissue microenvironment. This liberation from dependency on exogenously derived signals disrupts a critically important homeostatic mechanism that normally ensures a proper behavior of the various cell types within tissues (Hanahan *et al*., 2000). Aquired growth signal autonomy is achieved through alteration of extracellular growth signals, influence on transcellular transducers of growth signals and their impact on intracellular circuits that translate those signals into action. While most soluble mitogenic growth factors are made by one cell type in order to stimulate proliferation of another, many cancer cells acquire the ability to synthesize growth factors to which they are responsive, creating a positive feedback signaling loop often termed autocrine stimulation (Hanahan *et al*., 2000).
Cancer is a disorder that can be characterized by uncontrolled cell division or the cellular resistance to apoptosis. This is a physiological process that occurs in all tissues and under a variety of circumstances. The balance between normal cell division, differentiation and programmed cell death (apoptosis) is tightly regulated to ensure the integrity of organs and tissues. Non-malignant cells are programmed to maintain the function of the tissues of which they are a part. Development of cancer is a consequence of changes in somatic cells, which enable uncontrolled cell division or resistance to apoptosis. The DNA sequence itself is either affected (genetic origin) or changes in DNA methylation and demethylation (epigenetic origin) can cause uncontrolled cell division in cancer. Alterations of the genetic information in malignant cells can be single point mutations, deletions (a mutation in which a part of a chromosome or a sequence of DNA is missing), gains of genomic material (a mutation in which a part of a chromosome or a sequence of DNA is additional), chromosomal rearrangements, including translocations and epimutations (a change in heritable chromatin marks, such as an increase or decrease in the density of DNA methylation). According to current models, cells with genomic alterations that best promote growth and enhance cell survival are selected to multiply. Malignant cells with less efficient mutations may therefore be lost by competition within the tumor. This process is called ‘clonal evolution’ (Nowell *et al*., 1976; Gao *et al*., 2007). Only a few of these changes result in carcinogenesis and aberrations in a limited number of genes are sufficient for tumor formation. Proteins encoded by affected genes are generally involved in cellular maintenance, DNA repair machinery or regulatory mechanisms that control cell growth, proliferation and apoptosis.

1.1.2 Oncogenes

Genes are potential oncogenes, when their activation leads to enhanced cell growth, loss of differentiation and the resistance to undergo apoptosis. A proto-oncogene is a normal gene that can transform into an oncogene due to mutations or increased

expression, i.e. activation. Proteins encoded by proto-oncogenes participate in various ways to receive and process growth-stimulatory signals that originate from the extracellular environment. When these genes suffer mutation, the flow of growth-promoting signals released by these proteins becomes deregulated. According to the theory of Weinberg, the oncoproteins release a steady stream of growth stimulating signals resulting in a constant proliferation associated with cancer cells (Weinberg, 2007).

The activation of a proto-oncogene can be caused by one of the following events: (1) Gene duplication is a chromosome abnormality that may result in an increased amount of protein level. Amplifications of chromosomal bands coding for proto-oncogenes can result in the overexpression of the corresponding protein that causes increased proliferation or the resistance to apoptosis. *MYC* genes are one example for proto-oncogenes, activated in the described manner (Weiss *et al*., 1982). They encode transcription factors, which drive cell proliferation and regulate cell growth, differentiation, apoptosis and stem cell renewal when activated by cellular signals. (2) Point mutations within proto-oncogenes can generate constitutively active proteins or cause an increase in protein or enzyme activity. Alternatively, point mutations can lead to a loss of normal cell proliferation, i.e. the *RAS* oncogene. *RAS* proteins are GTPases and transfer signals from G-protein coupled receptors, following metabolism, into its inactive form GDP-RAS. Point mutations in *RAS* lead to amino-acid changes that can cause a reduction of GTPase activity. Consequently, GTP-RAS is inactivated, cannot perform its original function and leads to inadequate cellular signaling responses. (3) A chromosomal translocation can lead to increased gene expression by putting the proto-oncogene under the control of a strong promoter or enhancer leading to high gene expression levels, and it can lead to the formation of a constitutively active fusion protein. One example is the overexpression of cyclin D1 in mantle cell lymphoma. MCL is characterized by a t(11;14)(q13;q32) translocation (Espinet *et al*.,1999; Stamatopoulos *et al*., 1999) and an overexpression of *CCND1* promotes cell cycle progression. A gain-of-function mutation is always dominant on the cellular level. A single mutation in a gene is sufficient to promote carcinogenesis.

1.1.3 Tumor suppressor genes

Tumor suppressor genes (TSGs) are often involved in the regulation of the cell cycle, induction of apoptosis and decrease in cellular adhesion. TSGs are growth controlling genes that operate to constrain or suppress cell proliferation. When these genes are inactivated or lost, tumor formation progresses. To promote tumor formation, both alleles of a gene have to be inactivated by (a) mutation, (b) deletion or (c) silencing i.e. due to methylation of promoter-associated CpG islands or due to histone modifications.

The principle that both gene copies have to be lost was originally formulated by Alfred Knudson´s 'two-hit' hypothesis (Knudson *et al*., 1971). When a TSG is inactivated, it looses its growth-suppressing effects on the cell. A prominent example of a TSG is *TP53.* Loss or mutation of *TP53* is probably the most common aberration in human cancer. The wild type allele of *TP53* suppresses cell proliferation, and *p53* only acquires growth-promoting effects, when it sustains a point mutation in its reading frame. Because of this discovery, the *p53* gene was categorized as a tumor suppressor gene, which was finally confirmed (Vogelstein *et al*., 2000; Weinberg, 2007). *TP53* maps to chromosome 17p13 that is consistently deleted in CLL (Döhner *et al*., 1999; Döhner *et al*., 2000), and other cancers like colorectal carcinomas (Baker *et al*., 1990). Unlike oncogenes, an intact single copy of a tumor suppressor gene is usually sufficient to maintain its proper function.

1.2 Leukemia

Leukemia is a malignant cancer of the bone marrow and blood characterized by the uncontrolled proliferation of blood cells, usually white blood cells (leucocytes). Leukemia is clinically and pathologically subdivided into the following categories: myeloid or lymphocytic, each of which can be acute or chronic: Acute Myeloid Leukemia (AML), Acute Lymphocytic Leukemia (ALL), Chronic Myeloid Leukemia (CML) and Chronic Lymphocytic Leukemia (CLL). In lymphocytic leukemias, the cancerous change takes place in a type of marrow cell that normally forms lymphocytes like T-cells, B-cells, and natural killer cells. In myeloid leukemias, the cancerous change takes place in a type of marrow cell that forms granulocytes, erythrocytes, monocytes, and megakaryocytes.

1.2.1 Acute Leukemia

Acute leukemia is characterized by the rapid increase of immature blood cells. This process makes the bone marrow unable to produce healthy blood cells. Immediate treatment is required in acute leukemia due to the rapid progression and accumulation of malignant cells. Acute forms of leukemia are the most common forms of leukemia in children (Jemal *et al*., 2005).

1.2.2 Chronic Leukemia

Chronic leukemias have few or no blastoid cells. Compared to acute leukemias, chronic lymphocytic leukemia and chronic myelogenous leukemia usually progress more slowly. Chronic leukemias occur mostly, but not exclusively in older people and are often diagnosed in a routine blood test, as no symptoms manifest until the disease reaches an advanced stage. Aberrant cells are excessively accumulating, but it can take months or

even years for the disease progression. Treatment can frequently be postponed until the disease reaches a more malignant subform.

1.3 B-cell neoplasms

The World health organization classification of hematological malignancies categorizes neoplasms primarily to their cell lineage: myeloid, lymphoid, dendritic cells and mast cells. Within each category, distinct diseases are defined according to a combination of cell morphology, immunophenotype, genetic features and clinical syndromes (Martin-Subero *et al*., 2003). A so called 'cell of origin' is assigned for each neoplasm, which represents the stage of differentiation of the tumor. Two major categories of lymphoid neoplasms are described by the WHO classification: (1) Hodgkin lymphomas (HL), characterized by the growth of Reed-Sternberg cells and (2) non-Hodgkin lymphomas (NHL). The latter include B-cell neoplasms, T-cell neoplasms and NK (neutral killer cell) neoplasms. Lymphomas and lymphocytic leukemias are included in the category of lymphoid neoplasms. B-cell chronic lymphocytic leukemia and small B-cell lymphocytic leukemia are classified as different manifestations of the same neoplasm. B-cell lymphocytic leukemias comprise among others: small B-cell chronic lymphocytic leukemia (CLL) and mantle cell lymphoma (MCL).

B-cell lymphoma outcomes are extremely variable in the clinic. Some patients die within four weeks after diagnosis while others are cured or at least achieve 10-year survival without clinical symptoms. Interestingly, all of these tumors show similar phenotypes, but can be distinguished by their specific gene expression patterns (Küppers *et al*., 2005). About 95% of all lymphomas are of B-cell origin, the remaining are T-cell malignancies. This might be surprising, given similar frequency of B- and T-cells in the human body. This fact can be explained by the specific factors that influence the pathogenesis of B-cell lymphomas (Küppers *et al*., 2005). About 15 types of B-cell lymphomas are distinguished in the WHO lymphoma classification (Table 1). This is not only relevant in terms of lymphoma pathogenesis but also for the treatment of the patients. However, B-cell tumors are not as autonomous as previously thought. Key factors that are crucial for normal B-cell differentiation and survival are also required for the malignant growth of most B-cells lymphomas (Küppers *et al*., 2005).

Table 1: Human mature B-cell lymphomas (Küppers *et al.*, 2005)

Lymphoma/Leukemia	Cellular origin of B-cell	Frequency *
Diffuse large B-cell lymphoma	GC or post-GC B-cell	30-40%
Follicular lymphoma	GC B-cell	20%
Multiple myeloma	Plasma cell	10%
Classical Hodgkin´s lymphoma	Defective GC B-cell	10%
B-cell chronic lymphocytic leukemia	**Memory / naïve / marginal zone $CD5^+$ B-cell**	**7%**
MALT lymphoma	Marginal zone	7%
Mantle cell lymphoma	**Mantle zone, $CD5^+$ B-cell**	**5%**
Burkitt´s lymphoma	GC	2%
Nodal marginal zone lymphoma	Marginal zone	2%
Splenic marginal-zone lymphoma	Subset of naïve B-cells that have partially differentiated into marginal zone B-cells	1%
Primary mediastinal B-cell lymphoma	Thymic B-cell	2%
Post transplant lymphoma	GC B-cell	>1%
Lymphoplasmatic lymphoma	(Post) GC B-cell	1%
Hairy cell leukemia	Memory B-cell	<1%
B-cell prolymphocytic leukemia	Memory B-cell	<1%
Primary effusion B lymphoma	(Post) GC B-cell	0.5%
Lymphocyte-predominant Hodgkin´s lymphoma	GC B-cell	0.5%

*Frequency=Frequency among lymphomas. Numbers refer to frequencies in Europe and North America. GC=Germinal Center. Lymphomas investigated in this thesis work are highlighted in red.

1.3.1 B-cell development

B-cells are lymphocytes that play a key role in the immune response. The early development of B-cells takes place in differentiation steps, resulting in variable and specific structures of the B-cell receptor (BCR). Early B-cell development occurs in the bone marrow. The BCR is composed of two heavy chain and two light chain immunoglobulin (Ig) polypeptides which are covalently linked by bisulfite bridges. The intracellular signaling components activated by BCR crosslinking include activation of multiple tyrosine kinases. Signaling is depending on (1) the differentiation stage of the B-cell that recognizes the antigen and (2) the activation of other B-cell surface receptors that modulate BCR signaling. The activated B-cell might be stimulated to proliferate or to undergo further differentiation steps (Rajewsky *et al*., 1996). The BCR consists of variable (V) regions that bind the antigenes, and constant (C) regions that mediate the effector function of immunogobulins (Figure 2a). B-cells differentiate into mature naïve B-cells and leave the bone marrow. It was shown that B-cell precursors undergo apoptosis, if they fail to express a BCR or an autoreactive BCR (Rajewski *et al*., 1996). Mature naïve B-cells can be activated by antigen binding to the BCR and participate in immune responses. The activation of B-cells often depends on antigen-presenting T-cells and takes place in the germinal centers of lymph nodes, where the Ig genes are modified

by somatic hypermutation and class-switch recombinations upon activation (Figure 2b, c).

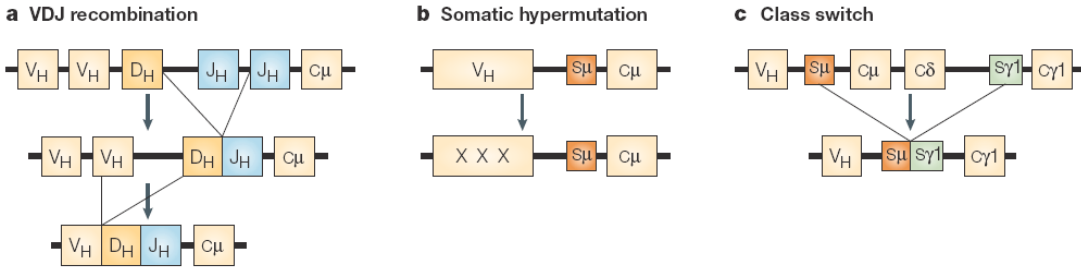

Figure 2: Molecular processes that remodel immunoglobulin genes (Küppers *et al*., 2005).

In T-cell dependent immune responses, antigen-activated B-cells undergo clonal expansion (Figure 3). Activated B-cells migrate into B-cell follicles, start to proliferate and differentiate into centroblasts thereby establishing germinal centers. The proliferating centroblasts activate the process of somatic hypermutation, generating mutations at a high rate in the V region genes and thereby leading to the formation of antibody variants. Centroblasts then differentiate into resting centrocytes, which are selected for high affinity of their BCR to the cognate antigen. Germinal-center B-cells with acquired affinity-increasing mutations will be able to interact with germinal-center T-cells and follicular dendritic cells (FDC) thus receiving survival signals and thereby escape the default apoptosis pathway of germinal-center B-cells. Finally, selected germinal-center B-cells differentiate into memory B-cells or plasma cells and leave the germinal center (Küppers *et al*., 2003; Küppers *et al*., 2005). However, the process can also proceed without T-cells in marginal zones, which occur all around the lymphoid foillicle (Chiorazzi *et al*., 2005).

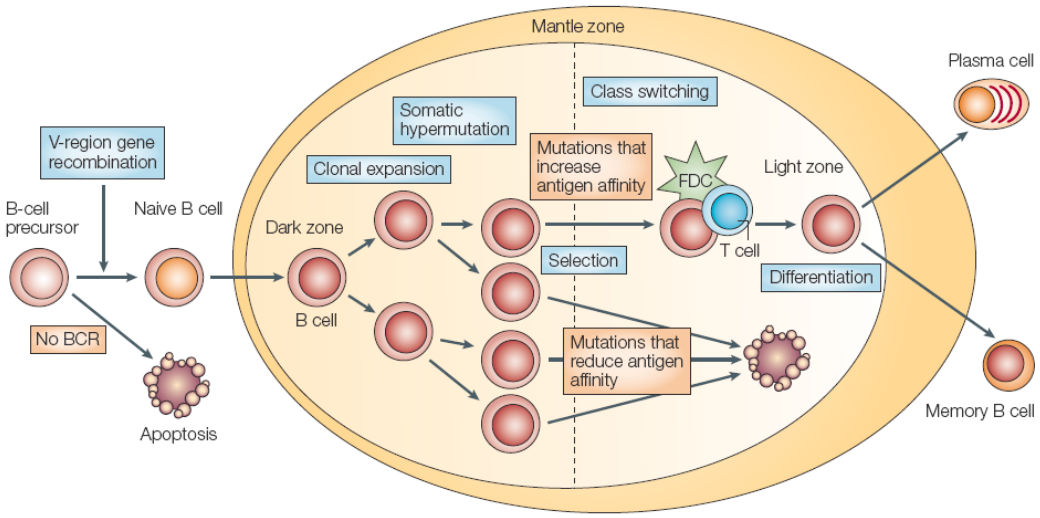

Figure 3: B-cell differentiation in a germinal center (Küppers *et al*., 2005).

1.3.2 The cellular origin of human B-cell lymphomas

Distinct stages of B-cell development and differentiation are characterized by the particular structure of the BCR and expression patterns of differentiation markers. These processes take place in specific histological structures and the analysis of these features is used to determine the origin of the various human B-cell lymphomas (Table 1). Classification of B-cell lymphomas is based on the observation that malignant B-cells seem to be arrested at a particular differentiation stage (Figure 4), which reflects their origin (Greaves *et al*., 1986; Küppers *et al*., 1999; Shaffer *et al*., 2002). The cellular origin of B-cell lymphomas was analyzed by gene expression profiling. These studies identified a germinal center B-cell gene expression profiling signature that is associated with follicular lymphoma (Alizadeh *et al*., 2000, Rosenwald *et al*., 2001, Rosenwald *et al*., 2003). Mantle cell lymphoma cells populate in the mantle zone of the follicles and constantly express *CD5*. Whereas most mantle cell lymphomas are believed to be derived from $CD5^+$ (naïve) B-cells of the mantle zone, about 20–30% of cases carry mutated V-region genes, indicating that they have passed through the germinal center. The marginal zone is located around the mantle zone and consists of post-germinal center memory B-cells and naïve B-cells that are involved in T-cell independent immune responses. The origin of B-cell chronic lymphocytic leukemia (B-CLL) cells still remains unclear but has been discussed to derive from $CD5^+$ B-cells, memory B-cells or naïve B-cells (Chiorazzi *et al*., 2003; Küppers *et al*., 2005).

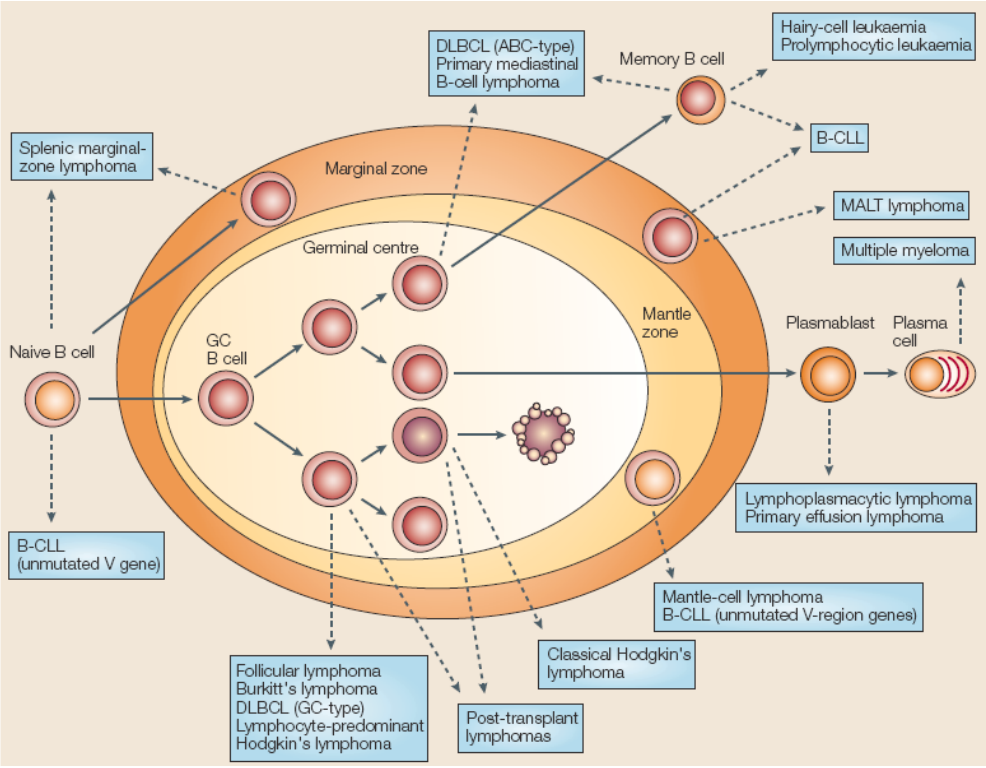

Figure 4: Cellular origin of B-cell lymphomas (Küppers *et al*., 2005).

1.4 Mantle cell lymphoma

Mantle cell lymphoma (MCL) is a lymphoid neoplasm characterized by abnormal proliferation of mature B-lymphocytes. It was discussed earlier that MCL cells probably derive from naïve B-cells residing in the primary follicles or in the mantle zones of secondary follicles (Weisenburger *et al*., 1996) and are expressing *CD5*. MCL represents 5–10% of all NHL and occurs more frequently in males (male:female ratio is 2.7:1) with advanced age (median age 60 years, range 29-85). This tumor is considered one of the aggressive clinical lymphoid neoplasms with poor responses to conventional chemotherapy and relatively short survival. The clinical evolution is usually very aggressive with frequent relapses. Only few patients are cured by current therapies.

1.4.1 Oncogenic mechanisms in MCL

The genetic and molecular mechanisms involved in the pathogenesis of MCL combine the dysregulation of cell proliferation and survival pathways with a high level of chromosome instability based on the disruption of DNA damage response pathways. MCL is also characterized by the proliferation of mature B-lymphocytes that have a striking tendency to disseminate throughout the body, infiltrate lymphoid tissues, bone marrow, peripheral blood and extranodal sites. They also enter territories that normally do not contain lymphoid cells. Concordant with its origin from pre-germinal center cells, MCL has been considered to carry no or very few somatic mutations in V-gene sequences of Ig (VH) genes. However, 15–40% of MCLs may carry somatic hypermutations indicating that some tumors originate from cells that have undergone the influence of mutations of the follicular germinal center (Welzel *et al*., 2001; Camacho *et al.,* 2003; Kienle *et al*., 2003; Orchard *et al*., 2003). The load of mutations in MCL is lower than in other lymphoid neoplasms such as chronic lymphocytic leukemia or follicular lymphoma (Hamblin *et al*., 1999; Crespo *et al*., 2003) suggesting a smaller influence of the germinal center microenvironment. Contrary to chronc lymphocytic leukemia, the Ig mutational status in MCL is not associated with the prognosis of the patients (Orchard *et al*., 2003; Welzel *et al*., 2001; Camacho *et al.,* 2003; Kienle *et al*., 2003, Carreras *et al*., 2005). The genetic hallmark of MCL is the t(11;14)(q13;q32) translocation that juxtaposes the proto-oncogene *CCND1,* which encodes cyclin D1 at chromosome 11q13, to the Ig heavy chain gene at chromosome 14q32 including regulatory sequences. This event leads to the overexpression of cyclin D1, which has an important pathogenetic role: deregulating cell cycle control by overcoming the suppressor effect of retinoblastoma 1 (*RB1*) and the cell cycle inhibitor *p27*. As a consequence of this translocation *CCND1*, which is not expressed in normal B-lymphocytes, becomes constitutively overexpressed. This genetic alteration is thought to be the primary event in the pathogenesis of the tumor, facilitating the deregulation of

the cell cycle at the G1–S phase transition (Campo *et al*., 1999; Jaffe *et al*., 2001). Breakpoint region analysis of the two chromosomes has suggested that the t(11;14)(q13;q32) translocation occurs in the bone marrow in an early B-cell at the pre-B stage of differentiation, when the cell is initiating the Ig gene rearrangement by the recombination of the V(D)J segments. In addition to this translocation, MCL tumor cells carry a high number of secondary chromosomal and molecular alterations targeting proteins that regulate cell cycle and senescence (*BMI1*, *INK4a*, *ARF*, *CDK4* and *RB1*) or interfere with the cellular response to DNA damage (*ATM*, *CHK2* and *p53*).

1.4.2 Secondary genetic alterations

Despite the important role of the t(11;14) translocation and cyclin D1 overexpression in the development of MCL, several observations suggest that these mechanisms may not be sufficient for the complete transformation and the aggressive behavior of the tumor. Transgenic mouse models show that the overexpression of cyclinD1 is not sufficient to induce malignant transformation of the cells. Moreover, cooperations with other oncogenes like *C-MYC* are neccessarry (Lovec *et al*., 1994). Cytogenetic studies identified secondary genetic alterations that may be involved in the progression of MCL (Bea *et al*., 1999; Bentz *et al*., 2000; Allen *et al*., 2002; Kohlhammer *et al*., 2004; Rubio-Moscardo *et al*., 2005; Tagawa *et al*., 2005; Rinaldi *et al*., 2006; Sander *et al*., 2008). MCL is a malignant lymphoid neoplasm with the highest level of genomic instability (Salaverria *et al*., 2007). Further studies suggest that genes involved in cell death may also be targeted by oncogenic events, and they may influence the tumor response to new therapeutic agents (Damle *et al*., 2002; Tobin *et al*., 2003). Previous investigation on genomic aberrations detected by fluorescence *in situ* hybridization (FISH) revealed the most common genomic changes in 103 MCL patients, all containing the translocation t(11;14)(q13;q32) (Table 2, Sander *et al*., 2008). Alterations of the 8q24 locus, including the t(8;14)(q24;q32) translocation that activates *MYC*, are uncommon, but have been identified in MCL with a very rapid clinical course. Crucial target genes such as *p16* ^{INK4a} on chromosome 9p21, *BMI-1* on 10p12, *ATM* on 11q22.3, *CDK4* on 12q14, and *p53* on 17p13 have been confirmed. Losses of 11q and 13q occur at similar frequencies in all histological variants of MCL, whereas the highly proliferative and clinically aggressive variants have more complex karyotypes with frequent losses of 9p, 9q and 17p and gains of 3q and 12q (Salaverria *et al*., 2007, Rubio-Moscardo *et al*., 2005). Copy number gains of 3q have been identified as prognostic markers of patients with low proliferation (Salaverria *et al.*, 2007).

Table 2: Genomic changes in t(11;14)(q13;q32) positive MCL, (Sander *et al*., 2008).

Aberration	Chromosome	Occurrence (%)
Gain	3q26	45
	8q24	19
	15q23	18
	12q12	17
	7p15	15
	18q21	14
Deletion	13q14	43
	11q22	41
	9p21	35
	13qter	33
	1p22	32
	17p13	26
	6q27	22
	8p22	21
	6q21	16
	10p15	13

1.5 B-cell chronic lymphocytic leukemia

B-cell chronic lymphocytic leukemia (B-CLL) is the most common leukemia of adults in the Western world (Rozman *et al*., 1995). It is characterized by a highly heterogenous clinical outcome, while some patients are dying within months, others have a normal lifespan.

1.5.1 Oncogenic mechanisms in CLL

Unlike other leukemias, there is only a small proportion of proliferating neoplastic cells, which are localized in the so-called 'pseudofollicles' in the lymph nodes and are scattered in the bone marrow of the patients (Granziero *et al*., 2001). Due to a selective survival advantage, the majority of leukemic cells in B-CLL are non-proliferating cells arrested in the G0/G1 phase, which accumulate gradually in lymphoid organs, bone marrow, and peripheral blood. This indicates that expansion of the tumor might take place in other tissues affected by the lymphoma. Indeed, proliferation of B-CLL is largely restricted to proliferation centers in lymph nodes and bone marrow, where the cells are in intimate contact with $CD4^+$ T-cells and dendritic cells. The *in vitro* survival of B-cells can be significantly extended in co-culture with stromal cells, and B-CLL proliferation can be induced by triggering the *CD40* receptor. As the ligand *CD40L* is expressed by a fraction of T-cells in the proliferation centers, it is intriguing to speculate that the T-cell/B-CLL cell interaction in *CD40* activated microenvironment provides important survival and proliferating signals for the malignant clone. Intrinsic defects, resistance to programmed cell death, and an altered, survival-stimulating microenvironment are

discussed as major pathogenic factors for B-CLL (Dighiero *et al*., 1991; Meinhardt *et al*., 1999; Caligaris-Cappio *et al*., 2003; Ghia *et al*., 2005).

1.5.2 Secondary genetic alterations

In contrast to many other types of B-cell lymphomas, which carry characteristic chromosomal translocations involving one of the Ig loci and a proto-oncogene (Willis and Dyer, 2000), translocations are very rare in B-CLL. However, genomic aberrations are very common and the clinical heterogeneity has been shown to correlate with the pattern of genetic changes. A comprehensive FISH analysis revealed the most common genomic changes in a set of 325 B-CLL patients (Table 3) (Döhner *et al.*, 2000). Further FISH analyses on 506 CLL patients have been conducted recently (Haferlach *et al*., 2007).

Table 3: Incidence of chromosomal abnormalities in 325 B-CLL patients (Döhner *et al*., 2000).

Aberration	Chromosome	Occurrence [%]
Deletion	13q	55
	11q	18
	17p	7
	6q	6
Gain	12q	16
	8q	5
	3q	3
Translocation	t(14q32)	4
Normal karyotype		18

The most frequent abnormalities are losses of genomic material. These deletions effect chromosome bands 13q14, 11q22-q23, 17p13 and 6q21. 17p and 11q deletions are associated with rapid progression of the disease and short survival times of the patients, whereas deletion of 13q14 as a single abnormality predicts longer survival times. The tumor suppressor gene *p53* is affected by 17p deletion; *ATM* (ataxia teleangiectasia mutated) is altered in a proportion of cases with 11q deletion (Schaffner *et al*., 1999; Schaffner *et al*., 2000). The most common gains of genomic material affect 12q13, 8q24 and 3q26 (Monni *et al*., 1998; Bea *et al*., 1999; Bentz *et al.*, 2000; Döhner *et al*., 2000).

1.6 Recurrent genomic patterns in MCL and CLL

MCL and CLL are characterized by recurrent chromosomal aberrations. Although MCL is associated with t(11;14)(q13;q32) and a higher karyotype complexity, there are striking similarities between their genetic aberrations. The two common deletions 11q and 13q are much more frequent in MCL and CLL when compared to other types of B-cell lymphomas. In addition, both malignancies share the frequently occurring chromosomal

gains in regions on 3q25-q29, 8q24, and 12q12-q14. For some chromosomal loci, the affected genes were recently identified such as *MYC* on chromosome 8q24, *TP53* on chromosome 17p13 and *ATM* on chromosome 11q23, whereas *CDK4* is predicted as candidate gene on chromosome 12q13. Among predicted candidate genes on chromosome 3q25-q29 were *BCL6*, *SERPINI2* and *ECT2* (Hernandez *et al*., 1996; el Rouby *et al.*, 1993; Schaffner *et al.*, 1999, Bentz *et al*., 1999; Schaffner *et al.*, 2000; Tagawa *et al*., 2005; Rubio-Moscardo *et al*., 2005; Jares *et al*., 2008; Sander *et al*., 2008).

1.6.1 Chromosomal gain of region 3q25-q29

Pathological relevant genes are located in gained genomic region 3q26-q29 (Bentz *et al*., 2000). One of the predicted candidate genes was the proto-oncogne *BCL6* which could not be confirmed in most of the investigated MCL cases (Bentz *et al*., 2000). Analysis of global gene expression profiling in MCL cells identified a proliferation signature based on the expression of 20 genes that enable to discriminate patients with different median survival, confirming increased proliferation as the best predictor for poor survival. Some genetic alterations, particularly the gains on chromosome 3q and losses on 9p, 9q and 17p have prognostic significance associated with a shorter survival (Bea *et al*., 1999; Allen *et al*., 2002; Rubio-Moscardo *et al*., 2005; Thelander *et al*., 2005). Most interesting, the impact of 3q gains and 9q losses on survival is independent of the proliferation activity of the tumor. Robust molecular and genetic prognostic predictors on 3q may therefore become an essential tool in clinical practice to define the best therapy for each patient.

1.6.2 Chromosomal gain of region 12q13-q14

Among their genomic aberrations, MCL and CLL show trisomy 12 as the most frequent ones (CLL 16%, MCL 17%) (Döhner *et al*., 1999; Döhner *et al*., 2000; Sander *et al*., 2008).
The segment that was duplicated in all cases included 12q13-q21.2, indicating that this region contains the relevant genes, involved in the pathomechanism of B-CLL tumors. Trisomy 12 was shown to result from one homolog, rather than from loss of one homolog and triplication of the remaining one (Döhner *et al*., 1999). In recent B-CLL studies the presence of trisomy 12 in combination with 11q deletions, was discussed to be associated with a bad clinical prognosis (Athanasiadou *et al*., 2006; Mittal *et al*., 2007). Nevertheless, the pathogenic role of trisomy 12 in MCL and CLL remains unresolved, but upregulated RNA expression levels have been observed for chromosome 12 candidate genes (Winkler *et al*., 2005). So far, *CDK4* is one of the most frequently discussed candidate gene on chromosome 12q13.

1.6.3 Chromosomal gain of region 18q21-q22

Gain of chromosome 18q and translocation t(14;18) are frequently found in B-cell non-Hodgkin lymphomas (B-NHL) (Galteland *et al*., 2005). Recent FISH analysis in primary MCL cases revealed a gain of chromosome 18q21 in 14% (Sander *et al*., 2008) leading to increased *BCL2* transcription levels. The anti-apoptotic role of *BCL2* in correlation to MCL and CLL disease pathways was described in recent publications. Therefore, *BCL2* is the most frequent discussed candidate gene on chromosome 18q21.

1.7 Recombinase Mediated Cassette Exchange

A molecular tool for the functional antagonization of inactivated tumor suppressor genes or activated oncogenes in MCL and CLL was recently established in our group (Pscherer *et al*., 2006). This system is based on the targeted integration of transgenes into a disease background, i.e. the parental tumor cell line, via recombinase mediated cassette exchange (RMCE). Genomic deletions can be compensated via integration of respective genomic DNA, whereas overexpression of genes can be antagonized by integrating short hairpin RNA (shRNA) coding plasmids (Figure 5). Notably, this site-specific shRNA-strategy circumvents the interferon response, often induced when applying transient RNAi knockdown (Pscherer *et al*., 2006). The production of stable cell lines is a multistep system based on site directed recombination events. In this work, overexpressed candidate genes were silenced via integration of shRNA coding plasmids into the genome (Figure 5). The RMCE system allows the antagonization of single overexpressed or downregulated genes without inducing further changes to the cell. The resulting functional changes identified upon supplementation of the gene/shRNA, show the biological relevance of the single genetic defects in CLL and MCL.

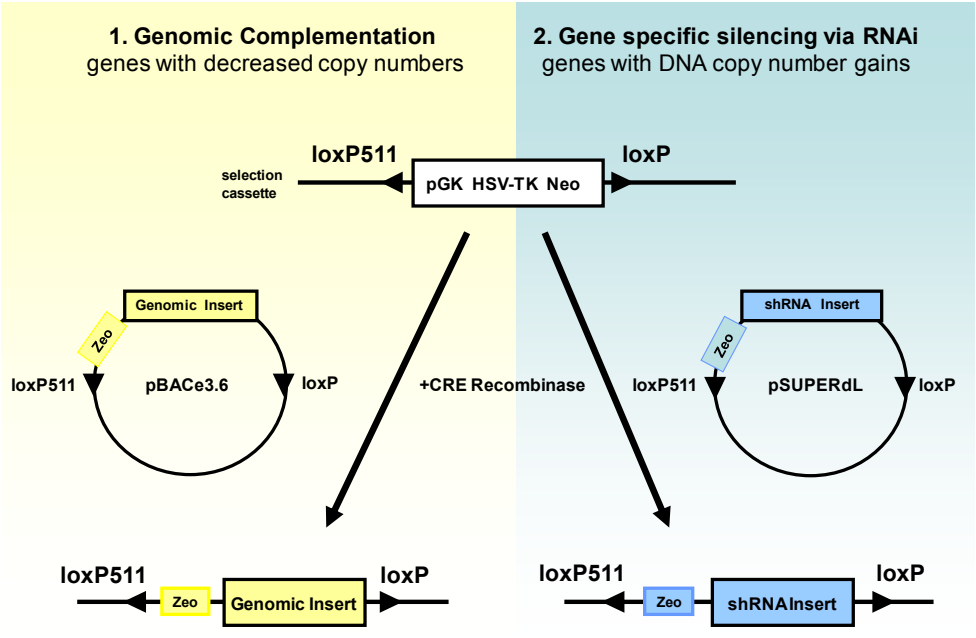

Figure 5: Schematic overview of recombinase mediated cassette exchange (RMCE). The selection cassette, carrying a Herpes Simplex Virus (HSV) Thymidin Kinase (TK) and a neomycine resistance gene (Neo) is flanked by two lox sites (loxP and loxP511). The cassette is randomly integrated into the genome of a cell line. (1) For genomic complementation, a BAC clone, inserted in the pBACe3.6 vector, can replace the selection cassette via homologous recombination (left side, yellow). (2) Gene specific silencing via RNAi is performed with a pSUPERdL (suppression of endogenous RNA) vector, carrying the shRNA for the gene of interest. Homologous recombination allows replacement of the neomycine selection cassette via the shRNA coding construct and the zeocin (Zeo) resistance cassette (right side, blue).

1.8 Cellular model systems

Along with other improvements, the advent of continuous human leukemia/lymphoma cell lines as a resource of abundant, accessible and manipulable living cells has contributed significantly to a better understanding of the pathophysiology of hematopoietic tumors (Drexler *et al*., 2006). The major advantages of continuous cell lines are the unlimited supply and worldwide availablility of identical cell material, and the infinite viable storability in liquid nitrogen. Leukemia/lymphoma cell lines are characterized generally by monoclonal origin and differentiation arrest, sustained proliferation in vitro under preservation of most cellular features, and specific genetic alterations. The most practical classification of leukemia/lymphoma cell lines assigns them to one of the physiologically occurring cell lineages, based on their immunophenotype, genotype and functional features (Drexler *et al*., 2006). MCL and CLL cell lines have been well characterized by matrix comparative genomic hybridization (mCGH), used to modulate specific gene activities and functionally analyze candidate genes within their genetic disease background (Korz *et al*., 2002; Pscherer *et al*., 2006). The MCL cell line JVM-2 shows gains on chromosomes 3q25-q29 and 12q13-q14 and the MCL cell line Granta-519 shows a typical gain on chromosome 18q21-q22 (Figure 6). Based on these results the two MCL cell lines were used in this study for gene modulation experiments.

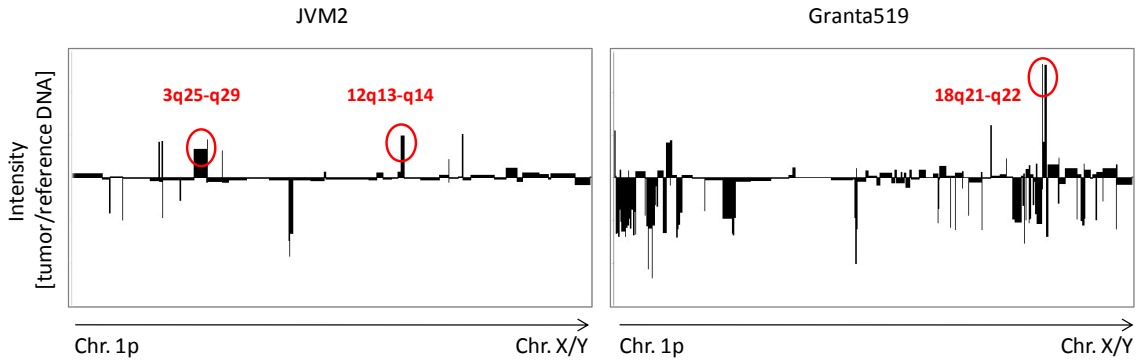

Figure 6: Array CGH in MCL cell lines JVM-2 and Granta-519. Recurrent chromosomal gains in the MCL cell line JVM-2 (3q25-q29 and 12q13-q14) and in the MCL cell line Granta-519 (18q21-q22) are highlighted in a red circle (modified according to Pscherer *et al*., 2006).

1.9 RNA interference

In 1998 RNA interference (RNAi) was discovered as a mechanism that can be exploited as an experimental tool by Andrew Fire and Craig Mello, a finding that was awarded with the Nobel Prize for Medicine in 2006 (Fire *et al*., 1998). Fire and co-workers discovered the presence of double stranded RNA (dsRNA) formed by the annealing of sense and antisense RNA. Although the biology of RNAi is not fully understood, it has become a powerful experimental tool and is currently being developed for human gene therapy. Silencing of candidate genes, thought to play a specific role in tumorigenesis and poor prognosis, is used as a technique to validate the predicted gene functions. RNAi can be directed against cancer through various pathways leading to suppression of tumor growth, metastasis and increased apoptosis.

1.9.1 Mechanisms of RNAi

RNAi is guided by small RNAs that include small interfering RNA (siRNA) and microRNAs (miRNAs). The process of RNAi begins with the cleavage of 21-23 bp long dsRNA by the Dicer enzyme complex into siRNAs. These siRNAs are incorporated into Argonaute 2 (*AGO2*) and the RNAi-induced silencing complex (RISC). In case the RNA duplex loaded onto RISC has perfect sequence complementarity, *AGO2* cleaves the passenger (sense) strand so that active RISC containing the guide (antisense) strand is produced. The siRNA guide strand recognizes target sites to direct mRNA cleavage, carried out by the catalytic domain of *AGO2* (Figure 7).

The processing of miRNAs begins with endogenously encoded primary miRNA transcripts (pri-miRNAs) that are transcribed by RNA polymerase II (Pol II) and are processed by the Drosha enzyme complex to yield precursor miRNAs (pre-miRNAs). These precursors are then exported to the cytoplasm by exportin 5 and subsequently bind to the Dicer enzyme complex, which processes the pre-miRNA for loading onto the AGO2–RISC complex. When the RNA duplex loaded onto RISC has imperfect sequence complementarity, the passenger (sense) strand is unwound leaving a mature miRNA bound to active RISC. The mature miRNA recognizes target sites (typically in the 3’-UTR) in the mRNA, leading to direct translational inhibition. Binding of miRNA to target mRNA may also lead to mRNA target degradation in processing (P)-bodies (de Fougerolles *et al*., 2007).

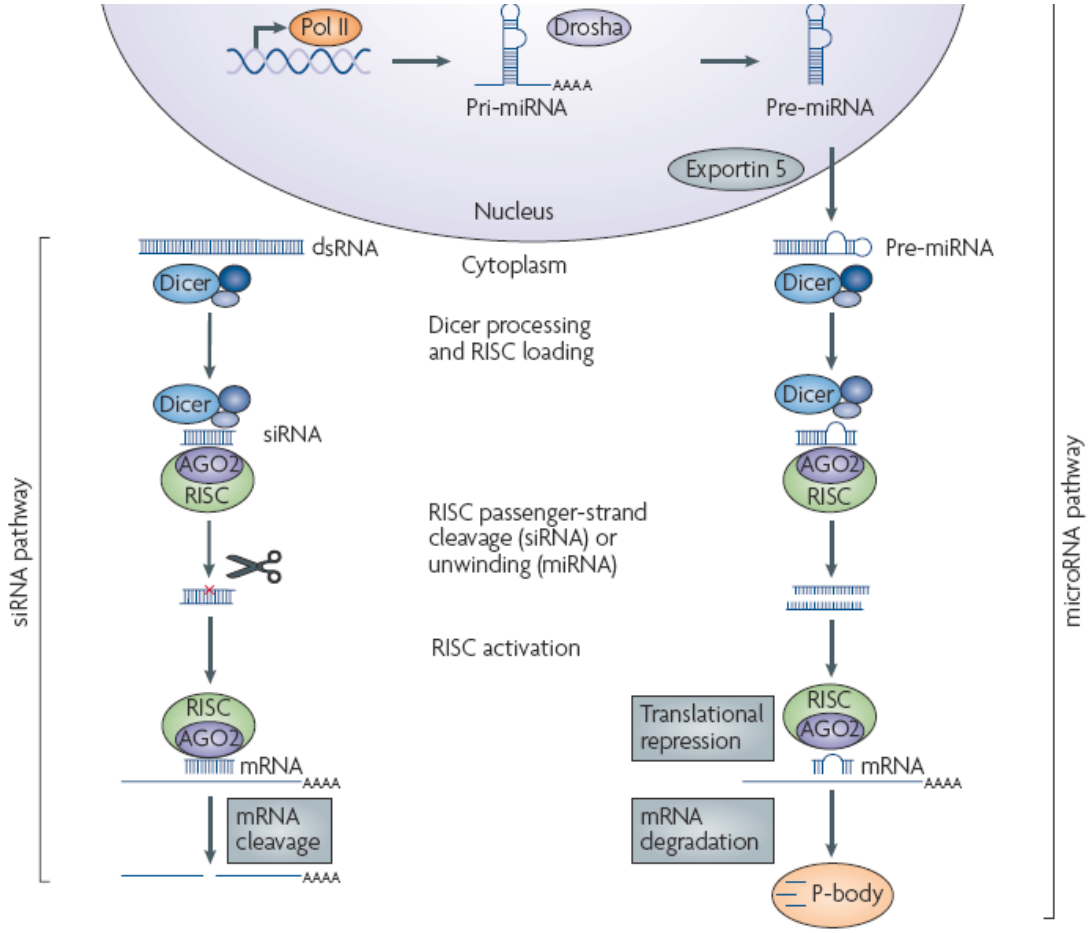

Figure 7: Mechanism of RNA interference in mammalian cells (de Fougerolles *et al*., 2007).

1.9.2 Loss-of-function screen

The most obvious application of RNAi screening, direct loss-of-function (LOF) screening, involves identifying and functionally characterizing genes of interest on the basis of their LOF phenotypes. Such studies offer the broadest discovery potential as they simply analyze single-gene LOF phenotypes in otherwise unmodified cells. This approach has proved effective for many types of genes, including those that encode structural components, cell-surface receptors, transcription factors and enzymes. The high activity, long protein half-life and high endogenous expression of some genes might make it difficult to generate detectable LOF phenotypes, especially in the case of certain enzymes, as residual activity might be sufficient to fulfill their cellular roles (Boutros *et al*., 2008). Importantly, using multiple siRNAs for the same target gene theoretically increases silencing from 70% to 95%. Although the concept of using such a pool of siRNAs (Figure 8c-d) is attractive for achieving a higher probability of strong silencing in fewer experimental samples, it assumes that the silencing performance of the pool is at least as good as the individual siRNAs (Figure 8a). In fact, when carefully optimized, such 'low-complexity siRNA pools' (3-6 siRNA molecules per pool) generally perform better than the worst of their constituent siRNAs but not quite as well as the best, because

poorly performing siRNAs have been found to compete with better ones. For validation of hits, shRNA coding inserts cloned in expression vectors (Figure 8e) can be used to establish stable cell lines (Echeverri *et al*., 2006). Various read out options are available to investigate the phenotype of a cell after functional gene knockdown. Until recently, assays that are based on the use of plate readers like those using luminescent reporters were the most favored ones for cell-based screening due to their simplicity of workflow, their strong robustness, and generally high reproducibility (Echeverri *et al*., 2006; Boutros *et al*., 2008). In the case of selection-based RNAi screens using pooled libraries, fluorescent reporter-based assays enable fluorescence activated cell sorting FACS of treated cells, offering powerful read-outs.

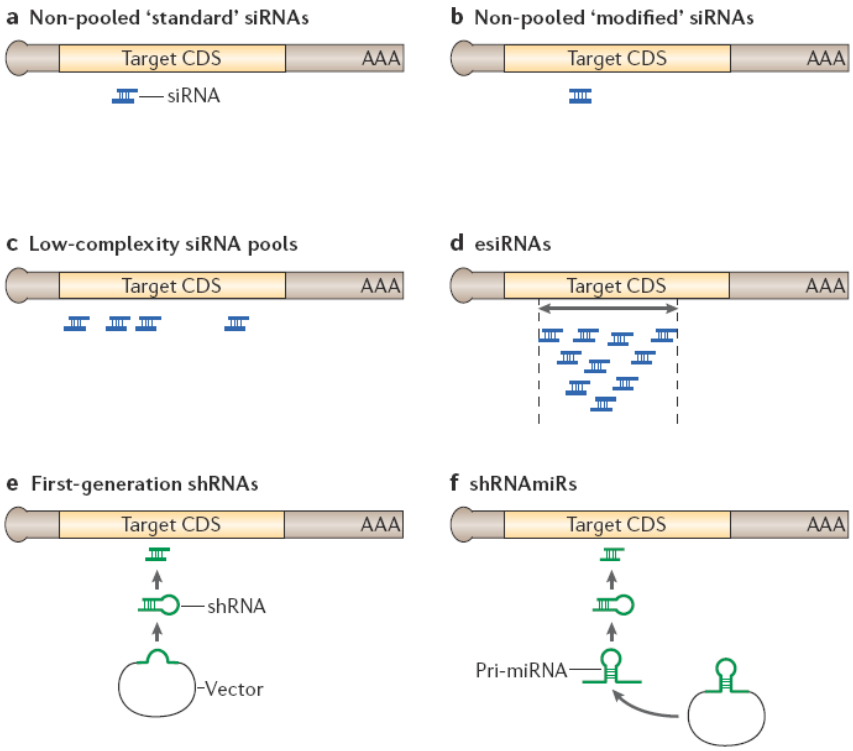

Figure 8: Silencing reagents for siRNA screens in mammalian cells (Echeverri *et al*., 2006). (a) siRNAs consist of a 19-bp duplex with 2-base overhangs at the 3´. (b) Synthetic siRNAs with non-canonical siRNA structures and/or a modified RNA backbone. (c) Low-complexity pools of <10 molecules that target the same transcript. (d) High-complexity pools of siRNA-like molecules can be synthesized by in vitro digestion of long dsRNAs and reveal endoribonuclase cleaved siRNAs (esiRNAs). (e) Vector-based library reagents, expressing short hairpin RNA (shRNA) constructs, are delivered virally. (f) A new vector design offers an RNase II- or RNase III-driven shRNA insert within a backbone from a known miRNA, producing 'shRNAmiRs' that enter the RNAi pathway as pri-miRNAs (primary miRNA), upstream from conventional shRNAs. Esi=endonuclease cleaved siRNA; CDS=coding sequence.

1.10 Aim of the work

The aim of the present work was to identify and functionally characterize genes with oncogenic potential in recurrently gained chromosomal regions of MCL and CLL (3q25-q29, 12q13-q14 and 18q21-q22). Profiling of MCL and CLL genomes and transcriptomes on array CGH and expression array platforms are methods of choice to reveal a focused set of overexpressed candidate genes located in the respective chromosomal regions. Antagonization of upregulated genes can be successfully achieved in a loss-of-function assay. A transient RNAi screen and subsequent functional analyses proving changes in cell viability are versataile approaches to uncover those genes with survival stimulating effects on MCL or CLL. Moreover, tumor model cell lines with stable gene knockdown, achieved for example by RMCE, can give even stronger evidence of the candidate gene´s role in the pathogenesis of MCL and CLL. Reporter-gene assays and genome wide expression profiling studies following overexpression and silencing of a candidate gene, can give detailled insights into its involvement in cell survival and cell proliferation pathways. Since genes identified through this approach promote tumor cell proliferation, the respective candiates are possible targets for diagnosis and anti-cancer therapies.

2 Material and Methods

2.1 Material

2.1.1 Chemicals and biochemicals

Chemicals	Supplier
2-mercaptoethanol (thioethylene glycol)	Sigma-Aldrich, Munich, Germany
2-Propanol (Isopropanol)	Merck, Darmstadt, Germany
α-Thioglycerol	Sigma-Aldrich, Munich, Germany
Acrylamide / Bis-Acrylamide (30% w/v)	Merck, Darmstadt, Germany
Acetic acid	Roth, Karlsruhe, Germany
Agarose	Sigma-Aldrich, Munich, Germany
Ammonium Persulphate (APS)	Sigma-Aldrich, Munich, Germany
Ammonium acetate solution 7.5 M	Sigma-Aldrich, Munich, Germany
Ampicillin	Roche Diagnostics, Mannheim, Germany
Bacto Agar	Difco Laboratories Inc, Detroit, USA
Bacto Tryptone	Difco Laboratories Inc, Detroit, USA
Bacto Yeast Extract	Difco Laboratories Inc, Detroit, USA
Bathocuproinedisulfonic acid disodium salt (BCS)	Sigma-Aldrich, Munich, Germany
Bicinchoninic acid (BCA)	Sigma-Aldrich, Munich, Germany
Bromphenoleblue	AppliChem GmbH, Darmstadt, Germany
Bovine serum albumine (BSA)	Sigma-Aldrich, Munich, Germany
Complete EDTA-free protease inhibitor cocktail	Roche Diagnostics, Mannheim, Germany
Copper-(III)-sulfate	Sigma-Aldrich, Munich, Germany
Chloroform	Merck, Darmstadt, Germany
DEPC treated water	Ambion, Austin, USA
Dithriotheital (DTT)	Sigma-Aldrich, Munich, Germany
Ethylenediaminetetraacetic acid (EDTA)	Merck, Darmstadt, Germany
Dimethylsulfoxid (DMSO)	Sigma-Aldrich, Munich, Germany
Ethanol	Merck, Darmstadt, Germany
Ethidium bromide	Sigma-Aldrich, Munich, Germany
Ficoll 400	Biochrom AG, Berlin, Germany
Formamide	Merck, Darmstadt, Germany
Glycerine	Roth, Karlsruhe, Germany
Glycine	Roth, Karlsruhe, Germany
Hepes	Sigma-Aldrich, Munich, Germany
Hydrochloride acid (HCl)	Merck, Darmstadt, Germany
Isoamylalcohol	Merck, Darmstadt, Germany
Maleic acid	Sigma-Aldrich, Munich, Germany
Magnesium chloride	Merck, Darmstadt, Germany
Methanol	Merck, Darmstadt, Germany
Milk powder	Sigma-Aldrich, Munich, Germany
N-Lauroylsarcosine sodium salt	Sigma-Aldrich, Munich, Germany

Chemicals	Supplier
Nuclease free water	Ambion, Austin, USA
Paraformaldehyde	Sigma-Aldrich, Munich, Germany
Pepsin	Sigma-Aldrich, Munich, Germany
Phenol	Roth, Karlsruhe, Germany
Potassium chloride (KCl)	Sigma-Aldrich, Munich, Germany
Potassium dihydrogen phosphate (KH_2PO_4)	Carl Roth, Karlsruhe, Germany
Sephadex-G50	Sigma-Aldrich, Munich, Germany
SOC medium	Invitrogen, Karlsruhe, Germany
Sodium acetate (NaAc)	Merck, Darmstadt, Germany
Sodium chloride (NaCl)	Merck, Darmstadt, Germany
Sodium citrate	Merck, Darmstadt, Germany
Sodium dodecyl sulfate (SDS)	Carl Roth, Karlsruhe, Germany
Sodium hydrogen phosphate (Na_2HPO_4)	Sigma-Aldrich, Munich, Germany
Sodium hydroxide (NaOH)	Merck, Darmstadt, Germany
Sodium pyruvate	Gibco BRL, Invitrogen, Karlsruhe, Germany
TEMED	Bio-Rad Laboratories, Munich, Germany
Tricine	Carl Roth, Karlsruhe, Germany
Tris-Base	Sigma-Aldrich, Munich, Germany
Triton X-100	Sigma-Aldrich, Munich, Germany
Trizol reagent	Invitrogen, Karlsruhe, Germany
Tween-20	Sigma-Aldrich, Munich, Germany
Xylencyanol	Sigma-Aldrich, Munich, Germany

2.1.2 Enzymes

Restriction Enzymes	Supplier
*Bam*HI (50 U/µl)	New England Biolabs, Frankfurt aM, Germany
*Bgl*II (50 U/µl)	New England Biolabs, Frankfurt aM, Germany
*Eco*RI (50 U/µl)	New England Biolabs, Frankfurt aM, Germany
*Hind*III (50 U/µl)	New England Biolabs, Frankfurt aM, Germany
*Nco*I (50 U/µl)	New England Biolabs, Frankfurt aM, Germany
*Not*I (50 U/µl)	New England Biolabs, Frankfurt aM, Germany
*Sca*I (50 U/µl)	New England Biolabs, Frankfurt aM, Germany

Enzymes	Supplier
Bca DNA Polymerase (2 U/µL)	Takara Bio Europe, Madion, USA
DNAseI (10 U/µl)	Roche Diagnostics, Mannheim, Germany
EuroTaq (5 U/µl)	EuroClone, Siziano, Italy
SuperScript II reverse transcriptase (200 U/µl)	Invitrogen, Karlsruhe, Germany
T4 DNA Ligase (200 U/µl)	New England Biolabs, Frankfurt aM, Germany
T4 Polynucleotide Kinase (1 U/µl)	New England Biolabs, Frankfurt aM, Germany
T4 DNA Polymerase (3 U/µl)	New England Biolabs, Frankfurt aM, Germany

2.1.3 Kits

Kit	Supplier
All Prep RNA Protein Kit	Qiagen, Hilden, Germany
ABsolute™ QPCR SYBR® Green ROX mix	ABgene, Epsome, UK
B-cell Isolation Kit II, untouched isolation	Miltenyi Biotech, Berglisch Gladbach, Germany
Big Dye Terminator Sequencing Kit	Applied Biosystems, Forster City, USA
CellTiter-Glo® Luminescent Cell Viability Assay	Promega, Karlsruhe, Germany
Caspase-Glo® 3/7 Assay Systems	Promega, Karlsruhe, Germany
Dual-Glo-Luciferase Assay System	Promega, Karlsruhe, Germany
ECL Western Blot Detection Kit	GE Healthcare Europe GmbH, Freiburg, Germany
ECL + Western Blot Detection Kit	GE Healthcare Europe GmbH, Freiburg, Germany
EndoFree Plasmid Maxi Kit	Qiagen, Hilden, Germany
MicroRNeasy Kit	Qiagen, Hilden, Germany
Qiagen DNA Gel Extraction Kit	Qiagen, Hilden, Germany
Qiagen DNA Purification Kit	Qiagen, Hilden, Germany
Qiagen Plasmid Purification Kit	Qiagen, Hilden, Germany
RNeasy Mini Kit	Qiagen, Hilden, Germany

2.1.4 Other materials

Name	Supplier
3MM Paper	Whatman, Dassel, Germany
ABI PRISM™ optical adhesive covers	Applied Biosystems, Forster City, USA
Adenosine 5´Triphosphate (ATP)	New England Biolabs, Frankfurt aM, Germany
Anti-Digoxigenin-AP, Fab fragments	Roche Diagnostics Mannheim, Germany
Blocking reagent	Roche Diagnostics Mannheim, Germany
CotI human DNA	Roche Diagnostics Mannheim, Germany
CDP Star	Roche Diagnostics Mannheim, Germany
Deoxynucleotide (dNTP) set	Amersham Bioscience, Freiburg, Germany
DNA mass standard (1 kB DNA ladder)	Invitrogen, Karlsruhe, Germany
DNA mass standard (smart ladder)	Eurogentec, Seraing, Belgium
DIG High Prime	Roche Diagnostics Mannheim, Germany
Hering sperm DNA solution	Invitrogen, Karlsruhe, Germany
FalconTM 50 ml conical tubes	BD Biosciences, San Jose, USA
FalconTM 15 ml conical tubes	BD Biosciences, San Jose, USA
Human genomic DNA (standard)	Roche Diagnostics Mannheim, Germany
Hyperfilm ECL	GE Healthcare Europe GmbH, Freiburg, Germany
Hybond N+ nylon membrane	GE Healthcare Europe GmbH, Freiburg, Germany
ImmobilinTM -P- PVDF membrane	Millipore, Schwalbach, Germany
Intensification screen	Dr.Goos-Suprema, Heidelberg, Germany
Lumi film chemiluminescent	Roche Diagnostics Mannheim, Germany
MACS® cell separation columns	Milentyi Biotech, Bergisch Gladbach, Germany
Midi MACS™ separator	Milentyi Biotech, Bergisch Gladbach, Germany
Microcentrifuge tubes, PCR, clean, 0.5 ml	Eppendorf, Hamburg, Germany
Microcentrifuge tubes, PCR, clean, 1.5 ml	Eppendorf, Hamburg, Germany
Microcentrifuge tubes, PCR, clean, 2.0 ml	Eppendorf, Hamburg, Germany

Name	Supplier
Microcon YM-100 centrifugal filter devices	Millipore, Schwalbach, Germany
Microcon YM-30 centrifugal filter devices	Millipore, Schwalbach, Germany
MicroAmp plates, optical 384-well reaction plate	PE Applied Biosystems, Weiterstadt, Germany
Millex-LCR filter, 0.45 µm, 25 mm, non-sterile	Millipore, Schwalbach, Germany
PCR tubes, 0.2 ml	Molecular Bioproducts, Dan Diego, USA
Propidium iodide	BD Bioscience, Heidelberg, Germany
Random hexamer primers	Invitrogen, Karlsruhe, Germany
Rnase Out	Invitrogen, Karlsruhe, Germany
RNAse ZAP	Ambion, Austin, USA
Salmon sperm DNA	Invitrogen, Karlsruhe, Germany
Second strand buffer for SSII cDNA synhesis	Invitrogen, Karlsruhe, Germany
T4 gene 32 protein	Roche Diagnostics Mannheim, Germany
TNFα	Calbiochem, Darmstadt, Germany
Universal human reference RNA	Stratagene, La Jolla, CA
VECTASHIELD with DAPI	Linaris, Wertheim-Bettingen, Germany
X-ray cassette	Dr. Goos-Suprema, Heidelberg, Germany

Bacteria	Supplier
OneShot^{R} Top10 Electrocomp^{TM} E.coli	Invitrogen, Karlsruhe, Germany

2.1.5 Solutions

2.1.5.1 Standard Solutions

Standard Solutions	Composition
20x SSC	3M NaCl 0.3 M Sodium citrate pH=7.0
10x PBS	137 mM NaCl 27 mM KCl 100 mM NaH_2PO_4 17 mM KH_2PO_4 dissolve in ddH_2O
1x TBS-T	20 mM Tris-Base 137 mM NaCl 3.8 ml 1M HCl 0.1% (v/v) Tween 20 dissolve in 1l ddH_20
5x Loading buffer	100 mM EDTA 30% (v/v) Glycerine 0.25% (w/v) Bromophenolblue dissolve in ddH_2O
5x TBE	0.445M Tris-Borat , pH=8.0 10mM EDTA, pH=8.0
20% SDS	20% SDS (w/v) dissolve in ddH_20

2.1.5.2 Medium and antibiotics

Medium and antibiotics	Composition
LB medium	1% (w/v) Bacto-Trypton 0.5% (w/v) Bacto-Yeast-Extract 1% (w/v) NaCl in H_2O adjust to pH=7.5
S.O.C. Medium	2% Trypton 0.5% Yeast Extract 10 mM NaCl 2.5 mM KCL 10 mM $MgCL_2$ 10 mM $MgSO_4$ 20 mM Glucose
Ampicillin	Stock solution: 100 mg/ml in H_2O sterile filtered and aliquoted, stored at -20°C working concentration: 100 µg/ml
Chloramphenicol	Stock solution: 34 mg/ ml in ethanol sterile filtered and aliquoted, stored at -20°C working concentration: 100 µg/ml
Kanamycin	Stock solution: 100 mg/ml in ethanol sterile filtered and aliquoted, stored at -20°C working concentration: 100 µg/ml

2.1.5.3 Southern blot solutions

Southern blot solutions	Composition
Denaturation Solution	0.5M NaOH 1.5M NaCl
Neutralization Solution	0.5 M TrisHCl 1.5M NaCl
Hybridisation buffer	5xSSC 0.1% N-lauroylsarcosine 0.02% SDS 1% Blocking Solution
Blocking Solution 10x	10 g Blocking Reagent 100 ml ddH_20
Low Stingency Buffer	2x SSC 0.1% SDS
High Stingency Buffer	0.5x SSC 0.1% SDS
DIG I	0.1 M Maleic acid 0.15M NaCl pH=7.5 adjust to pH=7.5 using 5M NaOH
DIG WASH	DIG I 0.3% Tween 20
DIG II	10 ml 10x Blocking 100 ml DIGI
DIG III	0.1 M NaCl 0.05M $MgCl_2$ adjust to pH 9.5 using 1M Tris-HCl pH=9.5

Southern blot solutions	Composition
Antibody Solution	DIG-AB-FAB-Fragments (1:10.000) in DIG II
CDP-Star solution	CDP-Star 1:100 in DIG III

2.1.5.4 Western blot solutions

Western blot solutions	Composition
2x Laemmli buffer	50 mM Tris/HCl pH=8.0 2.4% w/v SDS 8% Glycerin 0.2% w/v Bromphenol blue 2.5% v/v β-Mercaptoethanol
5x SDS-PAGE running buffer	25 mM Tris-Base 200 mM Glycine 10% (w/v) SDS ddH_2O
10x Western blot buffer	25 mM Tris-Base 192 mM Glycin 20% v/v Methanol (added when preparing 1x buffer)
BSA- blocking buffer	3% BSA in PBS
Milk-blocking buffer	10% Milk powder in TPBS-Tween (0.1%)
APS	10% APS w/v in ddH_20
Stripping buffer	100 nM β-Mercaptoethanol 2% SDS 62.5 nM Tris-HCl, pH=6.7

2.1.5.5 FISH solutions

FISH solutions	Composition
Hypotonic buffer	3g KCL 0.2 g EGTA 4.8 g HEPES dilute in 1l H_20 adjust with KOH to pH=7.4
Denaturation solution	49 ml Formamide 7 ml 20x SSC 14 ml ddH_2O adjust to pH=7.0
Wash A	50% (v/v) Formamide pH=7.0 30 ml 20x SSC 120 ml ddH_2O
Wash B	0.5x SSC
Wash C	0.1% (v/v) Tween 20 4x SSC
Blocking	3% (w/v) BSA 4x SSC
Detection	1% (w/v) BSA 4x SSC
DAPI	60 ml 2x SSC, pH 7.0 45 µl DAPI
Column buffer for Sephadex columns	10 mM Tris-HCl pH 8.0 1 mM EDTA pH 8.0 0.1% (w/v) SDS

2.1.6 siRNA sequences

siRNA	Sense Sequence (5´→ 3´)	Supplier	ID
CCDC50#1	GCUGGCUAUUGAGGCAGAGtt	Ambion	199977
CCDC50#2	GGAUGAGGACAUAGCUCGCtt	Ambion	129978
CCDC50#3	CCUCUAUGCUGCAUAUACUtt	Ambion	129979
siCONTROL Non-Targeting siRNA Pool #2	siRNA#1: AUGAACGUGAAUUGCUCAA siRNA#2: UAAGGCUAUGAAGAGAUAC siRNA#3: AUGUAUUGGCCUGUAUUAG siRNA#4: UAGCGACUAAACACAUCAA	Dharmacon	D-001206-14-05
ON-TARGET plus siCONTROL Non-targeting Pool	siRNA#1: UGGUUUACAUGUCGACUAA siRNA#2: UGGUUUACAUGUUGUGUG siRNA#3: UGGUUUACAUGUUUUCUGA siRNA#4: UGGUUUACAUGUUUUCCUA	Dharmacon	D-001810-10-05
Silencer Firefly Luc GL2/3	n/a	Ambion	AM4629
Silencer Negative Control #1	n/a	Ambion	AM4611
PLK1 Pool Pool	PLK1_6: CCGGATCAAGAAGAATGAATA PLK1_7: CGCGGGCAAGATTGTGCCTTAA PLK1_11: AACGAGCTGCTTAATGACGAG PLK1_2: CAACGGCAGCGTGCAGATCAA	Qiagen	SI 02223837 SI 02223844 SI 04376365 SI 00071624
DUSP5 Pool	DUSP5_14: CAAGTGAGCGTTCCTCGCCAA DUSP5_9: CGCGACCCACCTACACTACAA DUSP5_10: ATGAGTGTTGAGTGGATGTAA DUSP5_13: CTGCATGGCTTACCTTATGAA	Qiagen	SI 04345124 SI 03194282 SI 03206903 SI 04228700
KIF11 Pool	KIF11_7: GAAGATAAGATAGAAGATCAA KIF11_8: CTCGGAAGCTGGAAATATAA KIF11_6: ACGGAGGAGATAGTTCGTTTA KIF11_12: CAGGAATTGATTAATGTACTC	Qiagen	SI 02653770 SI 03019793 SI 02653693 SI 04376358
BCL2 Pool	BCL2_12: AACCGGGAGATGGTGATGAAG BCL2_9: TCCATTATAAGCTGTCGCAGA BCL2_10: AAGTTCGGTGGGTCATGTGT BCL2_11: AACTGGGGGAGGATTGTGGCC	Qiagen	SI 00299418 SI 00299397 SI00299404 SI 00299411
CCND1 Pool	CCND1_5: AACACCAGCTCCTGTGCTGCG CCND1_6: GCCCTCGGTGTCCTACTTCAA CCND1_1: AAGGCCAGTATGATTTATAAA CCND1_2: ATGCATGTAGTCACTTTATAA	Qiagen	SI 02654540 SI 02654547 SI 00147812 SI 00147819
All Stars Negative Control	n/a	Qiagen	1027280
All Stars Cell Death Control	n/a	Qiagen	1027298
ARHGAP9	CGGUUAGAUUUGGACAGUATT	Ambion	S34646
Ctrl_control_1	AATTCTCCGAACGTGTCACGT	Qiagen	SI 03650325
Ctrl_AllStars_1	n/a	Qiagen	SI 03650318
siGLO Risc Free	n/a	Dharmacon	D-001600-01-20

n/a=no sequence available

2.1.7 Vectors

Vector	Supplier
pSUPER	R. Agami, The Netherlands Cancer Institute, Amsterdam, NL
pSUPERdL	Pscherer *et al.*, 2006
pCMV6-XL4-CCDC50	OriGene Technologies Inc, Rockville, USA
pCMX_h-Cre	E. Greiner (DKFZ Heidelberg) with approval of F. Stewart (Desden)
pTER	H. Clevers, Netherlands Institure for Developmental Biology, NL
pGKneo	E.Greiner (DKFZ Heidelberg) with approval of F. Stewart (Desden)
pGKP511TkneoP	Pscherer *et al.*, 2006
pCMV-Renilla Luciferase	Dr. Mathas, Prof. Doerken, Max-Delbrueck Center in Berlin
p-6xNFKB-Firefly-luciferase	Dr. Mathas, Prof. Doerken, Max-Delbrueck Center in Berlin

2.1.8 Primers

2.1.8.1 Primer for PCR, sequencing, and cloning

Primer	Sequence (5´ → 3´)
castestLPr	CGCCAAGCTGGCGCGGGATAACT
castestf	GTGCCACCTGACGTCTAAGAAAC
pSUPER-intern_fw	TGCGCCCTGGCAGGAAGAT
pSUPER-intern_rev	AGCGAGTCAGTGAGCGAGGAA
pSUPER-up	CCATTCAGGCTGCGCAACTGTT
petra3_rev	CGAAGAACTCCAGCATGAGATCCC
pGKSacRf	GCT GGAGTTCTTCGCCGTTTC
P511OKrev2	TTCCATTGCTCAGAGGTGCTGT
sh_CCDC50_fw	GATCCCCCCTCTATGCTGCATATACTTTCAAGAGAAGTATATGCAGCATAGA GGTTTTTGGAAA
sh_CCDC50_rev	AGCTTTTCCAAAAACCTCTATGCTGCATATACTTCTCTTGAAAGTATATGCAG CATAGAGGGGG
sh_Luciferase_for	GATCCCCCTTACGCTGAGTACTTCGATTCAAGAGATCGAAGTACTCAGCGTA AGTTTTTGGAAA
sh_Luciferase_rev	AGCTTTTCCAAAAACTTACGCTGAGTACTTCGATCTCTTGAAGTATATGCAGC ATAGAGGGGG
TKneo-BglII_fw	CGTTCTCGCGGCCATAGCAA
TKneo-NcoI_rev	AACACGGCGGCATCAGAGCA
NotI_pTER_fw	CGATTGCGGCCGCTGATTTAAC
BamHI_pTER_rev	CGGAGGATCCAAGCTCTAGCTA
T7_fw	TAATACGACTCACTATAGGG
M13_rev	TTTCACACAGGAAACAGCTATGAC

2.1.8.2 Primer for quantitative real-time PCR

qRT-PCR Primer	Forward Sequence (5´→ 3´)	Reverse Sequence (5´→ 3´)
ACTL6A	TCTGTCAGTTTCTCTCTCTTTGCTC	AGAAGTGGTTGCAGTGCTGA
APOD	GGAAGTGCCCCAATCCTC	TTCGTACCATCTTCCGAGATACT
ARHGAP9	CCAACCATGACACTCTACGG	TGCGATTCTTATCTGAGTGTGC
DCTN2	ACTAGCGACCTACCTGAGGA	TCATAGGCAGCATTAGGATTGAC
DDIT3	CAGAGCTGGAACCTGAGGAG	CTGCAGTTGGATCAGTCTGG
CCDC50	TGACCGGGAAGCCCGCGTTAAAGG	TTCCTGCAGGCTGTGAGCCAGGGT
ECT2	CTCTAGGTGAGCACCCCTGT	TGTGCCGTTTTCTTGCTATCT
IL8	AGACAGCAGAGCACACAAGC	ATGGTTCCTTCCGGTGGT
ITGB7	CAGTTGGGGAGCTGAGTGAG	CACGGTGGAAGACAGGCTAT
YEATS2	ACGGAGTGTGTCGTTCAGC	AAATGCATGTCAAATCAGAAGC
LaminB1	CTGGAAATGTTTGCATCGAAGA	GCCTCCCATTGGTTGATCC
MALT1	TTGAATTCAGCCAGTGGTCA	GAGACGCCATCAACACTTCTC
PAK2	AAGGGGTTCAGCCAAAGAAT	TCCATGACCACAAACAATTCA
PFN2	AGGTGGGGAGCCAACATAC	CACCTTCCTTTCCCATGACTA
RHEBL1	TCTCTGAGCCCGCAGTTC	CACAAATTGATGTGCCAAAGA
RKHD2	TTGGGAGTGATCCTTCTGGT	AGGAGACAGACGAGGAGTAGATG
TIMELESS	AATTCGCCAGAAGGTTTCCT	AATTCGCCAGAAGGTTTCCT
TNFAIP3	TGCACACTGTGTTTCATCGAG	ACGCTGTGGGACTGACTTTC

2.1.9 Antibodies

2.1.9.1 Southern blot antibodies

Name	Blocking Solution	Dilution	Supplier
DIG-AB-FAB-Fragments	In DIG II	1:10000	Roche, Mannheim, Germany

2.1.9.2 Western blot antibodies

AB	Name	Produced in	Blocking Solution	Dilution	Supplier
1°	Anti-CCDC50-Antibody	rabbit	3% BSA-PBS	1:800	Sigma-Aldrich, Munich, Germany
1°	Anti-GAPDH-Antibody	mouse	5% Milk-TBST	1:5000	Calbiochem, Darmstadt, Germany
2°	Anti-mouse IgG, HRP-linked Antibody		5% Milk-TBST	1:5000	Cell Signaling Inc., Danvers, USA
2°	Anti-rabbit IgG, HRP-linked Antibody		5% Milk-TBST	1:2000	Cell Signaling Inc., Danvers, USA

2.1.9.3 FACS antibodies

Name	Supplier
CD19-PE antibody, clone LT19	Miltenyi Biotech, Bergisch Gladbach, Germany
CD20-PE antibody, clone LT20	Miltenyi Biotech, Bergisch Gladbach, Germany
Mouse IgG1 antibody	Miltenyi Biotech, Bergisch Gladbach, Germany

2.1.10 Cell culture

2.1.10.1 Cell lines

Cell line	No	Supplier
CA-46	ACC 73	DSMZ, Braunschweig, Germany
DG-75	ACC 83	DSMZ, Braunschweig, Germany
EHEB	ACC 67	DSMZ, Braunschweig, Germany
GRANTA-519	ACC 342	DSMZ, Braunschweig, Germany
HEK-293T	CRL-1573	ATCC, Manassas, VA, USA
HS5	CRL11882	ATCC, Manassas, VA, USA
HT	ACC 567	DSMZ, Braunschweig, Germany
JEKO-1	ACC 553	DSMZ, Braunschweig, Germany
JVM-2	ACC 12	DSMZ, Braunschweig, Germany
L428	ACC 197	DSMZ, Braunschweig, Germany
L540	ACC 72	DSMZ, Braunschweig, Germany
LCL-WEI	ACC 218	DSMZ, Braunschweig, Germany
MEC-1	ACC 497	DSMZ, Braunschweig, Germany
MEC-2	ACC 500	DSMZ, Braunschweig, Germany
MC-116	AC 82	DSMZ, Braunschweig, Germany
RAJI	ACC 319	DSMZ, Braunschweig, Germany
RAMOS	ACC 603	DSMZ, Braunschweig, Germany
SUDHL-5	ACC 571	DSMZ, Braunschweig, Germany
SUDHL-6	ACC 572	DSMZ, Braunschweig, Germany

2.1.10.2 Transfection reagents

Transfection Reagents	Supplier
Cell Line Nucleofector Kit V	Lonza, Cologne, Germany
Cell Line Nucleofector Kit T	Lonza, Cologne, Germany
Cell Line Optimization 96-well Nucleofector Kit	Lonza, Cologne, Germany
Cell Line 96-well Nucleofector Kit SF	Lonza, Cologne, Germany
DarmaFECT™ 1 siRNA transfection reagent	Dharmacon, Chicago, USA
Geneporter	Genlantis, San Diego, USA
HiPerfect	Qiagen, Hilden, Germany
Oligofectamine™	Invitrogen, Karlsruhe, Germany
Primary B-cell Nucleofector Kit	Lonza, Cologne, Germany
RNAiFECT	Qiagen, Hilden, Germany
TransIT	Mirus Bio LLC, Madison, USA
X-tremeGENE	Roche Diagnostics, Mannheim, Germany

2.1.10.3 Cell culture solutions

Product	Supplier
Dulbecco´s Modified Eagle Medium	Gibco BRL, Invitrogen, Karlsruhe, Germany
FCS (fetal cow serum)	Biochrom, Berlin, Germany
Ganciclovir	Sigma-Aldrich, Munich, Germany
L-Glutamin	Gibco BRL, Invitrogen, Karlsruhe, Germany
Penicillin-Steptomycin (1000 U/ml)	Gibco BRL, Invitrogen, Karlsruhe, Germany
RPMI 1640	Gibco BRL, Invitrogen, Karlsruhe, Germany
Geneticin (G418)	Invitrogen, Karlsruhe, Germany
Zeocin	Invitrogen, Karlsruhe, Germany

2.1.11 Tumor samples

2.1.11.1 MCL samples used for expression profiling

MCL Patient	Sex	Age at Dx	Follow-up (months)	State	Therapy	FISH on 3q27	Leukemic	MP
W-7466/02	M	39	22.9	0	CHOP	n.a.	?	C
W-16866/98	M	70	81.1	0	CHOP-like	Gain	No	C
W-19656/01	M	52	39.3	0	Unknown	Gain	?	C
W-2039/99	M	78	36.6	1	Unknown	Gain	?	C
W-28663/01	M	55	15.3	1	CHOP-like	Normal	?	C
W-H2568/97	M	56	94.2	0	intensified	normal	No	C

MCL patient: W=derived from A. Rosenwald, Würzburg; Dx=age at diagnosis; sex: M= Male; state: 0=alive, 1=dead; therapy: CHOP=Cyclophosphamid, Hydroxydaunorubicin (Doxorubicin), Vincristin (Oncovin), Predniso(lo)n); leukemic: No=not leukemic, ?=not investigated; MP=Morphology: C=Classical. All primary samples were derived from lymph nodes.

2.1.11.2 MCL samples used for qRT-PCR experiments

MCL Patient	Sex	Age at Dx	Follow-up (months)	State	Therapy	Derived from	FISH on 3q27	MP
W-15586/99	M	61	12.9	1	CHOP	LN	Normal	C
W-C2039/99	M	78	36.6	1	n.a.	LN	n.a.	C
W-28663/01	M	55	15.3	1	CHOP	LN	Normal	C
W-7466/02	M	39	22.9	0	CHOP	LN	n.a.	C
W-16866/98	M	78	81.1	0	CHOP	LN	gain	C
W-19656/01	M	52	39.3	0	n.a.	LN	gain	C
K-1363/04	M	75	n.a.	n.a.	n.a.	LN	n.a.	n.a.
K-184/92	M	75	n.a.	n.a.	n.a.	LN	n.a.	n.a.
K-1646/05	F	46	n.a.	n.a.	n.a.	BM	n.a.	n.a.

MCL patient: W=derived from A. Rosenwald, Würzburg, K=derived from R. Siebert, Kiel; Dx=age at diagnosis; sex: M=Male, F=Female; state: 0=alive, 1=dead; therapy: CHOP=Cyclophosphamid, Hydroxydaunorubicin (Doxorubicin), Vincristin (Oncovin), Predniso(lo)n); Derived from: LN=lymph node, BM=bone marrow; MP=Morphology: C=Classical.

2.1.11.3 CLL samples used for expression profiling

CLL	Sex	CD19+	FISH	VH status	VH-Gen gl
17-1	M	n.a.	17p-	n.a.	n.a.
17-2	M	n.a.	17p-	n.a.	n.a.
17-11	F	n.a.	17p-	n.a.	n.a.
17-15	F	n.a.	17p-	n.a.	n.a.
13-1 I	M	n.a.	13q-	n.a.	n.a.
13-1, II	M	n.a.	13q-	n.a.	n.a.
13-2	F	n.a.	13q-	n.a.	n.a.
12	M	96%	13q-	mutated/Ther	V3-72
14	F	n.a.	Normal	unmutated	V1-02
16	F	77%	13q-	unmutated	V1-69
34	M	66%	12q+	unmutated/C	V4-39
25	M	n.a.	13q	unmutated/C/Ther	V4-b
36	M	n.a.	13q-	mutated	V1-69
40	M	87.50%	13q-	mutated	V3-07
17-8	M	n.a.	17p- (94%)	n.a.	V7-4.1
17-10	F	n.a.	17p- (83%), 13q- (30%)	n.a.	V3-53
17-12	M	n.a.	17p- (78%), 6q- (71%)	n.a.	V1-03
17-14	F	n.a.	17p- (95%), 13q- (95%)	n.a.	V1-69
12-1	F	n.a.	12q (84%)	n.a.	V3-33
12-2	F	n.a.	12q (82%)	n.a.	V4-39
12-3	M	n.a.	12q (80%), 13q- (87%)	n.a.	V5-51
12-8	M	n.a.	12q (81%)	n.a.	V3-30/3-30.5

Sex: F=Female, M=Male, n.a.=no additional information / value not determined, source: H. Döhner and S. Stilgenbauer, University hospital, Ulm, Number of tumors is anonymous and assigned by M. Seiffert, DKFZ Heidelberg and H. Döhner and S. Stilgenbauer, University hospital, Ulm.

2.1.11.4 CLL samples used for qRT-PCR experiments

CLL	Sex	CD19+	FISH	VH status	VH-Gen gl
5	M	84%	normal	unmuated 100%	V3-11
6	M	80%	13q-	mutated 92%	V3-43 (of+stop)
7	M	80%	Normal	mutated 94,06%	V4-34
9	F	70%	13q-	mutated 91,78%	V3-72
11	M	n.a.	13q-	unmutated 99,21%	V2-70
12	M	96%	13q-	mutated 96,1%	V3-72
14	F	n.a.	Normal	unmutated 98,3%	V1-02
15	M	n.a.	13q-	mutated 90,99%	V3-23
16	F	77%	13q-	unmutated 100%	V1-69
18	M	89%	13q-	mutated	V4-39
19	M	78%	13q-	mutated	V5-51
21	M	61%	n.a	unmutated	V1-02
22	F	91%	11q-	unmutated/C/Ther	V1-02
25	M	n.a.	13q-	unmutated	V4-b
26	M	92%	13q-	unmutated	V3-30
28	F	93%	13q-	mutated	V4-34
29	M	89%	13q-	mutated	V1-69
30	F	71%	n.a.	n.a.	n.a.
32	M	90%	n.a.	mutated	V4-39
34	M	66%	12q+	unmutated	V4-39

CLL	Sex	CD19+	FISH	VH status	VH-Gen gl
37	M	78%	13q-	mutated/A	V5-51
39	M	98%	13q-	unmutated	V4-b
40	M	87.5%	13q-	mutated	V3-07
41	M	n.a.	13q-	mutated/Ther	V3-72
48	F	n.a.	n.a.	mutated/A/Ther	V1-18
50	M	n.a.	13q-	n.a.	n.a.
51	M	n.a.	13q-	mutated/Ther	V3-72
63	M	n.a.	13q-	mutated	n.a

Sex: F=Female, M=Male, n.a.=no additional information / value not determined, source: H. Döhner and S. Stilgenbauer, Ulm, Number of tumors is anonymous and assigned by M. Seiffert, DKFZ Heidelberg and H. Döhner and S. Stilgenbauer, University hospital, Ulm.

2.1.12 Instruments

Instrument	Supplier
7900 HT Fast Real Time PCR Systems	Applied Biosystems, Forster City, USA
ABI PRISM 3100 Genetic Analyzer, 16 Capillary DNA Sequencer	Applied Biosystems, Forster City, USA
ABI PRISM 7900 Sequence Detection System	Applied Biosystems, Forster City, USA
Agilent DNA microarray scanner	Agilent Technologies, Palo Alto, USA
Automatic developing machine	Amersham, Freiburg, Germany
Axioplan microscope	Carl Zeiss, Jena, Garmany
Balance BL 610 und BL150S	Sartorius AG, Goettingen, Germany
BD FACSArray™ Bioanalyzer System	BD Biosciences, San Jose, USA
BD FACSCanto II workstation	BD Biosciences, San Jose, USA
BD FACSCalibur workstation	BD Biosciences, San Jose, USA
Biofuge fresco refrigerated tabletop cantrifuge	Heraeus / Kendro, Hanau, Germany
Centrifuge 5810 R	Eppendorf, Hamburg, Germany
EAS gel documentation system	Herolab, Wiesloch, Germany
GS 6, GS 6KR, Centrifuge	Beckmann, Wiesloch, Germany
GSA- and SS34-Rotor	DuPont, Boston, USA
Gel electrophoresis power supply	E-C Apparatus Corporation, USA
Heating block QBT2	Grant Instruments/CLF, Emersacker
HMT 702 C Microwave oven	Robert Bosch GmbH, Stuttgart, Germany
Hybridization incubator	Bachofer GmbH, Reutlingen, Germany
LB-940 Mithras Multilabel Reader	Berthold Technologies, Bad Wildbach, Germany
Mastercycler PCR-Maschine	Eppendorf, Cologne, Germany
Micro-centrifuge	NeoLab Laborbedarf, Heidelberg
Mini-Protean 3 gel and electrophoresis system	Bio-Rad Laboratories, Munich, Germany
Multifuge 3 SR	Heraeus / Kendro, Hanau, Germany
NanoDrop ND-1000 Spectrophotometer	NanoDrop Technologies, San Diego, USA
Nucleofactor device	Lonza, Cologne, Germany
96-well-Shuttle Nucleofection System	Lonza, Cologne, Germany
SDS-PAGE gel apparatus	Biorad Laboratories, Munich, Germany
Speedvac concentrator apparatus	Eppendorf, Cologne, Germany
Thermomixer compact	Eppendorf, Cologne, Germany
Unimax 1010 Shaker	Heidolph Instruments, Schwabach, Germany
UV-Stratalinker 1800	Stratagene, La Jolla, CA
Varifuge 3.0/3.0R Labor centrifuge	Heraeus / Kendro, Hanau, Germany
Waterbath SW22	Julabo Labortechnik, Seelbach, Germany

2.1.13 Software

Software	Supplier
BD FACS Diva	BD Biosciences, San Jose, USA
CellQuest Pro™	BD Biosciences, San Jose, USA
Excel 2007	Microsoft, Redmond, USA
Fast PCR 5.4 Professional	Institute of Biotechnology, Helsinki, FL
Multiple Experiment Viewer	TM4, Boston, USA
SDS 2.0	Applied Biosystems, Forster City, USA
MikroWin 2000	Berthold Technologies, Bad Wildbach, Germany

2.2 Methods

2.2.1 Cell culture

2.2.1.1 Cultivation of cell lines

Cells were obtained from the DSMZ (Braunschweig, Germany). GRANTA-519 (ACC 342), MEC-1 (ACC 497) and MEC-2 (ACC 500) cells were cultured in Dulbecco's modified Eagle's medium (DMEM, Invitrogen, Karlsruhe, Germany). CA-46 (ACC 73), DG-75 (ACC 83), EHEB (ACC 67), HT (ACC 567), JEKO-1 (ACC 553), JVM-2 (ACC 12), L428 (ACC 197), L540 (ACC 72), LCL-WEI (ACC 218), MC-116 (AC 82), RAJI (ACC 319), RAMOS (ACC 603), SUDHL-5 (ACC 571) and SUDHL-6 (ACC 572) cells were cultured in RPMI 1640 medium (Invitrogen) supplemented with 2 mM L-glutamine (Invitrogen, Carlsbad, CA). Both media were supplemented with 10%-20% fetal calf serum (according to the instructions of the DSMZ) and 100 mg/ml penicillin/streptomycin. Cells were cultured at 37°C in a 5% CO_2 humidified incubator. The human bone marrow stroma cell line HS-5 was purchased from the American Type Culture Collection (Manassas, VA, USA). HS-5 cells were maintained in DMEM supplemented with 10% FCS, 4mM L-glutamine, 4.5 g/l glucose, 100 U/ml penicillin and 100 mg/ml streptomycin. Cells were cultured at 37°C in a 10% CO_2 humidified incubator.

2.2.1.2 Isolation of lymphocytes from whole blood

Human lymphocytes were isolated from peripheral blood by density centrifugation using a step gradient consisting of a mixture of the carbohydrate polymer Ficoll and the density iodine-containing compound metrizamide. This yields a population of mononuclear cells (lymphocytes) at the interface that has been depleted of red blood cells and most polymorophonuclear leukocytes and monocytes. Lymphocytes were isolated from whole blood using the Leucosep columns according to the manufacturer´s protocol (Greiner Bio-One, Frickenhausen, Germany).

2.2.1.3 Cultivation of primary B-CLL cells

Peripheral blood mononuclear cells were isolated by Ficoll density gradient from B-CLL patients. Thereafter, B-CLL preparations consisted of >80% CD19 positive cells as measured by fluorescent activated cell sorting and were used without further enrichment. Fractions of B-CLL cells were cryopreserved in cell culture medium containing 10% fetal calf serum and 10% dimethylsulfoxide. After thawing, B-CLL cells were cultured for 1 day with HS-5 stroma cell conditioned medium before experiments were performed. CD19 positive cells from healthy donors were enriched by magnetic bead-activated cell sorting using CD19-MicroBeads according to the manufacturer's

instructions (Miltenyi Biotec, Bergisch Gladbach, Germany). The purity of the CD19+ cell preparations was >95% as measured by flow cytometry. All cells were maintained in Dulbecco's modified Eagle's medium supplemented with 10% FCS, 4mM L-glutamine, 4.5 g/l glucose, 100 U/ml penicillin, 100 mg/ml streptomycin, and were cultured at 37°C in a 10% CO_2 humidified incubator. For experiments with conditioned medium from HS-5 cultures, the medium was removed from more than 70% confluent stromal cell layers, freed from cells by centrifugation for 10 minutes at 1000 g, sterile filtered through a Millipore 0.45 µM filter and added immediately to B-CLL cells in culture. For survival studies, lasting for several days, the conditioned medium was replaced daily. Primary cell samples were obtained from B-CLL and MCL patients and healthy donors after informed consent (University of Ulm, University of Kiel, and University of Würzburg). All MCL and B-CLL cases matched the standard diagnostic criteria according to the World Health Organization.

2.2.2 Transfection methods

2.2.2.1 Chemical transfection of cell lines

Chemical transfections using TransIT, DarmaFECT^{TM}1 siRNA transfection reagent (Dharmacon, Chicago, USA), OligofectamineTM (Invitrogen, Karlsruhe, Germany), RNAiFECT (Qiagen, Hilden, Germany), X-tremeGENE (Roche Diagnostics, Mannheim, Germany), HiPerfect (Qiagen, Hilden, Germany) and Geneporter (Genlantis, San Diego, USA) were performed according to the manufacturer´s instructions.

2.2.2.2 Nucleofection of cell lines and primary CLL cells

Transient transfections of cell lines were performed using the Nucleofector device (Lonza, Cologne, Germany) according to the manufacturer´s instructions with $2x10^6$ cells and 2 µg plasmid DNA or 500nM siRNA (in 100 µl volume) and applying the following parameters: solution T, program O-017 (GRANTA-519, JVM-2 and JEKO-1) and solution V, program X-001 (EHEB, JVM-2, MEC-1, MEC-2). Cells were harvested at 24h, 48h and 72h post transfection (p.t.) for isolation of RNA, protein or for functional assays. For transient transfections of primary CLL cells, a total of $5x10^6$ primary B-cells were electroporated using program U-015 and the primary B-cell solution with 500nM siRNA (in 100 µl volume). After nucleofection, primary cells were added to sterile filtered HS-5 conditioned media. Every 24h fresh HS-5 conditioned medium was added to the cells.
Using the 96-well shuttle nucleofection, a total of $4x10^5$ cells of the cell lines JVM-2 or GRANTA-519 and of primary CLL cells were transfected with 500nM siRNA (in 100 µl volume), solution SF with program 96-DN-100.

2.2.2.3 Stable transfection and Antioxidants

Many cell lines are sensitive to growth at low cell density and undergo apoptosis induced by oxidative stress, if the cell density is decreased below a critical threshold (Brielmeier *et al*., 1998). In stable transfection experiments this cell density-dependent growth may be the limiting factor, since during drug selection the cell density drops below the critical threshold, precluding outgrowth of transfected clones. Therefore, 0.1% α-thioglycerol, 0.02 mM BCS and 1% sodium pyruvate were added to stable transfected cells. $2x10^6$ JVM-2 cells were transfected with different concentrations of the vector pSUPERdL-Zeo_sh_CCDC50 (100ng, 200ng, 500ng, 1ug, 2ug and 5µg) using Lonza Solution T and program O-017. Cells were cultivated in medium containing antioxidants and zeocin (50 ng/ml). After four weeks of selection, stable cell clones grew out, while mock transfected cells died under the selection pressure.

2.2.3 Molecular biological standard methods

2.2.3.1 DNA isolation

$2x10^7$ cells were harvested by centrifugation (1000 rpm, 10 min, RT) and DNA was isolated using the Blood & Cell Culture DNA Midi Kit *(*Qiagen, Hilden, Germany) according to the manufacturer´s protocol. Quantification of DNA samples was carried out on the Nanodrop device (Nanodrop Technologies, Wilmington, DE) set for DNA measurement (A260 / A280 ratio).

2.2.3.2 Plasmid DNA isolation

E.coli colonies containing the plasmid of interest were picked from LB-agar plates and grown for mini preps in 5 ml LB medium and for maxi-preps in 300 ml LB-medium containing the respective antibiotic over night at 37◦C in a shaking incubator (200 rpm). Isolation of plasmid DNA was performed using the Plasmid Mini or Maxi Kit according to the manufacturer´s protocol (Qiagen, Hilden, Germany).

2.2.3.3 RNA Isolation

Total RNA was extracted using $2x10^6$ cells. The cells were centrifuged for 10 minutes at 1000 rpm at RT. The cell pellet was resuspended in 1 ml TRIZOL reagent (Invitrogen), incubated for 5 minutes at RT, then 300 µl chloroform was added. Cells were mixed thoroughly and incubated for another 5 minutes at RT. Cells were centrifuged for 15 minutes in a pre-cooled centrifuge at 4°C at 13000 rpm. The aqueous phase was placed into fresh tubes and mixed with an equal volume of 70% ethanol. The RNA solution was applied to miniRNeasy columns (Qiagen) and further isolation of RNA was performed according to the manufacturer´s protocol. RNA samples were finally dissolved in 20 µl RNAse free water and heated to 37°C for 30 min.

An alternative protocol was used to isolate both, RNA and protein. $2x10^6$ cells were harvested by centrifugation (800 rpm, 10 min, RT), cell pellets were lysed and column purified using the All Prep RNA / Protein Kit according to the manufacturer´s protocol (Qiagen, Hilden, Germany). Quantification of RNA samples were carried out on the Nanodrop device (Nanodrop Technologies, Wilmington, DE) set for RNA measurement (A260 / A280 ratio).

2.2.3.4 Protein isolation

A total of $2x10^6$ cells (primary CLL cells or cell lines) were harvested by centrifugation (800 rpm, 10 min, RT). Cell pellets were lysed and column purified using the All Prep RNA/Protein Kit according to the manufacturer´s protocol (Qiagen, Hilden, Germany).

2.2.3.5 Quantificatinon by spectrophotometry

The absorption maximum of proteins is at 280 nm due to the absorbance of aromatic amino acids. In addition, some contaminants (notably phenol) can significantly contribute to an error in concentration estimation as they also absorb strongly at 260nm. The ratio OD_{260}/OD_{280} can therefore be used as an indication for the purity of nucleic acid solutions. Pure DNA solutions have a ratio of > 1.8, whereas contaminations by phenol or proteins cause a decrease of this value. DNA solutions with a ratio smaller than 1.5 were considered inappropriate for further analysis.

2.2.3.6 Cloning

To obtain the vectors pSUPERdl_Zeo-sh_CCDC50 and pSUPERdl_Zeo-sh_luciferase, the short hairpin RNA coding oligonucleotides sh_CCDC50 and sh_Luciferase (chapter 2.1.8.1) were cloned into the expression vector pSUPERdL_Zeo. pSUPERdL_ZEO was obtained by cloning the zeocin expression unit SV40 promoter + Zeocin resistance gene + SV40 polyA out from the pTER plasmid (van de Wetering *et al.,* 2003) into the *Not* I and *BamH* I sites of pSUPERdL (Pscherer *et al.,* 2006) using te primers: NotI_pTER_fw and BamHI_pTER_rev (chapter 2.1.8.1). The sequence for the short hairpin RNA coding insert was designed according to siRNA sequence from CCDC50 (Ambion, 129979).

2.2.3.7 Vector restriction enzyme digests

Digests were carried out in 20 µl volume with a DNA content of 1 µg for 1 h with 10 U of each enzyme. For digestions over night, a minimum volume of at least 50 µl is recommended. For cloning of the short hairpin RNA coding insert sh_CCDC50 into the vector pSUPER_Zeo, 1µg vector was digested for 1h at 37°C using each 10 U each of the restriction endonucleases *Hind* III and *Bgl* II.

2.2.3.8 Annealing of oligos

To obtain DNA oligonucleotides for hairpin RNA expression, sense and antisense oligos were annealed. The oligonucleotides were dissolved in nuclease free water to a concentration of 3 mg/ml. For the annealing of the oligonucleotides, 1 µl of each 100pmol primer (sh_CCDC50_fw and sh_CCDC50_rev) were added to 48 µl annealing buffer (100nM potassium acetate, 30mM HEPES-KOH (pH=7.4), 2mM Mg-acetate), incubated 4 minutes at 95°C, then incubated 10 minutes at 70°C and subsequently slowly cooled down to 4°C.

2.2.3.9 Phosphorylation of oligos

Next the annealed oligos were phosphorylated by adding 2 µl of the annealed oligos to 1 µl PNK (polynucleotide kinase) buffer, 1 µl 10 mM ATP, 1 µl T4 PNK and 5 µl H_20. This mix was incubated 30 minutes at 37°C. To heat inactivate the PNK enzyme, the complete mix was incubated finally for 10 minutes at 70°C.

2.2.3.10 Ligation

For the ligation of the digested vector pSUPERdL_Zeo with the annealed and phosphorylated oligonucleotides, 2 µl of the latter were added to 1 µl T4 ligase buffer, 50 ng restriction enzyme digested pSUPERdL_Zeo, 5 µl H_20 and 1 µl T4 ligase (200 U). This ligation was incubated for 1 h at RT.

2.2.3.11 Transformation in competent bacteria

One Shot® TOP10 chemically competent *E.coli* (Invitrogen, Karlsruhe, Germany) was used to amplify plasmid DNA. The transfer of plasmids into bacteria requires that the cell membrane is permeable for the plasmids, which is achieved by a short time heat incubation at 42°C. 50 µl of electro-competent *E.coli* were thawed on ice, mixed with the complete ligation reaction and incubated on ice for 30 minutes. For the plasmid uptake, the bacteria were shifted to 42°C for 60 s and briefly equilibrated on ice. 250-300 µl of SOC medium (chapter 2.1.5.2) was added and cells were incubated for 1 h at 37°C while shaking (800 rpm). The suspension was plated onto LB-agar plates containing the respective antibiotic. LB plates were incubated over night at 37°C.

2.2.3.12 Primer design

Genomic DNA PCR primers were designed with the software tool “Fast PCR, 5.4 Professional” (Institute of Biotechnology, Helsinki, FL). To avoid conformation of primer dimers, it was insured that the 3’ end of the forward primer and the 3’ end of the reverse primer were not able to hybridize by homologous base pairing. The 5 first and 5 last residues of each primer should contain 2-3 G- or C-residues; if possible the last residue at the 3’ end should also be G or C to ensure a stable start position for the

enzyme. To avoid false primer annealing, stretches of more than 4 residues of the same nucleotides were excluded.

2.2.3.13 PCR reaction

Cyclic reaction series of denaturation, reannealing of forward and reverse primer and polymerization with a thermostable DNA polymerase allow the in vitro amplification of DNA (Saiki *et al.,* 1988). A PCR reaction contained: 150 ng DNA template, 5 µl of 1 pmol/µl forward primer, 5 µl of 1 pmol/µl reverse primer, 2 µl dNTP-mix (2.5 mM each), 2.5 µl 10xRB buffer (160mM $(NH_4)_2SO_4$; 670mM Tris-HCl (pH 8.8); 0.1% Tween-20), 2 µl of 1 pM DMSO, 1 µl (5Units) EuroTaq DNA polymerase (EuroClone, Siziano, Italy). The mixture was filled up with ddH_20 to a volume of 25 µl. Cycling reactions were 94°C for 5 minutes; 35 cycles of 94°C for 45s, 55°C for 45s, 72°C, for 45 s, 72° for 7 minutes, hold at 4°C. A minimum of 5 µl of the PCR reaction was analyzed on an agarose gel.

2.2.3.14 PCR purification and gel extraction

PCR product purification was performed using the QIAquick PCR Purification Kit according to the manufacturer´s protocol (Qiagen, Hilden, Germany). In cloning approaches, the restriction digested vector was separated in a 1% agarose gel and stained in with ethidium bromid for 5 minutes at RT. Under 254 UV nm light, vector and insert bands were carefully cutted out and extracted from the agarose gel using the QIAquick Gel Extraction Kit according to the manufacturer´s protocol (Qiagen, Hilden, Germany).

2.2.3.15 Sequencing

Sequencing of DNA was performed according to the Dideoxy-Sequencing method shown by Sanger (Sanger *et al.,* 1977). The reaction mix contained fluorescent labled dideoxy-derivates for all of the four nucleotides (Rosenblum *et al.,* 1997). Due to initial denaturation steps during the reaction, sequencing of dsDNA is possible. The sequencing reaction was done according to the manufacturer´s protocol using the PRISM Big DyeDeoxy Terminator Cycle Sequencing Kit. The reaction contained an initial denaturation step for 2 minutes at 96°C and 25 cycles of 5 s at 96°C, 10 s at 55°C, and 4 minutes at 60°C. After this reaction the samples were precipitated at RT with 2.5 Vol 100% ethanol and 1/10 Vol 3M NaAc, washed with 70% ethanol, dried and resuspended in 10 µl formamide. Fragment separation and detection via laser induced excitation of the fluorescently labeled dideoxynucleotides was performed using an ABI3100 capillary DNA sequencing apparatus (Applied Biosystems, Forster City, USA)

2.2.3.16 qRT-PCR Primer design

PCR primer for quantitative real-time PCR experiments were designed with the Primer design tool from Roche Applied Science: 'universal probe library' (https://www.roche-applied-science.com/sis/rtpcr /upl/index.jsp?id=UP030000). Primer pairs were chosen to include at least one intron sequence in order to avoid product amplification resulting from DNA contamination of the RNA template.

2.2.3.17 Synthesis of cDNA

Reverse transcription is the transcription of RNA into single strand complementary DNA (cDNA). For a final volume of 20 µl cDNA solution, 1 µg of total RNA (in 8µl) was used together with 2 µl of 5x 1st strand buffer (250 mM Tris-HCl, pH 8.3, 375 mM KCl, 15 mM $MgCl_2$) and 1 µl (10 units) DNAseI and incubated for 20 minutes at RT to allow genomic DNA digestion. 3 µl of a Master Mix1, which contained equal parts of 25mM EDTA, dNTP mix (10mM dNTP´s each), and 300 ng/µl random hexamer primer, were added to the mix and incubated in a thermo cycler for 10 minutes at 65°C and for 10 minutes at 25°C. This step removed secondary structures and allowed the annealing of primer to the RNA. After adding of 5 µl of a master mix 2 containing 5x 1st strand buffer, 0.1 M DTT and nuclease free water at a ratio of 2:2:1, the temperature was shifted to 42°C for 2 minutes before adding 1µl of reverse transcriptase and 0.2 µl of T4 gene P32 protein. After the reverse transcription reaction for 50 minutes at 42°C, the enzyme was inactivated for 10 minutes at 95°C.

2.2.3.18 Real-Time PCR analysis

The PCR reaction mixtures consisted of 6 µl SYBR Green mixture, 100nM forward and reverse primer, respectively, and 2 µl cDNA template in a reaction volume of 12 µl (Korz *et al*., 2002). A standard curve consisting of a dilution series of the 'Stratagene qPCR human reference' cDNA (1:1, 1:2, 1:4, 1:8, 1:16, 1:32, 1:64, 1:128), was used to determine the efficiency of the PCR reaction. To quantify cDNA templates obtained from RNA samples real-time PCR was performed in a 7900 HT Fast Real-Time PCR System (Applied Biosystems, Forster City, USA) with the following settings: 30 minutes at 37°C, 95°C for 15 minutes, then 40 cycles of 15 seconds at 95°C, 10 seconds at 60°C, 60 seconds at 72°C. Final steps comprized 15 seconds at 95°C, 15 seconds of 60°C, and 15 seconds at 95°C. The heating ramp between the last two steps was increased to 20 minutes to obtain a melting curve of the final RQ-PCR products. This is necesarry because SYBR Green fluorescence products may also be derived from side products such as pimer dimers. Calculation of efficiency and relative quantification was performed in correlation to the housekeeping genes (PGK, DCTN2). Individual samples were always measured in triplicates to ensure reliability.

2.2.4 Expression arrays

2.2.4.1 Probe Labeling and Illumina Sentrix BeadChip array Hybridization

Biotin-labeled cRNA samples for hybridization on Illumina Human Sentrix-6 BeadChip arrays (Illumina Inc., San Diego, USA) were prepared according to a modified protocol of Illumina's recommended sample labeling procedure. Briefly, 250 ng total RNA was used for complementary DNA (cDNA) synthesis, followed by an amplification/ labeling step (in vitro transcription) to synthesize biotin-labeled cRNA according to the MessageAmp II aRNA Amplification kit (Ambion Inc., Austin, TX). Biotin-16-UTP was purchased from Roche Applied Science (Penzberg, Germany). The cRNA was column purified according to TotalPrep RNA Amplification Kit (Ambion, Austin, USA) and eluted in 60 µl of water. The quality of cRNA was controlled using the RNA Nano Chip Assay on an Agilent 2100 Bioanalyzer and spectrophotometrically quantified by the NanoDrop device (NanoDrop, NanoDrop Technologies, San Diego, USA). Hybridization was performed at 58°C, in GEX-HCB buffer (Illumina Inc., San Diego, USA) at a concentration of 50 ng cRNA/µl, unsealed in a wet chamber for 20h. Spike-in controls for low, medium and highly abundant RNAs were added, as well as mismatch control and biotinylation control oligonucleotides. Microarrays were washed twice in E1BC buffer (Ambion Inc., Austin, TX) at room temperature for 5 minutes. After blocking for 5 minutes in 4 ml of 1% (w/v) Blocker Casein in phosphate buffered saline Hammarsten grade (Pierce Biotechnology Inc., Rockford, IL), array signals are developed by a 10-minutes incubation in 2 ml of 1 µg/ml Cy3-streptavidin (Amersham Biosciences, Buckinghamshire, UK) solution and 1% blocking solution. After a final wash in E1BC buffer (Ambion Inc., Austin, TX), the arrays were dried and scanned.

2.2.4.2 Scanning and data analysis

Microarray scanning was done using a Beadstation array scanner, setting adjusted to a scaling factor of 1 and PMT settings at 430. Raw data extraction was done using the beadarray R package (svn release 1.7.0) from bioconductor.org. Next, outliers were removed when their expression value dropped below a threshold: the median + *MAD (median absolute deviation) expression of all negative control beads. Individual bead types were also flagged as filtered when their bead replicate count dropped below 17. All data was then used for the mean expression value calculations within beadarray. Finally, we discarded a bead type when the bead type's filter flag was set across all samples. Data analysis was done by variance stabilizing and robust spline normalization of the remaining signals using the algorithms from lumi R package (release 1.1.0 from bioconductor.org). Subsequently, values of different time points were subtracted from values of the time point zero and related negative controls. The thresholds for individual samples were determined by calculating the median value of all values within one

sample and subtracting or adding the 1.5-fold standard deviation from each median value. Differentially regulated genes were defined by values higher (upregulated) or lower (downregulated) than each threshold.

2.2.5 Southern blot analysis

2.2.5.1 Digestion of genomic DNA with restriction enzymes and gel electrophoresis

For Southern blot analysis, $2x10^7$ cells were centrifuged (1000 rpm, 10 min, RT) and genomic DNA was isolated using the Blood & Cell Culture DNA Midi Kit (Qiagen) according to the manufacturer´s protocol. DNA quality was tested on a 1% TBE agaraose gel and the concentration measured by the NanoDrop device (NanoDrop Technologies, San Diego, USA) was compared to human genomic DNA standard on an agarose gel (Roche, Mannheim, Germany). 10 µg DNA was digested over night with 100 U of appropriate restriction endonucleases. Enzymes were finally heat inactivated at 65°C for 20 minutes. Digested genomic DNA and a molecular weight marker were separated on a 0.8% TBE agarose gel (15x17 cm) at 85V for 5 hours or 40V over night. Afterwards, the DNA was stained by soaking the gel for 5 minutes in 1 µg/ml ethidium bromide solution at RT. Images were taken with the digital camera device of the Gel Documentation System.

2.2.5.2 Southern blot procedure

To depurinate the DNA prior to transfer, the gel was soaked for 10 minutes at room temperature in 250 mM HCl. To denature the DNA in the gel, it was submerged in denaturation solution (0.5M NaOH, 1.5M NaCl) for 2 x 15 minutes at RT with gentle shaking, then rinsed with sterile, double distilled water and finally submerged in neutralization solution (0.5 M TrisHCl, 1.5M NaCl) for 2 x 15 minutes at RT. Before blotting, the gel was equilibrated for at least 10 minutes in 20x SSC. The transfer was performed over night. The wet membrane was finally exposed to UV-light using the UV-Stratlinker (Stratagene, La Jolla, CA), which cross-linked the DNA to the membrane.

2.2.5.3 Generation of a DIG-labeled probe

The DIG-labeling method is based on a steroid isolated from digitalis plants (*Digitalis purpurea* and *Digitalis lanata*). Hybridized DIG-labeled probes may be detected with high affinity anti-digoxigenin (anti-DIG) antibodies that are conjugated to alkaline phosphatase. The Southern blot probe was generated by restriction digestion of the pGK511TKneoP vector with the restriction endonucleases *Bgl*II and *NcoI*, generating a 1.7 kb insert and a 3.6 kb vector backbone. The digestion was analyzed on a 1% TBE agarose gel and the 1.7 kB insert was cut out of the gel and purified using the Qiaquick

Gel Extraction Kit (Qiagen, Hilden, Germany). In the random primed labeling reaction (DIG high prime, Roche, Mannheim, Germany), a Klenow enzyme copies the 1.7 kB TKneo template in the presence of hexameric primers and alkali-labile DIG-11-dUTP. On average, the enzyme inserts one DIG moiety in every stretch of 20-25 nucleotides. The resulting labeled product is a homogeneously labeled, sensitive hybridization probe (can detect as little as 0.10 – 0.03 pg target DNA).

2.2.5.4 Radioactive labelling

The 1.7 kb TKneo DNA probe was diluted to a concentration of 50ng in 6µl nuclease-free water and denaturated by heating at 90°C for 5 minutes. Then the probe was directly chilled on ice, and 3 µl dNTP (0.2 mM each), 2.5 µl 10x Bca buffer (Ladderman Labeling Kit, Takara Bio Europe) and 6 µl H_20 were added. Immediately before adding radioactivity, 1 µl (2 Units) of the Bca-polymerase was added following addition of 2.5 µl α^{32}P dATP and 30mM EDTA. The whole mixture was incubated 1h at 50°C. In order to clean the probe, 80 µl TE was added and loaded on a pre-equilibrated spin column (Pharmacia, MicroSpin column S-200HR). Centrifugation was performed for 2 minutes at 3000 rpm. The eluate was recovered. The incorporation of the radioactivity was checked by counting the labeled probe using a Scintillation Counter versus the probe with non-incorporated nucleotides. After denaturation of the labeled probe by heating at 95°C for 10 minutes, the probe was placed directly on ice, centrifuged and used for hybridization of the Southern blot membrane.

2.2.5.5 Probe hybridization and blot development

For pre-hybridization the membrane was placed in a glass tube containing 10 ml pre warmed (62°C) hybridization buffer (5xSSC, 0.1% N-lauroylsarcosine, 0.02% SDS, 1% Blocking Solution) and incubated by rotating for 2h at 62°C in a hybridization oven. The labeled probe was heated for 10 minutes at 95°C and directly added to 10 ml of fresh pre-warmed hybridization buffer. The pre-hybridization buffer was replaced quickly by the probe-containing hybridization buffer in order to avoid drying of the membrane. The latter was incubated by rotation over night at 62°C. The membrane was subsequently washed with low strigency buffer (2x SSC, 0.1% SDS) for 2x5 minutes, incubated by rotating for 2x15 minutes with pre-warmed (62°C) high-stringency buffer (0.5x SSC, 0.1% SDS), washed for 2 minutes with DIG-Wash (DIG I , 0.3% Tween 20) and blocked afterwards for 30 minutes in DIG II buffer (10 ml 10x Blocking , 100 ml DIGI). The DIG-antibody (Roche, Mannheim, Germany) was used for detection of DNA fragments, which the digoxigenin-labeled probe bound specifically. The antibody was diluted 1:10000 in blocking solution and incubated by shaking for 30 minutes at RT. The membrane was finally washed 3x5 minutes with DIG III buffer (0.1 M NaCl, 0.05M $MgCl_2$, adjust to pH 9.5 using 1M Tris-HCl pH=9.5). Immediately after substrate addition, CDP-Star generates

a luminescent signal. The membrane was placed in a plastic foil to prevent drying and then placed in a dark developing cassette and exposed to an X-ray film. Using DIG-labeled probes, the film exposure time was between 1-15 minutes. When applying radioactively labeled probes, the film exposure time was one week.

2.2.6 Western blot analysis

2.2.6.1 Protein quantification

For quantification of protein concentrations the enzymatic Biruet reaction was used, where proteins reduce Cu^{2+} ions to monovalent Cu^{+} ions in alkaline medium. Biuret reaction was performed with copper-(III)-sulfate and bicinchoninic acid (1:50 copper-(III)-sulfate : bicinchoninic acid). 10 µl of protein solution was added to 200 µl of reaction mixture, incubated at 37°C for 30 minutes and then determined using the NanoDrop reader at 550 nm wavelengths. Standard curves were performed by measuring BSA standard amounts ranging from 10 ng/µl to 2 µg/µL.

2.2.6.2 Western blot procedure

For SDS-PAGE, gel solutions with 10% acrylamide in the resovling part and 5% in the stacking part were prepared. 30% Ammonium Persulphate (APS) and 0.001% N,N,N´,N´-tetramethylethylendiamine (TEMED) were added to the gel solution to induce polymerization. Transfected B-CLL cells and cell lines were harvested by centrifugation (800 rpm, 10 min, RT). Cell pellets were lysed and column purified to isolate both RNA and protein from the same sample applying the All Prep RNA / Protein Kit (Qiagen). Protein samples were boiled in Laemmli buffer for 5 minutes and subsequently loaded into the slots of the gel. In addition a protein size maker (Spectra multicolor broad range protein ladder, Fermentas, St. Leon Rot, Germany) with 1x laemmli buffer was loaded into a slot of the gel. Electrophoresis was applied for 45 minutes at 160V and 70mA. The electrophoretic transfer of polypeptides from polyacrylamide (PAA) gel to a polyvinylidene floride (PVDF) membrane was performed by using a wet gel transfer apparatus. The PVDF membrane was briefly activated in 100% methanole and soaked for 5 minutes in Western blot buffer (25 mM Tris-Base, 192 mM Glycin, 20% v/v Methanol) for 10 minutes. The PAA gels were carefully removed from the electrophoresis chamber, the stacking gel was cut and the gel was soaked 3 minutes in Western blot buffer. The Western blot ‘sandwich’ was assembled and the transfer was carried out for 2h at 100V and 250mA in ice-cold buffer. For protein detection with antibodies, the membrane containing the separated polypeptides were placed in a tank and washed with washing buffer (15 minutes) following soaking in blocking buffer (1h) at RT. After blocking, the membrane was again washed (3x15 minutes) and the diluted primary antibody was added over night at 4°C. After washing (3x15 minutes) the membrane was incubated

with the secondary antibody conjugated with horse radish peroxidase for 1h at RT. While washing (3x15 minutes) the membrane, the ECL chemilumescent substrate was prepared (ECL Western Blot Detection Kit). Following incubation of the membrane with the ECL solution for 1 minute in the dark at RT, the solution was drained off. The membrane was placed in a plastic foil to prevent drying and then placed in a dark developing cassette and exposed to an ECL film. The exposure time of the film was between 10 seconds and 10 minutes.

2.2.7 Fluorescence *in situ* hybridization

Fluorescent *in situ* hybridization (FISH) is a cytogenetic technique that is used to detect and localize the presence or absence of specific DNA sequences on chromosomes. For preparation of probes, nick translation and PCR with labeled nucleotides was used. Metaphase chromosomes were firmly attached to glass slides, where repetitive DNA sequences were blocked by addition of CotI DNA to the sample. Finally the nick translated DNA probe was applied to the chromosomal DNA on the slide and binds to those parts of the chromosome to which they show a high degree of sequence similarity. Afterwards, fluorescence microscopy is used for the detection of the probe that is hybridized to a specific chromosome (Lichter and Ried, 1994).

2.2.7.1 Generation of FISH probes

Nick-translation is a conventional method for the generation of labeled DNA probes. DNA is incubated with a limited amount of DNaseI which introduces on the one hand single strand breaks (i.e. “nicks”) into the DNA, on the other results in limited double strand breaks in order to generate short DNA fragments. The enzyme DNaseI generates free 3’- and 5’-ends of DNA, which are necessary for DNA polymerase action. The latter enzyme is also included in a nick translation reaction, because it mediates the incorporation of labeled nucleotides into the DNA sequence. In nick translations, template DNA sequences are used to generate short labeled DNA probes for FISH, carried out by the combined action of DNaseI and DNA polymerase. DNaseI, DNA polymerase digestion and labeling of template DNA was allowed for at least 1 h at 15°C in a 100 µl reaction volume including 10 µl NEB2 buffer (New England Biolabs), 10 µl of the fluorophores, 10 µl of 0.1x β-mercaptoethanol, 4 µl of DNA-polymerase (1 U/µl) and 4 µl of 1:10.000 diluted DNAseI (10 U/µl). To control digestion efficiency, the DNA was denatured for 2 minutes at 100°C and analyzed by agarose gel electrophoresis. The DNA-fragments can be further used as probes if they are digested to a size of around 300-600 bp. DNAseI was inactivated by addition of 2 µl 0.5 M EDTA and 1 µl 10% SDS and incubation at 68°C for 10 minutes. Finally, the remaining enzymes and buffers were removed and DNA probes were isolated by custom prepared sephadex-columns. These

columns were filled with glass wool soaked with sephadex buffer, which is prepared by 30 g sephadex-G50 in 500 ml 1x column buffer. The probes were applied to the prepared sephadex-columns and centrifuged for 5 minutes at 2300 rpm. Sephadex columns allow rapid and convenient separation of nick-translated DNA from unlabeled nucleotides and similar separations by the process of gel filtration. Molecules larger than the largest pores in the matrix are excluded from the matrix and elute first. Intermediate size molecules penetrate the matrix to varying extents, depending on their size. After eluation the FISH-probes were transferred to fresh tubes and stored at -20°C until further use.

2.2.7.2 Generation of metaphase chromosomes

Colcemid is a derivative of colchicine and is commonly used to arrest mitosis, causing the dividing cells to accumulate in metaphase. In order to prepare metaphase chromosomes, cultured cell lines were arrested in their cell cycle by addition of 0.6% (v/v) colcemid and incubation for 70 minutes at 37°C and 5% CO_2. Colcemid was removed by centrifugation at 1000 rpm and subsequent removal of the supernatant. Cell pellets were carefully resupended in 12 ml pre-warmed 1x hypotonic buffer to swell the mitotic cells and incubated at 37°C for 30 min. The hypotonic buffer was removed by gentle centrifugation at 860 rpm at RT for 10 min. The supernatant was discarded and pellets were carefully resuspended in 2 ml of fixative, which was freshly prepared by combination of methanol and acetic acid in a 3:1 ratio. These prepared metaphase chromosomes were incubated for at least 30 minutes to a maximum of 4 h at -20°C followed by gentle centrifugation at 860 rpm and RT for 5 min. Then, pelleted metaphase chromosomes were washed with fixative and centrifuged as described above for three times, before they were carefully resuspended in 2 ml of the fixative. Glass slides were prepared prior to metaphase dropping by incubation for 5 minutes in absolute ethanol and subsequent 2x1 minute washing in ddH_2O to prepare a homogenous surface. Single drops of the metaphase cells pipetted on the slide were by using a glass pipette. The pre-fixed metaphase chromosome slides were dehydrated by incubation in increasing ethanol concentrations (70%, 90%, and 100%) for 5 minutes each and finally air dried.

2.2.7.3 FISH on metaphase chromosomes

For the removal of cytoplasm, nuclear membranes and cell membranes, and to enhance hybridization with the probe, treatment of the metaphase slides with pepsin was performed. Pepsin digestion of the metaphase chromosomes was carried out by incubation of the slides in 0.01 N HCl including 1 mg/ml pepsin at 37°C for 3 minutes. Residual pepsin or HCl was washed away by incubation in 1x PBS for 10 minutes. Subsequently, slides were post-fixed in 1x PBS containing 10% (v/v) PFA for 5 minutes at

4°C and washed again in 1x PBS for 10 minutes. Another step of dehydration in increasing ethanol concentrations (70%, 90%, 100%) at RT was followed by air-drying of slides for 10 minutes and final incubation at 63°C for 20 minutes. In order to denature the DNA fixed on the slides, they were incubated in denaturation solution for 2 minutes and 10 seconds at 65°C. Prior to application of the respective probes, a third dehydrating dilution series with 70%, 90% and absolute ethanol for 5 minutes in each dilution at 4°C was carried out. Centromere probes for chromosomes were precipitated together with 7 µl salmon sperm DNA (10 mg/ml) in 1/20 volume 3 M NaAc and 2.5 volumes absolute ethanol for 30 minutes at -80°C. Locus probes for chromosomes were precipitated together with 10 µl human CotI (1 µg/µl) DNA and 0.7 µl salmon sperm DNA in 1/20 volume 3 M NaAc and 2.5 volumes absolute ethanol for 30 minutes at -80°C. The probes were precipitated by centrifugation at 13.000 rpm and 4°C for 20 minutes, washed with 70% ethanol and finally dried for 10-15 minutes at 37°C. In order to denature the probe-DNA, 5 µl/slide de-ionized formamide and 5 µl/slide HybMix buffer (see material) were added to the probe, which then was incubated at 75°C for 6 minutes. After short incubation at 4°C the denatured single-stranded probe DNA was applied to the denatured single-stranded DNA on the slides, which were incubated overnight at 37°C in a humid chamber to allow hybridization. Hybridized slides were washed in WashA buffer (see material) at 42°C for 10 minutes and 3x5 minutes. After each incubation step the buffer was changed. The hybridized slides were incubated 3x5 minutes at 42°C in pre-warmed WashB buffer (see material). Prior to probe-detection the single stranded DNA on the slides was blocked in blocking buffer for 30 minutes at 37°C in a humid chamber. Successful hybridization of the probe was detected by addition of detection buffer (see material), FITC binds to avidin and DIG binds to antiDig-Rhodamin. The slides were incubated for 30 minutes at 37°C in the humid chamber. Unbound dyes and detection buffers were removed with WashC buffer 3x5 minutes at 42°C. The nuclei were stained with DAPI, which was contained in the mounting medium (Vectashield). The results were visualized and quantified using a fluorescence detecting microscope that was capable of exciting the dyes.

2.2.8 Functional assays

2.2.8.1 Dual-Luciferase Reporter assay

Genetic reporter systems are widely used to study regulation of eukaryotic gene expression. The term ‘dual’ refers to the simultaneous expression and measurement of two individual reporter enzymes within a single system. The experimental reporter (firefly luciferase) is correlated with specific experimental conditions, while the activity of the co-transfected ‘control’ (renilla luciferase) provides an internal control that serves as a baseline for transfection efficiency. Normalizing the activity of the firefly luciferase

to the activity of the renilla luciferase minimizes experimental variability caused by differences in cell viability or transfection efficiency. The firefly luciferase plasmid containing six binding sites for *NFkB* (Bergmann *et al.,* 1998) and the renilla luciferase plasmid were given to us as generous gifts from Dr. Mathas of the division of Prof. Doerken at the Max-Delbrueck Center in Berlin. A total of $4x10^5$ HEK-293T cells were transfected with 1.25 µg of the plasmid, coding for the gene of interest or 50nM of the siRNA of interest using the TransIT transfection reagent. In addition the two reporter plasmids (0.83 µg of the firefly plasmid containing the 6 *NFkB* binding sites and 0.42 µg of the renilla plasmid) were co-transfected. After 24h, NFκB activity was induced by adding 50 ng/ml TNFα to the cells. Immediately (0h), 3h, and 6h after TNFα induction, *firefly* and renilla luciferase activities were assayed using a Dual-Luciferase Reporter System (Promega, Madison, USA) and a luminometer (LB-940 Mithras Multilabel Reader, Berthold Technologies, Bad Wildbach, Germany). Transfected cells grown in a 6-well plate were centrifuged for 10 minutes at 1000 rpm at RT. Cell pellets were lysed with 65 µl of 1x passive lysis buffer (Promega) for 15 minutes at RT on a shaker (310 rpm). 15 µl of each lysate was pipette into a reader plate of the luminator in triplicates. The firefly luciferase activity was measured by adding 100 µl of LAR II reagent (Promega) to generate a stabilized luminescent signal. After quantifying the firefly luminescence, this reaction is quenched and the renilla luciferase reaction is initiated by adding 100 µl of Stop- and Glo reagent to the same tube. The Stop- and Glo reagent (Promega) produces a stabilized signal of the renilla luciferase, which is measured in the luminometer. After normalizing the firefly luciferase activity to the renilla luciferase activity, a direct comparison of samples regarding NFκB activity in the nucleus is possible.

2.2.8.2 Cell Viability assay

The proliferation of the transfected cells was assayed by Cell Titer Glo Luminescent Cell Viability Assay (Promega, Madison, USA) in opaque-walled multiwell plates (Costar, Baar, Germany). At 24h, 48h, and 72h after nucleofection, an aliquot of 100 µl suspension cells was assayed for its ATP content according to the maufacturer´s protocol. Each assay was performed in triplicate. An integration time of 0.3 second per well was used.

2.2.8.3 Fluorescence Activated Cell Sorting

Fluorescence activated cell sorting (FACS) is a type of flow cytometry (FCM), a method for sorting a suspension of cells into several fraction. Cells labeled with fluorescent dyes like propidium iodide are detected by emission of specific spectra. The intensity of light emission correlated with the amount of bound, labeled antibodies to specific epitopes on the cell surface.

Before staining, cells transfected by nucleofection were separated from medium by centrifugation (1000 rpm, 10 min) in tubes for FACS analysis. Cells were washed twice

with 1x sterile and cold PBS. $1x10^6$ cells were re-suspendend afterwards in 100 µl of the staining solution PBS:propidium iodide (500:1). Cells were incubated for 15 minutes at RT in the dark and analyzed with FACS. GFP expression after nucleofection was measured by flow cytometry, and transfection efficiency was calculated as percentage of 100% viable cells by excluding propidium iodide positive, i.e dead cells from the analysis. To determine the percentages of B-cells isolated from perpheral blood and purified over MACS columns, MACS preparations were quantified using PE-conjugated monoclonal antibodies specific to CD19 (clone LT19; Miltenyi Biotec) and CD20 (clone LT20; Miltenyi Biotec). All flow cytometry analyses were carried out using a FACS CantoII flow cytometer equipped with BD FACS Diva software (BD Biosciences).

3 Results

In order to identify, modulate, and functionally characterize upregulated candidate genes in MCL and CLL cells, a proper characterization of these cells were performed. Therefore, the utilization of different transfection techniques determined the optimal method and efficiency (chapter 3.1.). Gene expression profiling was suitable to discover a 'hit-list' of potential candidate genes (chapter 3.2). The use of a siRNA sceen could finally uncover those genes with impact on cell survival (chapter 3.3.). Following gene modulations, i.e. transient silencing of the candidate genes in primary cells (chapter 3.4) as well as stable knockdown or overexpression in tumor model cell lines (chapter 3.5), served to validate the impact of candidates in survival stimulating pathways in MCL and CLL cells.

3.1 Transfection of suspension cells

To functionally modulate gene expression, siRNAs and plasmid DNA need to enter the cell with high efficiency. The ability to specifically silence target genes at optimal low concentrations without inducing the interferon response or off-target effects depends on the efficient siRNA delivery and on the siRNA sequence itself. Low transfection efficiency is the most frequent cause of unsuccessful gene silencing experiments (Boutros *et al*., 2008; Zumbansen *et al*., 2008). Since MCL and CLL cells belong to the group of 'difficult-to-transfect' B-cells, determination and optimization of transfection efficiency was established in order to perform functional studies.

3.1.1 Optimization of transfection efficiencies

The non-viral introduction of recombinant DNA into cultured cells (transfection) has become an essential tool for studying gene function and regulation. Transfection technologies include chemical and lipid-mediated reagents or physical introduction through microinjection and electroporation. (1) Lipofection is a technique used to introduce genetic material into a cell by means of liposomes. It belongs to biochemical methods including also polymers, DEAE dextran (Diethylaminoethyl cellulose), and calcium phosphate. The main advantages of lipofection are its high efficiency, its ability to transfect all types of nucleic acids in a wide range of cell types, its ease of application, reproducibility and low toxicity. (2) Microinjection refers to the process of using a very fine needle to insert substances at a microscopic or borderline macroscopic level into a single living cell. (3) Nucleofection is a combination of chemical transfection and

electroporation that enables efficient and reproducible transfer of nucleic acids such as DNA, RNA and siRNA into hardly accessible cells. As DNA transfected by nucleofection can directly enter the nucleus, very high transfection efficiencies can be obtained (Gresch *et al*., 2004; 2006; Seiffert *et al*., 2007). MCL and CLL cell lines were either transfected via nucleofection and Superfect using a small GFP plasmid (pmaxGFP) or via RNAiFect, Dharmafect and X-tremeGENE using a Cy3-labeled siRNA (Figure 9). Moreover, transfection has been performed using the chemical reagents HiPerFect, Oligofectamine and Geneporter (not shown). Transfection efficiencies were determined by fluorescence activated cell sorting (FACS). The survival rates of cells and the transfection efficiencies after nucleofection are shown in Figure 10.

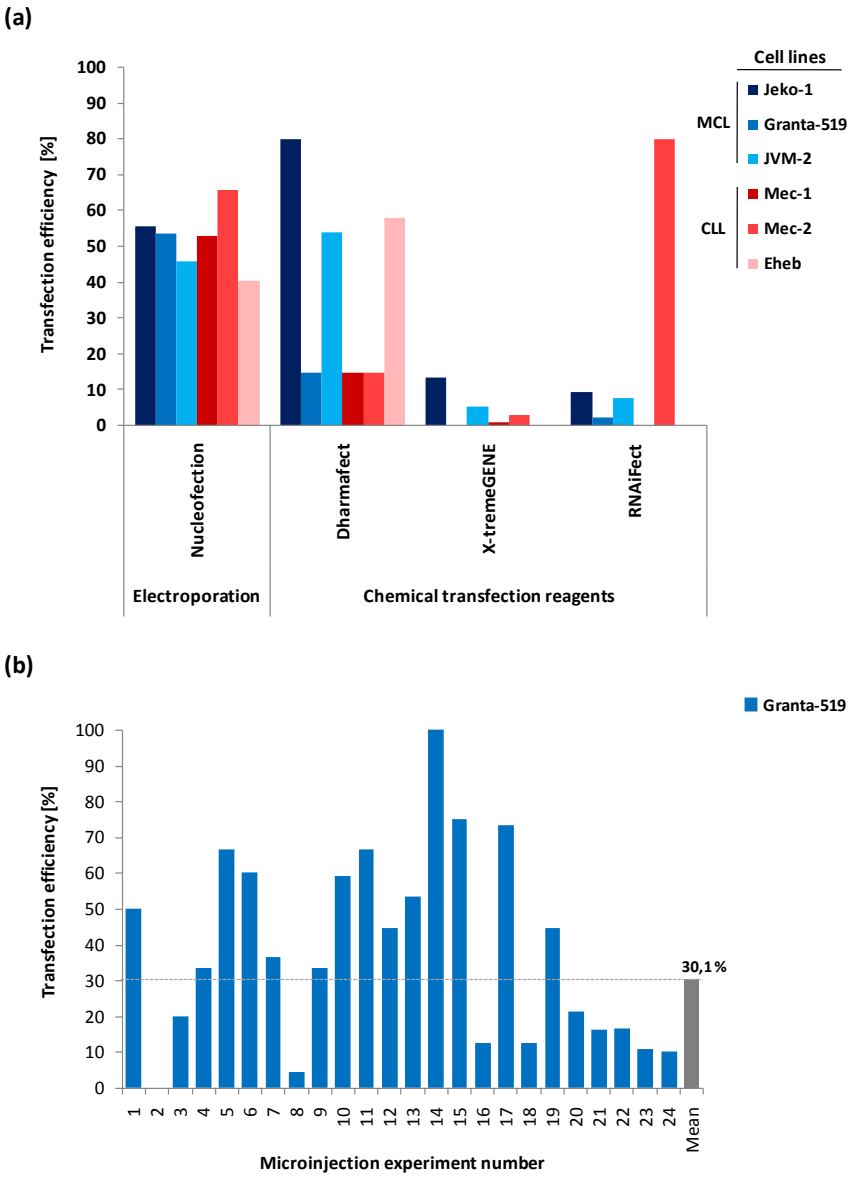

Figure 9: Transfection efficiencies of MCL and CLL cell lines. (a) Comparison of chemincal transfection efficiencies and nucleofection in three MCL (Jeko-1, Granta-519, JVM-2) cell lines and three CLL (Mec-1, Mec-2, Eheb) cell lines determined by FACS. (b) Microinjection of MCL cell line Granta-519. 24 microinjection approaches have been performed with a mean transfection efficiency of 30%, ranging between 0-100%.

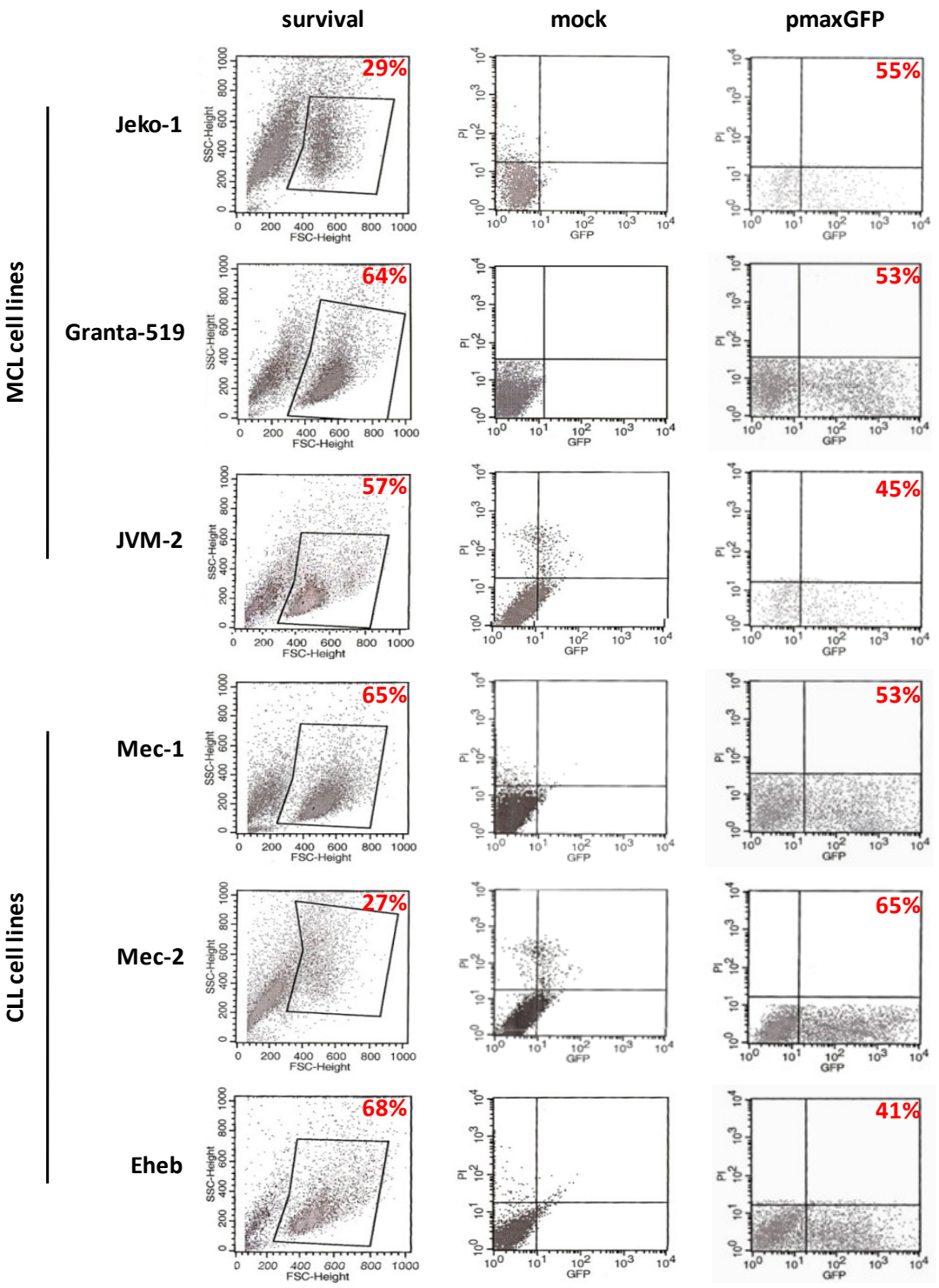

Figure 10: FACS results follwing transfection of the pmaxGFP vector into MCL and CLL cell lines via nucleofection. Surviving cells are highlighted as separate cell population in a black box and the number of surviving cells is shown in percentage for each experiment, respectively ('survival', left columns). Nucleofection without the pmaxGFP plasmid ('mock', central columns) and nucleofection using the pmaxGFP ('pmaxGFP', right columns) have been performed for each cell line using program O-017 and Solution T. The percentage of GFP-transfected, surviving cells are shown in the up-right corner of the appropriate boxes, respectively.

Most of the chemical and lipid-based reagents did not succeed in efficiently transfecting cell lines (true for Superfect, HiPerfect, Oligofectamie, and Geneporter). Dharmafect was a suitable reagent at least for the cell lines Eheb (58%), JVM-2 (53%), and Jeko-1 (80%). Xtremegene showed little overall transfection efficiencies (less than 5%). Transfection with RNAi-fect was successfull in the cell line Mec-2 (80%), but in none of the other cell lines tested. Microinjection of 10-40 individual cells per experiment revealed a median transfection efficiency of 30% (Figure 9) with large variations between individual experiments. Nucleofection resulted in the best and most importantly, overall constant transfection efficiencies between 41-65% (Figure 10). Even though many cells died after electroporation (Solution T, Program O-017), the optimization approach clearly showed most convincing transfection results using nucleofection.

3.1.2 Optimization of nucleofection parameters

As DNA transfected by nucleofection can directly enter the nucleus, very high transfection efficiencies can be obtained even in difficult to transfect cells such as MCL and CLL cell lines or freshly isolated primary CLL cells. One disadvantage of the nucleofection technology is the high percentage of cell death following electroporation. Initial testing for the optimal transfection method was performed using uniform nucleofection conditions: Solution T, Program O-017. In order to determine optimized nucleofection conditions for each cell line individually, MCL and CLL cell lines were transfected with different reagents and electroporation programs. Viable cells expressing GFP were measured 24h post transfection via FACS analysis (Figure 11a-c). A ‘no-program-control’ (NP) indicated the cell death rate, induced by the chemical component of the solution. Transfection approaches without plasmid (‘no GFP’) were performed to determine the influence of nucleofection pulses and the background fluorescence in cells for FACS analysis. For the cell lines JVM-2, Granta-519 and Mec-1 optimal conditions have already been established in our group. Optimal transfection conditions for all cell lines tested are summarized in Figure 11d. Mec-1, Mec-2, Eheb, JVM-2, and Jeko-1 show best transfection efficiencies with Solution V and program X-001. Granta-519 and JVM-2 show optimal transfection efficiencies with Solution T and program O-017. Granta-519 can moreover be electroporated using Solution V and program A-023. In all further transfection studies these optimized nucleofection conditions were applied.

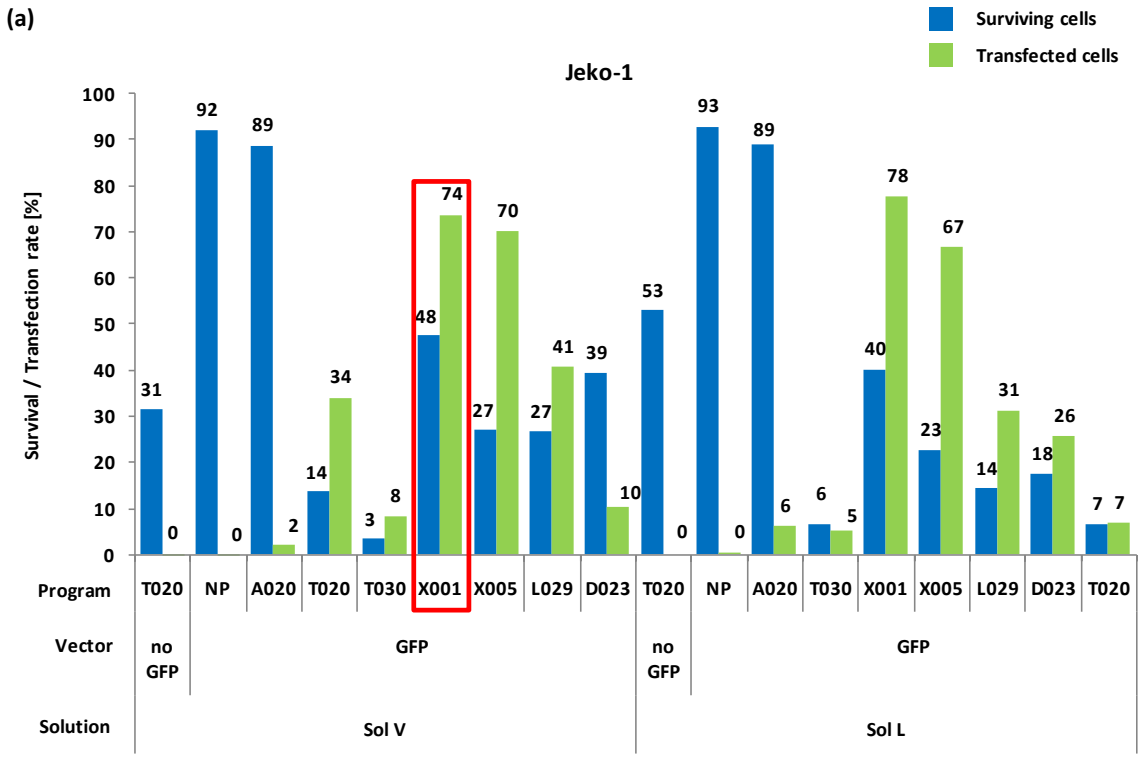
(a)
Surviving cells
Transfected cells
Jeko-1
Survival / Transfection rate [%]
100
90
80
70
60
50
40
30
20
10
0
31 0 92 0 89 2 14 34 3 8 48 74 27 70 27 41 39 10 53 0 93 0 89 6 6 5 40 78 23 67 14 31 18 26 7 7
Program T020 NP A020 T020 T030 X001 X005 L029 D023 T020 NP A020 T030 X001 X005 L029 D023 T020
Vector no GFP GFP no GFP GFP
Solution Sol V Sol L

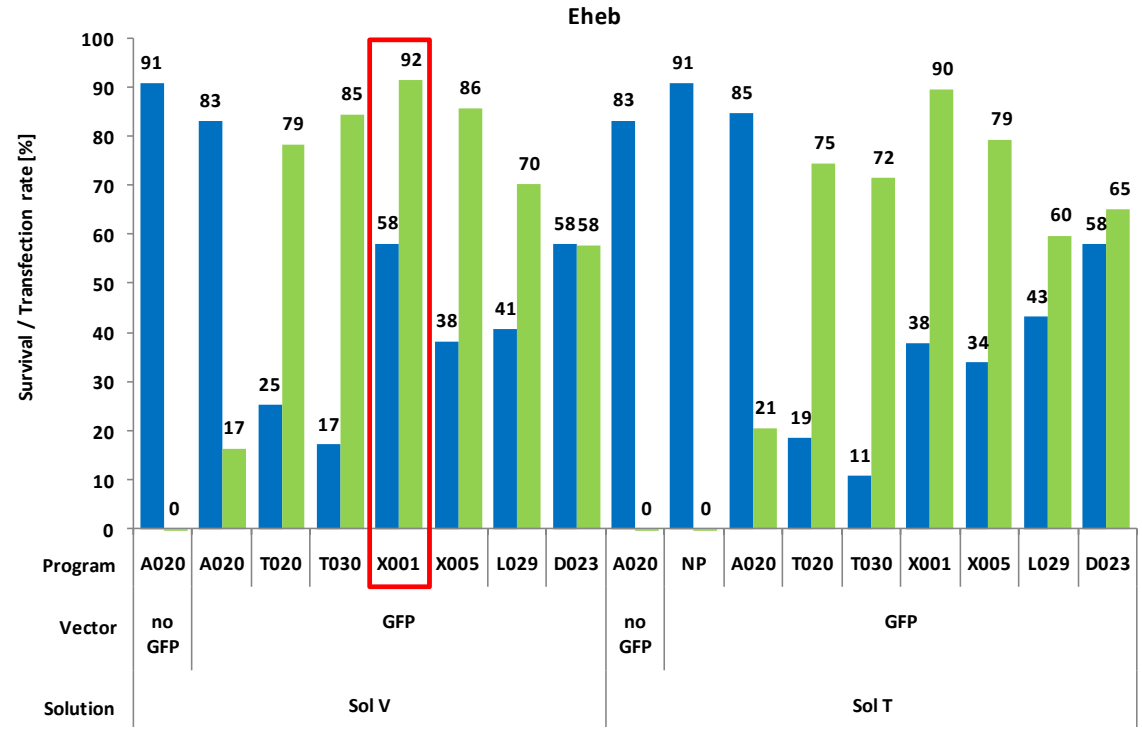
(b)
Eheb
Survival / Transfection rate [%]
100
90
80
70
60
50
40
30
20
10
0
91 0 83 17 25 79 17 85 58 92 38 86 41 70 58 58 83 0 91 0 85 21 19 75 11 72 38 90 34 79 43 60 58 65
Program A020 A020 T020 T030 X001 X005 L029 D023 A020 NP A020 T020 T030 X001 X005 L029 D023
Vector no GFP GFP no GFP GFP
Solution Sol V Sol T

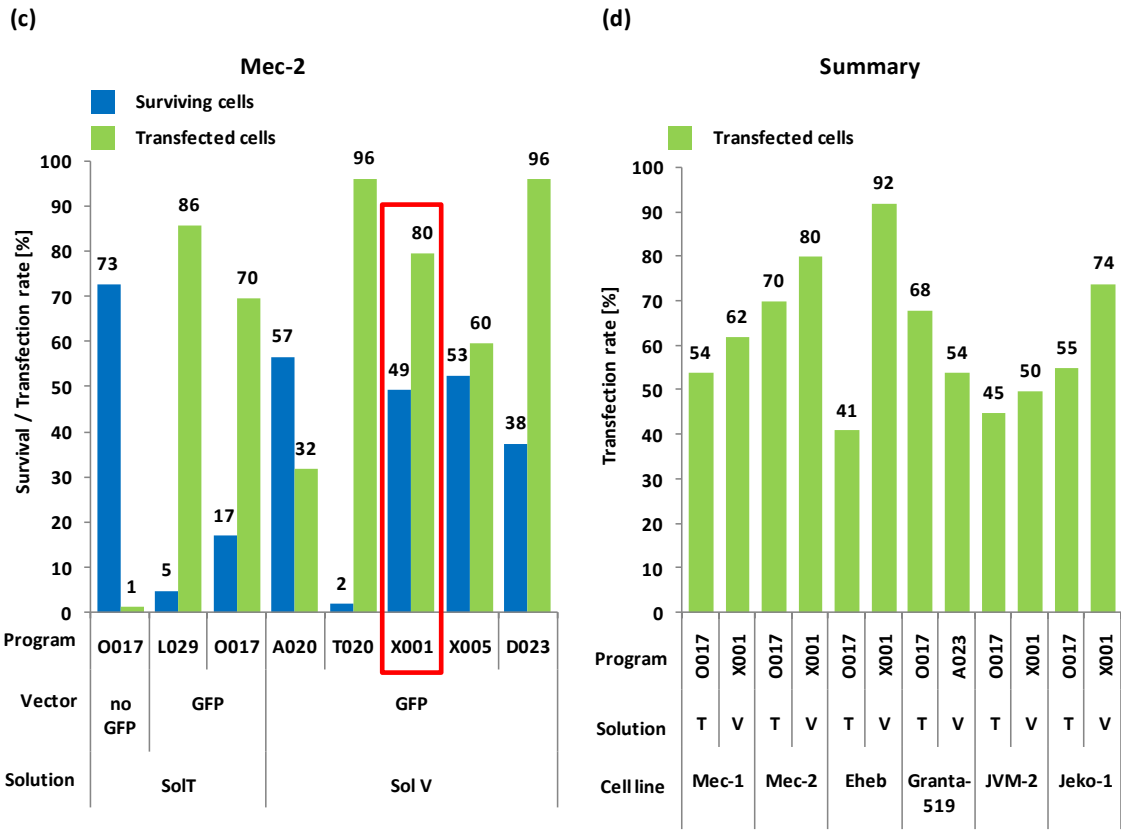

Figure 11: Advanced tranfection optimization using different transfection solutions and electroporation programs of the Lonza system. Transfection optimization is shown for (a) Jeko-1, (b) Eheb and (c) Mec-2 cell lines. Transfection optimization for cell lines Granta-519, Mec-1 and JVM-2 have been tested earlier. (a-c) Blue bars indicate the percentage of surviving cells after transfection. Setting the number of surviving cells to 100%, a certain percentage thereof was GFP transfected as indicated in green bars. The optimal transfection condition for each cell line is highlighted in a red box. (d) Summary of the electroporation programs and solution showing best transfection efficiencies and highest cell survival rates. NP=No Program, Sol=Solution, noGFP=Mock control, cells were pulsed without GFP.

3.1.3 96-well nucleofection of MCL cell lines and primary CLL cells

Based on the well established nucleofection technology, Lonza has developed a 96-well format shuttle approach for siRNA high-throughput screens in primary cells or difficult-to-transfect cell lines. Transfection is performed in a special disposable plate with conductive polymer electrodes that rule out any metal ion contamination. In this 'Nucleocuvette plate' the 96 samples are processed sequentially within three to four minutes, assuring reproducible homogeneous electrical conditions in each sample, thereby excluding plate effects and parameter variances. However, such screenings have so far mostly been limited to easy-to-transfect adherent cell lines. The efficiency of siRNA delivery into the cell needs to be as high as possible, as limits in the effectiveness of delivery lead to a decrease in knockdown. In this study the 96-well shuttle technology was optimized for MCL cell lines JVM-2 and Granta-519 as well as for primary CLL cells.

In MCL cell lines, the three chemical solutions SE, SF, and SG (termed by the company) were tested in combination with 31 different electroporation programs and one electroporation control ('No Program'). The combination of Solution SF with program 96-DN-100 showed best transfection efficiencies in JVM-2 and Granta-519 (Figure 12a,b) which were with 70% and 79% even higher than single cuvette nucleofection (50% and 68%, Figure 9). Transfection results of cell lines using solutions SE and SG are not shown. In primary CLL cells, the primary B-cell solution was tested using 31 electroporation programs and one electroporation control ('No Program'). Freshly isolated human B-cells were transfected with the plasmid pmaxGFP and 24 h later, cells were analyzed by flow cytometry. The overall transfection efficiency in primary CLL cells in this experiment was very low with a maximum efficiency of 16%. The overall comparison revealed 96-DN-100 as the optimal transfection program (Figure 12c).

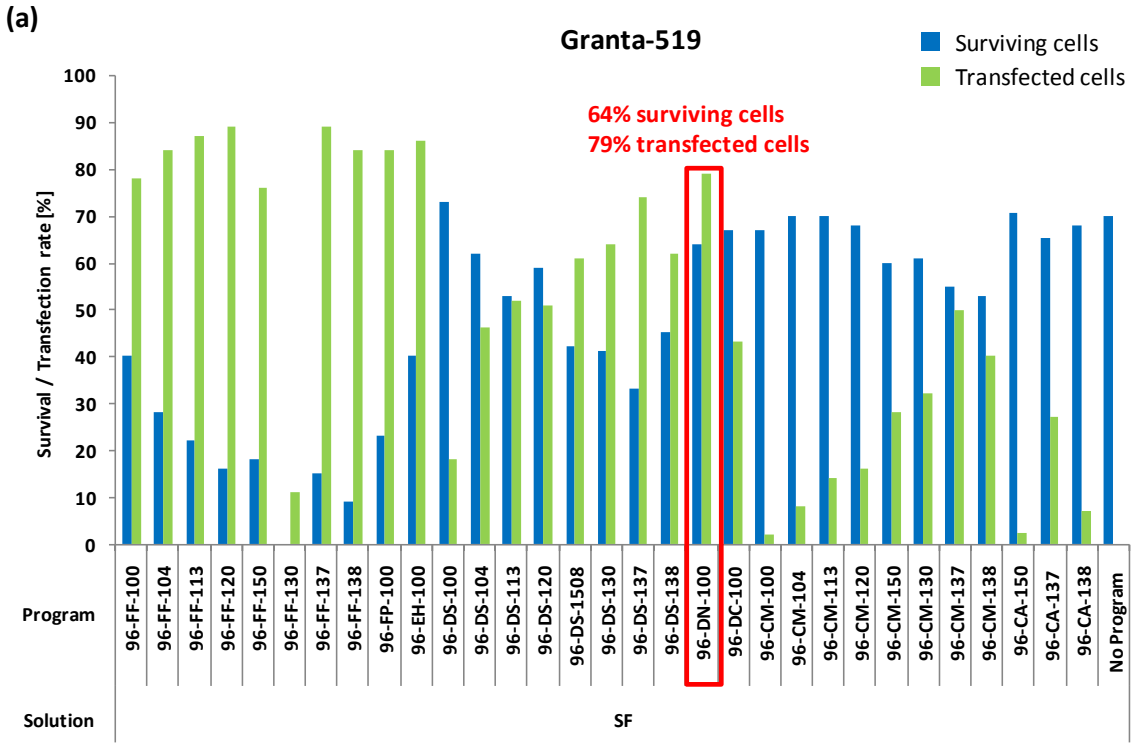

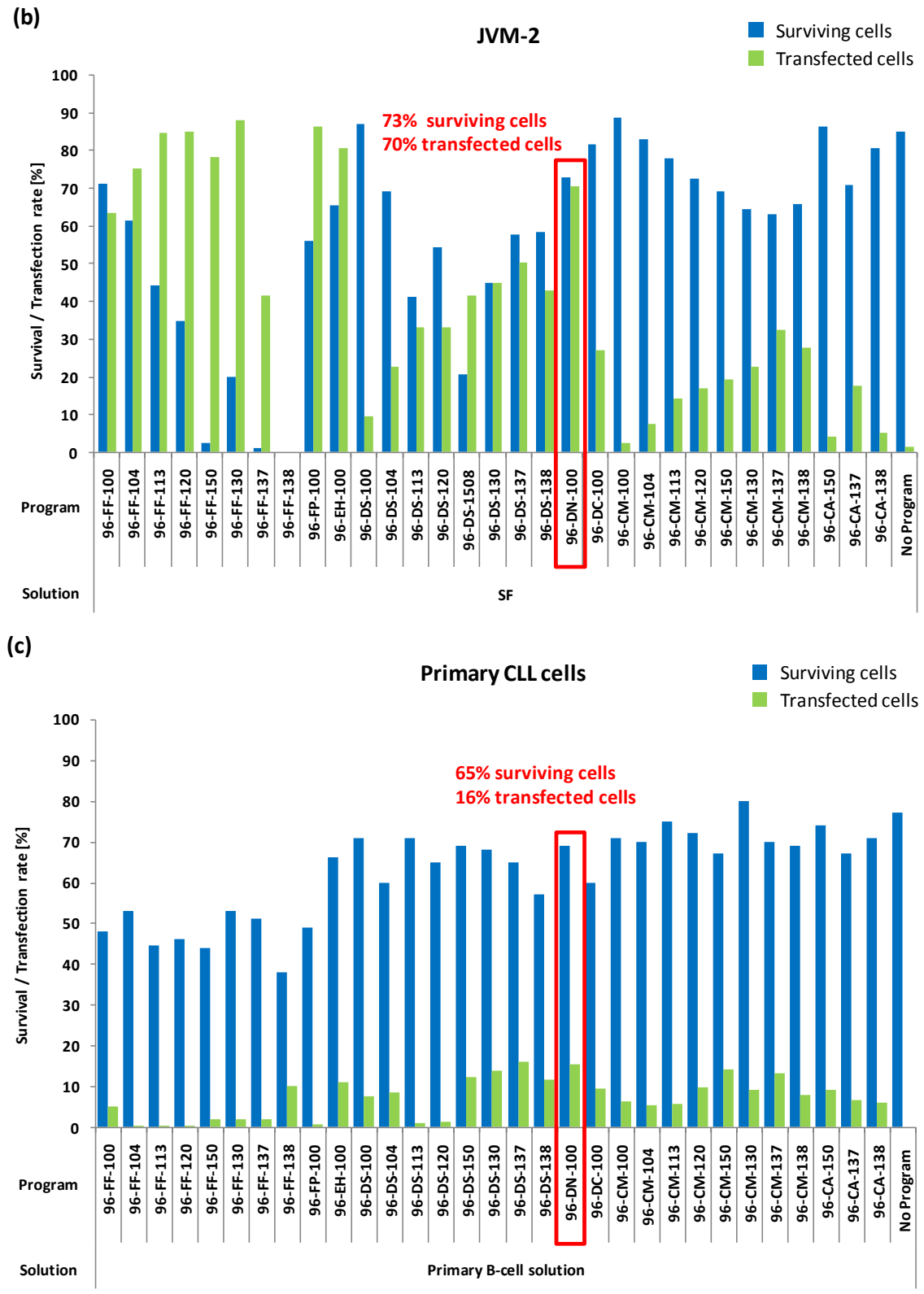

Figure 12: Optimization of 96-well nucleofection in cell lines and primary cells. FACS analysis was performed after 96-well nucleofection of the plasmid pmaxGFP in the MCL cell lines JVM-2 (a) and Granta-519 (b) and in primary CLL cells (c). The percentage of surviving cells is shown as a blue bar. Setting the number of surviving cells to 100%, a certain percentage thereof was successfullly GFP transfected, as indicated in green bars. Optimal transfection condition for each cell line is highlighted in a red box. Transfection of MCL cell lines JVM-2 and Granta-519 was performed using Solution SE, SF, and SG in

combination with 32 different electroporation programs including the 'No Program' control, respectively. Since Solution SF showed the best transfection efficiencies, transfection results using solution SE and SG are not shown. Transfection of primary CLL cells was performed using 32 different pulses in combination with the 'Primary B-cell solution'. In all of the tested cells the program 96-DN-100 showed the best transfection efficiency.

3.2 Expression arrays

In order to identify overexpressed genes in the frequent chromosomal gain regions 3q25-q29, 12q13-q14, and 18q21-q22 of MCL and CLL cells, high resolution expression arrays of primary cells and cell lines were performed. Overexpressed genes resulting from expression profiling were selected as potential candidates for further functional studies.

3.2.1 Expression profiling of cells from MCL and CLL patients and cell lines

Expression arrays are able to analyze changes in the transcriptome of MCL and CLL tumor cells in comparison to control cells of healthy donors. Transcriptomes of 6 primary MCL and 24 primary CLL patient samples, as well as 6 cell lines were profiled to identify overexpressed genes. Gene expression of cell lines was normalized to the lymphoblastoid non-tumor cell line LCL-WEI (Figure 27, supplementary material) whereas gene expression of primary MCL and CLL cells was normalized to a pool of CD19+ sorted B-cells from healthy donors (Figure 13). Thereby, four MCL patients were profiled in duplicate (MCL3-6, replicates 'a' and 'b', respectively) in order to test reproducibility of expression profiling results. Expression profiling performed in this study offered an increased resolution compared to the earlier published microarray platform (Rosenwald *et al*., 2003). Statistical analysis of microarray (SAM) and hierarchical clustering of significant overexpressed genes on chromosomes 3q25-q29, 12q13-q14, and 18q21-q22 were performed following normalization. The threshold for gene overexpression was defined as 1.5-fold compared to the control cells (LCL-WEI or CD19+). These results are shown as heatmaps in Figure 13. Obtained results were compared to recent publications and revealed 37 novel and 35 predicted candidate genes (Table 4). Detailled information about the gene expression levels and about recent publications discussing these candidate genes can be found in Table 6 (supplementary). This set of 72 genes was selected on the basis of high expression levels and localization of the respective genes in commonly gained chromosomal regions in MCL and CLL: 27 genes on chromosome 3q25-q29, 32 genes on chromosome 12q13-q14 and 13 genes on chromosome 18q21-q22.

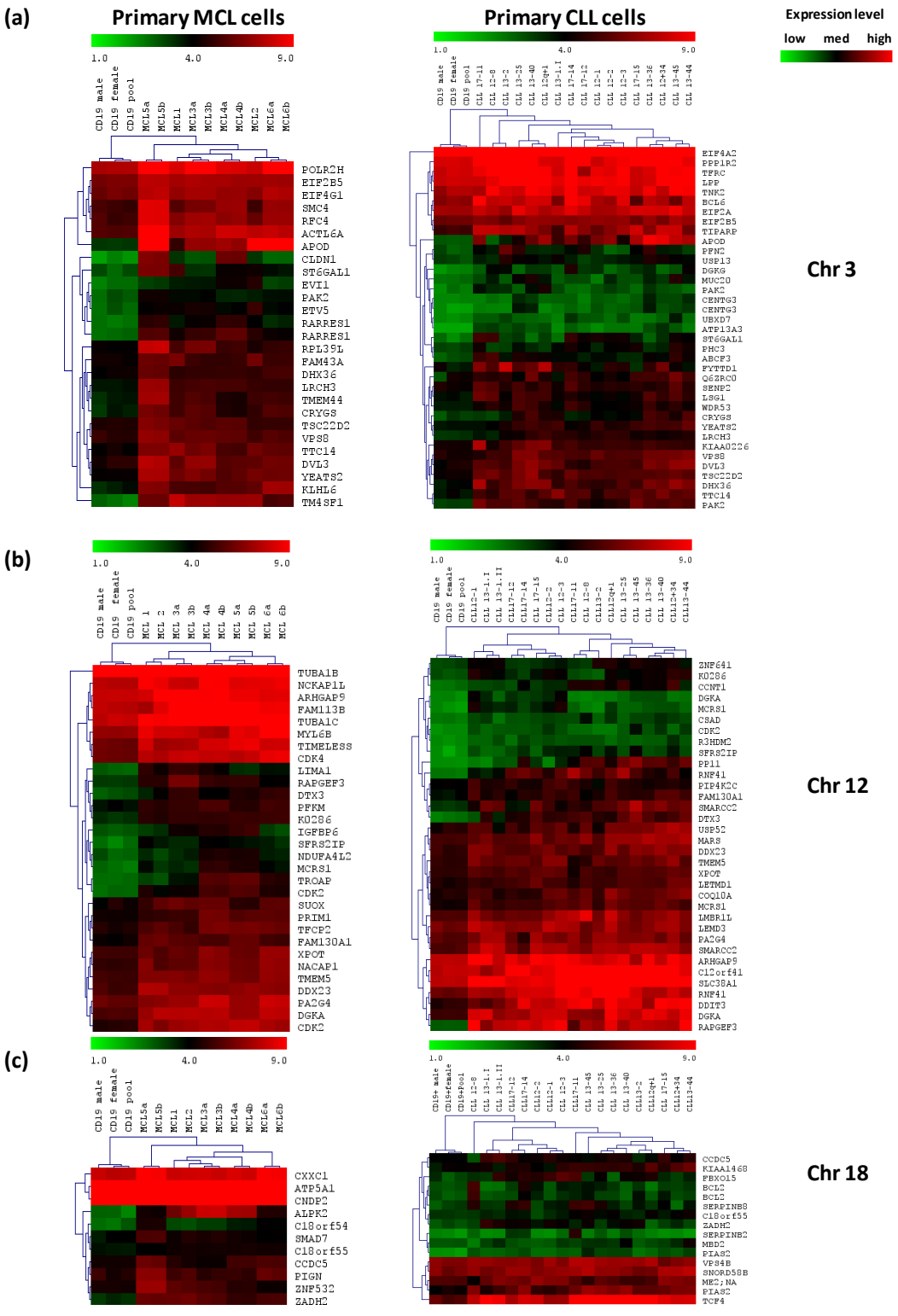

Figure 13: Differentially regulated genes in primary cells from MCL and CLL patients. Overexpressed genes in primary cells are shown for chromosomes 3q (a), 12q (b) and 18q (c) in comparison to CD19+ cells of healthy donors. Two-class unpaired SAM analysis was performed. Hierarchical clustering shows genes with similar gene expression patterns. Green=downregulated genes; black=median gene expression; red=upregulated genes. CD19 female/male=pool of two CD19 sorted B-cells of female/male origin. CD19 pool: pool of 2 male and 2 female CD19+ sorted B-cells. (a-c) Left heatmap=primary MCL, right heatmap=primary CLL. Four MCL patients were profiled in duplicate on the Illumina platform: MCL3-6 whereas 'a' and 'b' are duplicates. Chr=Chromosome.

Table 4: 72 overexpressed genes resulted from expression profiling and publications.

Chromosome 3		
No.	**Gene**	**Chr. band**
1	RARRES1	3q25
2	PFN2	3q25
3	GPR160*	3q26
4	ACTL6A	3q26
5	USP13	3q26
6	BCHE*	3q26
7	APOD	3q26
8	PIK3CA*	3q26
9	SerpinI2	3q26
10	ECT2	3q26
11	SMC4	3q26
12	YEATS2	3q27
13	RFC4	3q27
14	ECE2	3q27
15	C3ORF40*	3q27
16	DVL3	3q27
17	KLHL6	3q27
18	ETV5	3q28
19	LEPREL1	3q28
20	FLJ42393	3q28
21	CCDC50*	3q29
22	LAMP3	3q29
23	FAM43A	3q29
24	C3orf34*	3q29
25	RPL39L	3q29
26	PAK2	3q29
27	LRCH3	3q29

Chromosome 12		
No.	**Gene**	**Chr. band**
28	IRAK3*	12q13
29	SLC38A2*	12q13
30	HOXC6	12q13
31	RAPGEF3	12q13
32	KIAA0286	12q13
33	ARHGAP9	12q13
34	DDIT3	12q13
35	MBD6	12q13
36	RHEBL1*	12q13
37	TIMELESS	12q13
38	SMARCC2	12q13
39	RARG	12q13
40	STAT6*	12q13
41	CDK2	12q13
42	FAM112B*	12q13
43	PA2G4	12q13
44	FAM113B	12q13
45	ITGB7	12q13
46	INHBE*	12q13
47	GLI1*	12q13
48	MYL6B	12q13
49	METTL1	12q13
50	DTX3	12q13
51	DGKA	12q13
52	TUBA1B	12q13
53	PTGES3*	12q13
54	GDF11	12q14
55	CDK4	12q14
56	FAM119B	12q14
57	MARCH-IX	12q14
58	TSFM*	12q14
59	KUB3	12q14

Chromosome 18		
No.	**Gene**	**Chr. band**
60	PIAS2	18q21
61	IER3IP1*	18q21
62	RKHD2*	18q21
63	NARS*	18q21
64	TXNL1*	18q21
65	MALT1*	18q21
66	BCL2	18q21
67	VPS4B	18q21
68	ZNF532	18q21
69	SerpinB2	18q21
70	ZADH2	18q22
71	CCDC5	18q21
72	TCF4	18q21

Genes labeled with an asterisk (*) were previously published to be overexpressed in primary cells, but identified only overexpressed in cell lines in this study. Chr=Chromosome.

3.2.2 Validation of overexpressed candidate genes

Out of the set of 72 selected candidates, 13 genes were tested by quantitative real-time PCR (qRT-PCR) in MCL and CLL patient cells and cell lines. Three selection criteria were chosen for the validation of predicted gene expressions: (1) A different expression between MCL and CLL based on Illumina expression array results (*ACTL6A*, *DDIT3*, *PAK2* and *RHEBL1*), (2) high gene expression based on Illumina expression array results (*APOD* and *ARHGAP9*), and (3) predicted candidate genes from recent publications (*CCDC50*, *PFN2*, *ECT2*, *Timeless*, *IER3IP1*, *MALT1* and *RKHD2*). Validation of these overexpressed genes by qRT-PCR was shown in primary cells of 8 MCL and 28 CLL patients (Table 5), and in 6 cell lines including both neoplasias (Figure 14).

Table 5: Mean overexpression of candidate genes is shown in primary MCL and CLL cells on chromosomes 3q, 12q and 18q measured by qRT-PCR.

	Primary MCL		Primary CLL	
Gene	Mean	Range	Mean	Range
CCDC50	3.4	0.5 - 7.5	3.5	0.2 - 9.3
DDIT3	2.2	0.7 - 10.4	3.9	0.1 - 10.4
YEATS2	3.1	1.1 - 6.5	1.7	0.1 - 5.5
ARHGAP9	2.0	1.4 - 8.6	1.1	0.1 - 2.0
RHBL1	3.3	0.6 - 2.7	1.8	0.1 - 7.9
ACTL6A	2.0	0.5 - 3.0	2.6	0.1 - 9.5
Timeless	3.1	0.9 - 5.1	2.1	0.1 - 7.3
APOD	716	0 - 1273	262.0	0 - 1926
RKHD2	19.0	0 - 44.9	40.0	10.8 - 65.3
ECT2	68.7	0 - 213.0	6.5	2.3 - 14.1
PAK2	19.9	0.2 - 55.2	19.6	6.9 - 29.9
PFN2	14.7	14.6-15.8	58.8	4.3 - 346
MALT1	0.9	0.5 - 2.0	0.8	0.4 - 1.4

Correlation between gene overexpression and copy number gain was shown in the MCL cell line JVM-2 on chromosome 3q25-q29 for the genes *CCDC50*, *YEATS2*, *APOD,* and *PFN2*. The genomic copy number gains and a correlated gene overexpression on chromosomes 12q (chromosomal gain in JVM-2 and Jeko-1), and 18q (chromosomal gain in Granta-519) could be proven for all tested genes. Exemplary, the gene expression status of the gene *FLJ42393* that was not identified by microarray expression profiling, could be validated by qRT-PCR (Figure 14d).

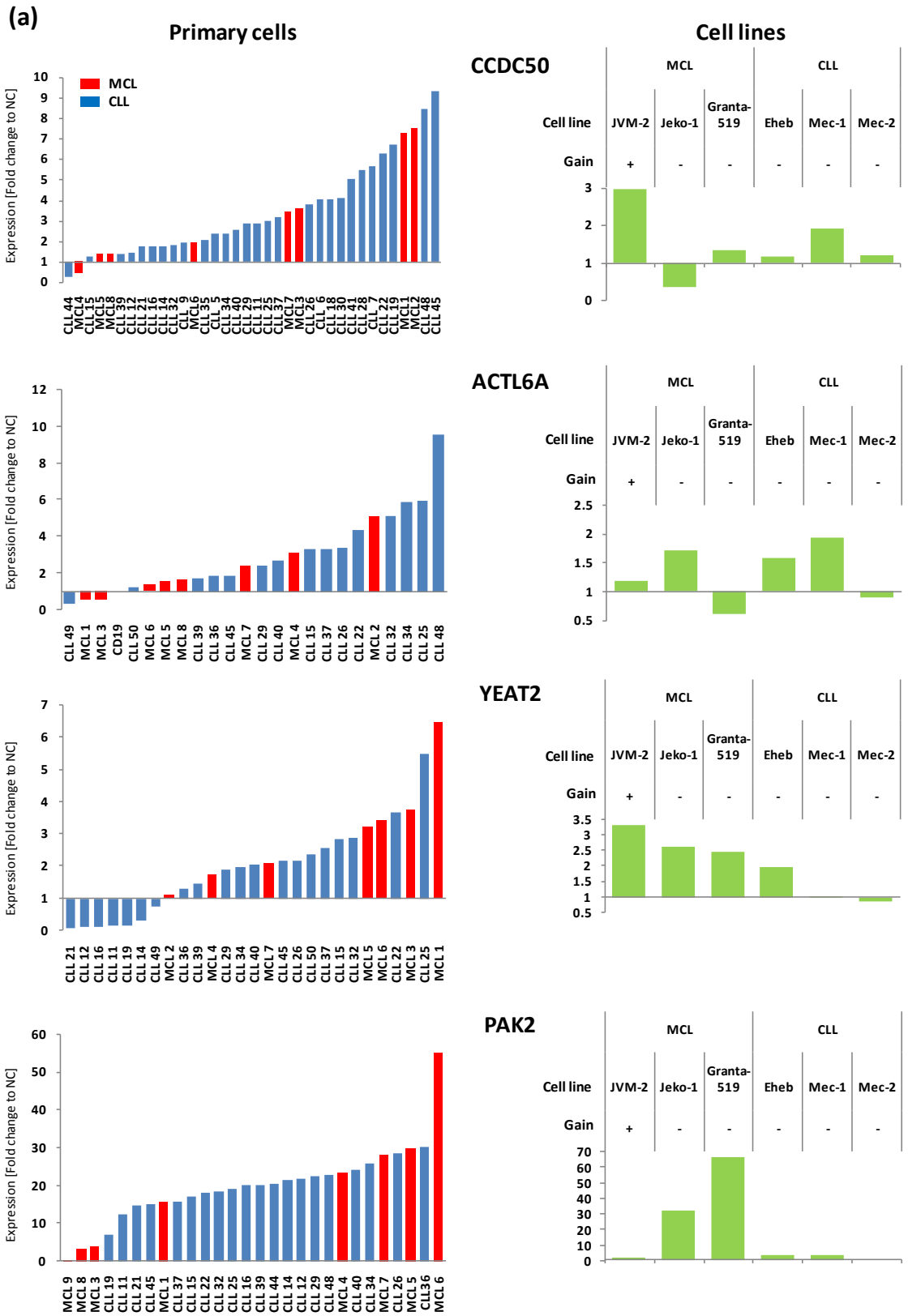
(a)
Primary cells
Cell lines
MCL
CLL
Expression [Fold change to NC]
CCDC50
ACTL6A
YEAT2
PAK2
Cell line
Gain
JVM-2
Jeko-1
Granta-519
Eheb
Mec-1
Mec-2
+
-

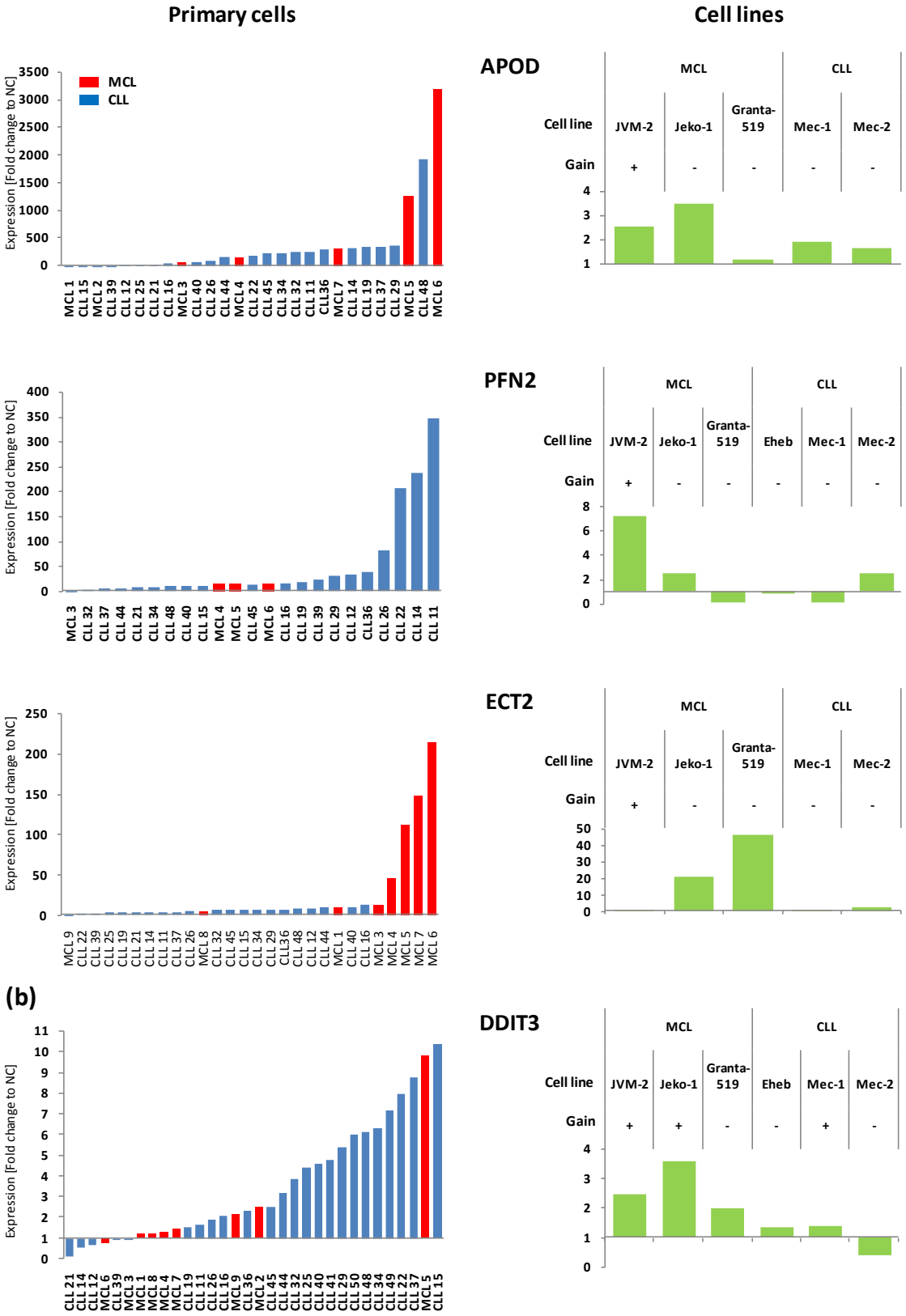
Primary cells
Cell lines
APOD
PFN2
ECT2
DDIT3
(b)
MCL
CLL
Expression [Fold change to NC]
Cell line
Gain
JVM-2
Jeko-1
Granta-519
Eheb
Mec-1
Mec-2

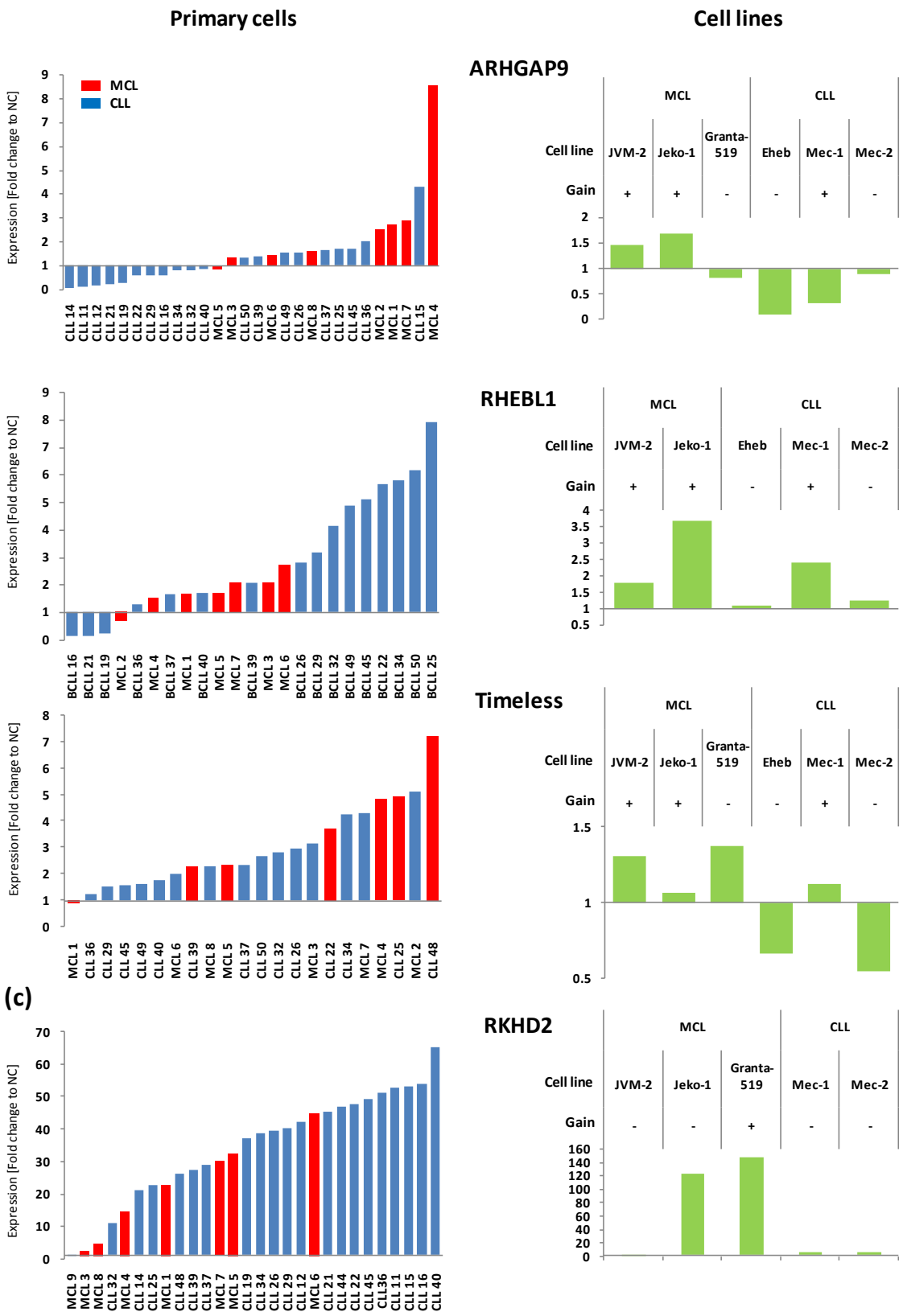
Primary cells
Cell lines
ARHGAP9
RHEBL1
Timeless
RKHD2
MCL
CLL
Expression [Fold change to NC]
Cell line
Gain
JVM-2
Jeko-1
Granta-519
Eheb
Mec-1
Mec-2
(c)

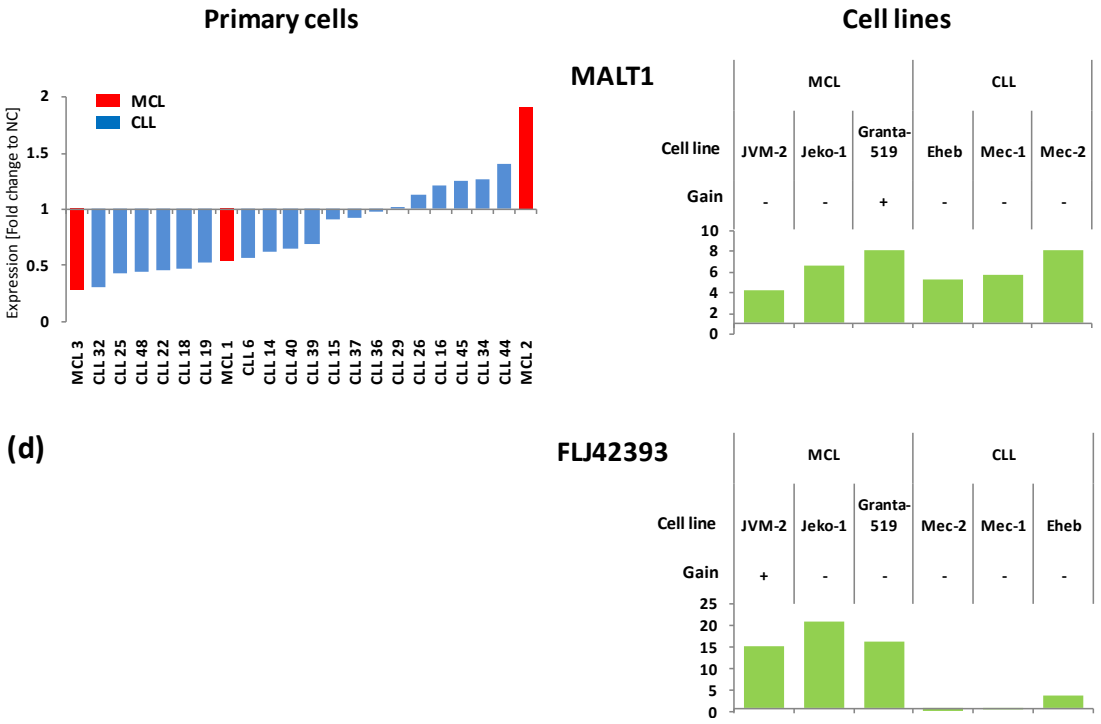

Figure 14: qRT-PCR of 14 selected candidate genes. Gene expression of candidates on chromosome 3q (a), 12q (b, d), and 18q (c) was measured in primary CLL and MCL cells (left column) and in cell lines (right column). X-axis reveals primary MCL (red bars) and CLL (blue bars) patients and cell lines (green bars). Y-axis shows fold change gene expression after correlating gene expression levels to the appropriate normalization control (NC). Expression levels of candidate genes in cell lines were normalized to the lymphoblastoid non-tumor cell line LCL-WEI. Expression levels of genes in primary cells were normalized to a pool of CD19+ B-cells (n=10). (a-d) Cell lines with chromosomal gain on the chromosome 3q, 12q, or 18q are labeled '+'. Cell lines with a normal caryotype in this genomic region are labled with '-'. (d) The recently predicted candidate gene in primary MCL cells (FLJ42393) was validated by qRT-PCR in cell lines.

3.3 RNAi screen

The 72 overexpressed genes were antagonized via siRNA pools applying the 96-well shuttle nucleofection technology in MCL cell lines JVM-2 and Granta-519. After transient gene knockdown in the leukemic cells, luminescent-based cell viability assays and FACS analyses were performed in order to reveal changes in cell viability and vitality.

3.3.1 Optimization of the screening set-up

During optimization of the screening set-up, experimental conditions were defined such that they offered the best possible screening window, reflecting good sensitivity, strong signal-to-noise ratio and low variability (high robustess and reproducibility). The dynamic range of the chosen read-out assay therefore represented the difference between 'baseline values' that were obtained from negative control genes and representative 'positive hit values' that were obtained from positive control genes. Negative control samples primarily allowed the evaluation of sequence-independent off-target effects

and the normalization of all data subsets from different plates into a single coherent data set. Positive control samples primarily offered a quality control to ensure that all screened genes are subjected to the same or at least a similar stringency of testing conditions. It was therefore crucial to select these control genes carefully. Negative control siRNAs were critical for setting the 'hit' threshold that determined, whether a siRNA was considered as having a positive, negative or neutral effect in a particular assay. These siRNAs lack similarity to nucleotide sequences in all known human genes. Therefore, it was worthwhile to screen multiple control genes in MCL and CLL cell lines before selecting one that accurately represents the baseline for each chosen cell line and assay (Figure 15). Different negative controls, such as scrambled siRNAs (pools and individual molecules), siRNAs directed against firefly luciferase and GFP, were tested to ascertain how faithfully they represent the baseline of each assay. Depending on the cell type and timepoint of readout, different siRNAs seem to positively or negatively induce cell proliferation.

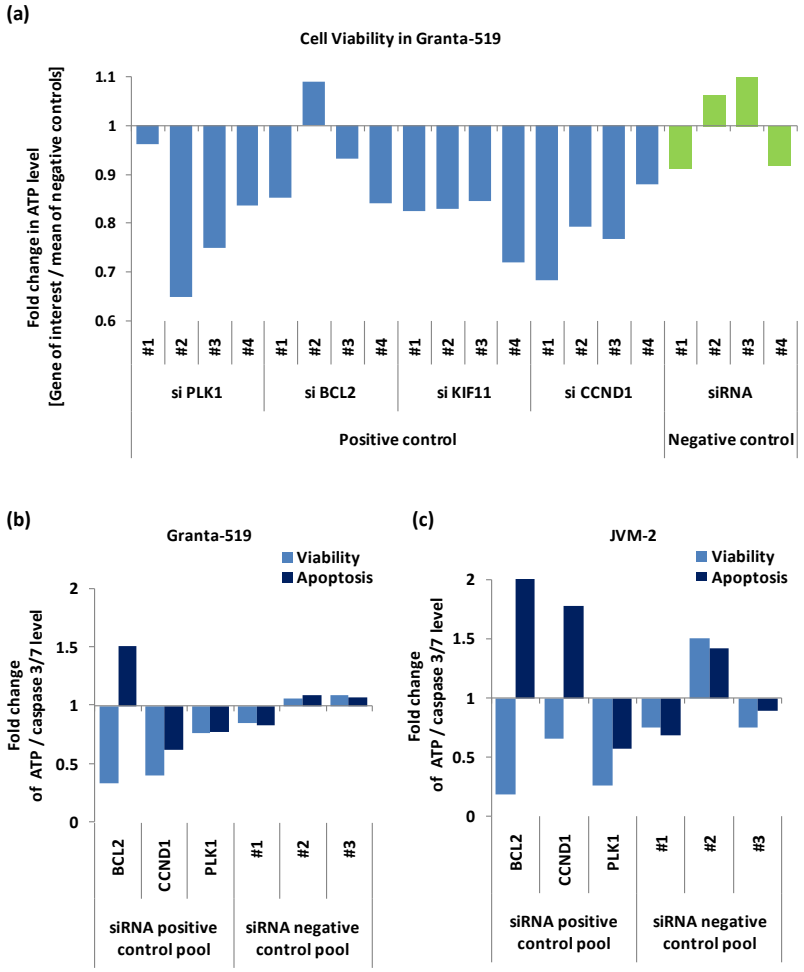

Figure 15: Testing of siRNA functionality in MCL cell lines JVM-2 and Granta-519. (a) Single siRNAs were transfected into Granta-519. Cell viability was measured as change of the ATP levels 72h post transfection (p.t.) compared to the mean of four negative controls (three scrambled siRNA molecules (siRNA #1-#3) and one siRNA molecule targeting GFP (siRNA#4)). (b-c) Cell viability and the induction of apoptosis were measured in Granta-519 (b) and JVM-2 (c) as ATP levels or caspase 3/7 activity 72h p.t.. Changes in cell

viability or apoptosis were compared to the mean of three different negative controls: two scrambled siRNA molecules (siRNA #1 and #2) and a siRNA targeting a luciferase sequence (siRNA #3).

3.3.2 siRNA screen to identify genes with impact on cell survival

The most obvious application of RNAi screening, i.e. loss-of-function (LOF) screening, involves identifying and functionally characterizing genes of interest on the basis of their LOF phenotypes. Such studies offer the broadest discovery potential, as they simply analyze single-gene LOF phenotypes in otherwise unmodified cells. Each of the 72 candidate genes was represented by a pool of four siRNA molecules transfected into the appropriate cell line. siRNAs targeting genes on chromosomes 3q and 12q were transfected into JVM-2, whereas siRNAs targeting genes on chromosome 18q were transfected into Granta-519 due to the presence of respective gained regions. The optimal siRNA concentration of 500nM and the optimal read-out timepoint at 72h post transfection (p.t.) had been previously determined. An ATP-dependent luminescent cell viability assay (Figure 16a) and FACS analysis in 96-well format (Figure 16b) were chosen as read-out approaches. Three biological replicates of the siRNA screen have been performed and positive 'hits' were selected according to four criteria. A candidate gene: (1) revealed a 'loss-of-viability' phenotype, (2) showed an increased cell death rate, (3) reached a certain threshold: >20% reduction in cell viability and >20% dead cells when compared to three independent negative controls and (4) showed criteria (1)-(3) in two out of the three biological replicates. Functional read-out assays of the loss-of-function screen revealed 18 genes that corresponded to these criteria and were selected for further validation experiments (Figure 16). The full data set resulting from the original screen is shown in the supplementary data (Figure 28-29).

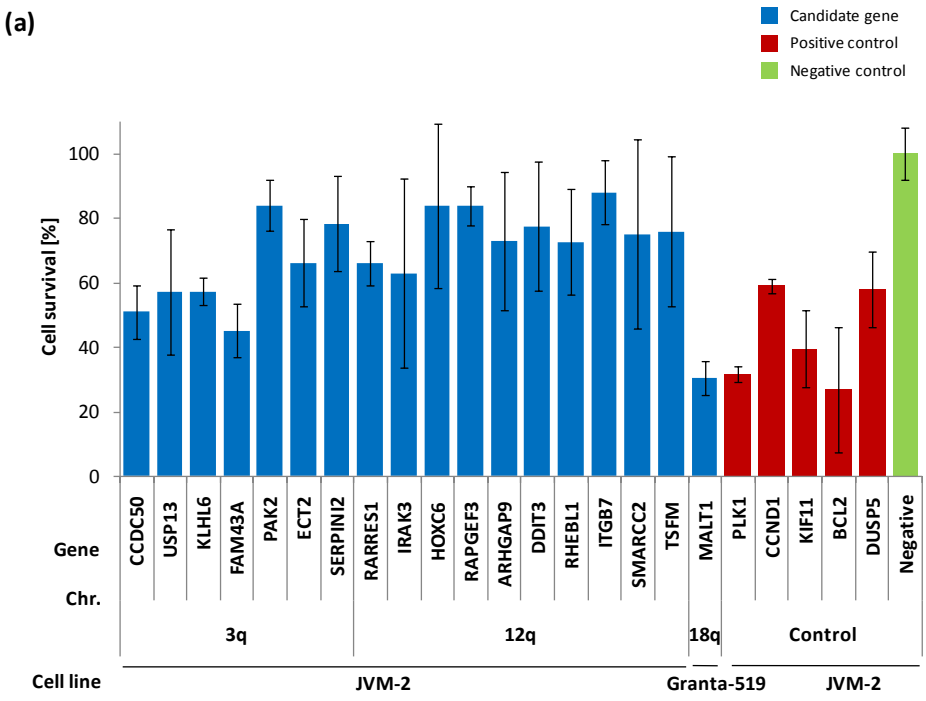

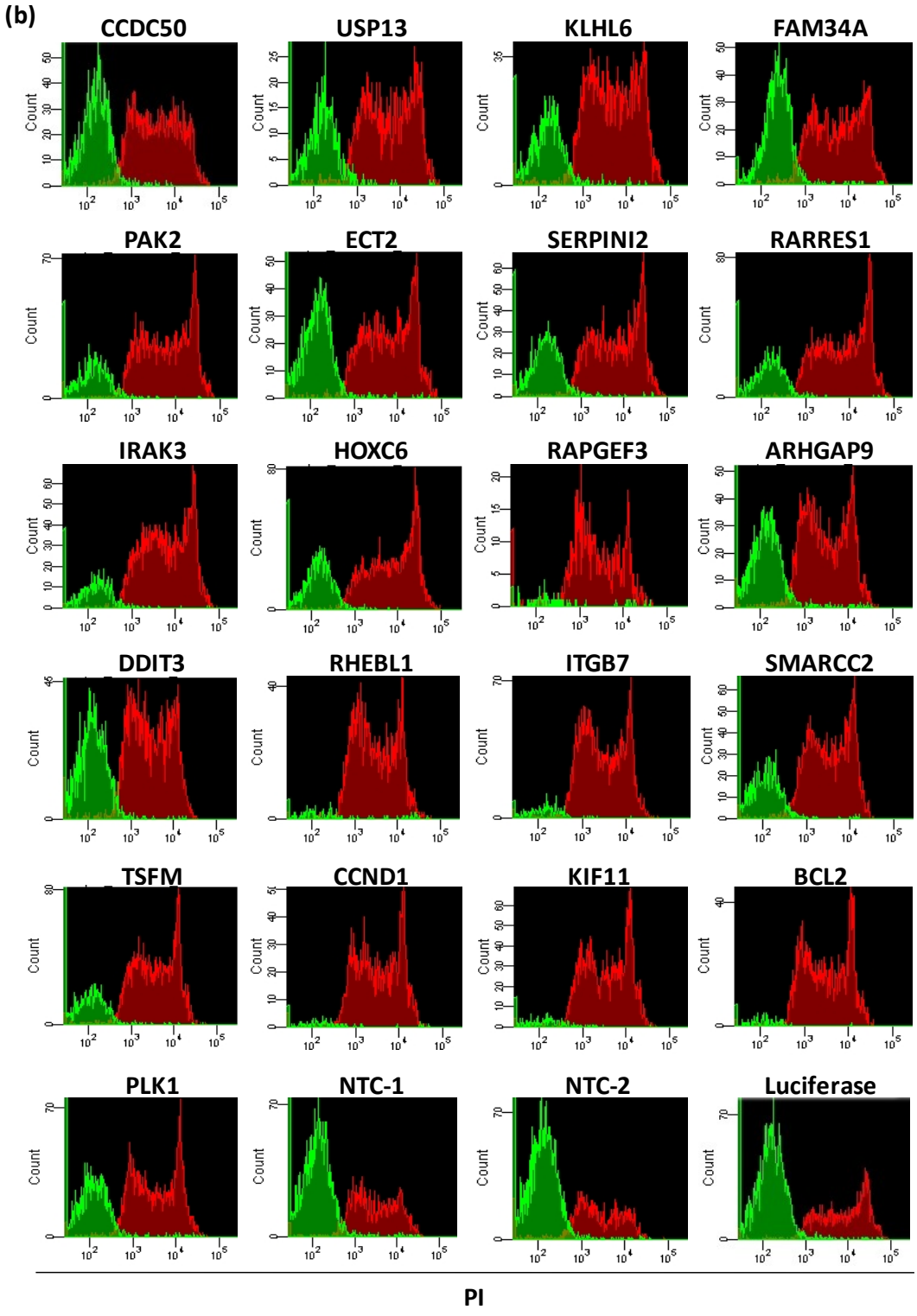

Figure 16: Cell viability assay and FACS analysis of the candidate genes resulting from the siRNA screen. (a) Cell viability assay shows the change in ATP levels after silencing of the gene of interest compared to the mean of three negative controls ('Negative'). The chromosomal location of the genes as well as the cell line, in which the knockdown was performed, is indicated. (b) FACS analysis was performed 72h after transfection. Cells were stained with propidium iodide (PI). Dead cells are indicated in red=PI positive cells. Living cells are indicated in green=PI negative cells. Positive controls shown are *CCND1*, *KIF11*, *BCL2*, and *PLK1*. The three negative controls are shown: two independent non-template controls ('NTC-1' and 'NTC-2') and a siRNA targeting the luciferase sequence ('Luciferase'). Cells after silencing of the gene *MALT1* are not shown by FACS analysis due to limited availability of cell material.

3.3.3 Validation of candidate genes

Validation of the 18 candidate genes was performed by transfecting up to four single siRNA molecules for each gene separately into the appropriate cell line. Due to limited availability of primary CLL material, pools of 2-4 siRNA molecules were transfected and cells were cultivated 72h in conditioned medium. Every 24h, fresh medium was added. Cell viability was measured at 24h, 48h, and 72h after transfection. Validation of a candidate gene was scored positive, if two out of four siRNA molecules reduced cell viability in cell lines and the pool of siRNAs reduced cell viability in primary CLL cells. The single siRNA or the pool of siRNAs, showing most significant reduction in cell viability is shown in Figure 17a,b. The whole data set from the validation experiment can be found in the supplementary data (Figure 30). For three genes, the reduction in cell viability was detected in cell lines and in primary cells: *CCDC50*, *SERPINI2*, and *SMARCC2*. Five genes were not tested in primary CLL cells due to limited availability of primary cell material (*USP13*, *FAM43A*, *PAK2*, *KLHL6* and *MALT1*). For four genes (*DDIT3*, *USP13*, *FAM43A*, *HOXC6*) the majority of tested individual siRNAs did not show a reduction in cell viability in the tested cell line. For nine genes, the loss-of-viability could only be shown in the JVM-2 cell line but not in primary CLL cells (*ARHGAP9*, *KLHL6*, *PAK2*, *ECT2*, *IRAK3*, *RAPGEF3*, *RHEBL1*, *ITGB7*, and *TSFM*). Interestingly, *DDIT3* showed a loss-of-viability only in primary CLL cells (Figure 17b). The successful knockdown of the two genes *CCDC50* and *SMARCC2* was validated by qRT-PCR in cell lines and primary cells (Figure 17c,d). The gene *CCDC50* showed most prominent reduction in cell viability after gene knockdown in primary cells and was selected for further analysis.

(a)

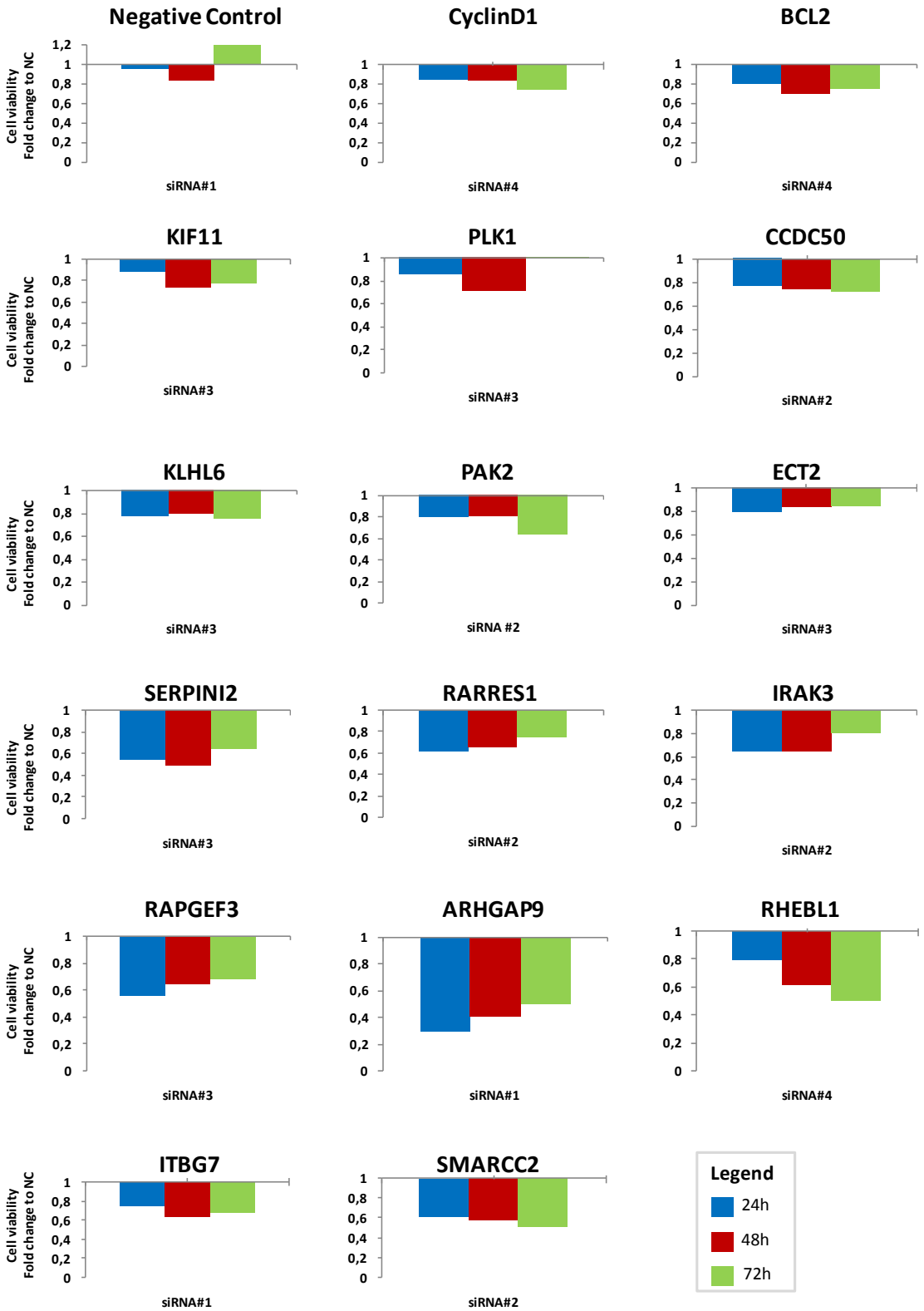
Negative Control
siRNA#1
CyclinD1
siRNA#4
BCL2
siRNA#4
KIF11
siRNA#3
PLK1
siRNA#3
CCDC50
siRNA#2
KLHL6
siRNA#3
PAK2
siRNA #2
ECT2
siRNA#3
SERPINI2
siRNA#3
RARRES1
siRNA#2
IRAK3
siRNA#2
RAPGEF3
siRNA#3
ARHGAP9
siRNA#1
RHEBL1
siRNA#4
ITBG7
siRNA#1
SMARCC2
siRNA#2
Cell viability
Fold change to NC
Legend
24h
48h
72h

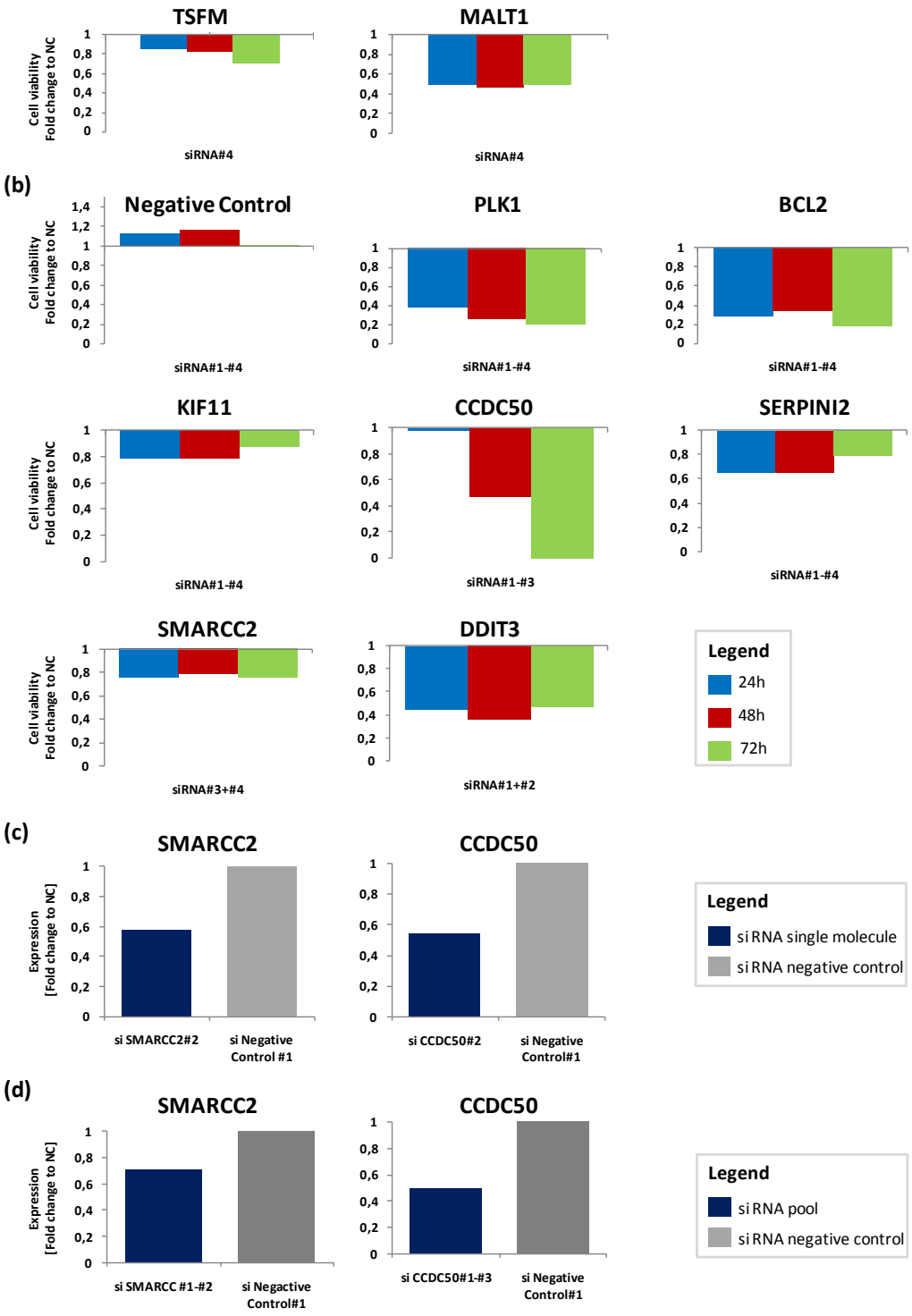

Figure 17: Cell viability assay after silencing of the candidate genes. (a) A single siRNA that revealed the most significant reduction in cell viability is shown for each candidate gene. Cell viability was measured as ATP level of the cells and was normalized to the mean of three negative controls ('NC'). Changes in cell viability are shown for one negative control and four positive controls (*BCL2*, *CyclinD1*, *KIF11*, and *PLK1*). Cell viability changes were measured 24h, 48h, and 72h after transfection (blue, red and green bars). (b) Primary CLL cells were transfected with a pool of siRNA molecules. Changes in cell viability were measured 24h, 48h, and 72h after transfection (blue, red, and green bars). The effect on cell survival after transfection of a negative control and three positive controls (*PLK1*, *BCL2*, and *KIF11*) is shown. (c-d) Knockdown was measured for *SMARCC2* and *CCDC50* via qRT-PCR in the cell line JVM-2 (c) and in primary CLL cells (d).

3.3.4 Determination of *CCDC50* RNA expression levels in various B-cell lymphomas

CCDC50 was analyzed in B-cell lymphoma cell lines and in primary MCL and CLL cells. Quantitative real-time PCR experiments performed with 16 lymphoma cell lines, comprising Burkitt lymphoma, Hodgkin lymphoma, diffuse large B-cell lymphoma, mantle cell lymphoma and chronic lymphocytic leukemia (Figure 18) revealed increased expression of *CCDC50* only in MCL and CLL cells (ranging from 1.3 - 2.9-fold), except in the cell line Jeko-1. The median upregulation of *CCDC50* in CLL (1.7-fold) and MCL (1.4-fold) cell lines was significantly higher than in burkitt lymphoma (0.28-fold), DLBCL (0.05-fold) and Hodgkin lymphoma (0.47-fold). Expression of genes was normalized to the housekeeping genes, *PGK1* (phosphoglycerate kinase 1) and *DCTN2* (dynactin 2), and was finally compared to the lymphoblastoid non-tumor cell line LCL-WEI (Figure 18a). Quantitative real-time PCR experiments with primary cells showed that 5 out of 8 MCL patients and 23 out of 26 CLL patients displayed an upregulation of *CCDC50* ranging from 1.5 – 10-fold with a mean expression of 3.4-fold (MCL) and 3.5-fold (CLL) and a threshold of 1.5-fold overexpression when compared to CD19+ selected B-cells of healthy donors (Figure 18b).

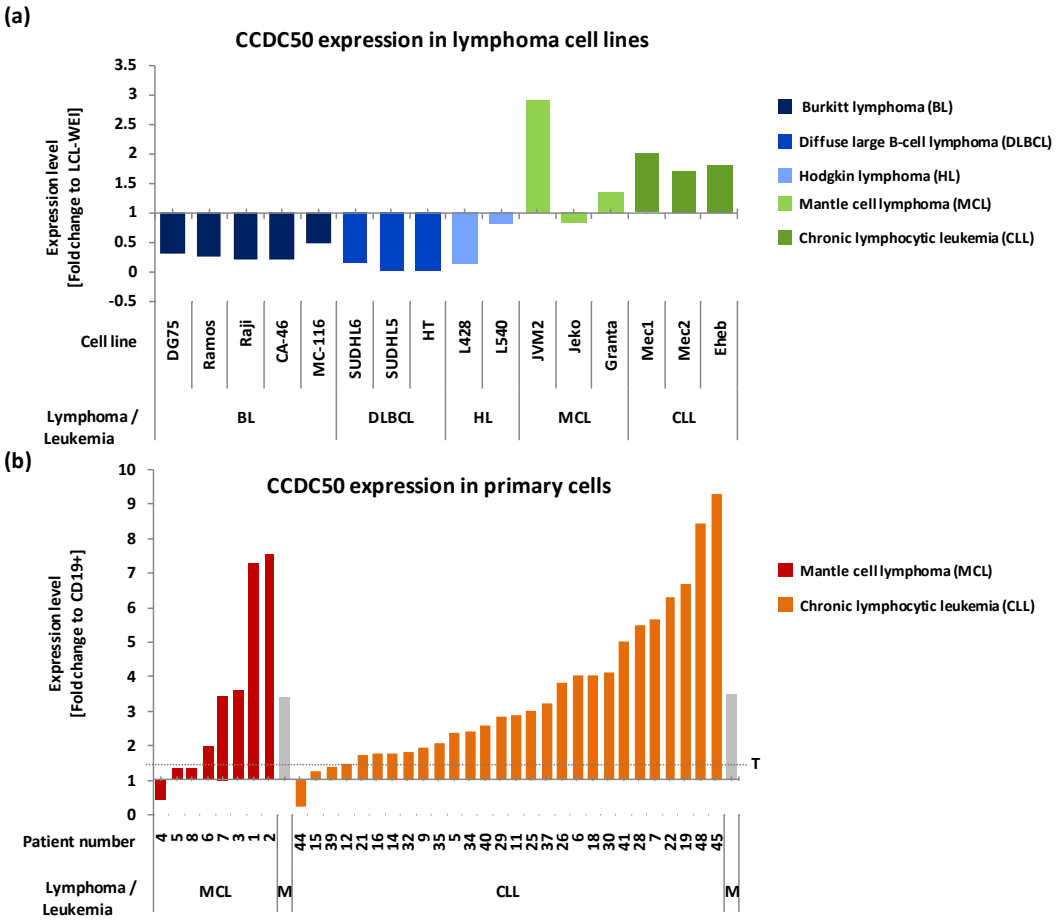

Figure 18: Expression of *CCDC50* in B-cell lines and primary MCL and CLL cells was measured by qRT-PCR. (a) Expression of *CCDC50* was analyzed by qRT-PCR in 16 cell lines: 5 Burkitt lymphoma (BL), 3 diffuse large

B-cell lymphoma (DLBCL), 2 Hodgkin lymphoma (HL), 3 mantle cell lymphoma (MCL), and 3 chronic lymphocytic leukemia (CLL) cell lines. Expression levels were first normalized to the expression of two housekeeping genes *PGK1* and *DCTN2*. Each sample was then compared to the lymphoblastoid non-tumor B-cell line LCL-WEI. (b) *CCDC50* expression was analyzed in 26 primary CLL and 8 primary MCL samples. Results were normalized to gene expression of CD19+ B-cells from healthy donors (n=10). M=median expression, T=Threshold for overexpression was set at 1.5-fold expression after normalization.

3.3.5 Transient knockdown of *CCDC50*

In order to validate the reduction in cell viability and identify the optimal siRNA sequence for efficient gene knockdown, the silencing effect of three independent siRNAs was determined (siCCDC50#1, siCCDC50#2, and siCCDC50#3) in the cell line JVM-2. All siRNAs tested, displayed reproducible gene knockdown 48h after transfection: siCCDC50#3 (92%), siCCDC50#2 (87%) and siCCDC50#1 (67%) (Figure 19). Functional investigations revealed the most significant decrease in cell viability after 72h. JVM-2+siCCDC50#1 showed comparable viability to JVM-2+siNegativeControl. In cells transiently transfected with siCCDC50#2 and #3, cell viability was reduced to 50% and 44%. *CCDC50* was therefore considered to play a crucial role in processes regulating cell cycle, proliferation and survival. The siRNA sequence siCCDC50#3 revealed the most efficient gene knockdown and was therefore used for stable knockdown experiments.

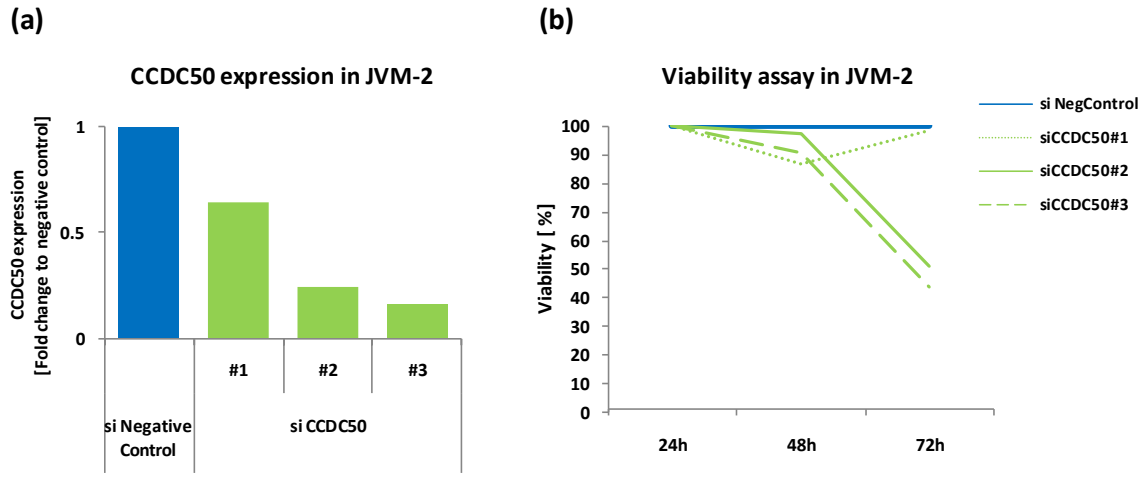

Figure 19: Transient knockdown of *CCDC50* in the MCL cell line JVM-2. (a) qRT-PCR 48h p.t. showed reduction in mRNA levels of transient transfected cells with siCCDC50#1, #2, and #3 in comparison to a GFP negative control ('si Negative Control'). (b) Cell viability assay was performed at 24h, 48h, and 72h p.t.. Cell viability was determined in an ATP-based viability assay.

3.4 Stable silencing of candidate genes

3.4.1 Generation of stable cell lines for RMCE

The first step for the generation of stable cell lines was the successful integration of a single selection cassette into the genome of parental cell lines. The cassette codes for a neomycin gene for positive selection, a Herpes Simplex Virus thymidine kinase (HSV-tk) gene for negative selection and harbors two lox sites (loxP and loxP511) for site specific Cre-mediated homologous recombination. To obtain subclones of successful transfected cells, selection was performed with 2mg/ml neomycin (G418) in MCL and CLL cell lines following limited dilution over a period of four weeks. PCR analysis confirmed the integration of the selection cassette in all further analyzed single cell clones. Southern blot analysis revealed the number of integration events and FISH analysis on metaphase chromosomes can identify the chromosomal site, where the integration of the cassette took place (Figure 20). The final step was the substitution of the selection cassette against the shRNA coding plasmid pSUPERdL (dL for 'double Lox'), which contained an additional zeocin gene for positive selection. Upon cotransfection with a Cre-expression plasmid (pCMXhCre), the recombinant pSUPERdL was exchanged against the selection cassette. Stable subclones were finally selected for ganciclovir (negative selection) and zeocin (positive selection) resistance. A successful recombination event was validated by genomic PCR.

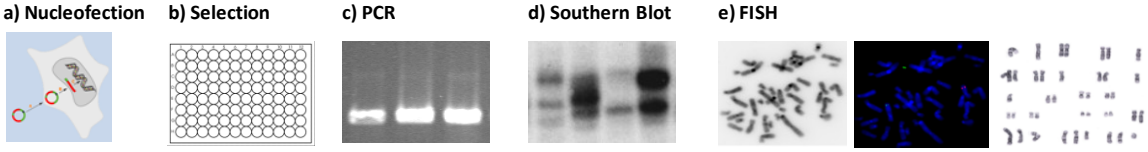

Figure 20: Schematic overview of the experimental procedure to generate and validate a single integration event of the selection cassette in cell lines. (a) Transfection of the cassette via nucleofection. (b) Selection of single cell clones in 96-well cultivation plates. (c) PCR analysis to validate the complete integration of the cassette. (d) Southern blot analysis to reveal the number of cassette integration events into the genome of a single cell clone. (e) FISH analysis to identify the chromosomal site of cassette integration.

Stable clones from MCL cell lines Granta-519 (GE82+) and JVM-2 (JEP4+C6) have already been established in previous work in our laboratories. Genomic DNA of these cells was chosen as positive control for Southern blot analysis. Successful generation of stable clones was shown for the cell lines Jeko-1, Eheb, Mec-2, and Mec-1. Single clones were tested by PCR for the integration of the selection cassette, which is exemplary shown for two single clones in Figure 21a. Single clones were further tested in Southern blot analysis, if PCR revealed a complete loxP and lox-P511 site and the full-length selection cassette (Figure 21a). Jeko-1+TKneo clones #3, #6, #8, #9, #12, #15 and #19 were

validated by Southern blot analysis for a single cassette integration event (Figure 21c). Jeko-1+TKneo clone #9 was in addition validated by FISH analysis on metaphase chromosomes (Figure 21e). Single clones of Mec-1+TKneo#8, #9 and #10, Mec-2+TKneo#4 and #29 and Eheb+TKneo#26 could also be validated by Southern blot analyses (Figure 21c). Single integration of the cassette in Mec-2+TKneo#4 and Eheb+TKneo#26 were validated further in FISH analysis (Figure 21e). Transfection of the TKneo selection cassette into the cell line Mec-1 showed repeated times multiple integration events in all cell clones (Figure 21d). Consequently, all of the selected single clones showed the same signal pattern after genomic DNA digestion in Southern blot analysis. The enzyme *Hind*III cuts only outside the selection cassette in the genome, whereas the enzymes *Nco*I and *Bgl*II are single cutters within the cassette. Digestion with one of the the later enzymes was therefore appropriate to reveal clones with multiple integration events. Double digestion with *Hind*III and *Bgl*II was appropriate to validate single integration of the HSV-TK-neo cassette (Figure 21c). FISH analyses have been performed for Mec-1+TKneo#17 and #34 (Figure 21e), showing multiple integration events (Figure 21d). Validated subclones carrying a single integration of the selection cassette could be further used for functional studies in the RMCE system for stable knockdown of shRNA coding inserts.

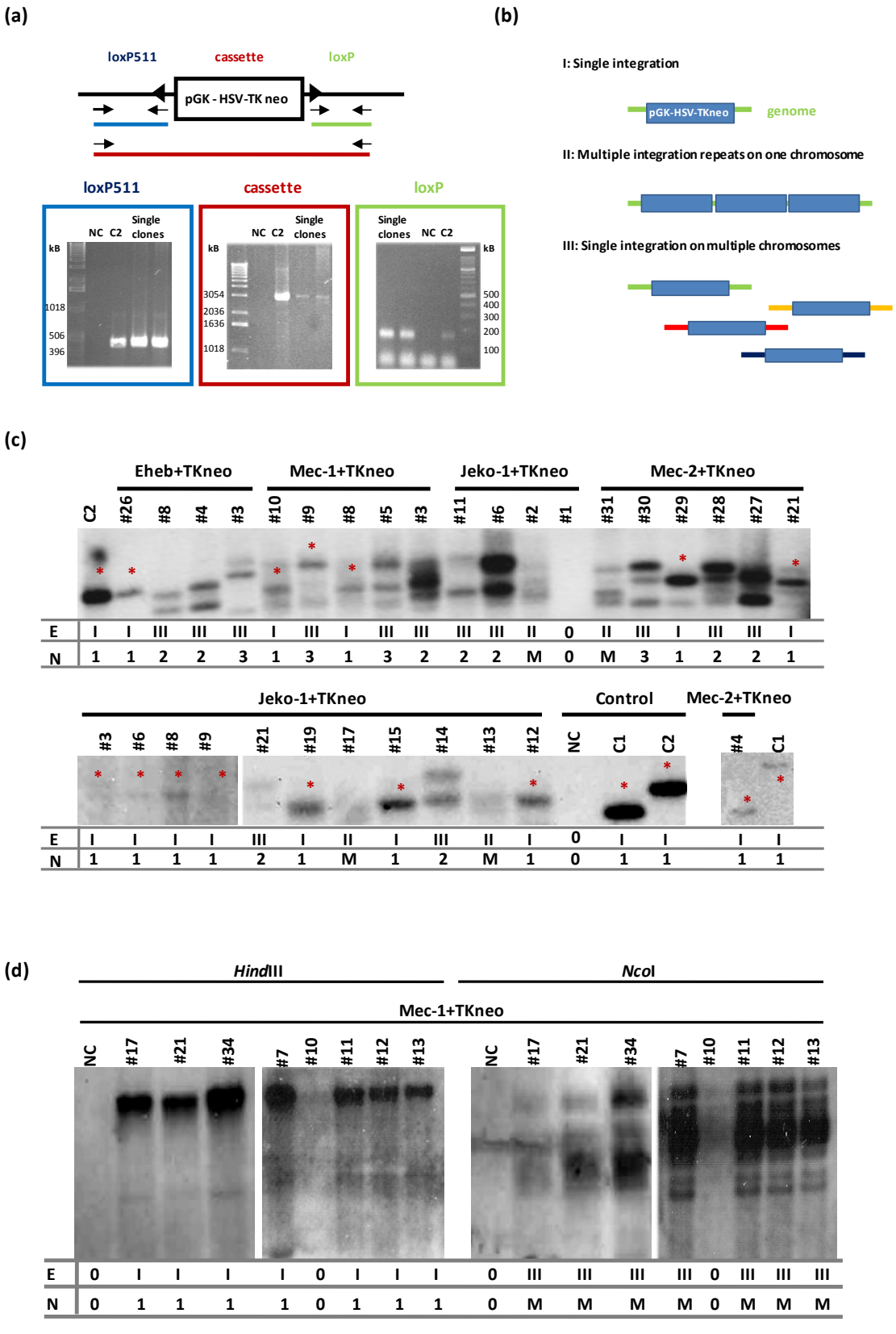
(a)
loxP511
cassette
loxP
pGK - HSV-TK neo
NC C2 Single clones
kB
1018
506
396
3054
2036
1636
1018
500
400
300
200
100
(b)
I: Single integration
pGK-HSV-TKneo
genome
II: Multiple integration repeats on one chromosome
III: Single integration on multiple chromosomes
(c)
Eheb+TKneo
Mec-1+TKneo
Jeko-1+TKneo
Mec-2+TKneo
C2 #26 #8 #4 #3 #10 #9 #8 #5 #3 #11 #6 #2 #1 #31 #30 #29 #28 #27 #21
E I I III III III I III I III III III III II 0 II III I III III I
N 1 1 2 2 3 1 3 1 3 2 2 2 M 0 M 3 1 2 2 1
Jeko-1+TKneo
Control
Mec-2+TKneo
#3 #6 #8 #9 #21 #19 #17 #15 #14 #13 #12 NC C1 C2 #4 C1
E I I I I III I II I III II I 0 I I I I
N 1 1 1 1 2 1 M 1 2 M 1 0 1 1 1 1
(d)
HindIII
NcoI
Mec-1+TKneo
NC #17 #21 #34 #7 #10 #11 #12 #13 NC #17 #21 #34 #7 #10 #11 #12 #13
E 0 I I I I 0 I I I 0 III III III III 0 III III III
N 0 1 1 1 1 0 1 1 1 0 M M M M 0 M M M

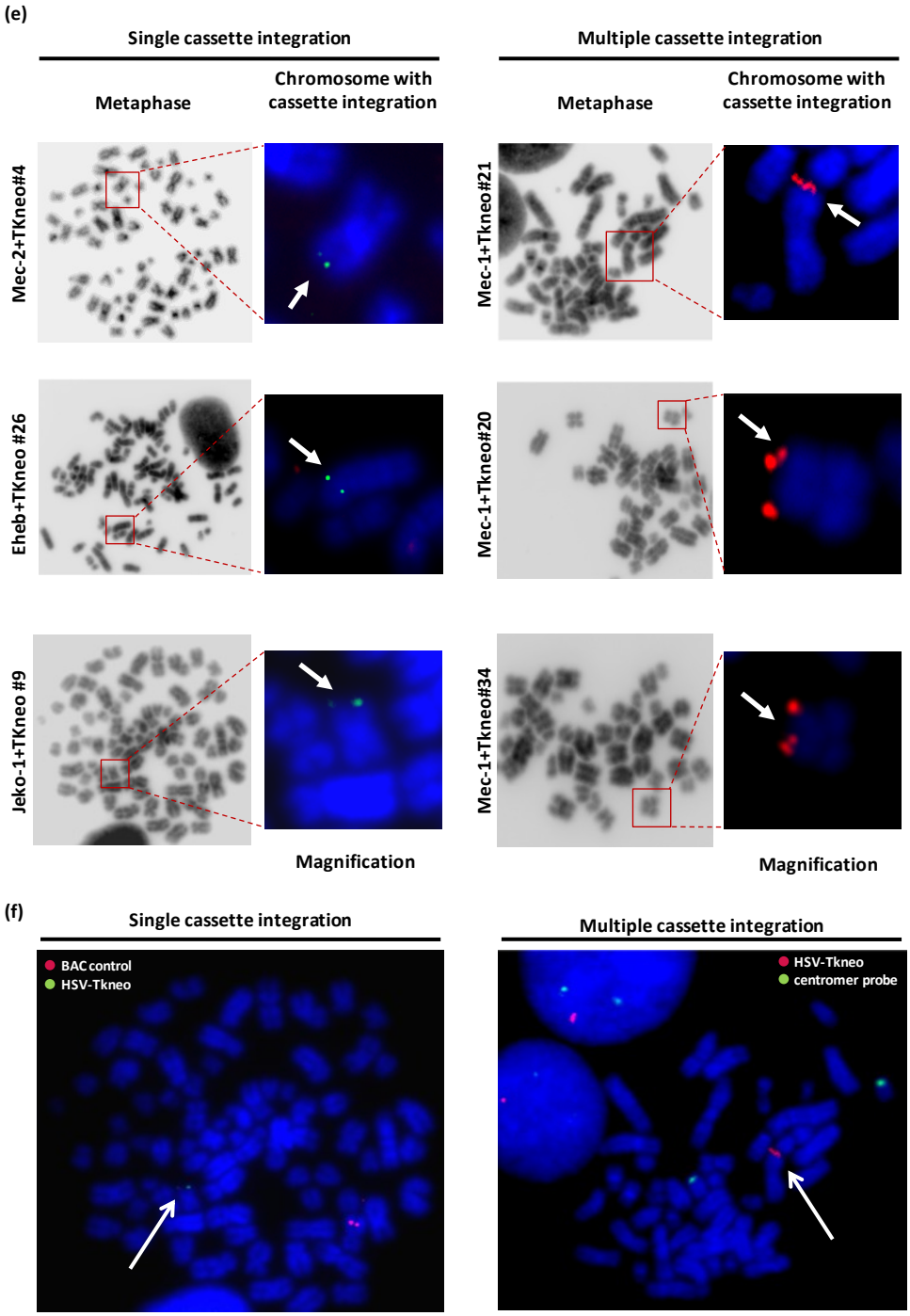

Figure 21: Generation of MCL and CLL cell lines with stable integration of the HSV-TK-neo cassette. (a) PCR amplification of loxP, loxP511 and the selection cassette. PCR analysis from two single Jeko-1 cell clones is shown. GE82+ cells served as a positive control (C2) and parental cells as negative control (NC). (b) Schematic overview of the possible integration events that could occur after transfection of the HSV-TK-neo cassette into the genome. (c) Southern blot analysis revealed the number of integration events. Clones with a single integration event were labeled with a red asterisk (*). C1=control JEP4+C6, C2=control GE81+, E=event of integration, N=number of integrations. I, II, III represent integration events shown in (b). (d) In the cell line Mec-1 multiple integration events occured. (e) FISH analysis identified the chromosomal site, where the stable integration event occurred. FISH was performed using a FITC-labeled (green) TKneo probe (Mec-2+TKneo#4, Jeko-1#TKneo#9, Eheb+TKneo#26) or a DIG-labeled (red) TKneo probe (Mec-1+TKneo#20, #21 and #34). (f) FISH analysis is exemplary shown for metaphase cells of the cell line Jeko#TKneo#9 (left side), and for Mec1+TKneo#21. The arrow indicates the site of chromosomal integration of the TKneo cassette. BAC contol= RP11-369L4.

3.4.2 Stable *CCDC50* knockdown via RMCE ?

In order to stably knock down *CCDC50* in the disease background of MCL and CLL, the siRNA sequence of siCCDC50#3 was cloned as a short-hairpin coding insert into the pSUPERdL-Zeo expression vector. To establish an appropriate negative control, a luciferase short hairpin coding insert was cloned in an independent approach. Stable transfection approaches were performed in the stable JVM-2 clone JEP4+C6, carrying a single TKneo cassette for RMCE. Following co-transfection of a Cre-expression plasmid (pCMXhCre) with the recombinant pSUPERdL-Zeo, the selection markers HSV-Tk and neo should be substituted by the cloned insert. New subclones were negatively selected by ganciclovir and positively selected by zeocin. Tranfected JEP4+C6 cell lines were selected over a period of four weeks. Alternating antibiotic treatments, the addition of antioxidants (sodium pyruvate, α-thioglycerol and bathocuproine disulfonate) and the addition of 10% conditioned medium was intended to increase the survival rate of transfected cells and avoid long selection periods with both antibiotics. This approach did not reveal stable cell lines, neither for *CCDC50* nor for the recombination of the luciferase sh-coding insert. All cells died within four weeks while under selection. Even the transfection of different plasmid concentrations in order to increase the possibility of a recombination event as well as the decrease of the antibiotic selection pressure by lowering the antibiotics concentration did not promote the generation of stable cell lines that exchanged the selection cassette for the sh-coding construct. The use of an alternative Cre-recombinase plasmid did not overcome initial problems. In summary, it was not possible to generate stable MCL cell lines by exchanging the single cassette via RMCE. Therefore random integration of sh_CCDC50 was the method of choice.

3.5 Functional studies of *CCDC50*

3.5.1 Stable *CCDC50* silencing in MCL and CLL cell lines

The generation of stable cell lines with random integration of the short hairpin coding insert sh_CCDC50 was performed in the MCL cell line JVM-2 and the CLL the cell line Mec-1. According to qRT-PCR results (Figure 18) JVM-2 and Mec-1 showed high expression values for *CCDC50* among all cell lines (2.9 and 2.0-fold). The strategy to validate the genomic integration of pSUPERdL-Zeo-sh_CCDC50 is shown in Figure 22a. Transfected cells were selected over a period of four weeks for zeocin resistance. PCR on genomic DNA validated the availability of the short hairpin coding *CCDC50* insert (PCR I) and the vector backbone including the zeocin resistance gene (PCR II) in stable cell clones (Figure 22b). This PCR demonstrated which part of the original pSUPERdL-Zeo-sh_CCDC50 vector has integrated into the genome of the stable selected cell lines.

CCDC50 RNA levels were reduced after stable *CCDC50* silencing by 50% (JVM-2+sh_CCDC50#1,#3) and by 80% (Mec-1+sh_CCDC50#1) when compared to their parental cell lines (Figure 22c), and was accompanied by reduced protein levels (Figure 22Figure 21d) and reduced cell viability (Figure 22e, f).

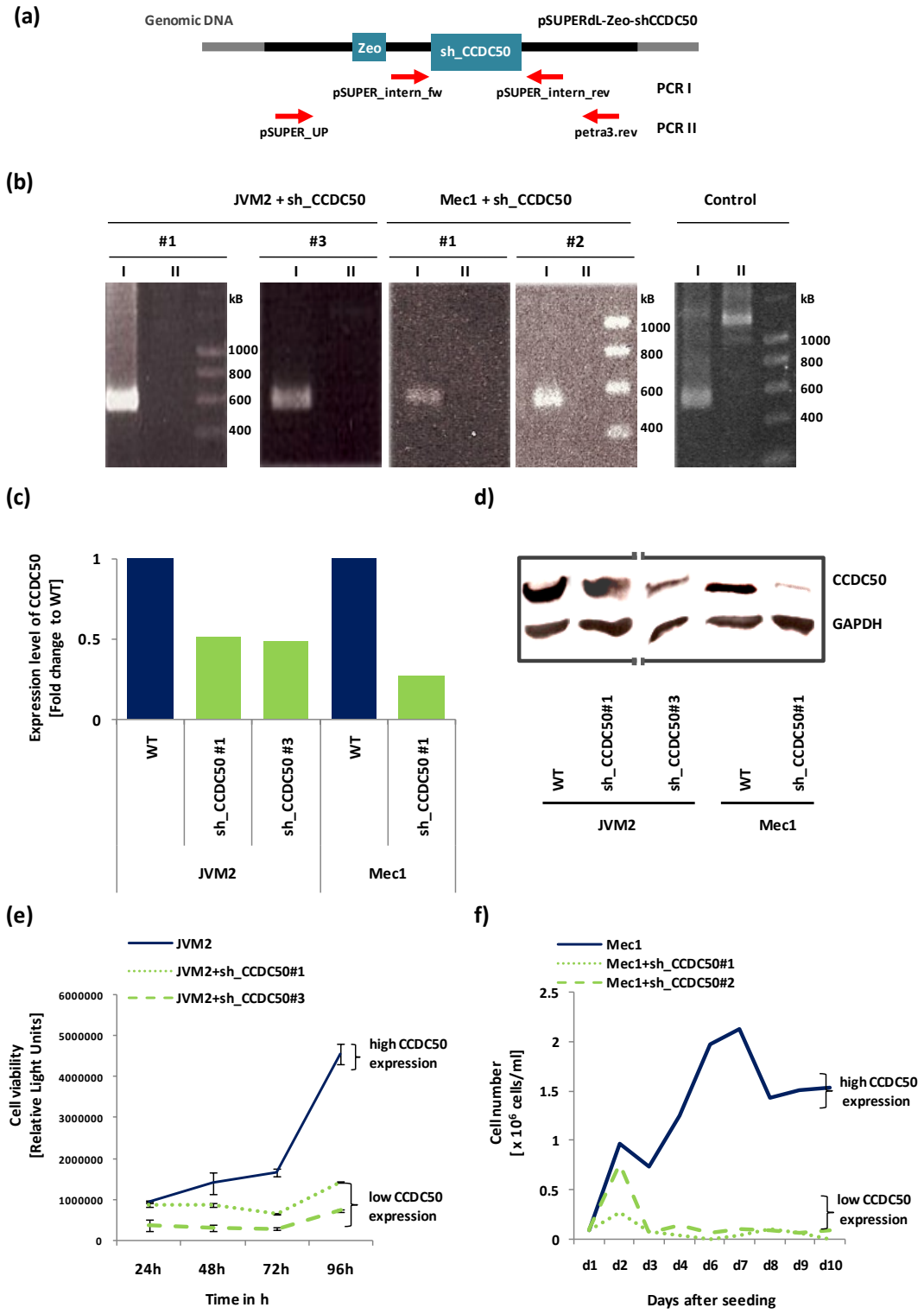

Figure 22: Stable *CCDC50* knockdown and functional analysis in JVM-2 and Mec-1 cell lines. (a) Strategy to validate genomic integration of pSUPERdL-Zeo-sh_CCDC50. (b) PCR to validate integration of sh_CCDC50

insert in JVM-2 and Mec-1 cell lines. The integrated sh_CCDC50 is shown with PCR I. PCR II showed which part of the vector backbone was additionally integrated. Control=pSUPERdL-Zeo-sh_CCDC50 vector. (c) Analysis of *CCDC50* expression by qRT-PCR in parental and stable cell clones. LCL-WEI was used as a reference cell line due to a balanced *CCDC50* expression status. Expression of *CCDC50* was finally normalized to wild type (WT) cells JVM-2 or Mec-1. (d) Western blot analysis showed the reduction in protein levels of *CCDC50* in parental and stable cell lines. GAPDH served as a loading control. (e) Cell viability assay was performed by seeding $3x10^6$ parental JVM-2 and stable transfected JVM-2 cells and measuring ATP-dependent cell viability every 24h for 4 days. (f) Cell proliferation was measured in Mec-1 WT and Mec-1 stable clones by counting cells via a cell counter device. Measurement was performed after initial seeding of $1x10^5$ cells every 24h for 10 days.

3.5.2 Silencing of *CCDC50* in primary CLL cells

Interestingly, quantitative real-time PCR experiments revealed overexpression of CCDC50 in five out of eight MCL patients (mean: 3.4-fold) and 24 out of 28 CLL patients (mean: 3.5-fold) in comparison to CD19+ selected B-cells of healthy donors. In order to investigate whether silencing of CCDC50 has also an antiproliferative impact on primary cells, transient knockdown experiments were performed in freshly isolated B-cells from peripheral blood of CLL patients. Transfection of primary B-cells was performed via nucleofection of $5x10^6$ cells with an optimized concentration of 500nM siRNA. CLL cells were cultured in conditioned medium of HS5 stroma cells. Every 24h fresh and sterile filtered medium was added to the CLL cells. Following transient transfection of siCCDC50#3 into primary B-cells from CLL patients (B-CLL 48, 49, 50, 51, and 61), the cells were cultured for 72h in conditioned medium. Quantitative real-time PCR and a cell viability assay revealed in all patients a CCDC50 gene knockdown between 40-80% (Figure 23a) correlating with 50-60% reduction in cell viability (Figure 23c). Analysis of the CCDC50 protein level in CLL patient 49 at 48h and 72h after transfection showed a reduction compared to a negative and a mock control (Figure 23b).

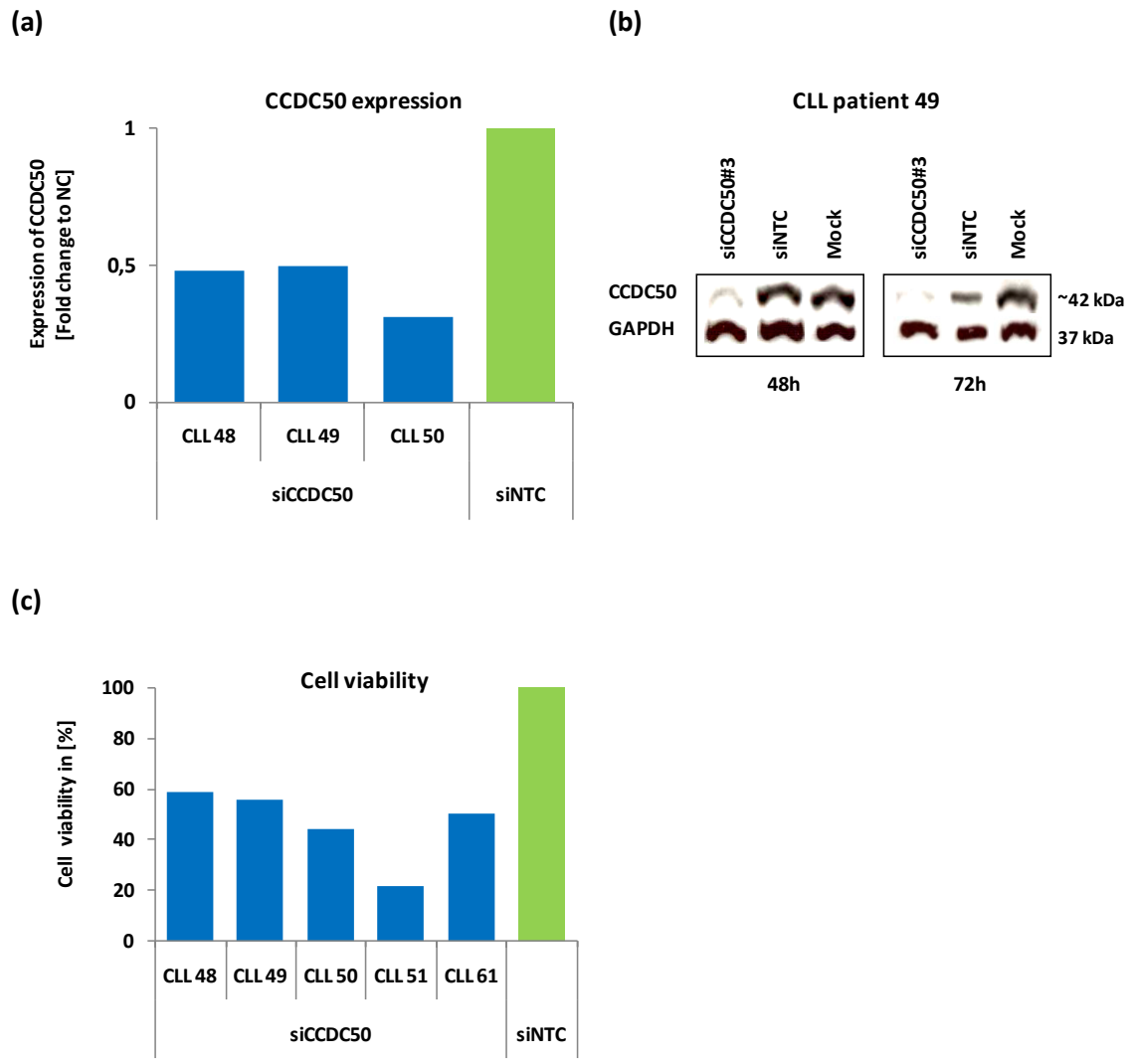

Figure 23: Silencing of *CCDC50* in primary CLL cells. (a) qRT-PCR showed *CCDC50* knockdown in patients 48, 49, and 50 in comparison to a non-template control ('siNTC'). (b) Western blot analysis showed *CCDC50* protein expression in CLL patient 49 at 48h and 72h after transfection of siCCDC50#3. *CCDC50* protein expression was measured additionally in cells transfected with siNTC and in mock transfected cells. GAPDH served as loading control. (c) Cell viability assay in CLL patients 48, 49, 50, 51, and 61 was performed, measuring the ATP level of primary CLL cells, transiently transfected with siCCDC50 and siNTC.

3.5.3 Involvement of *CCDC50* in the NFκB pathway

CCDC50 was previously identified to suppress NFκB activity through its interaction with *TNFAIP3*. Knockdown of *CCDC50* was shown to activate NFκB signaling, even without *TNF*α stimulation (Bohgaki *et al.*, 2008). *NFκB* can either promote or inhibit carcinogenesis and cancer progression. In MCL and CLL, NFκB activity is often correlated with increased cell survival (Malynn *et al.*, 2009; Schmitz *et al.,* 2009). To investigate the correlation between *CCDC50* induced cell survival and NFκB signaling, NFκB reporter assays have been performed in HEK-293T cells. These cells combine three major advantages: (1) a higher transfection efficiency (90%) than MCL or CLL cells (40-80%), (2)

a high inducibility of the NFκB reporter by TNFα (7-fold) and (3) low *CCDC50* expression levels (0.9-fold) in comparison to JVM-2 cells (8.4-fold), when comared to the mean of two housekeeping genes (Figure 24a). NFκB reporter plasmids (p6xNFκB-firefly-luciferase and pCMV-renilla-luciferase) were co-transfected together with either a siCCDC50 or a plasmid coding for *CCDC50* (pCMV_CCDC50). 24 h after transfection, the NFκB activity was induced by 50 ng/ml TNFα and measured before (0h) as well as 3h and 6h post induction (Figure 24b). After normalizing the activity of the firefly luciferase to the activity of the renilla luciferase, our results showed a direct correlation of inducibility and *CCDC50* expression. High *CCDC50* expression levels resulted in a 16-fold NFκB induction by TNFα, while low *CCDC50* expression levels only showed a 6-7-fold induction.

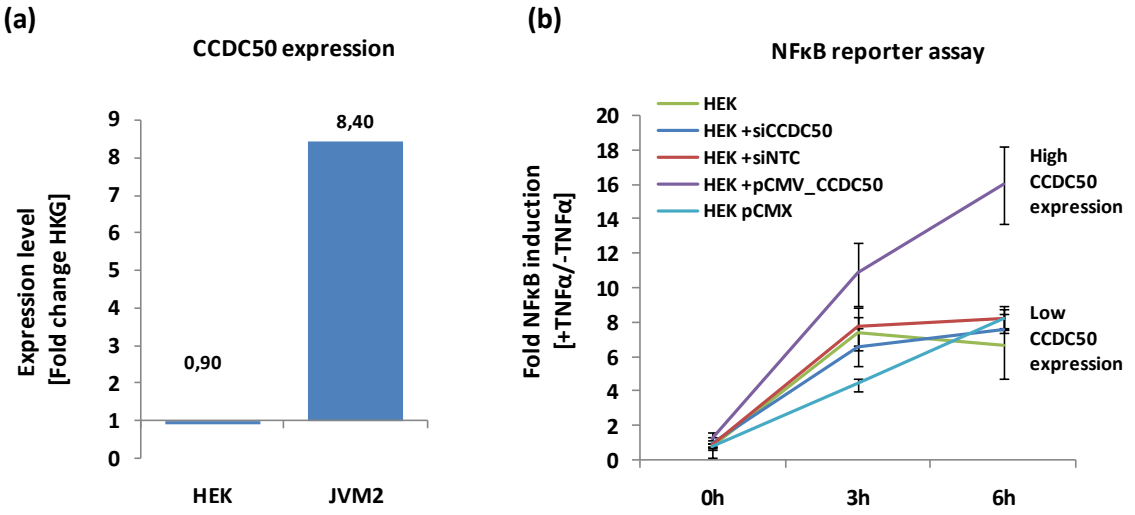

Figure 24: NFκB reporter assay in HEK-293T cells after *CCDC50* gene modulation. (a) Quantitative RT-PCR shows the *CCDC50* expression level of HEK-293T and JVM-2 cells after normalization to the mean of two housekeeping genes (*PGK1* and *DCTN2*). (b) TNFα induction in HEK-293T cells was performed 24h after co-transfection of the reporter plasmids alone (HEK-293T) or together with either a siRNA (siCCDC50, siNTC) or an expression plasmid (pCMV_CCDC50 or pCMX). NFκB reporter activity was measured before (0h) as well as 3h and 6h after TNFα induction. Normalization was performed when comparing the activity of the firefly luciferase to the activity of the renilla luciferase. Finally, the fold induction was calculated as correlation between TNFα induced cells to uninduced cells.

3.5.4 Involvement of *CCDC50* in CLL cell survival

As previously shown, conditioned medium obtained from HS5 cells have promotional effects on primary CLL cell survival (Seiffert *et al.*, 2007). Expression array data comparing CLL cells before and after co-culture with HS5 cells provide evidence that the NFκB cascade is induced, explaining the enhanced *in vitro* survival of CLL cells in co-culture. In CLL cells, the NFκB cascade is discussed in having promotional effects on cell proliferation. The *IL8* expression is induced following *NFκB* activation and found among

the top genes upregulated after co-cultivation (Seiffert *et al.,* manuscript in preparation). *TNFAIP3* is, on the one hand, induced after *NFκB* activation but is, on the other hand, a negative feedback regulator of *NFκB* signaling. *TNFAIP3* is downregulated in co-culture experiments. These findings support the hypothesis, that *NFκB* has promotional effects on cell survival. To answer the question whether *CCDC50* was differentially expressed during co-cultivation of primary CLL cells and to understand the effects that *CCDC50* has on NFκB-induced cell survival, freshly isolated CLL cells from peripheral blood were cultivated in conditioned medium for 48h. In qRT-PCR experiments the gene expressions of *CCDC50*, *TNFAIP3* and *IL8* were measured before and after cultivation (Figure 25). Interestingly, in CLL patient 48, a decrease of *CCDC50* and *TNFAIP3* expression was observed 48h after cultivation in conditioned medium. The *IL8* expression level increased which correlated with the induction of the NFκB pathway and the survival of B-cells.

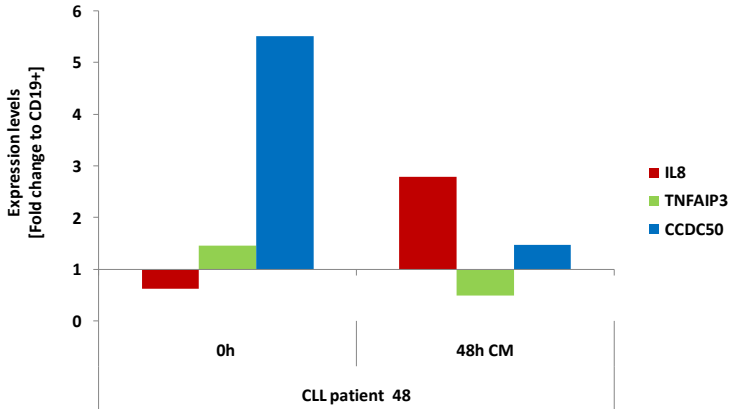

Figure 25: Quantitative RT-PCR showing the expression levels of *IL8*, *TNFAIP3* and *CCDC50* in primary cells of CLL patient 48. Expression levels were measured in B-cells directly after their isolation from peripheral blood (0h) and after cultivation in conditioned media (CM) for 48h. Genes were first normalized to housekeeping genes PGK1 and DCTN2. Finally, expression was compared to CD19+ B-cells of healthy donors (n=9).

3.5.5 Genome wide expression changes after *CCDC50* modulation

As investigated in this study by quantitative real-time PCR experiments, the three MCL cell lines JVM-2, Granta-519, and Jeko showed different *CCDC50* expression levels (2.9-fold, 1.3-fold and not detectable). Therefore, genome wide gene expression changes after *CCDC50* modulation in the two MCL cell lines JVM-2 and Granta-519 were performed on the Illumina expression array platform. For modulation of *CCDC50* expression, siCCDC50#3 and pCMV_CCDC50 as well as the negative controls siNTC ('Non-Template-Control') and pCMX were transiently transfected into JVM-2 and Granta-519. After seventy two hours, RNA was isolated, examined for the *CCDC50* expression status, and profiled for genome wide expression changes. Quantitative RT-PCR revealed a 0.6-fold expression of cells silenced for *CCDC50* and a 4.3-fold overexpression in JVM-2 cells

after transfection of pCMV_CCDC50, setting the controls siNTC and pCMX to basal level expression. In the cell line Granta-519 similar results were achieved after modulation of *CCDC50* expression (Figure 26a,b).

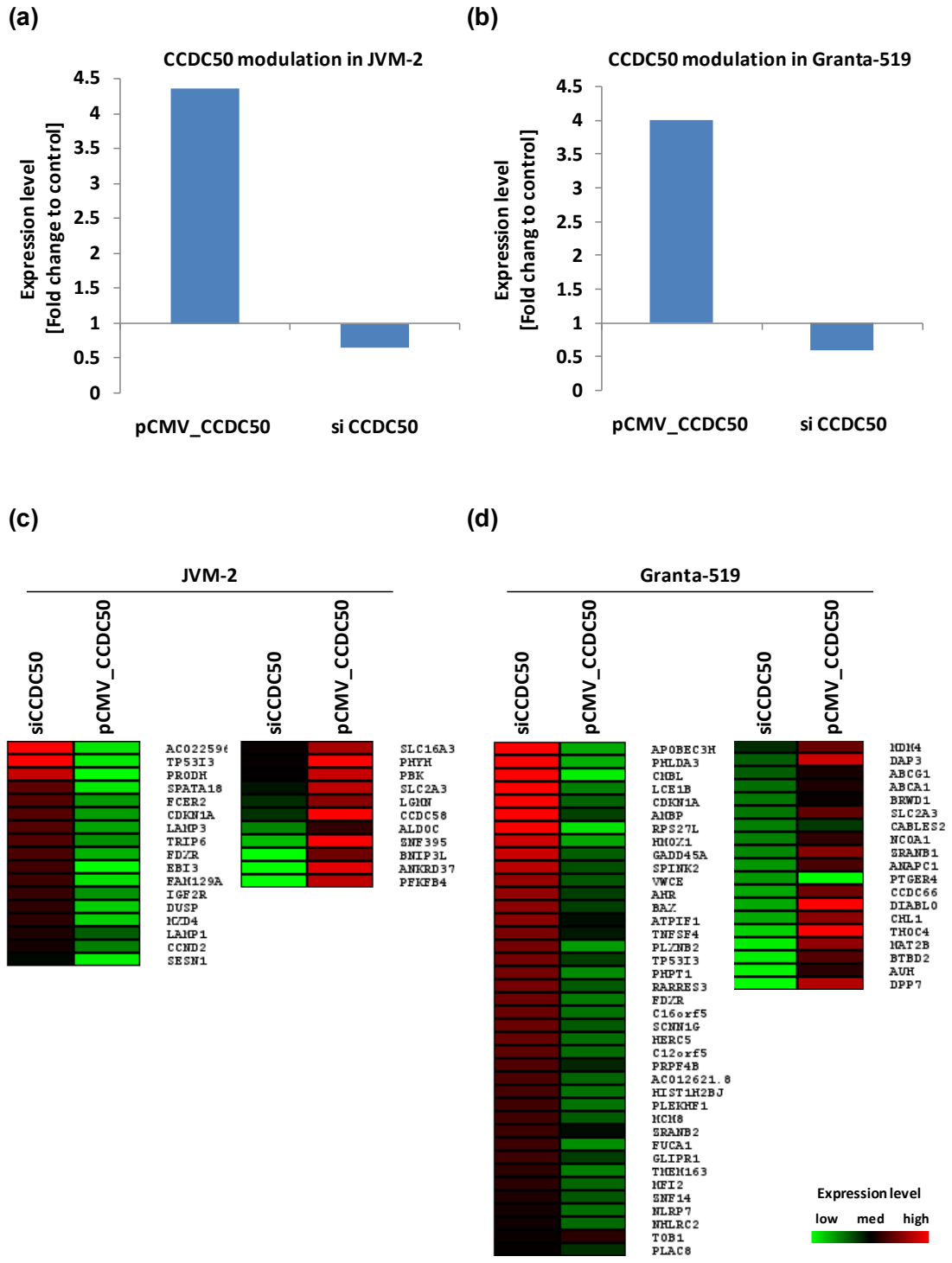

Figure 26: Modulation of *CCDC50* gene expression in MCL cell lines. *CCDC50* silencing and overexpression was performed in MCL cell lines JVM-2 (a) and Granta-519 (b). Genome wide gene modifications after *CCDC50* downregulation (siCCDC50) or overexpression (pCMV_CCDC50) are shown in JVM-2 (c) and Granta-519 (d). Expression was normalized to a non-template control, which is siNTC or pCMX. Green=downregulated genes; black=median gene expression; red=upregulated genes.

Expression profiling revealed in the cell line JVM-2 a total of 28 deregulated genes (17 upregulated and 11 downregulated), and in the cell line Granta-519, 39 aberrantly expressed genes (20 upregulated and 19 downregulated) as shown in Figure 26c-d and in Table 7-8 (see supplementary). Among them, a majority of genes was involved in p53 signaling pathways. Beside *TP53I3*, two further oxidoreductases were found overexpressed in JVM-2: *FDXR* (rank 9) and *SESN1* (rank 17). In the cell lines JVM-2 and Granta-519 the genes *TP53I3* (rank 2, 17), *CDKN1A* (rank 6, 5), and FDXR (rank 9, 20) were upregulated following *CCDC50* silencing. Among upregulated genes affected only in the cell line JVM-2 that are involved in apoptosis induction or cell cycle inhibition, were *PRODH* (rank 3), *LAMP3* (rank7), FAM129A (rank 11), *MXD4* (rank 14), and SENS1 (rank 17), whereas genes found upregulated only in Granta-519 were *PHLDA3* (rank 2), *GADD45A* (rank 9), *BAX* (rank 13), and *RARRES3* (rank19). Among the downregulated genes, involved in maintenance of cell cycle affected in JVM-2 were *BNIP3L* (rank 3) and *LGMN* (rank 7), whereas in Granta-519 the genes *MDM4* (rank 19), and *BRWD1* (rank 15) were identified.

4 Discussion

The two B-cell non-Hodgkin lymphoma entities CLL and MCL show recurrent chromosomal gains of 3q25-q29, 12q13-q14 and 18q21-q22. The genetic pathomechanisms affected by these aberrations are mainly not understood. The aim of this study was to identify genes, located within these gained regions, which are involved in cell survival pathways. 24 CLL patients, 6 MCL patients and 6 cell lines, representing both malignancies, were analyzed by expression profiling. 72 candidate genes were identified through comparison of array CGH and expression profiling studies. After gene silencing of these 72 genes in a microtiter-format-based RNAi screen, changes in cell viability were investigated. *CCDC50*, *SERPINI2* and *SMARCC2* emerged as candidates mediating reduction in cell viability. Furthermore, gene knockdown and reporter gene assays revealed a role of *CCDC50* in cell survival pathways of MCL and CLL cells.

4.1 Optimal transfection of MCL and CLL cells via nucleofection

RNAi-based screening has become a powerful *in vitro* tool to identify drug targets that play a role in disease development and progression (Zumbansen *et al*., 2008). Successful screening experiments using siRNAs require efficient delivery of highly functional and specific siRNA molecules into appropriate cells (Boutros *et al*., 2008). While lipid-mediated transfection is a common approach for siRNA delivery, many cell types, including B-lymphocytes like MCL and CLL cells, are not accessible using this technology (Gresch *et al*., 2004; Pscherer *et al*., 2006; Seiffert *et al*., 2007). This limitation prevents analysis of many biologically relevant cell types and restricts siRNA screenings mainly to adherent cell lines that often exhibit specific phenotypic and genetic abnormalities after extended periods of culturing. The use of cancer cells for functional screening is a relevant approach for studying cancer mechanisms. Moreover, the diversity of biological questions requires functional studies in primary cells (Zumbansen *et al*., 2008).

In this work, optimization of transfection conditions for three MCL and CLL cell lines and for primary CLL cells were performed for cuvette nucleofection, as well as for the 96-well shuttle transfection. Using nucleofection, transfection efficiencies between 40-80% could be achieved. In contrast, MCL cells showed very low transfection efficiencies using microinjection (Figure 9). Moreover, microinjection is usually applied for stable transfection of single clones and is not applicable in the context of transient transfection approaches. Most of the tested chemical transfection reagents were highly inefficient in MCL and CLL cell lines. Dharmafect showed good transfection efficiencies for Jeko-1 (80%), JVM-2 (53%) and Eheb (58%) but not for Mec-1, Mec-2 and Granta-519 (all 0%).

For siRNA screening in a 96-well format, a transfection method suitable for all MCL and CLL cell lines had to be established. Nucleofection was therefore the method of choice, which showed best overall transfection efficiencies. The only disadvantage applying this method was the induction of 20-50% cell death. Since the extent of cell death was comparable among different transfection experiments, and since positive and negative controls set the 'hit' threshold that determined whether an siRNA is considered as mediating a positive, negative, or neutral effect in a particular assay, this side effect can be neglected (Echeverri *et al*., 2006). These experiments were the basis for the siRNA screen discussed in chapter 4.4.

4.2 Limitations of the RMCE system in cell lines

In the field of reverse genetics, a technique like RMCE (recombinase-mediated cassette exchange) is of increasing relevance (Baer *et al.*, 2001; Wirth *et al.*, 2007). The procedure permits the systematic modification of higher eukaryotic genomes by targeted integration (Sauer *et al*., 1988; Gu *et al*., 1993; Araki *et al*., 1997; Seibler *et al*., 1997; Seibler *et al*., 1998). For the RMCE strategy applied in our group, this is achieved by the complete exchange of a preexisting 'selection cassette' (HSV-TK-neo) for an analogous cassette carrying the 'gene of interest', either a short hairpin RNA coding insert for gene knockdown or a coding insert for stable gene overexpression. The Cre-lox recombination system has proven to be a useful tool for complementation or genetic manipulation of mammalian cells (Sauer *et al*., 1988; Gu *et al*., 1993; Araki *et al*., 1997; Baer *et al*., 2001; Oumard *et al*., 2006). Integration of the gene of interest into inactive heterochromatin results in little or no transgene expression, whereas integration into active euchromatin frequently allows transgene expression. Since the site of integration can have severe effects on the transcription rate of the gene of interest, the RMCE system clearly defines the integration site and avoids unspecific phenotypic effects (Baer *et al*., 2001). Recently, our lab could show stable integration following cassette exchange thereby stably silencing *CyclinD1* or overexpressing *CDKN2a* in the MCL cell line Granta-519 (Pscherer *et al*., 2006). This current work, in addition, shows the stable integrate the HSV-TK-neo selection cassette into further MCL and CLL cell lines (Eheb, Mec-1, Mec-2, and Jeko-1). The growth of transfected cell clones carrying multiple cassette integration events has been observed repeated times in the cell line Mec-1 (Figure 21). Consequently, most of the selected Mec-1 clones showed the same signal pattern after genomic DNA digestion in Southern blot analysis (Figure 21b). Multiple cassette integration may also be the reason for the high signal intensity and the occurrence of numerous cassette signals in FISH analysis (Figure 21e). The selection of one 'dominant clone' may occur due to a high neomicine (G418) concentration. In this scenario, only cells with multiple integration events may have a certain survival advantage (i.e.

Mec-1+TKneo#17, #21, #34, Figure 21c). Limited dilution following nucleofection and a decreased neomicine concentration, from 2mg/ml to 1mg/ml, solved the problem of the 'dominant' clone selection. In this way Mec-1+TKneo clones, carrying a single integration event, were successfully generated (Mec-1+TKneo#8, #9, and #10, Figure 21b). One major limitaton of the RMCE approach was the site directed cassette exchange against the gene of interest. After co-transfection with the Cre-recombinase and pSUPERdL vectors, cells died under optimized selection conditions, independently of the integrated sh-RNA sequence. The short hairpin constructs targeting *CCDC50* and luciferase (pSUPERdL_Zeo-shCCDC50 and pSUPERdL_Zeo-shLuciferase) have been tested repeated times for RMCE, but none of the transfected cells survived. Titration of plasmid concentrations have been tested in addition to decreasing antibiotic concentration without any success. Two further system limitations were identified during validation of the cassette integration: Low signal intensities in Southern blot and FISH analyses. Southern blot analyses were perfomed using digoxigenin-labled probes (Figure 21c) as well as radioactively labled probes (Figure 21b). Most prominent results were achieved, when (1) probes were radioactively labeled, (2) a minimum of 10µg of endogen-free, highly purified DNA was used for restriction analysis, (3) X-ray intensification screens were applied for higher signal intensities, and (4) a minimum film exposure time of one week was applied (Figure 21b). In FISH analyses the low signal intensity of a 3 kb probe resulted in hardly detectable localization of a single integrated HSV-TK-neo cassette on metaphase chromosomes. In cell clones with multiple HSV-TKneo cassette integration events, as validated in advance by Southern blot analysis, the fluorescent signals on metaphase chromosomes could easily be detected (Figure 21e). The utilization of increased fluorescent dyes resulted in high background signals and did not overcome these limitations. Since the attempts for the generation of a stable JVM-2 cell line via RMCE did not reveal the homologous recombination event, random integration was the method of choice in order to establish stable cell lines for functional approaches. To overcome locus dependent integration effects, two independent clones of each stable cell line were functionally characterized. When both clones showed comparable phenotypic behavior, which differed from the parental cells, the phenotype was further analyzed and correlated with stable silencing of the candidate gene. A successful stable silencing of *CCDC50* was performed in MCL cell line JVM-2 and CLL cell line Mec-1. Two independent stable clones for JVM-2 and Mec-1, showing a random integration of sh_CCDC50, were obtained after the first round of transfection and zeocin selection (Figure 22b). In summary, the RMCE system is a tool for the directed site specific recombination event, but is most probably limited to easy to transfect cells. Failure of RMCE may be caused by the nucleofection procedure, which caused up to 50% cell death. In this study, the integration and characterization of a single recombination event turned out to cause unexpected problems. Therefore, random integration of the short

hairpin construct was the method of choice showing successful and time efficient generation of stable cell lines for functional analysis.

4.3 Expression profiling studies of MCL and CLL cells reveal candidate genes

Expression analysis of genes located in commonly gained chromosomal regions revealed 72 overexpressed genes in MCL and CLL. Antagonizing these genes using the RNAi technology identified 18 of these as candidates, of which 12 were novel and 6 were previously discussed: *CCDC50* (Schmechel *et al*., 2004; Bertoni *et al*., 2006; Salaverria *et al*., 2007), *ECT2* (Rubio-Moscardo *et al*., 2005; Jares *et al*., 2008; Sander *et al*., 2008), *SERPINI2* (Tagawa *et al*., 2005), PAK2 (Salaverria *et al*., 2007), *KLHL6* (Salaverria *et al*., 2007) and ITGB7 (Greiner *et al*., 2006). *DDIT3*, which showed loss-of-viability only in primary CLL, was previously identified as expressing increased RNA levels in progressive CLL in comparison to stable CLL primary cells (Falt *et al*., 2005). Other previously reported genes like *GLI1* (Sander *et al*., 2008), *Timeless* (Haslinger *et al*., 2004) or *TCF4* (Rizzatti *et al*., 2005) did not induce reduction in cell viability after their gene knockdown.

It was recently shown that highly proliferative and clinically aggressive variants of MCL have a complex phenotype with frequent gains on 3q and 12q (Bea *et al*., 1999; Rubio-Moscardo *et al*., 2005; Salaverria *et al*., 2007). Based on the expression profiling of 71 primary MCL patients on the lymphochip platform, a recent publication characterized especially overexpressed candidate genes on chromosome 3 (Salaverria *et al*., 2007). Among them are genes involved in cell proliferation (*YEATS2*, *PICK3*, *ACTL6A*, *RFC4*, and *CENTB2*) and cellular homeostasis (*SIAH2*). Ten genes were identified as being specifically upregulated in MCL compared to B-cell like diffuse large B-cell lymphoma (DLBCL): *GPR160*, *PH3*, *PIK3CA*, *FXR1*, *SIAT1*, *LPP*, *CCDC50*, *CENTB2*, *ACK1* and *TFRC*. Seven genes were found upregulated in MCL and DLBCL: *SIAH2*, *PDCD10*, *RFC4*, *OPA1*, *PPP1R2*, *PAK2* and *KIAA0226*. Further overexpressed genes, detected on the lymphochip platform, were *KLHL6*, *ETV5*, *DVL3* and *GPR160*. Expression profiling, performed in this work, confirmed the candidates *YEATS2*, *CCDC50*, *ACTL6A*, *BCL6*, *RFC4*, *PAK2*, *DVL3*, *KLHL6* and *KIAA00226*. An interesting candidate gene identified on expression array was *APOD* with a mean overexpression of 130-fold in primary MCL and 15-fold in primary CLL cells. Knockdown of *APOD* did not reveal changes in cell viability in primary CLL cells or in MCL cell lines (not shown). So far, none of the discussed candidate genes located on chromosome 3q was functionally characterized for its role in the pathogenesis of MCL or CLL. Gains on chromosome 12 are found frequently in CLL and MCL (17% and 16%, respectively) (Bea *et al*., 2008). Overexpression of *CDK4*, the most frequently discussed

candidate gene on chromosome 12q13, was successfully correlated with enhanced induction of cell survival pathways and thereby inhibited apoptotic stimuli.
In this study, a large set of further candidate genes were identified as overexpressed on chromsome 12q in primary CLL cells: *RAPGEF3* (47-fold), *DGKA* (7.6-fold), *SMARCC2* (3.5-fold), *Timeless* (3.4-fold), *DDIT3* (3-fold), and *ARHGAP9* (2.3-fold). Among overexpressed genes in MCL cells, the following genes were discovered: *CDK2* (6-fold), *HOXC6* (4-fold), *DGKA* (4-fold), *Timeless* (3.7-fold), *CDK4* (3.7-fold), *MYL6B* (3.6-fold), *TUBA1B* (3.5-fold), *KIAA0286* (3-fold) and *ARHGAP9* (2-fold). An overexpressed gene in recurrently gained genomic region 18q21 was *TCF4* that showed an even higher expression level (8.3-fold) than the candidate gene *BCL2* (2-fold) in patients (Rosenwald *et al*., 2003, Rizatti *et al*., 2005, Rubio-Moscardo *et al*., 2005; Jares *et al*., 2008). In summary, expression profiling of primary MCL and CLL cells identified recently published as well as novel candidate genes on chromosomes 3q, 12q, and 18q. Previous studies reported overexpressed genes predominantly without their functional investigation. In this work, further characterization of the 72 candidate genes was performed applying an RNAi screen in MCL and CLL cells and investigating the effects on cell survival and cell proliferation.

4.4 siRNA screen in MCL cell lines JVM-2 and Granta-519

The remarkable gene knockdown technique based on RNAi has opened exciting new avenues for genetic screens in human cells. The success of large-scale RNAi studies depends on a careful development of phenotypic assays and their interpretation in a relevant biological context (Boutros *et al*., 2008). The focused RNAi screen, which was performed in this study using the MCL cell lines Granta-519 and JVM-2, will only be the first step in the comprehensive analysis of the pathomechanisms affected by the genomic gains 3q, 12q, and 18q; the end of the screen is actually the beginning of a new experiment.

4.4.1 The use of siRNA, shRNA and esiRNA

In this work, a loss-of-function screen was applied using a pool of four siRNA sequences per gene in a primary screen. Validation of candidates was performed in a validation experiment by testing the phenoypic effect of the four siRNA sequences separately. Investigations of a specific gene function were analyzed in stable silencing experiments using a shRNA coding expression vector. Because long intracellular dsRNAs activate the interferon response, leading to unspecific apoptosis, RNAi in human cells need to be initiated by siRNAs of 21–23 nucleotides in length, which evade the interferon response (Elbashir *et al*., 2001). Since the knockdown efficiencies of single siRNAs vary strongly,

multiple independent siRNAs per gene are required. These can be screened individually or in pools. Pooling of siRNAs can reduce the costs of screening, but it increases the likelihood that the phenotype is caused by an off-target effect of a single siRNA (Elbashir *et al*., 2001). This can be determined by retesting hits with multiple independent siRNAs separately. Several laboratories have developed vector-based shRNA libraries that can be either transfected into cells or packaged into viruses, and transduced into cells that are difficult to transfect, such as primary cells. Because retroviruses and lentiviruses integrate stably, these libraries are often screened in pools. Clonal cell populations of the desired phenotype can be selected and the 'causative' shRNA is identified. Alternatively, barcoding screens can be performed in which cells are transduced with pooled viruses that contain shRNAs, which can be uniquely identified with a molecular barcode (Berns *et al*., 2004; Paddison *et al*., 2004; Silva *et al*., 2008; Schlabach *et al*., 2008). After phenotypic selection, enrichment of integrated shRNAs fused to barcode sequences is measured using a microarray that contains sequences of the barcode (Berns *et al*., 2004; Paddison *et al*., 2004; Silva *et al*., 2008; Schlabach *et al*., 2008). Another approach for generating a large-scale RNAi library involves endoribonuclease-cleaved siRNAs (esiRNAs). In this approach, long dsRNA are synthesized in vitro, digested into smaller dsRNA fragments, and transfected into cells. Such libraries have been shown to be highly efficient and have fewer off-target effects than siRNAs (Kittler *et al*., 2007). The smaller the transfected construct, the better the transfection efficiency in MCL and CLL cell lines. siRNAs are more easily to transfect than larger expression plasmids coding for shRNAs. In this study, the use of 21–23 nucleotide long siRNAs showed better transfection efficiencies compared to esiRNAs (not shown). Therefore the siRNA screen was performed with a pool of four siRNA molecules. Positive controls such as *PLK1*, *CCND1*, *DUSP5*, *KIF11* or *BCL2* resulted, as expected, in a reduction in cell viability. Testing a variety of independent negative controls such as scrambled siRNAs (pools or single sequences) or siRNAs targeting luciferase or GFP was necessary to reveal controls mediating no off-target effect or interferon response in MCL and CLL cell lines. Since each negative control can cause an unspecific effect on the cells, a minimum of three negative control siRNAs were included in each experiment. In this way, a reliable baseline was established, which was calculated as the mean of all negative controls. The dynamic range of the chosen read-out assay therefore represented the difference between 'baseline values' that were obtained from negative control genes and representative 'positive hit values' that were obtained from positive control genes. The focused loss-of-function screen was performed by applying siRNA pools (Qiagen) in the primary screen, while using either the single siRNA sequences from the initial screen or three to four independent siRNA duplexes from a different supplier (Ambion, Dharmacon) in the validation experiments. After successful validation of the 'loss-of-viability' phenotype, shRNA coding plasmids were used for stable silencing experiments.

4.4.2 Candidate genes with impact on cell survival

In this study, a loss-of-function screen was performed in MCL cell lines applying the 96-well shuttle nucleofection technology. A previous siRNA screen had been performed in Granta-519 applying the single nucleofection approach (Ortega-Paino *et al*., 2008). The reliable transfection efficiency of primary CLL cells and cell lines using nucleofection has been reported earlier (Gresch *et al*., 2004; Seiffert *et al*., 2007; Pscherer *et al*., 2006). A lentiviral-based RNAi screen has recently been performed in B-NHL cell line RAMOS (Ruiz-Vela *et al*., 2008) and in diffuse large B-cell lymphoma cell lines (Shaffer *et al*., 2006). Moreover, shRNA libraries were used succesfully to screen for phenotypes in cancer cells, leading to the discovery of five target genes of *p53* that regulate p53-dependent cell cycle arrest and a new tumor suppressor gene for the phosphatidyl-inositol-3 kinase (PI3K) pathway (Berns *et al*., 2004; Westbrook *et al*., 2005). In contrast to the screen applied in this work, the shRNA screens by Berns and Westerbrook employed a 'positive selection' experimental scheme. First selective pressure was exerted that prevented cells from growing and/or surviving. shRNAs that allowed cells to circumvent these inhibitory constraints were positively selected. Three to six different shRNA coding vectors that were inducible by tetracycline were transduced into DLBCL cell lines. The aim of this work was to screen for genes with oncogenic potential, which induced cell cycle arrest or inhibition of cell survival after functional gene knockdown. The 96-well nucleofection technology enabled a simultaneous and efficient transfection of siRNAs into cells in a multiwell format. The focused set of 72 siRNAs was selected according to identified overexpressed genes coded on the gained regions 3q, 12q and 18q. The initial screen resulted in 18 candidates with a phenotype of reduced cell viability (Figure 16). Off-target effects, low silencing efficiency of the respective gene or technical limitations may have contributed to the results of 4 of 18 genes, where the loss of cell viability could not be validated in the majority of tested individual siRNA sequences (*DDIT3*, *USP13*, *FAM43A* and *HOXC6*) as shown in Figure 30. The reason may be technical limitations, low knockdown efficiencies or off-target effects of single siRNA sequences. The latter play major roles in the generation of false positives and are key limitations in all types of screening approaches. siRNAs are known to produce a 'signature' of inhibited transcripts in addition to the targets being analyzed (Jackson *et al*., 2003; Snove *et al*., 2004; Tschuch *et al*., 2008). Off-target effects and induction of the interferon response can be examined to rule out non-specific effects of the introduced sequence. At first, by studying similar target sequences using bioinformatics; secondly, by examination of interferon markers such as *OAS1* (Bridge *et al*., 2003); and thirdly, by transcriptional profiling with multiple siRNAs that are directed against the same target (Jackson *et al*., 2004). In this work, 14 of 18 candidate genes from the initial screen were validated by the use of different individual siRNA sequences for each investigated gene

(*ARHGAP9*, *CCDC50*, *ECT2*, *IRAK3*, *ITGB7*, *KLHL6*, *MALT1*, *PAK2*, *RAPGEF3*, *RARRES1*, *RHEBL1*, *SERPINI2*, *SMARCC2*, and *TSFM*; Figure 17a). In this validation experiment, primary CLL cells have also been tested for the phenotypic changes after gene knockdown. Interestingly, *DDIT3* showed a reduction in cell viability only in primary CLL cells. Six genes (*USP13*, *FAM43A*, *PAK2*, *KLHL6*, and *MALT1*) were not tested in primary CLL cells due to limited availability of primary cell material. Eight candidate genes (*ECT2*, *PAK2*, *IRAK3*, ARHGAP9, *RAPGEF3*, *RHEBL1*, *ITGB7*, and *TSFM*) displayed the phenotype only in MCL cell lines. Interestingly, three candidates showed a loss-of-viability phenotype both cell lines and primary CLL cells: *CCDC50*, *SERPINI2* and *SMARCC2*. Published data on these candididates documented an overexpression for *SERPINI2* in 32-70% and for *CCDC50* in 80% of MCL patients (Tagawa *et al*., 2005; Rosenwald *et al*., 2003). *SMARCC2* is a novel, so far unpublished gene on 12q13 related to MCL and CLL neoplasias.

4.4.3 The importance of screening conditions

Primary screens are usually conducted in replicates to increase the confidence of positives and to avoid the false negatives that arise in large-scale screening (Boutros *et al*., 2008). All candidate hits are usually retested to confirm specificity. The result of a primary screen will be a list of candidates that reproducibly score as positive in the primary assay (Boutros *et al*., 2008). It is important to have a detailed screening schedule of every step in the process and to keep track of the screen parameters: date, time of day, person setting up the assay, person scoring the screen, lot numbers of reagents used, equipment used, temperature variations, drying of plates and possible contaminations. To keep all screening parameters constant, each replicate in this study was set up at the same time of the day (morning) and a single task (siRNA preparation, cultivation of cells, 96-well nucleofection, pipetting of the transfected cells from 96-well-cuvette-plate into cultivation plates, adding medium, and conduct read-out assays) was carried out repeatedly by the same person. Pipettes and tips were used from the same supplier and kept constant throughout the screening and read-out procedure. In order to avoid evaporation effects, due to multiple opening of the incubator following uncontrolled temperature and $C0_2$ decrease, the incubator was only occupied by screening plates from one person. Throughout the incubation period of 72h, the incubator remained closed and cultivation plates were placed in the same position in each replicate. All reagents for the read-out-assays (Cell Titer Glo Reagent, Propidium-Iodide) were used from one batch. The read-out time (72h) and pipetting procedure was also kept constant for all replicates throughout the screen. Following these rules, the occurrence of false positives or false negatives, due to technical or handling approaches, was minimized as much as possible.

A recent publication showed a loss-of-function study in MCL cell line Granta-519 by applying the single nucleofection method (Ortega-Paino *et al*., 2008). Major advantages of the 96-well-shuttle format are the simultaneous treatment of all transfections within a short time window (three to four minutes), enhanced transfection efficiency and low variations when compared to single transfections. By minimizing (1) edge dependent evaporation effects ('edge effects') by filling two outer rows of a 96-well plate with medium, (2) plate variances by using one batch of cultivation plates and (3) positives and negatives by applying a minimum of 3 different negative and positive controls on each cultivation plate, aimed to increase the number of true positive candidates. Applying these guidelines, three out of 72 genes could be validated as functionally related to cell survival in MCL and CLL cells.

4.4.4 The selection of proper controls

The false negative rate is usually estimated by measuring the hit rate for known positive genes. Comparing reproducibility between duplicate or triplicate wells can also provide information on false negative rates (Boutros *et al*., 2008). In some cases, the insufficient silencing of a gene might not generate an observable phenotype, thereby contributing to the false negative rate of the screen. In addition, there can be considerable experimental variability in the degree of knockdown. The false positive rate of a primary screen can be estimated using the results of the secondary assays. In a well-designed and well-controlled screen, the final false positive rate should be negligible. Nevertheless, the false negative rate in this work was unexpectedly high. In previous studies, the knockdown of genes like *BCL2*, *CCND1*, *KIF11*, *PLK1* or *DUSP5* were reported to decrease cell viability in MCL cells (Guan *et al*., 2005; Reagan-Shaw *et al*., 2005; Pscherer *et al*., 2006; Ortega-Paino *et al*., 2008, Tucker *et al*., 2008). In this work, these positive controls did not show the expected phenotype in all of the three replicates. A reproducible decrease in cell viability was achieved after functional gene knockdown of *PLK1*, which was placed in four independent wells of a screening plate. Surprisingly, reduction in cell viability could not be observed in all of the four wells on a 96-well plate. Position dependent effects were excluded since the well position on a plate, where *PLK1* was showing the corresponding loss-of-viability phenotype, was different in each of the three replicates. All of the other controls were used just once per plate and did not show reduction in viability in all of the three replicates. A possible explanation could be an unequal transfection efficiency throughout one plate resulting in a low knockdown of the gene. Evidence for this explanation was given by corresponding FACS analysis, which showed a comparable result for the same *PLK1* sample as the cell viability assay. In summary, the cell viability assay was highly sensitive and reliable, that could be validated by FACS analysis (Figure 16). 14 of the 18 candidates from the primary screen

could be validated in the validation experiment. The occurrence of false negatives was most probably due to the siRNA sequence itself or technical difficulties (i.e. unequal transfection efficiency) in the nucleofection approach.

4.4.5 The identification of weak and strong targets

The five independent controls (*PLK1*, *BCL2*, *CCND1*, *KIF11*, and *DUSP5*) used in this screen covered both weak and strong positives that allowed for the detection of weak and strong candidate genes. Weak read-out effects could be caused either by partial knockdown of a gene with a strong effect or a strong knockdown of a gene with a weak effect (Boutros *et al*., 2008). Since the gene knockdown was not tested in the RNAi screen, siRNAs causing a reduction in cell viability comparable to the positive controls were further tested in the validation assay. To also take partial knockdown events into consideration, siRNAs fulfilling a lower threshold (chapter 3.3.2) were additionally retested in the validation experiment.

4.4.6 Hit validation of the siRNA screen

No matter how specific a primary screen is, validation experiments are important for identifying the genes that are particularly relevant (Moffat *et al*., 2006; Boutros *et al*., 2008). Validation of the 18 candidate genes was performed by transfecting up to four single siRNA sequences for each gene separately into the appropriate cell line. Due to limited availability of primary material, pools of two to four siRNA sequences were transfected into primary CLL cells. Validation of a candidate gene was scored positive, if two out of four siRNA sequences reduced cell viability in cell lines and the pool of siRNAs reduced the cell viability in primary CLL cells. Recent publications discussed that two or more siRNA sequences that knockdown target protein levels and elicit the same phenotype, are a sufficient proof of target specificity (Moffat *et al*., 2006; Boutros *et al*., 2008). Moreover, independent siRNA sequences from different suppliers were used in this work in order to minimize the rate of sequence dependent effects. In addition, the multiwell format was changed to a 6-well format and cuvette nucleofection for the validation assays. Following this straight forward approach, validation of 14 of the 18 candidate genes from the primary screen was successful in the validation analysis. For three genes, the loss-of-viability was detected in cell lines and in primary cells: *CCDC50*, *SERPINI2*, and *SMARCC2*. The most prominent reduction in cell viability after gene knockdown in primary cells and cell lines revealed the gene *CCDC50*. Although an unexpected number of false negatives occurred in the primary screen, the high validation rate of candidates in the validation experiment revealed that a reliable cut-off for the selection of candidates was chosen in this study (chapter 3.3.2).

4.4.7 Validation of a candidate gene with different siRNA sequences

RNAi screens in mammalian cells have the potential to shed light on processes that are directly relevant to human health; however, important challenges remain. Validation strategies have to be carefully adapted for RNAi screens. One approach is to only consider and validate common hits that are identified using different libraries or siRNA sequences. This would yield in a short list of highly validated phenotypes, although it would greatly increase the false negative rate. Because siRNA efficiency and specificity is still improving, certain issues remain unresolved and recommendations of how many independent siRNAs should be used are evolving (Boutros *et al*., 2008). One way to overcome sequence dependent effects is to use multiple siRNAs from different suppliers. The candidate gene *CCDC50* has been identified using a pool of four siRNA sequences (Qiagen). Validation experiments were set up with three different individual siRNA duplexes (Ambion). Due to a comparable phenotype that could be shown in both approaches, *CCDC50* was proven as candidate gene, showing effects on cell survival in MCL and CLL cells.

4.5 The candidate genes *CCDC50*, *SERPINI2* and *SMARCC2*

Loss-of-function screens offer the highest discovery potential, as they simply analyze single gene loss-of-function phenotypes in otherwise unmodified cells. In this study, *CCDC50*, *SERPINI2* and *SMARCC2* were identified as inducing reduction in cell viability following functional gene knockdown in MCL cell line JVM-2 and in primary CLL cells. Moreover, *CCDC50* was shown to be overexpressed in MCL and CLL cell lines specifically. *CCDC50* is located in genomic gained region 3q29 which is reported to have prognostic impact, mainly in MCL patients with low survival (Salaverria *et al*., 2007). Pathologically relevant genes are reported to be located in genomic gained region 3q26-q29 (Bentz *et al*., 2000). So far, none of the predicted candidate genes (mainly: *SERPINI2* and *ECT2*) were functionally characterized in MCL or CLL cells (Rubio-Moscardo *et al*., 2005; Tagawa *et al*., 2005; Jares *et al*., 2008; Sander *et al*., 2008). This study showed that *CCDC50* has survival stimulating effects in both neoplasias. The identification of robust molecular and genetic prognostic predictors on chromosome 3q may become an essential tool in the clinical practice. As each patient shows different chromosomal aberrations, the identification of novel molecular markers is a significant prerequisite in order to predict the best therapy for each patient.

4.5.1 *CCDC50* is involved in NFκB signaling pathways and has survival stimulating effects

CCDC50 was shown during the course of this thesis work to be overexpressed in MCL cells in comparison to other lymphomas (Salaverria *et al*., 2007) and to benign reactive lymph node tissue of MCL patients (Schmechel *et al*., 2004). We showed that *CCDC50* is upregulated in primary MCL and CLL cells and in respective cell lines, in comparison to CD19 positive cells of healthy donors, or to the cell line LCL-WEI. *CCDC50* was identified as a candidate gene with a 3.5-fold mean overexpression ranging from 1.5-fold up to 10-fold, in 5 MCL and in 24 CLL patients. This is in accordance with published data, showing *CCDC50* as 2.6-fold overexpressed in MCL in comparison to B-cells of healthy donors (Schmechel *et al*., 2004). Moreover, this study showed that *CCDC50* was upregulated in MCL and CLL cell lines. The mean RNA expression of *CCDC50* in CLL (1.7-fold) and MCL (1.4-fold) cell lines was significantly higher than in Burkitt´s lymphoma (0.28-fold), DLBCL (0.05-fold) and Hodgkin´s lymphoma (0.47-fold). Recent publications reported an involvement of *CCDC50* in NFκB and EGFR signaling pathways (Bohgaki *et al*., 2008; Tashiro *et al*., 2006; Kameda *et al*., 2009). CCDC50 is phosphorylated and ubiquitinated upon EGF stimulation and inhibits EGF receptor downregulation (Tashiro *et al*., 2006). Phosphorylated CCDC50 is mainly located at the plasma membrane together with the EGF receptor and functions in EGF receptor endocytosis and its degradation. Consequently, *CCDC50* plays an essential role for the positive maintenance of the growth factor receptor expression on the cell surface. When activated, overexpressed or phosphorylated, *CCDC50* contributes to positive receptor signaling and acts tumorigenic. *CCDC50* was also postulated as a negative regulator of the NFκB pathway, investigated in Hela cells (Bohgaki *et al*., 2008 and Kameda *et al*., 2009). Interestingly, *CCDC50* was found to interact with the cytoplasmatic zinc finger protein *TNFAIP3* that inhibits NFκB activation. In addition, IKKγ and CCDC50 were described to interact with the K63-linked polyubiquitin chain of the RIP1 protein. Therefore, *CCDC50* competes for the interaction between *IKKγ* and *RIPK1*, resulting in the attenuation of the NFκB signaling. Furthermore, *CCDC50* can directly interact with *RIPK1* and thereby inhibit its function (Bohgaki *et al*., 2008). In contrast to results shown in Hela cells, our data gave rise to a survival stimulating effect of *CCDC50* (Figure 17, Figure 19) and since knockdown of *CCDC50* in primary CLL cells and in cell lines showed a loss-of-viability phenotype (Figure 22, Figure 23). We could validate the reduction in cell viability in 6 CLL patients and in MCL and CLL cell lines, following *CCDC50* knockdown. Reduction in *CCDC50* expression levels correlated with decreasing cell proliferation in stable cell lines. Expression of *TNFAIP3* is induced by TNFα stimulation, i.e. an active NFκB pathway. On the other hand, once expressed *TNFAIP3* functions as a negative regulator of NFκB signaling and inhibited cell survival (Pham *et al*., 2003). Depending on the cell type in which NFκB acts,

it can either inhibit or promote carcinogenesis and cancer progression (Yamaoka *et al.,* 1996; Dajee *et al*., 2003; Bogaki *et al*., 2008). It is broadly discussed, that NFκB signaling is constitutively active in MCL cell lines and stimulates cell survival (Beyaert *et al*., 2000; Pham *et al*., 2003; Malynn *et al*., 2009; Schmitz *et al*., 2009). Therefore, further activation by TNFα may be difficult to detect and could not be seen in MCL cell line JVM-2 and CLL cell line Mec-1 (not shown). In order to validate the involvement of *CCDC50* in NFκB signaling, reporter assays have been performed in HEK-293T cells. These cells were easy and efficient to transfect (90%) and showed a 7-fold stimulation of the NFκB reporter plasmid following TNFα stimulation. Our data showed that TNFα induction of the NFκB reporter plasmid revealed 50% less inducibility in cells transiently silenced for *CCDC50* compared to cells with *CCDC50* overexpression (Figure 24). These findings supported the hypothesis, that *CCDC50* has a survival stimulating effect. Low *CCDC50* expression levels correlated with reduced cell viability that may be caused by low NFκB inducibility.

4.5.2 *SMARCC2* is upregulated in MCL and CLL and promotes cell survival

SMARCC2, also called *BAF170*, was identified in this study as candidate gene in the loss-of-function screen. Silencing of *SCMARCC2* resulted in decreased cell viability in the MCL cell line JVM-2 and in primary CLL cells. *SMARCC2* is mapped to the recurrently gained genomic region 12q13 and is a so far unpublished candidate in the pathogenesis of MCL or CLL. *SMARCC2* is a member of the SWI/SNF family of proteins, which display helicase and ATPase activities and which are identified as transcriptional regulators by modifying chromantin accessibility in the context of target genes (Phelan *et al*., 1999; Decristofaro *et al*., 2001; Chen *et al*., 2005; Wang *et al*., 2005; Zhang *et al*., 2007). *SMARCC2* is involved in transcriptional activation and repression of target genes by chromatin remodeling (alteration of DNA-nucleosome topology) (Nagl *et al*., 2006). The protein is part of the large ATP-dependent chromatin remodeling complex *SNF/SWI* and contains a leucine zipper motif typical of many transcription factors. In lymphoid cells, *SWI/SNF* subunits are also associated with the transcriptional regulator Ikaros required for normal B- and T-cell differentiation (Kim *et al*., 1999; O'Neill *et al*., 2000). In mice, heterozygous mutation of some *SWI/SNF* components results in an increased risk of cancer, whereas homozygous mutation causes embryonic lethality (Klochendler-Yeivin *et al*., 2000). These studies suggest that *SWI/SNF* complexes play important roles during normal development and differentiation in mammals. This would also explain the reduction in cell viability following functional gene knockdown. Therefore, further functional characterization of *SMARCC2* in CLL and MCL pathogenesis is necessary.

4.5.3 *SERPINI2* has proliferation stimulating activity in MCL and CLL

In this study, *SERPINI2* was identified in this loss-of-function screen to reduce cell viability in MCL cell line JVM-2 and in primary CLL cells after functional gene knockdown. *SERPINI2* was published earlier as a candidate gene on chromosome 3q26 in MCL, although no correlation to its functional impact on MCL cells has been shown so far (Tagawa *et al*., 2005). *SERPINI2* was initially identified and implicated as a potential tumor suppressor gene because it was downregulated in pancreatic cancer cell lines when compared to normal pancreatic cells (Ozaki *et al*., 1998). *SERPINI2*, also known as *MEPI*, is expressed in normal breast myoepithelial cells, but not in malignant breast carcinoma cells (Xiao *et al*., 1999). It is a member of the serpin superfamily of proteins that have been implicated in a variety of functions, including blood coagulation, angiogenesis, inflammation, and programmed cell death (Scarff *et al*., 2004). *SERPINI2* is involved in growth control, growth-suppressing pathways and, when impaired, is involved in pancreatic carcinogenesis. *SERPINI2* is a highly interesting candidate in MCL and CLL showing survival stimulating effects. In future experiments, functional assays have to be performed in primary MCL and CLL cells to gain further insights into its function in the pathogenesis of both neoplasias.

4.6 Involvement of *CCDC50* in survival of primary CLL cells

In CLL patient 48, a decrease of *CCDC50* and *TNFAIP3* expression was measured 48h after cultivation in conditioned medium by qRT-PCR experiments. In addition, the *IL8* level increased, which correlated with the induction of the NFκB pathway and the survival of B-cells. These results indicate that *CCDC50* is maybe not essential for B-cell survival, while cells were cultivated in HS5 conditioned medium or were in co-culture. This co-culture system mainly resembles the natural environment in bone marrow or lymph node. Here cells can survive due to cytokine stimuli of T-cells and nurse-like cells, while cells in peripheral blood may show different expression patterns and may need distinct survival factors due to a changing environment (Shen *et al*., 2004; Caligaris-Cappio *et al*., 2008). The overexpression of *CCDC50* in most primary CLL cells isolated from peripheral blood may therefore reflect the original expression pattern of cells in peripheral blood. As soon as they enter the bone marrow, lymph node or the so called proliferation center (Caligaris-Cappio *et al*., 2008), they might change their gene expression according to their microenvironment and survive due to T-cell or stroma-cell contact. Proliferation centers are focal aggregates of variable size scattered in lymph nodes and to a lesser extent in the bone marrow (Schmid *et al*., 1994; Granziero *et al*., 2001; Soma *et al*., 2006). The changing expression patterns due to their location and survival stimuli in lymph node, bone marrow and peripheral blood may be a reasonable

explanation for the decrease of *CCDC50* expression levels seen in primary CLL cells, cultured in conditioned medium. Future studies showing evidence on this theory need to be performed in cells deriving from these different tissues.

4.7 *CCDC50* is involved in p53 signaling pathways

Genome wide expression arrays were performed in order to identify differentially regulated genes following *CCDC50* modulation, i.e. silencing and overexpression. Bioinformatic analysis revealed that after *CCDC50* knockdown, a majority of overexpressed genes were involved in p53 signaling pathways (*CDKN1A*, *FDXR*, *GADD45A*, *LAMP3*, *PRODH*, *PHLDA3*, *SESN1*, and *TP53I3*). Further upregulated genes identified in this study were tumor suppressor genes and genes, inducing cell death or the suppression of cell proliferation (*BAX*, *FAM129A*, *MDX4*, and *RARRES3*). Downregulated genes following *CCDC50* silencing were predominantly involved in the activation of cell survival pathways (*BNIP3L*, *BRWD1*, *LGMN*, and *MDM4*). *TP53I3* was identified as overexpressed in JVM-2 and Granta-519 following a decrease in *CCDC50* expression levels (Figure 26). Further publications showed that the protein encoded by this gene is similar to oxidoreductases which are activated upon oxidative stress and irradiation (Contente *et al*., 2002). *TP53I3* was described as activated by the tumor suppressor gene *p53* and mediated cell death (Contente *et al*., 2002). As a component of the response to acute stress, *p53* has a well established role in protecting against cancer development. It was shown that *p53* directly binds and activates the *TP53I3* promoter (Contente *et al*., 2002). Beside *TP53I3*, *CDKN1A*, and *FDXR* were upregulated in both cell lines JVM-2 and Granta-519, and were reported as *p53* target genes (Kerley-Hamilton *et al*., 2005). *CDKN1A* is a potent, tight-binding inhibitor of CDKs that inhibits phosphorylation of the retinoblastoma protein and mediates p53 suppression of tumor cell growth i.e. acts pro-apoptotic. *PHLDA3*, *GADD45A*, *BAX*, and *RARRES3* were upregulated only in Granta-519 and described to be involved in p53 signaling (Smith *et al*., 1994; Chipuk *et al*., 2004; Kerley-Hamilton *et al*., 2005). Kawase *et al*. identified *PHLDA3* as a *p53* target gene. Activation of *PHLDA3* depended on phosphorylation of *p53*, and endogenous *PHLDA3* was required for p53-dependent apoptosis (Kawase *et al*., 2009). *BAX* was identified as a protein partner of *BCL2* and is responsible in the p53-regulated pathway for the induction of apoptosis (Oltavi *et al*., 1993; Chipuk *et al*., 2004). *GADD45A* was shown to stimulate DNA excision repair *in vitro* and inhibited entry of cells into S-phase. These results established *GADD45A* as a link between the p53-dependent cell cycle checkpoint and DNA repair (Smith *et al*., 1994). Moreover, *GADD45A* was found to be involved in JNK signaling and in the MAPK pathway, which promoted the induction of apoptosis. *PRODH*, *LAMP3*, and *SESN1* were described as apoptosis inducing genes in the p53 pathway. *FAM129A* was identified to inhibit cell

proliferation and *MXD4* was described as tumor-suppressor gene and contributed to the regulation of cell growth in differentiating tissues (Pulverer *et al.*, 2000; Adamsen *et al*., 2007; Phang *et al*., 2008). *LAMP3* was found as a novel *TP53* target (Adamsen *et al*., 2007). Among the downregulated genes with functions in cell cycle progression were *BNIP3L*, *LGMN* (JVM-2), as well as *MDM4* and *BRWD1* (Granta-519) (Pulverer *et al*., 2000; Contente *et al*., 2002). Apoptosis-protecting genes like *BNIP3L* and *LGMN* were downregulated in accordance with *CCDC50* silencing. In recent studies it was shown that *BNIP3L* and *CCDC50* were both found overexpressed in a cohort of 71 primary MCL cells (Salaverria *et al*., 2007). Since silencing of *CCDC50* in our study was accompanied by *BNIP3L* downregulation, a direct correlation of both genes can be assumed. The decrease of the anti-apoptotic gene *BNIP3L* may therefore be a plausible explanation for the reduction in cell viability seen in MCL and CLL cells with low *CCDC50* expression levels. In summary, the observed reduction in cell viability following *CCDC50* knockdown can be explained by the overexpression of apoptosis-stimulating genes involved in the p53 signaling pathways like *TP53I3* and the downregulation of apoptosis protecting genes like *BNIP3L*.

4.8 Conclusion

In this study primary cells of 24 CLL and 6 MCL patients and cells of 3 MCL and 3 CLL cell lines were profiled in order to identify novel overexpressed genes in recurrently genomic gained regions. When correlating these data with recent publications, a set of 72 upregulated genes was identified on chromosomes 3q25-q29, 12q13-q14, and 18q21-q22. These genes were investigated for their phenotypic behavior after functional gene knockdown applying an RNAi screen. This study uncovered three major candidate genes with survival promoting effects in CLL and MCL cells: *CCDC50*, *SERPINI2* and *SMARCC2*. Functional investigations on the candidate gene *CCDC50* confirmed its involvement in NFκB signaling. Genome wide expression profiling identified several target genes of the p53 signaling pathway as significantly upregulated in accordance with low *CCDC50* transcript levels. Overexpression of pro-apoptotic genes like *TP53I3* and *BAX* and downregulation of apoptosis protecting genes like *BNIP3L* and *GADD45A* were a plausible cause for the reduction in cell viability in primary CLL cells and MCL cell lines after *CCDC50* silencing. Detailed analysis have to be performed to get a deeper insight into *CCDC50* function, its involvement in the NFκB and the p53 pathway, and its influence in mechanisms leading to the pathogenesis of MCL and CLL.

References

Adamsen BL, Kravik KL, Clausen OP, De Angelis PM (2007): Apoptosis, cell cycle progression and gene expression in TP53-depleted HCT116 colon cancer cells in response to short-term 5-fluorouracil treatment. Int J Oncol 31, 1491-500

Alizadeh AA *et al*. (2000): Distinct types of diffuse large B-cell lymphoma identified by gene expression profiling. Nature 403, 503-11

Allen JE, Hough RE, Goepel JR, Bottomley S, Wilson GA, Alcock HE, Baird M, Lorigan PC, Vandenberghe EA, Hancock BW, Hammond DW (2002): Identification of novel regions of amplification and deletion within mantle cell lymphoma DNA by comparative genomic hybridization. Br J Haematol 116, 291-8

Araki K, Imaizumi T, Okuyama K, Oike Y, Yamamura K (1997): Efficiency of recombination by Cre transient expression in embryonic stem cells: comparison of various promoters. J Biochem 122, 977-82

Athanasiadou A, Stamatopoulos K, Tsompanakou A, Gaitatzi M, Kalogiannidis P, Anagnostopoulos A*, et al.* Clinical, immunophenotypic, and molecular profiling of trisomy 12 in chronic lymphocytic leukemia and comparison with other karyotypic subgroups defined by cytogenetic analysis. *Cancer Genet Cytogenet* 2006 Jul 15; 168(2): 109-119.

Baer A, Bode J (2001): Coping with kinetic and thermodynamic barriers: RMCE, an efficient strategy for the targeted integration of transgenes. Curr Opin Biotechnol 12, 473-80

Baker SJ, Preisinger AC, Jessup JM, Paraskeva C, Markowitz S, Willson JK, Hamilton S, Vogelstein B (1990): p53 gene mutations occur in combination with 17p allelic deletions as late events in colorectal tumorigenesis. Cancer Res 50, 7717-22

Bea S, Ribas M, Hernandez JM, Bosch F, Pinyol M, Hernandez L, Garcia JL, Flores T, Gonzalez M, Lopez-Guillermo A, Piris MA, Cardesa A, Montserrat E, Miro R, Campo E (1999): Increased number of chromosomal imbalances and high-level DNA amplifications in mantle cell lymphoma are associated with blastoid variants. Blood 93, 4365-74

Bea S, Campo E (2008): Secondary genomic alterations in non-Hodgkin's lymphomas: tumor-specific profiles with impact on clinical behavior. Haematologica 93, 641-5

Bentz M, Stilgenbauer S, Lichter P, Dohner H (1999): Interphase FISH in chronic lymphoproliferative disorders and comparative genomic hybridization in the study of lymphomas. Haematologica 84 Suppl EHA-4, 102-6

Bentz M, Plesch A, Bullinger L, Stilgenbauer S, Ott G, Muller-Hermelink HK, Baudis M, Barth TF, Moller P, Lichter P, Dohner H (2000): t(11;14)-positive mantle cell lymphomas exhibit complex karyotypes and share similarities with B-cell chronic lymphocytic leukemia. Genes Chromosomes Cancer 27, 285-94

Bergmann M, Hart L, Lindsay M, Barnes PJ, Newton R (1998): IkappaBalpha degradation and nuclear factor-kappaB DNA binding are insufficient for interleukin-1beta and tumor necrosis factor-alpha-induced kappaB-dependent transcription. Requirement for an additional activation pathway. J Biol Chem 273, 6607-10

Berns K, Hijmans EM, Mullenders J, Brummelkamp TR, Velds A, Heimerikx M, Kerkhoven RM, Madiredjo M, Nijkamp W, Weigelt B, Agami R, Ge W, Cavet G, Linsley PS, Beijersbergen RL, Bernards R (2004): A large-scale RNAi screen in human cells identifies new components of the p53 pathway. Nature 428, 431-7

Bertoni F, Rinaldi A, Zucca E, Cavalli F (2006): Update on the molecular biology of mantle cell lymphoma. Hematol Oncol 24, 22-7

Beyaert R, Heyninck K, Van Huffel S (2000): A20 and A20-binding proteins as cellular inhibitors of nuclear factor-kappa B-dependent gene expression and apoptosis. Biochem Pharmacol 60, 1143-51

Bohgaki M, Tsukiyama T, Nakajima A, Maruyama S, Watanabe M, Koike T, Hatakeyama S (2008): Involvement of Ymer in suppression of NF-kappaB activation by regulated interaction with lysine-63-linked polyubiquitin chain. Biochim Biophys Acta 1783, 826-37

Boutros M, Ahringer J (2008): The art and design of genetic screens: RNA interference. Nat Rev Genet 9, 554-66

Brielmeier M, Bechet JM, Falk MH, Pawlita M, Polack A, Bornkamm GW (1998): Improving stable transfection efficiency: antioxidants dramatically improve the outgrowth of clones under dominant marker selection. Nucleic Acids Res 26, 2082-5

Bridge AJ, Pebernard S, Ducraux A, Nicoulaz AL, Iggo R (2003): Induction of an interferon response by RNAi vectors in mammalian cells. Nat Genet 34, 263-4

Caligaris-Cappio F (2003): Role of the microenvironment in chronic lymphocytic leukaemia. Br J Haematol 123, 380-8

Caligaris-Cappio F, Ghia P (2008): Novel insights in chronic lymphocytic leukemia: are we getting closer to understanding the pathogenesis of the disease? J Clin Oncol 26, 4497-503

Camacho FI, Algara P, Rodriguez A, Ruiz-Ballesteros E, Mollejo M, Martinez N, Martinez-Climent JA, Gonzalez M, Mateo M, Caleo A, Sanchez-Beato M, Menarguez J, Garcia-Conde J, Sole F, Campo E, Piris MA (2003): Molecular heterogeneity in MCL defined by the use of specific VH genes and the frequency of somatic mutations. Blood 101, 4042-6

Campo E, Raffeld M, Jaffe ES (1999): Mantle-cell lymphoma. Semin Hematol 36, 115-27

Carreras J, Villamor N, Colomo L, Moreno C, Ramon y Cajal S, Crespo M, Tort F, Bosch F, Lopez-Guillermo A, Colomer D, Montserrat E, Campo E (2005): Immunohistochemical analysis of ZAP-70 expression in B-cell lymphoid neoplasms. J Pathol 205, 507-13

Chen J, Archer TK (2005): Regulating SWI/SNF subunit levels via protein-protein interactions and proteasomal degradation: BAF155 and BAF170 limit expression of BAF57. Mol Cell Biol 25, 9016-27

Chiorazzi N, Rai KR, Ferrarini M (2005): Chronic lymphocytic leukemia. N Engl J Med 352, 804-15

Chipuk JE, Kuwana T, Bouchier-Hayes L, Droin NM, Newmeyer DD, Schuler M, Green DR (2004): Direct activation of Bax by p53 mediates mitochondrial membrane permeabilization and apoptosis. Science 303, 1010-4

Contente A, Dittmer A, Koch MC, Roth J, Dobbelstein M (2002): A polymorphic microsatellite that mediates induction ofPIG3 by p53. Nat Genet 30, 315-20

Crespo M, Bosch F, Villamor N, Bellosillo B, Colomer D, Rozman M, Marce S, Lopez-Guillermo A, Campo E, Montserrat E (2003): ZAP-70 expression as a surrogate for immunoglobulin-variable-region mutations in chronic lymphocytic leukemia. N Engl J Med 348, 1764-75

Dajee M, Lazarov M, Zhang JY, Cai T, Green CL, Russell AJ, Marinkovich MP, Tao S, Lin Q, Kubo Y, Khavari PA (2003): NF-kappaB blockade and oncogenic Ras trigger invasive human epidermal neoplasia. Nature 421, 639-43

Damle RN, Ghiotto F, Valetto A, Albesiano E, Fais F, Yan XJ, Sison CP, Allen SL, Kolitz J, Schulman P, Vinciguerra VP, Budde P, Frey J, Rai KR, Ferrarini M, Chiorazzi N (2002): B-cell chronic lymphocytic leukemia cells express a surface membrane phenotype of activated, antigen-experienced B lymphocytes. Blood 99, 4087-93

de Fougerolles A, Vornlocher HP, Maraganore J, Lieberman J (2007): Interfering with disease: a progress report on siRNA-based therapeutics. Nat Rev Drug Discov 6, 443-53

Decristofaro MF, Betz BL, Rorie CJ, Reisman DN, Wang W, Weissman BE (2001): Characterization of SWI/SNF protein expression in human breast cancer cell lines and other malignancies. J Cell Physiol 186, 136-45

Demidova AR, Aau MY, Zhuang L, Yu Q (2009): Dual regulation of Cdc25A by Chk1 and p53-ATF3 in DNA replication checkpoint control. J Biol Chem 284, 4132-9

Dighiero G, Travade P, Chevret S, Fenaux P, Chastang C, Binet JL (1991): B-cell chronic lymphocytic leukemia: present status and future directions. French Cooperative Group on CLL. Blood 78, 1901-14

Dohner H, Stilgenbauer S, Dohner K, Bentz M, Lichter P. Chromosome aberrations in B-cell chronic lymphocytic leukemia: reassessment based on molecular cytogenetic analysis. *J Mol Med* 1999 Feb; 77(2): 266-281.

Dohner H, Stilgenbauer S, Benner A, Leupolt E, Krober A, Bullinger L, Dohner K, Bentz M, Lichter P (2000): Genomic aberrations and survival in chronic lymphocytic leukemia. N Engl J Med 343, 1910-6

Drexler HG, MacLeod RA. Mantle cell lymphoma-derived cell lines: unique research tools. *Leuk Res* 2006 Aug; 30(8): 911-913

Echeverri CJ, Perrimon N (2006): High-throughput RNAi screening in cultured cells: a user's guide. Nat Rev Genet 7, 373-84

el Rouby S, Thomas A, Costin D, Rosenberg CR, Potmesil M, Silber R, Newcomb EW (1993): p53 gene mutation in B-cell chronic lymphocytic leukemia is associated with drug resistance and is independent of MDR1/MDR3 gene expression. Blood 82, 3452-9

Elbashir SM, Lendeckel W, Tuschl T (2001): RNA interference is mediated by 21- and 22-nucleotide RNAs. Genes Dev 15, 188-200

Espinet B, Sole F, Woessner S, Bosch F, Florensa L, Campo E, Costa D, Lloveras E, Vila RM, Besses C, Montserrat E, Sans-Sabrafen J (1999): Translocation (11;14)(q13;q32) and preferential involvement of chromosomes 1, 2, 9, 13, and 17 in mantle cell lymphoma. Cancer Genet Cytogenet 111, 92-8

Falt S, Merup M, Gahrton G, Lambert B, Wennborg A (2005): Identification of progression markers in B-CLL by gene expression profiling. Exp Hematol 33, 883-93

Fire A, Xu S, Montgomery MK, Kostas SA, Driver SE, Mello CC (1998): Potent and specific genetic interference by double-stranded RNA in Caenorhabditis elegans. Nature 391, 806-11

Galteland E, Sivertsen EA, Svendsrud DH, Smedshammer L, Kresse SH, Meza-Zepeda LA, Myklebost O, Suo Z, Mu D, Deangelis PM, Stokke T (2005): Translocation t(14;18) and gain of chromosome 18/BCL2: effects on BCL2 expression and apoptosis in B-cell non-Hodgkin's lymphomas. Leukemia 19, 2313-23

Gao C, Furge K, Koeman J, Dykema K, Su Y, Cutler ML, Werts A, Haak P, Vande Woude GF (2007): Chromosome instability, chromosome transcriptome, and clonal evolution of tumor cell populations. Proc Natl Acad Sci U S A 104, 8995-9000

Ghia P, Circosta P, Scielzo C, Vallario A, Camporeale A, Granziero L, Caligaris-Cappio F (2005): Differential effects on CLL cell survival exerted by different microenvironmental elements. Curr Top Microbiol Immunol 294, 135-45

Granziero L, Ghia P, Circosta P, Gottardi D, Strola G, Geuna M, Montagna L, Piccoli P, Chilosi M, Caligaris-Cappio F (2001): Survivin is expressed on CD40 stimulation and interfaces proliferation and apoptosis in B-cell chronic lymphocytic leukemia. Blood 97, 2777-83

Greaves MF (1986): Differentiation-linked leukemogenesis in lymphocytes. Science 234, 697-704

Greiner TC *et al*. (2006): Mutation and genomic deletion status of ataxia telangiectasia mutated (ATM) and p53 confer specific gene expression profiles in mantle cell lymphoma. Proc Natl Acad Sci U S A 103, 2352-7

Gresch O, Engel FB, Nesic D, Tran TT, England HM, Hickman ES, Korner I, Gan L, Chen S, Castro-Obregon S, Hammermann R, Wolf J, Muller-Hartmann H, Nix M, Siebenkotten G, Kraus G, Lun K (2004): New non-viral method for gene transfer into primary cells. Methods 33, 151-63

Gu H, Zou YR, Rajewsky K (1993): Independent control of immunoglobulin switch recombination at individual switch regions evidenced through Cre-loxP-mediated gene targeting. Cell 73, 1155-64

Guan R, Tapang P, Leverson JD, Albert D, Giranda VL, Luo Y (2005): Small interfering RNA-mediated Polo-like kinase 1 depletion preferentially reduces the survival of p53-defective, oncogenic transformed cells and inhibits tumor growth in animals. Cancer Res 65, 2698-704

Haferlach C, Dicker F, Schnittger S, Kern W, Haferlach T. Comprehensive genetic characterization of CLL: a study on 506 cases analysed with chromosome banding analysis, interphase FISH, IgV(H) status and immunophenotyping. *Leukemia* 2007 Dec; 21(12): 2442-2451

Hamblin TJ, Davis Z, Gardiner A, Oscier DG, Stevenson FK (1999): Unmutated Ig V(H) genes are associated with a more aggressive form of chronic lymphocytic leukemia. Blood 94, 1848-54

Hanahan D, Weinberg RA (2000): The hallmarks of cancer. Cell 100, 57-70

Haslinger C, Schweifer N, Stilgenbauer S, Dohner H, Lichter P, Kraut N, Stratowa C, Abseher R (2004): Microarray gene expression profiling of B-cell chronic lymphocytic leukemia subgroups defined by genomic aberrations and VH mutation status. J Clin Oncol 22, 3937-49

Hernandez L, Fest T, Cazorla M, Teruya-Feldstein J, Bosch F, Peinado MA, Piris MA, Montserrat E, Cardesa A, Jaffe ES, Campo E, Raffeld M (1996): p53 gene mutations and protein overexpression are associated with aggressive variants of mantle cell lymphomas. Blood 87, 3351-9

Jaffe ES, Harris NL, Stein H, Vardiman JW, World Health Organization Classification of Tumors. Pathology and Genetics of Tumors of Hematopoietic and Lymphoid Tissues (eds Kleihuis, P. & Sobin, L.) (IARC, Lyon, 2001).

Jackson AL, Bartz SR, Schelter J, Kobayashi SV, Burchard J, Mao M, Li B, Cavet G, Linsley PS (2003): Expression profiling reveals off-target gene regulation by RNAi. Nat Biotechnol 21, 635-7

Jackson AL, Linsley PS (2004): Noise amidst the silence: off-target effects of siRNAs? Trends Genet 20, 521-4

Jares P, Campo E (2008): Advances in the understanding of mantle cell lymphoma. Br J Haematol

Jemal A, Murray T, Ward E, Samuels A, Tiwari RC, Ghafoor A, Feuer EJ, Thun MJ (2005): Cancer statistics, 2005. CA Cancer J Clin 55, 10-30

Kameda H, Watanabe M, Bohgaki M, Tsukiyama T, Hatakeyama S (2009): Inhibition of NF-kappaB signaling via tyrosine phosphorylation of Ymer. Biochem Biophys Res Commun 378, 744-9

Kawase T, Ohki R, Shibata T, Tsutsumi S, Kamimura N, Inazawa J, Ohta T, Ichikawa H, Aburatani H, Tashiro F, Taya Y (2009): PH domain-only protein PHLDA3 is a p53-regulated repressor of Akt. Cell 136, 535-50

Kerley-Hamilton JS, Pike AM, Li N, DiRenzo J, Spinella MJ. A p53-dominant transcriptional response to cisplatin in testicular germ cell tumor-derived human embryonal carcinoma. *Oncogene* 2005 Sep 8; 24(40): 6090-6100.

Kienle D, Krober A, Katzenberger T, Ott G, Leupolt E, Barth TF, Moller P, Benner A, Habermann A, Muller-Hermelink HK, Bentz M, Lichter P, Dohner H, Stilgenbauer S (2003): VH mutation status and VDJ rearrangement structure in mantle cell lymphoma: correlation with genomic aberrations, clinical characteristics, and outcome. Blood 102, 3003-9

Kim J, Sif S, Jones B, Jackson A, Koipally J, Heller E, Winandy S, Viel A, Sawyer A, Ikeda T, Kingston R, Georgopoulos K (1999): Ikaros DNA-binding proteins direct formation of chromatin remodeling complexes in lymphocytes. Immunity 10, 345-55

Kittler R *et al*. (2007): Genome-wide resources of endoribonuclease-prepared short interfering RNAs for specific loss-of-function studies. Nat Methods 4, 337-44

Klein G, Imreh S, Zabarovsky ER (2007): Why do we not all die of cancer at an early age? Adv Cancer Res 98, 1-16

Klochendler-Yeivin A, Fiette L, Barra J, Muchardt C, Babinet C, Yaniv M (2000): The murine SNF5/INI1 chromatin remodeling factor is essential for embryonic development and tumor suppression. EMBO Rep 1, 500-6

Knudson AG, Jr. (1971): Mutation and cancer: statistical study of retinoblastoma. Proc Natl Acad Sci U S A 68, 820-3

Kohlhammer H, Schwaenen C, Wessendorf S, Holzmann K, Kestler HA, Kienle D, Barth TF, Moller P, Ott G, Kalla J, Radlwimmer B, Pscherer A, Stilgenbauer S, Dohner H, Lichter P, Bentz M (2004): Genomic DNA-chip hybridization in t(11;14)-positive mantle cell lymphomas shows a high frequency of aberrations and allows a refined characterization of consensus regions. Blood 104, 795-801

Korz C, Pscherer A, Benner A, Mertens D, Schaffner C, Leupolt E*, et al.* Evidence for distinct pathomechanisms in B-cell chronic lymphocytic leukemia and mantle cell lymphoma by quantitative expression analysis of cell cycle and apoptosis-associated genes. *Blood* 2002 Jun 15; 99(12)**:** 4554-4561.

Kuppers R, Klein U, Hansmann ML, Rajewsky K (1999): Cellular origin of human B-cell lymphomas. N Engl J Med 341, 1520-9

Kuppers R (2003): Somatic hypermutation and B-cell receptor selection in normal and transformed human B-cells. Ann N Y Acad Sci 987, 173-9

Kuppers R (2005): Mechanisms of B-cell lymphoma pathogenesis. Nat Rev Cancer 5, 251-62

Malynn BA, Ma A. A20 takes on tumors: tumor suppression by an ubiquitin-editing enzyme. J Exp Med 2009 Apr 20.

Lovec H, Grzeschiczek A, Kowalski MB, Moroy T. Cyclin D1/bcl-1 cooperates with myc genes in the generation of B-cell lymphoma in transgenic mice. *EMBO J* 1994 Aug 1; 13(15): 3487-3495.

Malynn BA, Ma A. A20 takes on tumors: tumor suppression by an ubiquitin-editing enzyme. *J Exp Med* 2009 Apr 20.

Martin-Subero JI, Knippschild U, Harder L, Barth TF, Riemke J, Grohmann S, Gesk S, Hoppner J, Moller P, Parwaresch RM, Siebert R (2003): Segmental chromosomal aberrations and centrosome amplifications: pathogenetic mechanisms in Hodgkin and Reed-Sternberg cells of classical Hodgkin's lymphoma? Leukemia 17, 2214-9

Meinhardt G, Wendtner CM, Hallek M (1999): Molecular pathogenesis of chronic lymphocytic leukemia: factors and signaling pathways regulating cell growth and survival. J Mol Med 77, 282-93

Mittal AK, Hegde GV, Aoun P, Bociek RG, Dave BJ, Joshi AD*, et al.* Molecular basis of aggressive disease in chronic lymphocytic leukemia patients with 11q deletion and trisomy 12 chromosomal abnormalities. *Int J Mol Med* 2007 Oct; 20(4): 461-469.

Moffat J, Grueneberg DA, Yang X, Kim SY, Kloepfer AM, Hinkle G, Piqani B, Eisenhaure TM, Luo B, Grenier JK, Carpenter AE, Foo SY, Stewart SA, Stockwell BR, Hacohen N, Hahn WC, Lander ES, Sabatini DM, Root DE (2006): A lentiviral RNAi library for human and mouse genes applied to an arrayed viral high-content screen. Cell 124, 1283-98

Monni O, Oinonen R, Elonen E, Franssila K, Teerenhovi L, Joensuu H, Knuutila S (1998): Gain of 3q and deletion of 11q22 are frequent aberrations in mantle cell lymphoma. Genes Chromosomes Cancer 21, 298-307

Nagl NG, Jr., Zweitzig DR, Thimmapaya B, Beck GR, Jr., Moran E (2006): The c-myc gene is a direct target of mammalian SWI/SNF-related complexes during differentiation-associated cell cycle arrest. Cancer Res 66, 1289-93

Nowell PC (1976): The clonal evolution of tumor cell populations. Science 194, 23-8

Oltvai ZN, Milliman CL, Korsmeyer SJ (1993): Bcl-2 heterodimerizes in vivo with a conserved homolog, Bax, that accelerates programmed cell death. Cell 74, 609-19

O'Neill DW, Schoetz SS, Lopez RA, Castle M, Rabinowitz L, Shor E, Krawchuk D, Goll MG, Renz M, Seelig HP, Han S, Seong RH, Park SD, Agalioti T, Munshi N, Thanos D, Erdjument-Bromage H, Tempst P, Bank A (2000):

An ikaros-containing chromatin-remodeling complex in adult-type erythroid cells. Mol Cell Biol 20, 7572-82

Orchard J, Garand R, Davis Z, Babbage G, Sahota S, Matutes E, Catovsky D, Thomas PW, Avet-Loiseau H, Oscier D (2003): A subset of t(11;14) lymphoma with mantle cell features displays mutated IgVH genes and includes patients with good prognosis, nonnodal disease. Blood 101, 4975-81

Ortega-Paino E, Fransson J, Ek S, Borrebaeck CA (2008): Functionally associated targets in mantle cell lymphoma as defined by DNA microarrays and RNA interference. Blood 111, 1617-24

Oumard A, Qiao J, Jostock T, Li J, Bode J (2006): Recommended Method for Chromosome Exploitation: RMCE-based Cassette-exchange Systems in Animal Cell Biotechnology. Cytotechnology 50, 93-108

Ozaki K, Nagata M, Suzuki M, Fujiwara T, Miyoshi Y, Ishikawa O, Ohigashi H, Imaoka S, Takahashi E, Nakamura Y (1998): Isolation and characterization of a novel human pancreas-specific gene, pancpin, that is down-regulated in pancreatic cancer cells. Genes Chromosomes Cancer 22, 179-85

Paddison PJ, Cleary M, Silva JM, Chang K, Sheth N, Sachidanandam R, Hannon GJ (2004): Cloning of short hairpin RNAs for gene knockdown in mammalian cells. Nat Methods 1, 163-7

Pham LV, Tamayo AT, Yoshimura LC, Lo P, Ford RJ (2003): Inhibition of constitutive NF-kappa B activation in mantle cell lymphoma B-cells leads to induction of cell cycle arrest and apoptosis. J Immunol 171, 88-95

Phang JM, Donald SP, Pandhare J, Liu Y. The metabolism of proline, a stress substrate, modulates carcinogenic pathways. *Amino Acids* 2008 Nov; 35(4): 681-690.

Phelan ML, Sif S, Narlikar GJ, Kingston RE (1999): Reconstitution of a core chromatin remodeling complex from SWI/SNF subunits. Mol Cell 3, 247-53

Pscherer A, Schliwka J, Wildenberger K, Mincheva A, Schwaenen C, Dohner H, Stilgenbauer S, Lichter P (2006): Antagonizing inactivated tumor suppressor genes and activated oncogenes by a versatile transgenesis system: application in mantle cell lymphoma. FASEB J 20, 1188-90

Pulverer B, Sommer A, McArthur GA, Eisenman RN, Luscher B. Analysis of Myc/Max/Mad network members in adipogenesis: inhibition of the proliferative burst and differentiation by ectopically expressed Mad1. *J Cell Physiol* 2000 Jun; 183(3): 399-410

Rajewsky K (1996): Clonal selection and learning in the antibody system. Nature 381, 751-8

Reagan-Shaw S, Ahmad N (2005): Silencing of polo-like kinase (Plk) 1 via siRNA causes induction of apoptosis and impairment of mitosis machinery in human prostate cancer cells: implications for the treatment of prostate cancer. FASEB J 19, 611-3

Rinaldi A, Kwee I, Taborelli M, Largo C, Uccella S, Martin V, Poretti G, Gaidano G, Calabrese G, Martinelli G, Baldini L, Pruneri G, Capella C, Zucca E, Cotter FE, Cigudosa JC, Catapano CV, Tibiletti MG, Bertoni F (2006): Genomic and expression profiling identifies the B-cell associated tyrosine kinase Syk as a possible therapeutic target in mantle cell lymphoma. Br J Haematol 132, 303-16

Rizzatti EG, Falcao RP, Panepucci RA, Proto-Siqueira R, Anselmo-Lima WT, Okamoto OK, Zago MA (2005): Gene expression profiling of mantle cell lymphoma cells reveals aberrant expression of genes from the PI3K-AKT, WNT and TGFbeta signaling pathways. Br J Haematol 130, 516-26

Rosenblum BB, Lee LG, Spurgeon SL, Khan SH, Menchen SM, Heiner CR, Chen SM (1997): New dye-labeled terminators for improved DNA sequencing patterns. Nucleic Acids Res 25, 4500-4

Rosenwald A, Alizadeh AA, Widhopf G, Simon R, Davis RE, Yu X, Yang L, Pickeral OK, Rassenti LZ, Powell J, Botstein D, Byrd JC, Grever MR, Cheson BD, Chiorazzi N, Wilson WH, Kipps TJ, Brown PO, Staudt LM (2001): Relation of gene expression phenotype to immunoglobulin mutation genotype in B-cell chronic lymphocytic leukemia. J Exp Med 194, 1639-47

Rosenwald A *et al*. (2003): The proliferation gene expression signature is a quantitative integrator of oncogenic events that predicts survival in mantle cell lymphoma. Cancer Cell 3, 185-97

Rozman C, Montserrat E (1995): Chronic lymphocytic leukemia. N Engl J Med 333, 1052-7

Rubio-Moscardo F, Climent J, Siebert R, Piris MA, Martin-Subero JI, Nielander I, Garcia-Conde J, Dyer MJ, Terol MJ, Pinkel D, Martinez-Climent JA (2005): Mantle-cell lymphoma genotypes identified with CGH to BAC microarrays define a leukemic subgroup of disease and predict patient outcome. Blood 105, 4445-54

Ruiz-Vela A, Aggarwal M, de la Cueva P, Treda C, Herreros B, Martin-Perez D, Dominguez O, Piris MA (2008): Lentiviral (HIV)-based RNA interference screen in human B-cell receptor regulatory networks reveals MCL1-induced oncogenic pathways. Blood 111, 1665-76

Saiki RK, Gelfand DH, Stoffel S, Scharf SJ, Higuchi R, Horn GT, Mullis KB, Erlich HA (1988): Primer-directed enzymatic amplification of DNA with a thermostable DNA polymerase. Science 239, 487-91

Salaverria I *et al*. (2007): Specific secondary genetic alterations in mantle cell lymphoma provide prognostic information independent of the gene expression-based proliferation signature. J Clin Oncol 25, 1216-22

Sander S, Bullinger L, Leupolt E, Benner A, Kienle D, Katzenberger T, Kalla J, Ott G, Muller-Hermelink HK, Barth TF, Moller P, Lichter P, Dohner H, Stilgenbauer S (2008): Genomic aberrations in mantle cell lymphoma detected by interphase fluorescence in situ hybridization. Incidence and clinicopathological correlations. Haematologica 93, 680-7

Sanger F, Nicklen S, Coulson AR (1977): DNA sequencing with chain-terminating inhibitors. Proc Natl Acad Sci U S A 74, 5463-7

Sauer B, Henderson N (1988): Site-specific DNA recombination in mammalian cells by the Cre recombinase of bacteriophage P1. Proc Natl Acad Sci U S A 85, 5166-70

Scarff KL, Ung KS, Nandurkar H, Crack PJ, Bird CH, Bird PI (2004): Targeted disruption of SPI3/Serpinb6 does not result in developmental or growth defects, leukocyte dysfunction, or susceptibility to stroke. Mol Cell Biol 24, 4075-82

Schaffner C, Stilgenbauer S, Rappold GA, Dohner H, Lichter P (1999): Somatic ATM mutations indicate a pathogenic role of ATM in B-cell chronic lymphocytic leukemia. Blood 94, 748-53

Schaffner C, Idler I, Stilgenbauer S, Dohner H, Lichter P (2000): Mantle cell lymphoma is characterized by inactivation of the ATM gene. Proc Natl Acad Sci U S A 97, 2773-8

Schlabach MR, Luo J, Solimini NL, Hu G, Xu Q, Li MZ, Zhao Z, Smogorzewska A, Sowa ME, Ang XL, Westbrook TF, Liang AC, Chang K, Hackett JA, Harper JW, Hannon GJ, Elledge SJ (2008): Cancer proliferation gene discovery through functional genomics. Science 319, 620-4

Schmechel SC, LeVasseur RJ, Yang KH, Koehler KM, Kussick SJ, Sabath DE (2004): Identification of genes whose expression patterns differ in benign lymphoid tissue and follicular, mantle cell, and small lymphocytic lymphoma. Leukemia 18, 841-55

Schmid C, Vazquez JJ, Diss TC, Isaacson PG (1994): Primary B-cell mucosa-associated lymphoid tissue lymphoma presenting as a solitary colorectal polyp. Histopathology 24, 357-62

Schmitz R, Hansmann ML, Bohle V, Martin-Subero JI, Hartmann S, Mechtersheimer G*, et al.* TNFAIP3 (A20) is a tumor suppressor gene in Hodgkin lymphoma and primary mediastinal B cell lymphoma. *J Exp Med* 2009 Apr 20.

Seibler J, Bode J (1997): Double-reciprocal crossover mediated by FLP-recombinase: a concept and an assay. Biochemistry 36, 1740-7

Seibler J, Schubeler D, Fiering S, Groudine M, Bode J (1998): DNA cassette exchange in ES cells mediated by Flp recombinase: an efficient strategy for repeated modification of tagged loci by marker-free constructs. Biochemistry 37, 6229-34

Seiffert M, Stilgenbauer S, Dohner H, Lichter P (2007): Efficient nucleofection of primary human B-cells and B-CLL cells induces apoptosis, which depends on the microenvironment and on the structure of transfected nucleic acids. Leukemia 21, 1977-83

Schaffner C, Stilgenbauer S, Rappold GA, Dohner H, Lichter P. Somatic ATM mutations indicate a pathogenic role of ATM in B-cell chronic lymphocytic leukemia. *Blood* 1999 Jul 15; 94(2): 748-753

Schaffner C, Idler I, Stilgenbauer S, Dohner H, Lichter P. Mantle cell lymphoma is characterized by inactivation of the ATM gene. *Proc Natl Acad Sci U S A* 2000 Mar 14; 97(6): 2773-2778

Shaffer AL, Rosenwald A, Staudt LM (2002): Lymphoid malignancies: the dark side of B-cell differentiation. Nat Rev Immunol 2, 920-32

Shaffer AL, Wright G, Yang L, Powell J, Ngo V, Lamy L, Lam LT, Davis RE, Staudt LM (2006): A library of gene expression signatures to illuminate normal and pathological lymphoid biology. Immunol Rev 210, 67-85

Shen Y, Iqbal J, Xiao L, Lynch RC, Rosenwald A, Staudt LM, Sherman S, Dybkaer K, Zhou G, Eudy JD, Delabie J, McKeithan TW, Chan WC (2004): Distinct gene expression profiles in different B-cell compartments in human peripheral lymphoid organs. BMC Immunol 5, 20

Silva JM, Marran K, Parker JS, Silva J, Golding M, Schlabach MR, Elledge SJ, Hannon GJ, Chang K (2008): Profiling essential genes in human mammary cells by multiplex RNAi screening. Science 319, 617-20

Smith ML, Chen IT, Zhan Q, Bae I, Chen CY, Gilmer TM, Kastan MB, O'Connor PM, Fornace AJ, Jr. (1994): Interaction of the p53-regulated protein Gadd45 with proliferating cell nuclear antigen. Science 266, 1376-80

Snove O, Jr., Nedland M, Fjeldstad SH, Humberset H, Birkeland OR, Grunfeld T, Saetrom P (2004): Designing effective siRNAs with off-target control. Biochem Biophys Res Commun 325, 769-73

Soma LA, Craig FE, Swerdlow SH (2006): The proliferation center microenvironment and prognostic markers in chronic lymphocytic leukemia/small lymphocytic lymphoma. Hum Pathol 37, 152-9

Stamatopoulos K, Kosmas C, Belessi C, Kyriazopoulos P, Papadaki T, Anagnostou D, Loukopoulos D (1999): Molecular analysis of bcl-1/IgH junctional sequences in mantle cell lymphoma: potential mechanism of the t(11;14) chromosomal translocation. Br J Haematol 105, 190-7

Tagawa H, Karnan S, Suzuki R, Matsuo K, Zhang X, Ota A, Morishima Y, Nakamura S, Seto M (2005): Genome-wide array-based CGH for mantle cell lymphoma: identification of homozygous deletions of the proapoptotic gene BIM. Oncogene 24, 1348-58

Tashiro K, Konishi H, Sano E, Nabeshi H, Yamauchi E, Taniguchi H (2006): Suppression of the ligand-mediated down-regulation of epidermal growth factor receptor by Ymer, a novel tyrosine-phosphorylated and ubiquitinated protein. J Biol Chem 281, 24612-22

Thelander EF, Walsh SH, Thorselius M, Laurell A, Landgren O, Larsson C, Rosenquist R, Lagercrantz S (2005): Mantle cell lymphomas with clonal immunoglobulin V(H)3-21 gene rearrangements exhibit fewer genomic imbalances than mantle cell lymphomas utilizing other immunoglobulin V(H) genes. Mod Pathol 18, 331-9

Tobin G, Thunberg U, Johnson A, Eriksson I, Soderberg O, Karlsson K, Merup M, Juliusson G, Vilpo J, Enblad G, Sundstrom C, Roos G, Rosenquist R (2003): Chronic lymphocytic leukemias utilizing the VH3-21 gene display highly restricted Vlambda2-14 gene use and homologous CDR3s: implicating recognition of a common antigen epitope. Blood 101, 4952-7

Tschuch C, Schulz A, Pscherer A, Werft W, Benner A, Hotz-Wagenblatt A, Barrionuevo LS, Lichter P, Mertens D (2008): Off-target effects of siRNA specific for GFP. BMC Mol Biol 9, 60

Tucker CA, Kapanen AI, Chikh G, Hoffman BG, Kyle AH, Wilson IM, Masin D, Gascoyne RD, Bally M, Klasa RJ (2008): Silencing Bcl-2 in models of mantle cell lymphoma is associated with decreases in cyclin D1, nuclear factor-kappaB, p53, bax, and p27 levels. Mol Cancer Ther 7, 749-58

van de Wetering M, Oving I, Muncan V, Pon Fong MT, Brantjes H, van Leenen D, Holstege FC, Brummelkamp TR, Agami R, Clevers H (2003): Specific inhibition of gene expression using a stably integrated, inducible small-interfering-RNA vector. EMBO Rep 4, 609-15

Vogelstein B, Lane D, Levine AJ (2000): Surfing the p53 network. Nature 408, 307-10

Wang X, Liao DW, Scoy MV, Pacchione S, Yaciuk P, Moran E (2005): Monoclonal antibodies reactive with the BAF155 (SMARCC1) and BAF170 (SMARCC2) components of human SWI/SNF-related complexes. Hybridoma (Larchmt) 24, 55-7

Weinberg, R.A. (2007) The Biology of Cancer. Garland Science, New York City.

Weisenburger DD, Armitage JO (1996): Mantle cell lymphoma-- an entity comes of age. Blood 87, 4483-94

Weiss R (1982): The myc oncogene in man and birds. Nature 299, 9-10

Welzel N, Le T, Marculescu R, Mitterbauer G, Chott A, Pott C, Kneba M, Du MQ, Kusec R, Drach J, Raderer M, Mannhalter C, Lechner K, Nadel B, Jaeger U (2001): Templated nucleotide addition and immunoglobulin JH-gene utilization in t(11;14) junctions: implications for the mechanism of translocation and the origin of mantle cell lymphoma. Cancer Res 61, 1629-36

Westbrook TF, Stegmeier F, Elledge SJ (2005): Dissecting cancer pathways and vulnerabilities with RNAi. Cold Spring Harb Symp Quant Biol 70, 435-44

Winkler D, Schneider C, Krober A, Pasqualucci L, Lichter P, Dohner H, Stilgenbauer S (2005): Protein expression analysis of chromosome 12 candidate genes in chronic lymphocytic leukemia (CLL). Leukemia 19, 1211-5

Wirth D, Gama-Norton L, Riemer P, Sandhu U, Schucht R, Hauser H (2007): Road to precision: recombinase-based targeting technologies for genome engineering. Curr Opin Biotechnol 18, 411-9

Xiao G, Liu YE, Gentz R, Sang QA, Ni J, Goldberg ID, Shi YE (1999): Suppression of breast cancer growth and metastasis by a serpin myoepithelium-derived serine proteinase inhibitor expressed in the mammary myoepithelial cells. Proc Natl Acad Sci U S A 96, 3700-5

Yamaoka S, Inoue H, Sakurai M, Sugiyama T, Hazama M, Yamada T, Hatanaka M (1996): Constitutive activation of NF-kappa B is essential for transformation of rat fibroblasts by the human T-cell leukemia virus type I Tax protein. EMBO J 15, 873-87

Zhang B, Chambers KJ, Faller DV, Wang S (2007): Reprogramming of the SWI/SNF complex for co-activation or co-repression in prohibitin-mediated estrogen receptor regulation. Oncogene 26, 7153-7

Zumbansen M, Altrogge L, Toell A, Leake D, Müller-Hartmann H (2008) First siRNA Library Screening in Hard-to-Transfect HUVEC and Jurkat Cells, Application Note.

Supplementary

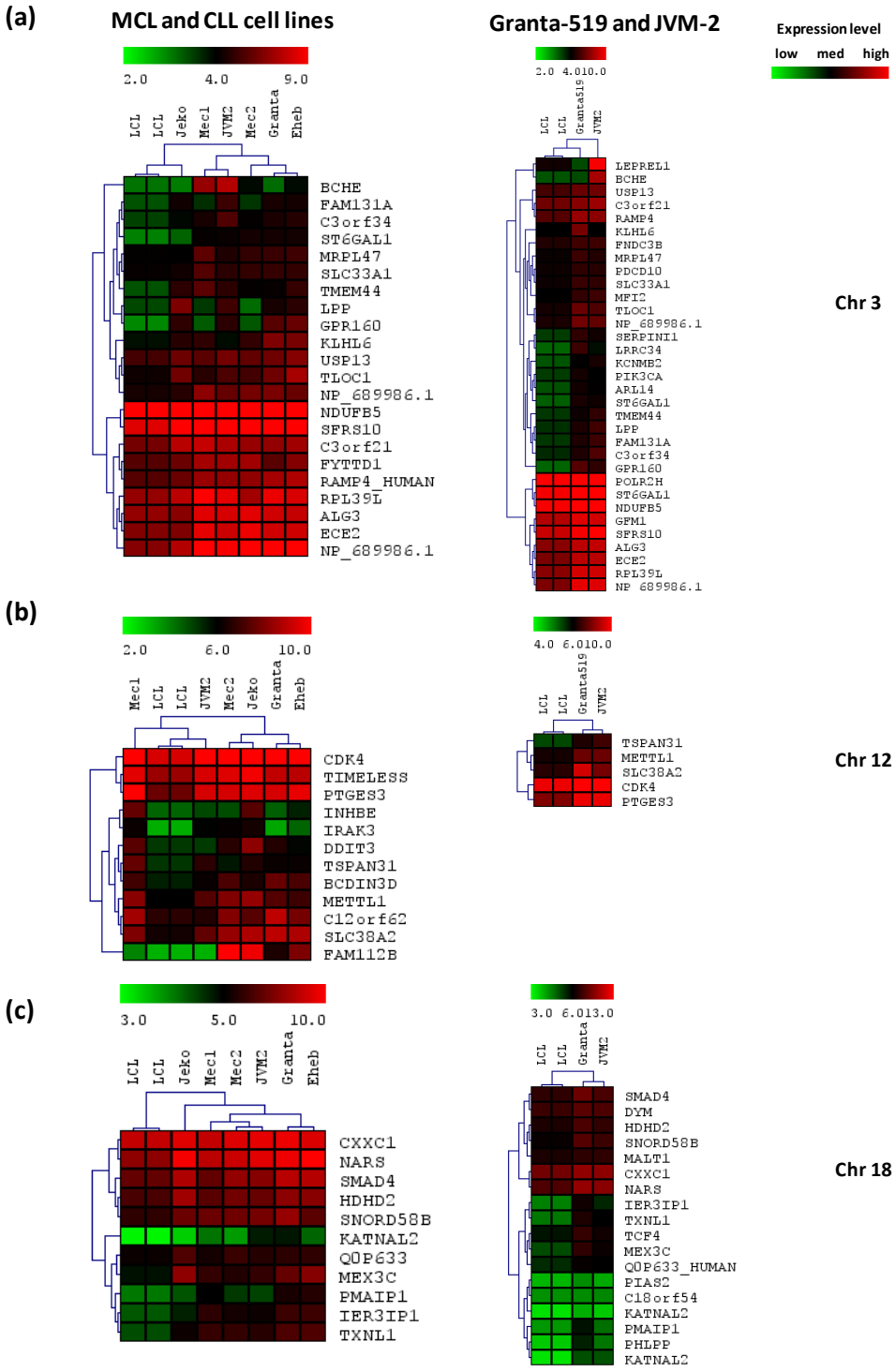

Figure 27: Expression profiling of MCL and CLL cell lines. Expression of three MCL and CLL cell lines compared to the lymphoblastoid non-tumor cell line LCL-WEI (left column). Expression profiling of the MCL cell lines JVM-2 and Granta-519 compared to the non-tumor cell line LCL-WEI (right column). Two class unpaired SAM analyses and hierachical clustering were performed for genes in recurrently genomic gained regions 3q25-q29 (a), 12q13-q14 (b) and 18q21-q22 (c).

Table 6: 72 overexpressed candidate genes identified by expression profiling and/or prediction in recent publications.

No.	Gene	Chr.	Log2 (MCL/CD19+)	Log2 (CLL/CD19+)	Recent publications
1	RARRES1	3q25	5.4	-	-
2	PFN2	3q25	1.6	2.3	Salaverria *et al.*, 2007
3	*GPR160	3q26		*CL : 5.3	Salaverria *et al.*, 2007
4	ACTL6A	3q26	6.0	1.2	Salaverria *et al.*, 2007
5	USP13	3q26	1.8	1.7	-
6	*BCHE	3q26		*CL : 7.2	Schraders *et al.*, 2005
7	APOD	3q26	130.0	15.0	Schmechel *et al.*, 2004
8	*PIK3CA	3q26		*CL: 1.7	Salaverria *et al.*, 2007
9	SerpinI2	3q26	-	-	Tagawa *et al.*, 2005
10	ECT2	3q26	2.0	-	Rubio-Moscardo *et al.*, 2005; Jares *et al.*, 2008; Sander *et al.*, 2008
11	SMC4	3q26	3.8	1.2	-
12	YEATS2	3q27	5.0	2.3	Salaverria *et al.*, 2007
13	RFC4	3q27	4.0	1.1	Salaverria *et al.*, 2007
14	ECE2	3q27	1.8	-	-
15	*C3ORF40	3q27		*CL : 1.9	-
16	DVL3	3q27	3.6	3.0	Salaverria *et al.*, 2007
17	KLHL6	3q27	6.0	-	Salaverria *et al.*, 2007
18	ETV5	3q28	2.7	-	Korz *et al.*, 2002, Salaverria *et al.*, 2007, Sander *et al.*, 2008
19	LEPREL1	3q28	1.5	1.2	-
20	FLJ42393	3q28	-	-	Salaverria *et al.*, 2007
21	*CCDC50	3q29		*CL: 1.5	Schmechel *et al.*, 2004; 2007; Bertoni *et al.*, 2006; Salaverria *et al.*, 2007
22	LAMP3	3q29	1.95	-	Rinaldi *et al.*, 2005
23	FAM43A	3q29	3.6	5.4	-
24	*C3orf34	3q29	*CL: 2.3		-
25	RPL39L	3q29	4.8	-	-
26	PAK2	3q29	2.0	4.6	Salaverria *et al.*, 2007
27	LRCH3	3q29	4.1	2.3	-
28	*IRAK3	12q13		*CL: 4.0	-
29	*SLC38A2	12q13		*CL: 4.4	-
30	HOXC6	12q13	4.0	-	-
31	RAPGEF3	12q13	3.8	35.0	-
32	KIAA0286	12q13	3.0	2.0	-
33	ARHGAP9	12q13	2.0	2.3	-
34	DDIT3	12q13	0.7	10.0	Rosenwald *et al.*, 2003
35	MBD6	12q13	1.4	1.3	Rosenwald *et al.*, 2003
36	*RHEBL1	12q13		*CL : 1.7	-
37	TIMELESS	12q13	3.7	2.0	Haslinger *et al.*, 2004
38	SMARCC2	12q13	1.8	5.4	-
39	RARG	12q13			Rosenwald *et al.*, 2003
40	*STAT6	12q13		*CL: 1.5	Rosenwald *et al.*, 2003; Winkler *et al.*, 2005
41	CDK2	12q13	6.0	1.5	Korz *et al.*, 2002

No.	Gene	Chr.	Log2 (MCL/CD19+)	Log2 (CLL/CD19+)	Recent publications
42	*FAM112B	12q13		*CL: 41	-
43	PA2G4	12q13	2.7	1.9	-
44	FAM113B	12q13	2.9	1.3	-
45	ITGB7	12q13	-	1.3	Rosenwald *et al.*, 2003; Greiner *et al.*, 2006
46	*INHBE	12q13		*CL : 3.8	-
47	*GLI1	12q13		*CL : 1.4	Sander *et al.*, 2008
48	MYL6B	12q13	3.6	1.3	-
49	METTL1	12q13	1.7	-	-
50	DTX3	12q13	2.9	6.3	-
51	DGKA	12q13	4.0	6.9	Rosenwald *et al.*, 2003
52	TUBA1B	12q13	3.5	-	Rosenwald *et al.*, 2003
53	*PTGES3	12q13		*CL: 3.1	-
54	GDF11	13q13		*CL : 1.5	-
55	CDK4	12q14	3.7	-	Hoffmann *et al.*, 2001; de Leuuw *et al.*, 2005; Rubio-Moscardo *et al.*,2005; Kienle *et al.*, 2005; Jares *et al.*, 2008
56	FAM119B	12q14	1.5	-	-
57	MARCH-IX	12q14	-	-	Rosenwald *et al.*, 2003
58	*TSFM	12q14	*CL : 1.4		-
59	KUB3	12q14	1.4	1.5	-
60	PIAS2	18q21	-	3.7	-
61	*IER3IP1	18q21		*CL: 3.0	-
62	*RKHD2	18q21		*CL: 3.5	Rosenwald *et al.*, 2003
63	*NARS	18q21		*CL: 3.4	-
64	*TXNL1	18q21		*CL : 3.7	-
65	*MALT1	18q21		*CL : 1.5	Rosenwald *et al.*, 2003
66	BCL2	18q21	-	1.5	Hofmann *et al.*, 2001 ; Korz *et al.*, 2002 ; Martinez *et al.*, 2003; de Leeuw *et al.*, 2004
67	VPS4B	18q21	1.8	1.3	Rinaldi *et al.*, 2005 ; Rizatti *et al.*, 2005, Rubio-Moscardo *et al.*, 2005
68	ZNF532	18q21	2.6	-	Rinaldi *et al.*, 2005
69	SerpinB2	18q21	2.0	1.5	-
70	ZADH2	18q22	4.7	1.8	-
71	CCDC5	18q21	1.8	1.5	-
72	TCF4	18q21	3.2	-	Rizatti *et al.*, 2005

Expression levels are calculated as log2 (tumor cells/healthy control), Chr=Chromosome, CL=Cell lines, (*)=Overexpressed only in cell lines, not in primary cells, 3 genes were not identified by expression profiling in this study, 37 genes were novel identified by expression profiling in this study and not correlated previously with MCL or CLL, 32 genes were identified both, in recent publications and by expression profiling in this study.

(a)

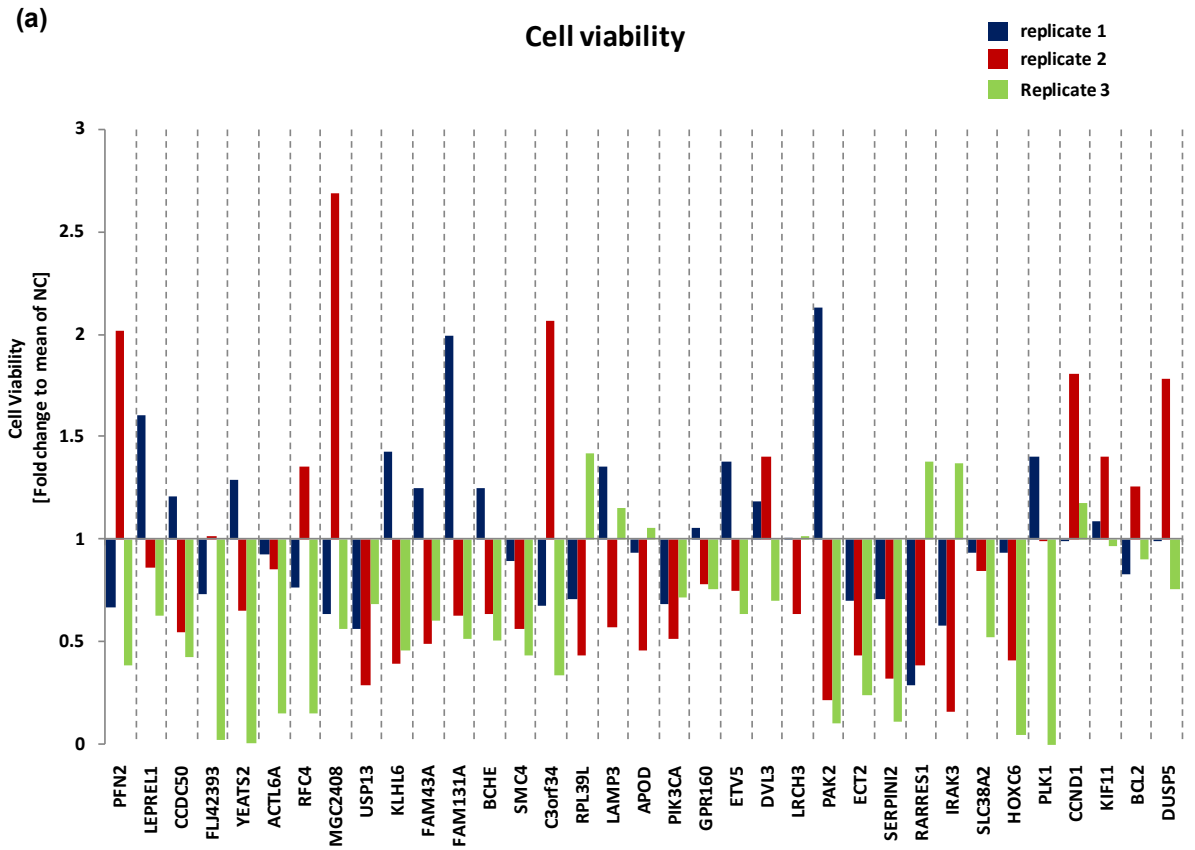
Cell viability
replicate 1
replicate 2
Replicate 3
Cell Viability
[Fold change to mean of NC]
3
2.5
2
1.5
1
0.5
0
PFN2
LEPREL1
CCDC50
FLJ42393
YEATS2
ACTL6A
RFC4
MGC2408
USP13
KLHL6
FAM43A
FAM131A
BCHE
SMC4
C3orf34
RPL39L
LAMP3
APOD
PIK3CA
GPR160
ETV5
DVL3
LRCH3
PAK2
ECT2
SERPINI2
RARRES1
IRAK3
SLC38A2
HOXC6
PLK1
CCND1
KIF11
BCL2
DUSP5

(b)

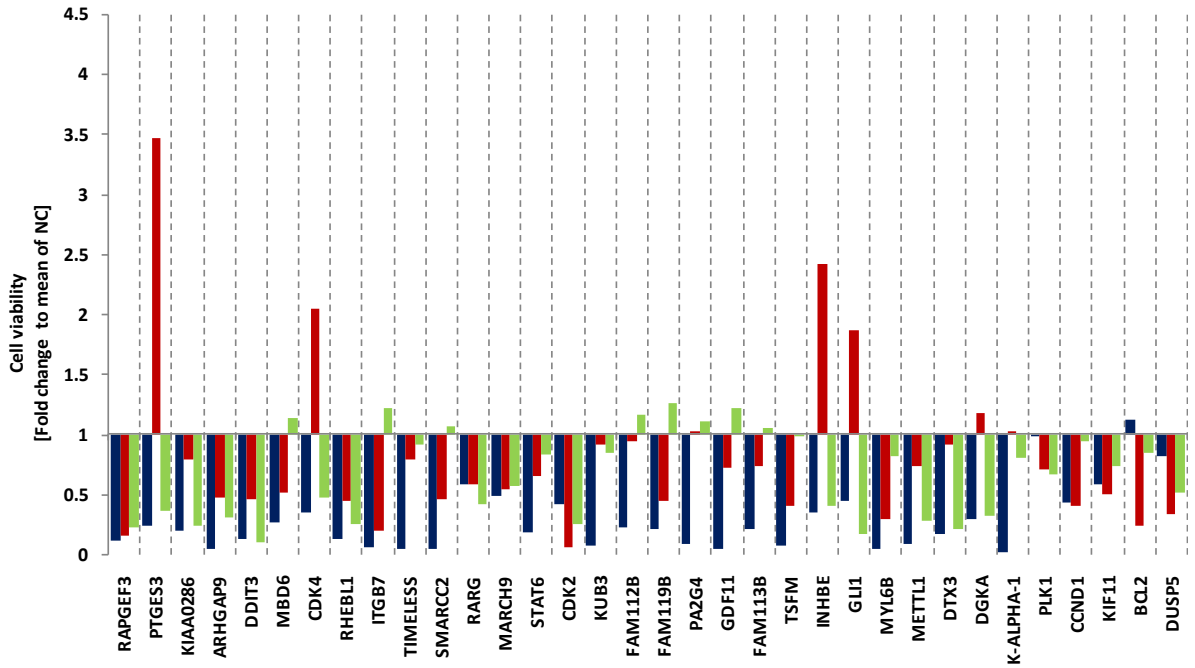
Cell viability
[Fold change to mean of NC]
4.5
4
3.5
3
2.5
2
1.5
1
0.5
0
RAPGEF3
PTGES3
KIAA0286
ARHGAP9
DDIT3
MBD6
CDK4
RHEBL1
ITGB7
TIMELESS
SMARCC2
RARG
MARCH9
STAT6
CDK2
KUB3
FAM112B
FAM119B
PA2G4
GDF11
FAM113B
TSFM
INHBE
GLI1
MYL6B
METTL1
DTX3
DGKA
K-ALPHA-1
PLK1
CCND1
KIF11
BCL2
DUSP5

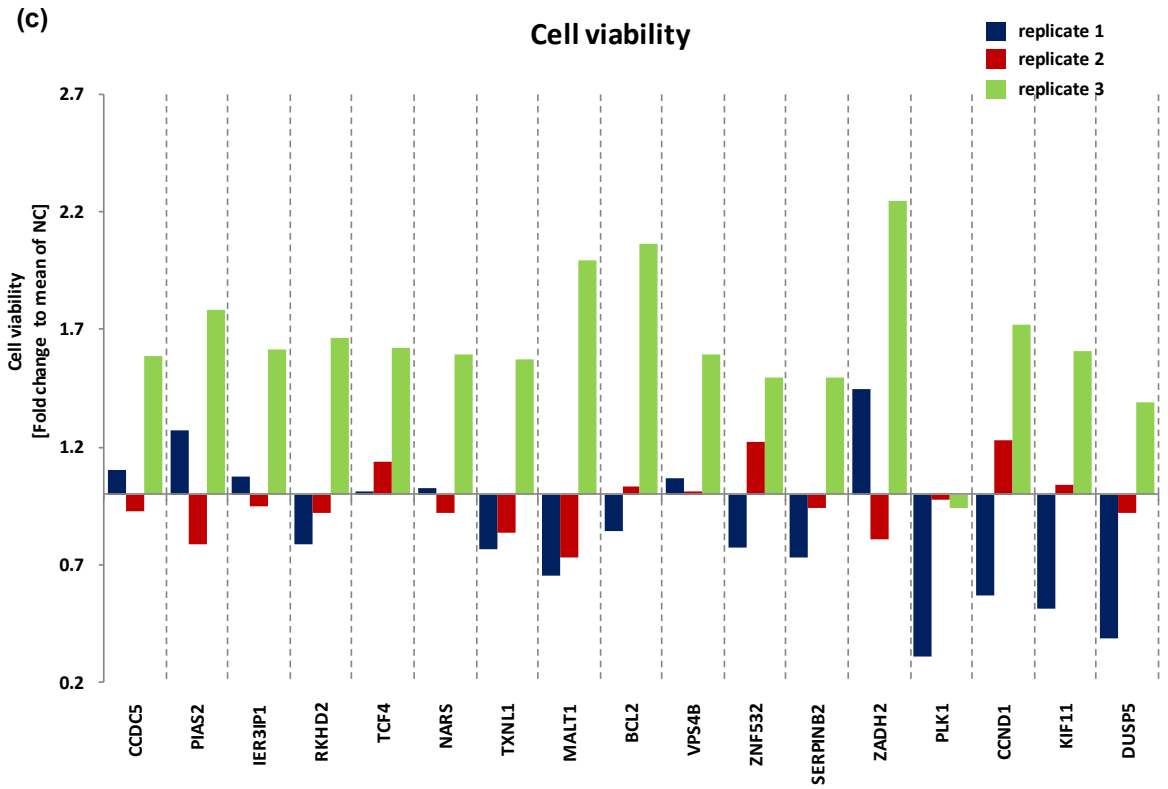

Figure 28: Cell viability assay of the three replicates of the siRNA screen. Cell viability was measured 72h p.t. of the 72 candidate genes and the controls, which are distributed in three independent 96-well plates: plate1 (a), plate 2 (b) and plate 3 (c). Cell viability assay was measured as the change in ATP levels after transfection of the gene of interest compared to transfection of a negative control ('NC'). The three replicates of the screen (replicate 1, 2, and 3) are shown as blue, red and green bars.

Chromosome	Gene	Replicate 1		Replicate 2		Replicate 3	
		Viability	FACS	Viability	FACS	Viability	FACS
Chromosome 3	PFN2						
	LEPREL1						
	CCDC50						
	FLJ42393						
	YEATS2						
	ACTL6A						
	RFC4						
	MGC2408						
	USP13						
	KLHL6						
	FAM43A						
	FAM131A						
	FAM79B						
	BCHE						
	SMC4						
	C3orf34						
	RPL39L						
	LAMP3						
	APOD						
	PIK3CA						
	GPR160						
	ETV5						
	DVL3						
	LRCH3						
	PAK2						
	ECT2						
	SERPINI2						
	RARRES1						
Chromosome 12	IRAK3						
	SLC38A2						
	HOXC6						
	RAPGEF3						
	PTGES3						
	KIAA0286						
	ARHGAP9						
	DDIT3						
	MBD6						
	CDK4						
	RHEBL1						
	ITGB7						
	TIMELESS						
	SMARCC2						

Chromosome	Gene	Replicate 1		Replicate 2		Replicate 3	
		Viability	FACS	Viability	FACS	Viability	FACS
Chromosome 12	RARG						
	MARCH9						
	STAT6						
	MAP3K12						
	CDK2						
	XRCC6BP1						
	FLJ32942						
	FAM119B						
	PA2G4_9						
	GDF11_6						
	FAM113B						
	DKFZP586A0522						
	TSFM						
	RACGAP1						
	INHBE						
	GLI1						
	MYL6B						
	METTL1						
	DTX3						
	DGKA						
	K-ALPHA-1						
Chromosome 18	CCDC5						
	PIAS2						
	IER3IP1						
	RKHD2						
	TCF4						
	NARS						
	TXNL1						
	MALT1				n.a.	n.a.	n.a.
	BCL2						
	VPS4B						
	MAPK4						
	MBD2						
	ZNF532						
	TNFRSF11A						
	SERPINB2						
	SOCS6						
	ZADH2						

Figure 29: Evaluation of cell viability assay and FACS analysis. Blue boxes indicate cells, after gene knockdown, which fulfilled the following criteria: (1) 'loss-of-viability' phenotype (luminescent based viability assay), (2) increased cell death rate (FACS), (3) a certain threshold: >20% reduction in cell viability in assay (1) and >20% dead cells in assay (2) compared to the mean of three independent negative controls, and (4) criteria (1)-(3) are fulfilled in two out of the three biological replicates. n.a.=value was not determined.

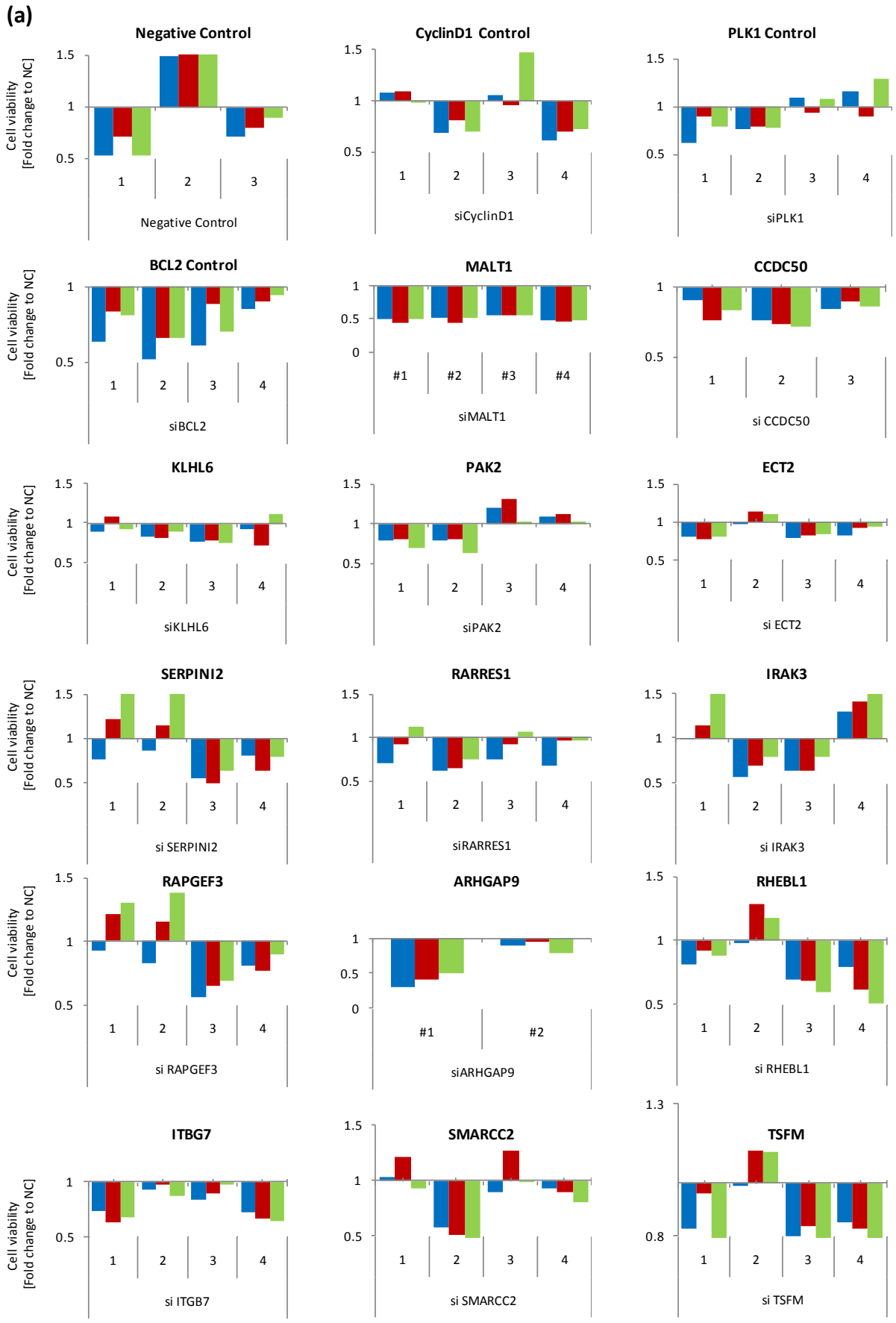
(a)
Negative Control
Cell viability [Fold change to NC]
Negative Control
CyclinD1 Control
siCyclinD1
PLK1 Control
siPLK1
BCL2 Control
siBCL2
MALT1
siMALT1
CCDC50
si CCDC50
KLHL6
siKLHL6
PAK2
siPAK2
ECT2
si ECT2
SERPINI2
si SERPINI2
RARRES1
siRARRES1
IRAK3
si IRAK3
RAPGEF3
si RAPGEF3
ARHGAP9
siARHGAP9
RHEBL1
si RHEBL1
ITBG7
si ITBG7
SMARCC2
si SMARCC2
TSFM
si TSFM

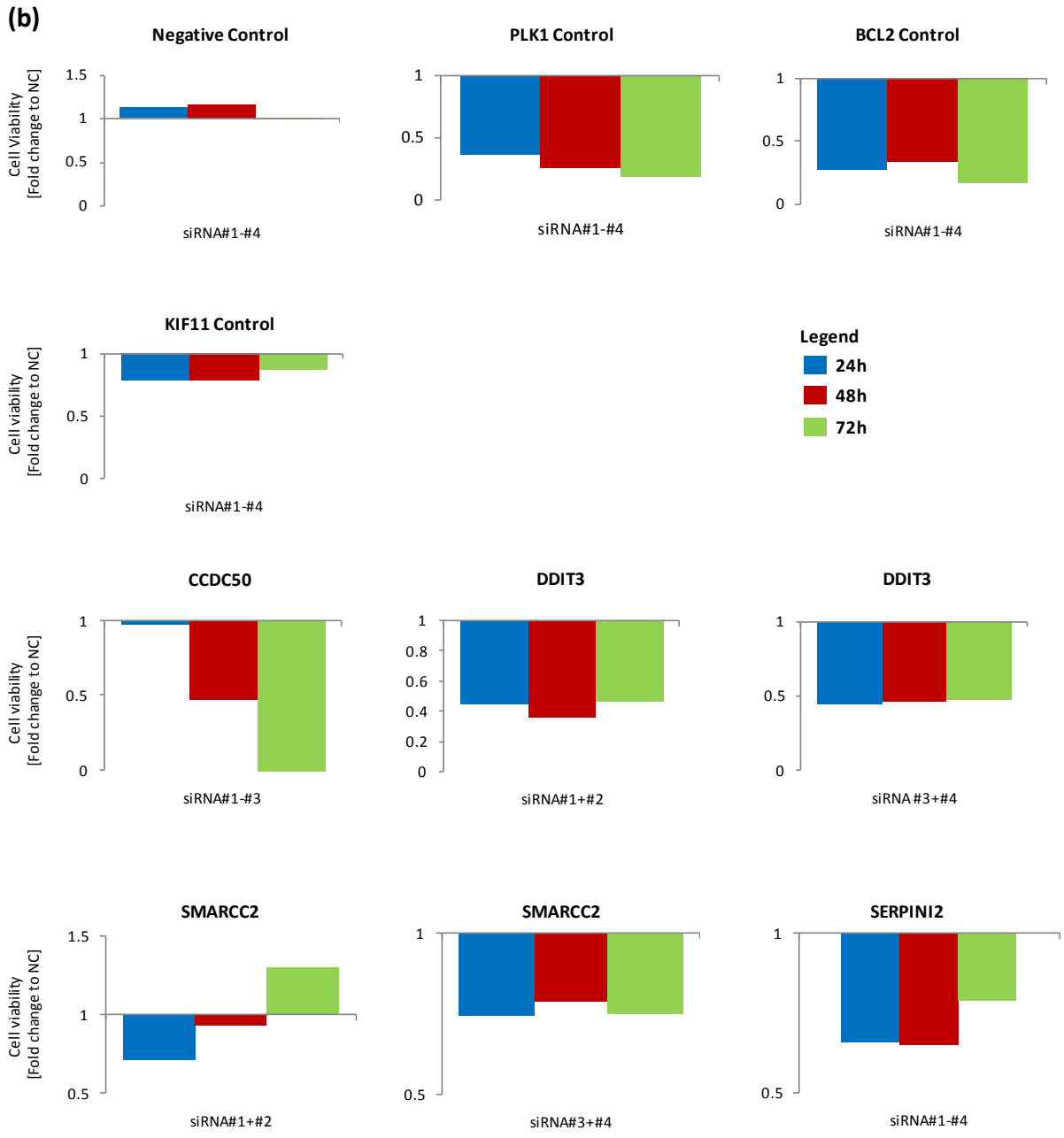
(b)
Negative Control
PLK1 Control
BCL2 Control
Cell Viability [Fold change to NC]
siRNA#1-#4
KIF11 Control
Cell viability [Fold change to NC]
Legend
24h
48h
72h
CCDC50
DDIT3
DDIT3
siRNA#1-#3
siRNA#1+#2
siRNA #3+#4
SMARCC2
SMARCC2
SERPINI2
siRNA#3+#4

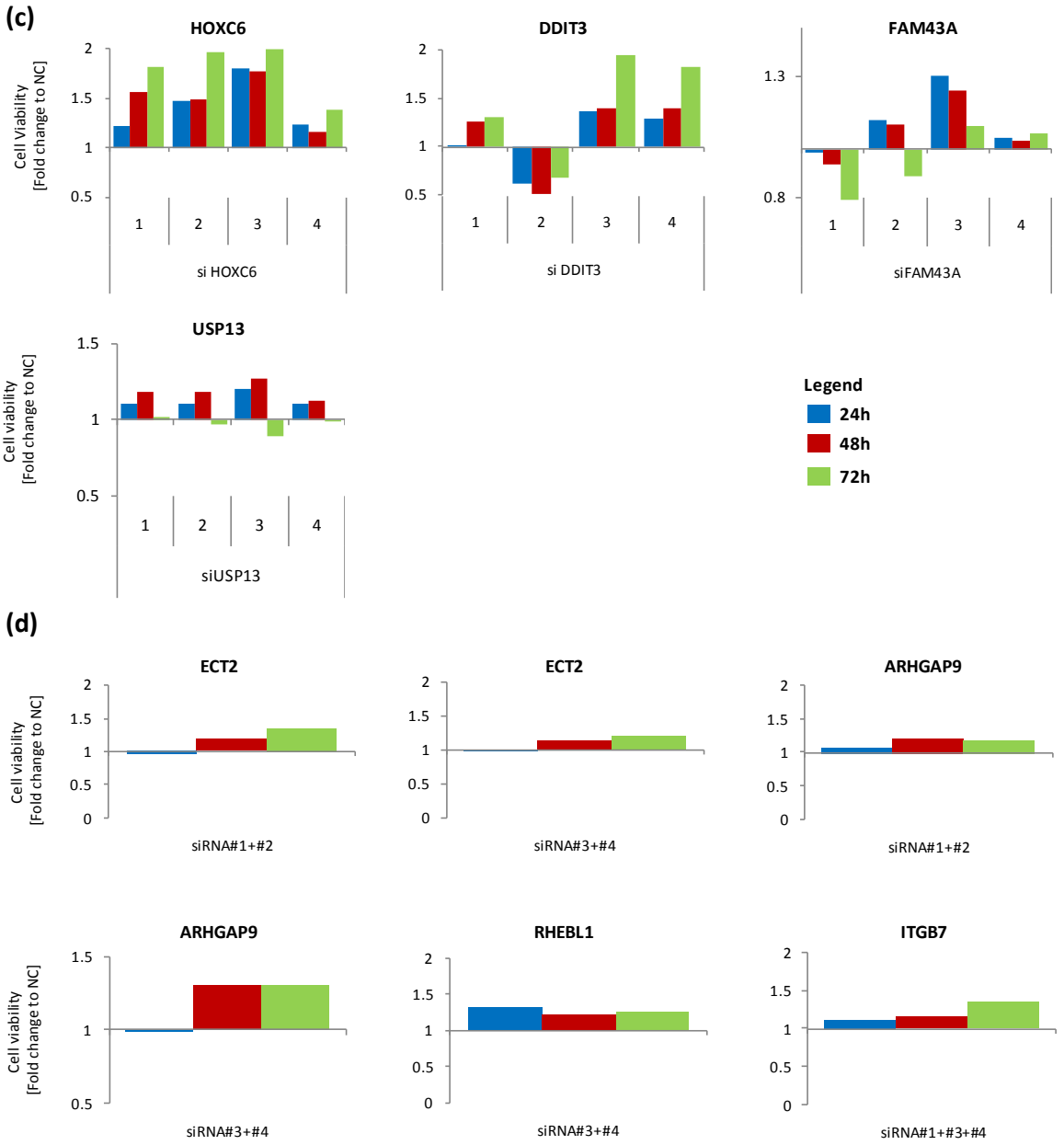

Figure 30: Cell viability assay of candidate genes from the siRNA screen. Cell viability was measured 24h, 48h, and 72h post transfection (blue, red and green bars). (a) Validation of the 'loss-of-viability' phenotype after silencing of 14 candidate genes in the MCL cell lines JVM-2 and Granta-519 using single siRNA molecules. Change in cell viability was measured 72 h post transfection in comparison to the mean of 3 negative controls: Control-AllStars-1, NegativeControl #1, and Silencer Firefly Luc GL2/3. (b) Validation of the 'loss-of-viability' phenotype in primary CLL cells using siRNA pools of 2-4 molecules. Changes in cell viability were measured in primary CLL cells at 72 h post transfection in comparison to the mean of 4 negative controls: si Silencer Firefly Luc GL2/3, ON TARGET plus siCONTROL, si Control Non-Targeting siRNA, siNegative Control. Positive controls (*BCL2*, *PLK1*, and *KIF11*) were used as pool of four siRNA molecules. (c) The four candidate genes *HOXC6*, *DDIT3*, *FAM42A*, and *USP13* could not be validated in the majority of tested individual siRNA sequences to reduce cell viability in the cell line JVM-2. (d) The four candidate genes *ECT2*, *ARHGAP9*, *RHEBL1*, and *ITGB7* could not be validated in the majority of tested pooled siRNA molecules to reduce cell viability primary CLL cells.

Table 7: Results after expression profiling of JVM-2 cells after CCDC50 knockdown (siCCDC50) and CCDC50 overexpression (pCMV_CCDC50).

JVM-2	Rank	Symbol	CCDC50 Silencing		CCDC50 Overexpression	
			log2 (siCCDC50/siNTC)	Fold change	log2 (pCMV-CCDC50 / pCMX)	Fold change
Upregulated	1	KRT17	1.02	2.03	-0.40	0.76
	2	TP53I3	1.01	2.01	-0.42	0.75
	3	PRODH	0.89	1.85	-0.66	0.63
	4	SPATA18	0.69	1.61	-0.41	0.75
	5	FCER2	0.67	1.59	-0.10	0.93
	6	CDKN1A	0.67	1.59	-0.12	0.92
	7	LAMP3	0.67	1.59	-0.14	0.91
	8	TRIP6	0.66	1.58	-0.06	0.96
	9	FDXR	0.65	1.57	-0.19	0.88
	10	EBI3	0.63	1.55	-0.55	0.68
	11	FAM129A	0.62	1.54	-0.38	0.77
	12	IGF2R	0.61	1.53	-0.07	0.95
	13	DUSP	0.59	1.51	-0.30	0.81
	14	MXD4	0.59	1.51	-0.31	0.81
	15	LAMP1	0.56	1.47	0.13	1.09
	16	CCND2	0.54	1.45	-0.00	1.00
	17	SESN1	0.47	1.39	-0.44	0.74
Downregulated	11	SLC16A3	-0.57	0.67	-0.13	0.91
	10	PHYH	-0.58	0.67	0.10	1.07
	9	PBK	-0.59	0.66	-0.04	0.97
	8	SLC2A3	-0.63	0.65	-0.07	0.95
	7	LGMN	-0.67	0.63	-0.22	0.86
	6	CCDC58	-0.68	0.62	0.22	1.16
	5	ALDOC	-0.81	0.57	-0.45	0.73
	4	ZNF395	-0.9	0.54	0.14	1.10
	3	BNIP3L	-1	0.50	-0.29	0.82
	2	ANKRD37	-1.48	0.36	0.02	1.01
	1	PFKFB4	-2.05	0.24	-0.07	0.95

Table 8: Results after expression profiling of Granta-519 cells after CCDC50 knockdown (siCCDC50) and CCDC50 overexpression (pCMV_CCDC50).

Granta-519	Rank	Symbol	CCDC50 Silencing		CCDC50 Overexpression	
			log2 (siCCDC50/siNTC)	Fold change	log2 (pCMV-CCDC50 / pCMX)	Fold change
Upregulated	1	APOBEC3H	1.81	3.51	-0.50	0.71
	2	PHLDA3	1.51	2.85	-0.55	0.68
	3	CMBL	1.38	2.60	-0.92	0.53
	4	LCE1B	1.37	2.58	-0.26	0.84
	5	CDKN1A	1.28	2.43	-0.09	0.94
	6	AMBP	1.11	2.16	0.11	1.08
	7	RPS27L	0.99	1.99	-0.84	0.56
	8	HMOX1	0.91	1.88	-0.49	0.71
	9	GADD45A	0.90	1.87	-0.06	0.96
	10	SPINK2	0.87	1.83	0.03	1.02
	11	VWCE	0.80	1.74	-0.02	0.99

Granta-519	Rank	Symbol	CCDC50 Silencing		CCDC50 Overexpression	
			log2 (siCCDC50/siNTC)	Fold change	log2 (pCMV-CCDC50 / pCMX)	Fold change
Upregulated	12	AHR	0.79	1.73	0.13	1.09
	13	BAX	0.78	1.72	0.13	1.09
	14	ATPIF1	0.77	1.71	0.43	1.35
	15	TNFSF4	0.74	1.67	0.36	1.29
	16	PLXNB2	0.73	1.66	-0.42	0.75
	17	TP53I3	0.73	1.66	0.14	1.10
	18	PHPT1	0.73	1.66	-0.33	0.80
	19	RARRES3	0.73	1.66	-0.03	0.98
	20	FDXR	0.71	1.64	-0.23	0.85
	21	C16orf5	0.71	1.64	-0.18	0.89
	22	SCNN1G	0.71	1.64	-0.03	0.98
	23	HERC5	0.70	1.62	-0.14	0.91
	24	C12orf5	0.69	1.61	-0.14	0.91
	25	PRPF4B	0.66	1.58	0.28	1.21
	26	AC012621.8	0.65	1.57	-0.09	0.94
	27	HIST1H2BJ	0.64	1.56	-0.19	0.88
	28	PLEKHF1	0.63	1.55	-0.19	0.88
	29	MCM8	0.63	1.55	-0.03	0.98
	30	ZRANB2	0.62	1.54	0.44	1.35
	31	FUCA1	0.62	1.54	-0.35	0.79
	32	GLIPR1	0.62	1.54	0.14	1.10
	33	TMEM163	0.59	1.51	-0.25	0.84
	34	MFI2	0.59	1.51	-0.11	0.93
	35	ZNF14	0.56	1.47	-0.02	0.99
	36	NLRP7	0.54	1.45	-0.15	0.90
	37	NHLRC2	0.53	1.44	-0.14	0.91
	38	TOB1	0.52	1.43	0.59	1.50
	39	PLAC8	0.51	1.42	0.22	1.17
Downregulated	19	MDM4	-0.45	0.73	0.18	1.13
	18	DAP3	-0.51	0.70	0.76	1.69
	17	ABCG1	-0.51	0.70	-0.27	0.83
	16	ABCA1	-0.53	0.69	-0.24	0.85
	15	BRWD1	-0.54	0.69	-0.34	0.79
	14	SLC2A3	-0.54	0.69	0.14	1.10
	13	CABLES2	-0.55	0.68	-0.47	0.72
	12	NCOA1	-0.55	0.68	-0.14	0.91
	11	ZRANB1	-0.56	0.68	0.34	1.27
	10	ANAPC1	-0.58	0.67	0.01	1.01
	9	PTGER4	-0.58	0.67	-0.73	0.60
	8	CCDC66	-0.60	0.66	0.22	1.17
	7	DIABLO	-0.60	0.66	1.25	2.38
	6	CHL1	-0.60	0.66	0.38	1.30
	5	THOC4	-0.65	0.64	4.10	17.12
	4	MAT2B	-0.68	0.62	0.40	1.32
	3	BTBD2	-0.68	0.62	0.06	1.04
	2	AUH	-0.69	0.62	-0.17	0.89
	1	DPP7	-0.91	0.53	0.59	1.51

Table 9: Information on siRNAs used for screening

Plate Name	Row	Col	Entrez Gene Id	NCBI gene symbol	siRNA Target Sequence 5´→3´	Product ID	Product Name
Farfsing No.2	A	1	5217	PFN2	CTGATTTAATATGCATTTAAA	SI02653959	Hs_PFN2_7
Farfsing No.2	A	2	8975	USP13	AGCGACGATTATGAATATGAA	SI00058100	Hs_USP13_2
Farfsing No.2	A	3	116832	RPL39L	TTGCCTCTTTGGAGTAGGAAA	SI00706552	Hs_RPL39L_4
Farfsing No.2	A	4	5062	PAK2	AAGAAAAGGAACGGCCAGAAA	SI00301077	Hs_PAK2_6
Farfsing No.2	A	5	10411	RAPGEF3	CTGGAGCCTCTTCAACAGTAT	SI04377296	Hs_RAPGEF3_6
Farfsing No.2	A	6	3695	ITGB7	ACGCACCTATGTGGAAACTAA	SI00017836	Hs_ITGB7_2
Farfsing No.2	A	7	91419	XRCC6BP1	GACGCTGGAGACAAATCCATA	SI04313078	Hs_XRCC6BP1_2
Farfsing No.2	A	8	29127	RACGAP1	CTGAATGTATCTCCTAGCTAT	SI00101171	Hs_RACGAP1_2
Farfsing No.2	A	9	115106	CCDC5	AAGCGAGAACTAGATAGCATT	SI04359824	Hs_CCDC5_10
Farfsing No.2	A	10	596	BCL2	AACTGGGGGAGGATTGTGGCC	SI00299411	Hs_BCL2_11
Farfsing No.2	A	11	284273	ZADH2	ACGCTTACATTCAATTCTTTA	SI00159551	Hs_ZADH2_1
Farfsing No.2	A	12			AACGTACGCGGAATACTTCGA	1022070	Unspecific_LuciferaseGL2_1
Farfsing No.2	B	1	55214	LEPREL1	CTGAACCGAATTATTGGATCA	SI04265184	Hs_LEPREL1_8
Farfsing No.2	B	2	23043	TNIK	CTGGAATATAAGCGCAAACAA	SI02225510	Hs_TNIK_6
Farfsing No.2	B	3	27074	LAMP3	AGGGCGGATTTGTGAATCTCA	SI04231311	Hs_LAMP3_6
Farfsing No.2	B	4	1894	ECT2	TTGCCTAGAGATAGCAAGAAA	SI02643067	Hs_ECT2_5
Farfsing No.2	B	5	10728	PTGES3	CAGATATGCTGTATTTGCCTA	SI02781170	Hs_PTGES3_2
Farfsing No.2	B	6	8914	TIMELESS	ACGGGCCCGAATAGTGGATAA	SI04140297	Hs_TIMELESS_5
Farfsing No.2	B	7	121355	GTSF1	AACTCACTACTCTGACAACAA	SI04346965	Hs_FAM112B_2
Farfsing No.2	B	8	83729	INHBE	AGGGCTGTTGAGGTACCTTAA	SI02779875	Hs_INHBE_8
Farfsing No.2	B	9	9063	PIAS2	AGCCCTGCGGTTCAGATTAAA	SI03143749	Hs_PIAS2_5
Farfsing No.2	B	10	9525	VPS4B	AGCGATAGATCTGGCTAGCAA	SI03144456	Hs_VPS4B_5
Farfsing No.2	B	11	5347	PLK1	CACCATATGAATTGTACAGAA	SI00071631	Hs_PLK1_3
Farfsing No.2	B	12	5347	PLK1	CACCATATGAATTGTACAGAA	SI00071631	Hs_PLK1_3
Farfsing No.2	C	1	152137	CCDC50	GACCGGGAAGCCCGCGTTAAA	SI04261201	Hs_CCDC50_1
Farfsing No.2	C	2	131583	FAM43A	CTGAGCTGTCGCAACTTATTA	SI04278001	Hs_FAM43A_7
Farfsing No.2	C	3	347	APOD	ATCTCGGAAGATGGTACGAAA	SI04309305	Hs_APOD_9
Farfsing No.2	C	4	5276	SERPINI2	CTGGCTCAAAGCCAATTTATA	SI00085813	Hs_SERPINI2_2
Farfsing No.2	C	5	23306	TMEM194A	CACGGATACAGATCCGAGTAA	SI04304867	Hs_KIAA0286_6
Farfsing No.2	C	6	6601	SMARCC2	CGCCGCCGCAGTGAAAGCTAA	SI04173169	Hs_SMARCC2_7
Farfsing No.2	C	7	25895	FAM119B	AGCACTAGTGTTAGAACACCA	SI04280052	Hs_FAM119B_2
Farfsing No.2	C	8	2735	GLI1	ACCCAACTTGCCCAATCACAA	SI00074802	Hs_GLI1_2
Farfsing No.2	C	9	51124	IER3IP1	TGAGTGGTTATCCCTAGATAA	SI04172175	Hs_IER3IP1_6
Farfsing No.2	C	10	5596	MAPK4	AAGGATCGTTGATCAGCATTA	SI00606011	Hs_MAPK4_5
Farfsing No.2	C	11	595	CCND1	GCCCTCGGTGTCCTACTTCAA	SI02654547	Hs_CCND1_6
Farfsing No.2	C	12	595	CCND1	GCCCTCGGTGTCCTACTTCAA	SI02654547	Hs_CCND1_6
Farfsing No.2	D	1	401105	FLJ42393	TAGGATGTTGTGATCGACACA	SI04773685	Hs_FLJ42393_5
Farfsing No.2	D	2	131408	FAM131A	CAGGGTGTTAATGCCCACGTA	SI00635313	Hs_MGC21688_3
Farfsing No.2	D	3	5290	PIK3CA	CTCCGTGAGGCTACATTAATA	SI02665369	Hs_PIK3CA_8
Farfsing No.2	D	4	10644	IGF2BP2	CAGGGCGTTAAATTCACAGAT	SI03176593	Hs_IGF2BP2_1
Farfsing No.2	D	5	64333	ARHGAP9	CCGCGTGCGCAACAAACTAAA	SI00302603	Hs_ARHGAP9_3
Farfsing No.2	D	6	5916	RARG	TACGACTGTATGGAAACGTTT	SI04025609	Hs_RARG_8
Farfsing No.2	D	7	5036	PA2G4	ATGCCATGCCGTTTACTTTAA	SI02636858	Hs_PA2G4_4
Farfsing No.2	D	8	140465	MYL6B	CAGGCAGTGGCCAAGAACCGA	SI03175312	Hs_MYL6B_1
Farfsing No.2	D	9	51320	MEX3C	CCGCGCAAGAATGATATCCAA	SI00703682	Hs_RKHD2_2
Farfsing No.2	D	10	8932	MBD2	TGGAAAGATGATGCCTAGTAA	SI02632280	Hs_MBD2_7
Farfsing No.2	D	11	3832	KIF11	GCCGATAAGATAGAAGATCAA	SI02653770	Hs_KIF11_7
Farfsing No.2	D	12	3832	KIF11	GCCGATAAGATAGAAGATCAA	SI02653770	Hs_KIF11_7
Farfsing No.2	E	1	55689	YEATS2	CACAAGGACAACAAACGCTAA	SI04174639	Hs_YEATS2_5
Farfsing No.2	E	2	285386	TPRG1	CAAGACTCTCTTGATCTGCAA	SI04197781	Hs_FAM79B_3
Farfsing No.2	E	3	26996	GPR160	ACAGCTGTCATAAGATCATAA	SI00105329	Hs_GPR160_3
Farfsing No.2	E	4	5918	RARRES1	CCCTTGGAAATAGTCAGCATA	SI03079762	Hs_RARRES1_8
Farfsing No.2	E	5	1649	DDIT3	CAGCTTGTATATAGAGATTGT	SI00059535	Hs_DDIT3_2
Farfsing No.2	E	6	92979	MARCH-9	CAGGTTGGATGCCGTTGCAGA	SI04236694	Hs_MARCH9_2
Farfsing No.2	E	7	10220	GDF11	CAGAGCATCGACTTCAAGCAA	SI00081529	Hs_GDF11_4
Farfsing No.2	E	8	4234	METTL1	CTGGTGTATACCATAACCGAT	SI00076132	Hs_METTL1_3
Farfsing No.2	E	9	6925	TCF4	AGCCGAATTGAAGATCGTTTA	SI00048965	Hs_TCF4_4
Farfsing No.2	E	10	55205	ZNF532	CACATAGGTCCGAATAACCTA	SI04195765	Hs_ZNF532_7
Farfsing No.2	E	11	596	BCL2	AACTGGGGGAGGATTGTGGCC	SI00299411	Hs_BCL2_11
Farfsing No.2	E	12	1847	DUSP5	CTGAGTGTTGCGTGGATGTAA	SI03206903	Hs_DUSP5_10
Farfsing No.2	F	1	86	ACTL6A	CAACAGTGGAACGGAGGTTTA	SI02779994	Hs_ACTL6A_6
Farfsing No.2	F	2	590	BCHE	CAGGAGTGAGTGAGTTTGGAA	SI00000924	Hs_BCHE_3
Farfsing No.2	F	3	2119	ETV5	CCCACCTCCAACCAAGATCAA	SI04251835	Hs_ETV5_8
Farfsing No.2	F	4	11213	IRAK3	CTGGATGTTCGTCATATTGAA	SI02224285	Hs_IRAK3_6
Farfsing No.2	F	5	114785	MBD6	CAGGCACGCGGGAGCTGATTA	SI04182353	Hs_MBD6_7
Farfsing No.2	F	6	6778	STAT6	CAGGATGGCTCTCCACAGATA	SI00048447	Hs_STAT6_1
Farfsing No.2	F	7	91523	FAM113B	CCGTCTGGTCACAATGATCTA	SI00633941	Hs_MGC16044_3
Farfsing No.2	F	8	196403	DTX3	TGGGCGGATGCTGGTCTCTAA	SI03020871	Hs_DTX3_5
Farfsing No.2	F	9	4677	NARS	AACGTGGATTCTGAATAGGTA	SI03126592	Hs_NARS_6
Farfsing No.2	F	10	8792	TNFRSF11A	TTCCTTGGAAAGAGAGTAGAA	SI03022544	Hs_TNFRSF11A_5
Farfsing No.2	F	11	1847	DUSP5	CTGAGTGTTGCGTGGATGTAA	SI03206903	Hs_DUSP5_10
Farfsing No.2	G	1	5984	RFC4	CCGATTCTGTCTTATCTGTAA	SI02665719	Hs_RFC4_6
Farfsing No.2	G	2	10051	SMC4	AAGGGACTTTGTTGAACTTTA	SI00727013	Hs_SMC4L1_3

Plate Name	Row	Col	Entrez Gene Id	NCBI gene symbol	siRNA Target Sequence 5´→3´	Product ID	Product Name
Farfsing No.2	G	3	1857	DVL3	TCGGATGACAATGCCAAGCTA	SI03116799	Hs_DVL3_8
Farfsing No.2	G	4	54407	SLC38A2	CAGCGACTTCAACTACTCCTA	SI03066756	Hs_SLC38A2_8
Farfsing No.2	G	5	1019	CDK4	AAGCCTCTCTTCTGTGGAAAC	SI00299789	Hs_CDK4_4
Farfsing No.2	G	6	7786	MAP3K12	CTCAGGCGAGAGCAAGCTTTA	SI00087206	Hs_MAP3K12_4
Farfsing No.2	G	7	25840	METTL7A	TAGGTTGGTTAGAGGGTTTAA	SI00102928	Hs_DKFZP586A0522_2
Farfsing No.2	G	8	1606	DGKA	ATCCATCTTCTCAACATGCAA	SI00605199	Hs_DGKA_5
Farfsing No.2	G	9	9352	TXNL1	AACTATATTTGTTCAGTCGAA	SI03030482	Hs_TXNL1_7
Farfsing No.2	G	10	5055	SERPINB2	AACCTATGACAAACTCAACAA	SI02628962	Hs_SERPINB2_5
Farfsing No.2	H	1	9718	ECE2	CAGCTCCAACTAGATCCAGAA	SI00635845	Hs_MGC2408_3
Farfsing No.2	H	2	84984	C3orf34	TCCAGCTATTATCTTAATCTA	SI00632954	Hs_MGC14126_2
Farfsing No.2	H	3	84859	LRCH3	AACGGCGGAGTGGAACATGAT	SI04271575	Hs_LRCH3_5
Farfsing No.2	H	4	3223	HOXC6	CGCCCTCAATTCCACCGCCTA	SI03193778	Hs_HOXC6_5
Farfsing No.2	H	5	121268	RHEBL1	TTGGCACATCAATTTGTGGAA	SI04216800	Hs_RHEBL1_7
Farfsing No.2	H	6	1017	CDK2	CACGTACGGAGTTGTGTACAA	SI00605353	Hs_CDK2_7
Farfsing No.2	H	7	10102	TSFM	AAGGATCAGTTGGCTTTAGCA	SI04200091	Hs_TSFM_6
Farfsing No.2	H	8	10376	TUBA1B	AAGGAGAGGAATACTAATTAT	SI00084329	Hs_K-ALPHA-1_4
Farfsing No.2	H	9	10892	MALT1	CACAGTTGATACATAGTTGTA	SI00091903	Hs_MALT1_2
Farfsing No.2	H	10	9306	SOCS6	TTGATCTAATTGAGCATTCAA	SI00061369	Hs_SOCS6_1
Farfsing No.2	H	12			AACGTACGCGGAATACTTCGA	1022070	Unspecific_LuciferaseGL2_1
Farfsing No.4	A	1	5217	PFN2	CAAACTGTAGATGGTAGCTAA	SI00040677	Hs_PFN2_2
Farfsing No.4	A	2	8975	USP13	CCACCCGGAATTCTCCTCTAA	SI03074498	Hs_USP13_6
Farfsing No.4	A	3	116832	RPL39L	CTGTATCAAGTTCACGATCAT	SI04232655	Hs_RPL39L_5
Farfsing No.4	A	4	5062	PAK2	CCGGATCATACGAAATCAATT	SI00605717	Hs_PAK2_9
Farfsing No.4	A	5	10411	RAPGEF3	AGGGACCGTGTTGTTCAGCCA	SI04378157	Hs_RAPGEF3_7
Farfsing No.4	A	6	3695	ITGB7	GACGGCTACTATGGTGCTCTA	SI00017843	Hs_ITGB7_3
Farfsing No.4	A	7	91419	XRCC6BP1	TTCCATGATGTTGATAGGTGA	SI04372228	Hs_XRCC6BP1_4
Farfsing No.4	A	8	29127	RACGAP1	CTGGTAGATAGAAGAGCTAAA	SI02639840	Hs_RACGAP1_5
Farfsing No.4	A	9	115106	CCDC5	TGGAGTCCTATTTAGACTTAA	SI04776926	Hs_CCDC5_13
Farfsing No.4	A	10	596	BCL2	AAGTTCGGTGGGGTCATGTGT	SI00299404	Hs_BCL2_10
Farfsing No.4	A	11	284273	ZADH2	AAAGGGCGCTTGATAGTAATA	SI03026835	Hs_ZADH2_6
Farfsing No.4	A	12			AACGTACGCGGAATACTTCGA	1022070	Unspecific_LuciferaseGL2_1
Farfsing No.4	B	1	55214	LEPREL1	CCGAAGCCCTCTCGAGCGTAA	SI04252640	Hs_LEPREL1_7
Farfsing No.4	B	2	23043	TNIK	CCGGAATATTGCTACATACTA	SI02794470	Hs_TNIK_8
Farfsing No.4	B	3	27074	LAMP3	AAGGTGTCAATCATCTGGATA	SI04356303	Hs_LAMP3_8
Farfsing No.4	B	4	1894	ECT2	GTCGCCCGTTGTATTGTACAA	SI03106390	Hs_ECT2_7
Farfsing No.4	B	5	10728	PTGES3	TTCCAGGTGTATCTTAGCTAA	SI04438735	Hs_PTGES3_6
Farfsing No.4	B	6	8914	TIMELESS	ACCGGCTCATGGGATCAGTAA	SI04282880	Hs_TIMELESS_7
Farfsing No.4	B	7	121355	GTSF1	GAGCAAGATGTTGTCAACCAA	SI00407477	Hs_FLJ32942_4
Farfsing No.4	B	8	83729	INHBE	AAGGGTTAGGGTGATGGTCCA	SI02646399	Hs_INHBE_6
Farfsing No.4	B	9	9063	PIAS2	AAGCCCACGAGTTTAGTTCAA	SI04367433	Hs_PIAS2_7
Farfsing No.4	B	10	9525	VPS4B	CAGGAAAGTCCTACTTAGCCA	SI04198579	Hs_VPS4B_8
Farfsing No.4	B	11	5347	PLK1	CCCGAGGTGCTGAGCAAGAAA	SI00071638	Hs_PLK1_4
Farfsing No.4	B	12	5347	PLK1	CCCGAGGTGCTGAGCAAGAAA	SI00071638	Hs_PLK1_4
Farfsing No.4	C	1	152137	CCDC50	CTGTATCTACTCCATCACGAA	SI04372074	Hs_CCDC50_4
Farfsing No.4	C	2	131583	FAM43A	TACACGGACCCTGCTGCTATA	SI04327757	Hs_FAM43A_8
Farfsing No.4	C	3	347	APOD	TTGGGAGAGGCCAGTCACCAA	SI04225760	Hs_APOD_8
Farfsing No.4	C	4	5276	SERPINI2	CTCCCTAGATTTAAAGTAGAA	SI00085820	Hs_SERPINI2_3
Farfsing No.4	C	5	23306	TMEM194A	CCAGACTTACTGGCTCACCAA	SI04334288	Hs_KIAA0286_8
Farfsing No.4	C	6	6601	SMARCC2	CACCGTGACCCAGTTCGACAA	SI04277560	Hs_SMARCC2_8
Farfsing No.4	C	7	25895	FAM119B	CCGAGGCAAGAAGGTGATCGA	SI04316221	Hs_FAM119B_4
Farfsing No.4	C	8	2735	GLI1	CAGACGGTTATCCGCACCTCA	SI03063641	Hs_GLI1_6
Farfsing No.4	C	9	51124	IER3IP1	CAGACCAGTGTCTACAGATTT	SI04299477	Hs_IER3IP1_8
Farfsing No.4	C	10	5596	MAPK4	GAGGACCTGCCGGACAATAAA	SI00042497	Hs_MAPK4_4
Farfsing No.4	C	11	595	CCND1	ATGCATGTAGTCACTTTATAA	SI00147819	Hs_CCND1_2
Farfsing No.4	C	12	595	CCND1	ATGCATGTAGTCACTTTATAA	SI00147819	Hs_CCND1_2
Farfsing No.4	D	1	401105	FLJ42393	CTGTGCCTGACTGGTCAGAAA	SI04773699	Hs_FLJ42393_7
Farfsing No.4	D	2	131408	FAM131A	ATGGGTTGAGCCGTCCCTCAA	SI04263469	Hs_FAM131A_1
Farfsing No.4	D	3	5290	PIK3CA	TGCGAAATTCTCACACTATTA	SI00085841	Hs_PIK3CA_2
Farfsing No.4	D	4	10644	IGF2BP2	CCCGGGTAGATATCCATAGAA	SI04367020	Hs_IGF2BP2_4
Farfsing No.4	D	5	64333	ARHGAP9	CCAGGACAAGAAGGTCGGTTA	SI04373950	Hs_ARHGAP9_6
Farfsing No.4	D	6	5916	RARG	AAGCCGGGTCGCGATGTACGA	SI04025602	Hs_RARG_7
Farfsing No.4	D	7	5036	PA2G4	CTACAGAACAGGGCTAAATTA	SI04383253	Hs_PA2G4_9
Farfsing No.4	D	8	140465	MYL6B	CGAGGCCTTCTTGAAACACAT	SI04337697	Hs_MYL6B_4
Farfsing No.4	D	9	51320	MEX3C	AACCATGTTGGCCTTCCAATA	SI03028487	Hs_RKHD2_5
Farfsing No.4	D	10	8932	MBD2	CGAAACGATCCTCTCAATCAA	SI03083605	Hs_MBD2_10
Farfsing No.4	D	11	3832	KIF11	CTAGATGGCTTTCTCAGTATA	SI00064855	Hs_KIF11_4
Farfsing No.4	D	12	3832	KIF11	CTAGATGGCTTTCTCAGTATA	SI00064855	Hs_KIF11_4
Farfsing No.4	E	1	55689	YEATS2	TACGGTCAGTTCTGTAACGAA	SI04351032	Hs_YEATS2_7
Farfsing No.4	E	2	285386	TPRG1	ATCCTTATCATCAGCCTTATA	SI04287864	Hs_FAM79B_4
Farfsing No.4	E	3	26996	GPR160	TTGGTACAGGCTATCAGGATA	SI04901043	Hs_GPR160_11
Farfsing No.4	E	4	5918	RARRES1	TACCTGATAATCATGGACATA	SI03109225	Hs_RARRES1_10
Farfsing No.4	E	5	1649	DDIT3	AGGGAGAACCAGGAAACGGAA	SI00059542	Hs_DDIT3_3
Farfsing No.4	E	6	92979	MARCH-9	CCAGCAGTGGAAGGTCCTAAA	SI04316424	Hs_MARCH9_4
Farfsing No.4	E	7	10220	GDF11	TGCGAGTACATGTTCATGCAA	SI03118724	Hs_GDF11_6

Plate Name	Row	Col	Entrez Gene Id	NCBI gene symbol	siRNA Target Sequence 5´→3´	Product ID	Product Name
Farfsing No.4	E	8	4234	METTL1	CAGAAGCGCTACTACCGGCAA	SI03063088	Hs_METTL1_5
Farfsing No.4	E	9	6925	TCF4	CACGAAATCTTCGGAGGACAA	SI00048944	Hs_TCF4_1
Farfsing No.4	E	10	55205	ZNF532	AACGAAAGGGCTGGACTACTA	SI04243393	Hs_ZNF532_9
Farfsing No.4	E	11	596	BCL2	AAGTTCGGTGGGGTCATGTGT	SI00299404	Hs_BCL2_10
Farfsing No.4	E	12	1847	DUSP5	CAAGTGCGAGTTCCTCGCCAA	SI04345124	Hs_DUSP5_14
Farfsing No.4	F	1	86	ACTL6A	TACGAGGTCTTGGCACAATTA	SI00062405	Hs_ACTL6A_1
Farfsing No.4	F	2	590	BCHE	CAGAACGTTGAACTTAGCTAA	SI00000931	Hs_BCHE_4
Farfsing No.4	F	3	2119	ETV5	CAGGCTCTTGGTGCTAACTAT	SI04189738	Hs_ETV5_7
Farfsing No.4	F	4	11213	IRAK3	TCGGTCATCTGTGGCAGTATA	SI00095431	Hs_IRAK3_4
Farfsing No.4	F	5	114785	MBD6	CGGTCTGGAGTGTCCACTTAA	SI04272044	Hs_MBD6_9
Farfsing No.4	F	6	6778	STAT6	CAGCGGCTCTATGTCGACTTT	SI03067414	Hs_STAT6_6
Farfsing No.4	F	7	91523	FAM113B	CACCGAGGCACGTAAACATAA	SI04216506	Hs_FAM113B_2
Farfsing No.4	F	8	196403	DTX3	TGGCGAGACTTCTGACATCTA	SI03120264	Hs_DTX3_7
Farfsing No.4	F	9	4677	NARS	TTGGTGCGTTAGAAGGATATA	SI04324719	Hs_NARS_8
Farfsing No.4	F	10	8792	TNFRSF11A	CTGGGACGGTGCTGTAACAAA	SI03098578	Hs_TNFRSF11A_7
Farfsing No.4	F	11	1847	DUSP5	CAAGTGCGAGTTCCTCGCCAA	SI04345124	Hs_DUSP5_14
Farfsing No.4	G	1	5984	RFC4	GCCGAAGTTGACAAATGCCTA	SI00045689	Hs_RFC4_2
Farfsing No.4	G	2	10051	SMC4	GCCCGGTGTCATGAAATGAAA	SI04294738	Hs_SMC4_2
Farfsing No.4	G	3	1857	DVL3	CCCGGCTAAATGGAACTGCGA	SI00063476	Hs_DVL3_3
Farfsing No.4	G	4	54407	SLC38A2	TACGAACATGTTGAGTCAGAA	SI02643550	Hs_SLC38A2_5
Farfsing No.4	G	5	1019	CDK4	CAAGGTAACCCTGGTGTTTGA	SI00001421	Hs_CDK4_2
Farfsing No.4	G	6	7786	MAP3K12	CTCGTATTCCTTGTACATAGA	SI02637194	Hs_MAP3K12_6
Farfsing No.4	G	7	25840	METTL7A	GACAGTTTAGTATATCCATAA	SI00102942	Hs_DKFZP586A0522_4
Farfsing No.4	G	8	1606	DGKA	CGGAAGGACATTGGTGTCCAA	SI04434871	Hs_DGKA_10
Farfsing No.4	G	9	9352	TXNL1	CAGCTGCTTATTACTGTGGCA	SI03068394	Hs_TXNL1_9
Farfsing No.4	G	10	5055	SERPINB2	TGCGAGCTTCCGGGAAGAATA	SI03118710	Hs_SERPINB2_7
Farfsing No.4	H	1	9718	ECE2	CAGATCATGAGGACTTCCTTA	SI03064656	Hs_MGC2408_5
Farfsing No.4	H	2	84984	C3orf34	CAGCGCATTATGCCAGTTCGA	SI04180120	Hs_C3orf34_1
Farfsing No.4	H	3	84859	LRCH3	CACGGTAGCGTCGGGAGGTAA	SI04292162	Hs_LRCH3_7
Farfsing No.4	H	4	3223	HOXC6	CCGTATGACTATGGATCTAAT	SI04178377	Hs_HOXC6_7
Farfsing No.4	H	5	121268	RHEBL1	CTGGGCATTATTTATCCAGGA	SI04243463	Hs_RHEBL1_8
Farfsing No.4	H	6	1017	CDK2	GACGGAGCTTGTTATCGCAAA	SI00299782	Hs_CDK2_6
Farfsing No.4	H	7	10102	TSFM	TGGGTTCTACGTTGGCTCTTA	SI04360132	Hs_TSFM_8
Farfsing No.4	H	8	10376	TUBA1B	CAGCTTAACTGACAGACGTTA	SI02636634	Hs_K-ALPHA-1_6
Farfsing No.4	H	9	10892	MALT1	CTGGATGTTTGCGACATCCCA	SI03097724	Hs_MALT1_6
Farfsing No.4	H	10	9306	SOCS6	CAGCTGCGATATCAACGGTGA	SI03068359	Hs_SOCS6_5
Farfsing No.4	H	12			AACGTACGCGGAATACTTCGA	1022070	Unspecific_LuciferaseGL2_1
Farfsing No.1	A	1	5217	PFN2	CAGACAGATGAAATAAATTTA	SI02654127	Hs_PFN2_8
Farfsing No.1	A	2	8975	USP13	TCGCTTATGAACTAACGAGAA	SI00058093	Hs_USP13_1
Farfsing No.1	A	3	116832	RPL39L	CAGATGAAACCTGGTAGTAAA	SI00706531	Hs_RPL39L_1
Farfsing No.1	A	4	5062	PAK2	CCGCGACCGGATCATACGAAA	SI00605710	Hs_PAK2_8
Farfsing No.1	A	5	10411	RAPGEF3	AGGGCACTTCGTGGTACATTA	SI00698530	Hs_RAPGEF3_2
Farfsing No.1	A	6	3695	ITGB7	CCGGCTCTCGGTGGAAATCTA	SI00017829	Hs_ITGB7_1
Farfsing No.1	A	7	91419	XRCC6BP1	ACCGTGATCGGTATTATTCAA	SI00467411	Hs_KUB3_2
Farfsing No.1	A	8	29127	RACGAP1	CACCACAGACACCAGATATTA	SI00101164	Hs_RACGAP1_1
Farfsing No.1	A	9	115106	CCDC5	CCGCTAGGAGTTCCTAGTAAA	SI00339465	Hs_CCDC5_1
Farfsing No.1	A	10	596	BCL2	TCCATTATAAGCTGTCGCAGA	SI00299397	Hs_BCL2_9
Farfsing No.1	A	11	284273	ZADH2	TACGATGGTCTCAACACCTTT	SI02779518	Hs_ZADH2_5
Farfsing No.1	A	12			AACTTACGCTGAGTACTTCGA	1022073	Unspecific_LuciferaseGL3_1
Farfsing No.1	B	1	55214	LEPREL1	CCCAAGATAGATCGAGACCTA	SI04179539	Hs_LEPREL1_5
Farfsing No.1	B	2	23043	TNIK	AAGGACCATATTGATAGAACA	SI02225503	Hs_TNIK_5
Farfsing No.1	B	3	27074	LAMP3	ACAACCGATGTCCAACTTCAA	SI04287458	Hs_LAMP3_7
Farfsing No.1	B	4	1894	ECT2	ATCGCAAACGACGTCGTTTAA	SI00120568	Hs_ECT2_4
Farfsing No.1	B	5	10728	PTGES3	CAGCTTAGGGAAAGAGAATAA	SI02780911	Hs_PTGES3_1
Farfsing No.1	B	6	8914	TIMELESS	TTGGAGCTCCTTAGCAAATAA	SI00745017	Hs_TIMELESS_3
Farfsing No.1	B	7	121355	GTSF1	TTGAATCCTCATTTAATGCAA	SI04240628	Hs_FAM112B_1
Farfsing No.1	B	8	83729	INHBE	TAGGGTGATGGTCCAGAGCAA	SI02779854	Hs_INHBE_7
Farfsing No.1	B	9	9063	PIAS2	CAGGTGGTAGGAGAGATTATA	SI00684397	Hs_PIAS2_3
Farfsing No.1	B	10	9525	VPS4B	AAGACGGAGTTCCTAGTGCAA	SI04194127	Hs_VPS4B_7
Farfsing No.1	B	11	5347	PLK1	CGCGGGCAAGATTGTGCCTAA	SI02223844	Hs_PLK1_7
Farfsing No.1	B	12	5347	PLK1	CGCGGGCAAGATTGTGCCTAA	SI02223844	Hs_PLK1_7
Farfsing No.1	C	1	152137	CCDC50	AAGAAATCGCTCGACTTCTAA	SI04338544	Hs_CCDC50_3
Farfsing No.1	C	2	131583	FAM43A	AACGCGCTGGCGGAATTTAAA	SI00383915	Hs_FAM43A_3
Farfsing No.1	C	3	347	APOD	TCCCATCTTTGTGTTTCGATA	SI04152939	Hs_APOD_6
Farfsing No.1	C	4	5276	SERPINI2	AAGGTGATGAATTTAGCTTAA	SI00085806	Hs_SERPINI2_1
Farfsing No.1	C	5	23306	TMEM194A	TCAGATGGATGCCTACGTAAA	SI04244240	Hs_KIAA0286_5
Farfsing No.1	C	6	6601	SMARCC2	CAGGTGGATGCTGAGAGTCGA	SI04134466	Hs_SMARCC2_5
Farfsing No.1	C	7	25895	FAM119B	CTCCTTCAGTCCATTCCGCAA	SI04207770	Hs_FAM119B_1
Farfsing No.1	C	8	2735	GLI1	CCAGCCCAGATGAATCACCAA	SI00074795	Hs_GLI1_1
Farfsing No.1	C	9	51124	IER3IP1	CAGCTAATGAACCTTATTCGA	SI04153569	Hs_IER3IP1_5
Farfsing No.1	C	10	5596	MAPK4	CGCCTTAAATCTAATCAGCAA	SI00606018	Hs_MAPK4_6
Farfsing No.1	C	11	595	CCND1	AACACCAGCTCCTGTGCTGCG	SI02654540	Hs_CCND1_5
Farfsing No.1	C	12	595	CCND1	AACACCAGCTCCTGTGCTGCG	SI02654540	Hs_CCND1_5
Farfsing No.1	D	1	401105	FLJ42393	CTGGTCTCTGTTTATGATATA	SI00415457	Hs_FLJ42393_4

Plate Name	Row	Col	Entrez Gene Id	NCBI gene symbol	siRNA Target Sequence 5´→3´	Product ID	Product Name
Farfsing No.1	D	2	131408	FAM131A	TCGGATAATGTGAACCACTAA	SI00635299	Hs_MGC21688_1
Farfsing No.1	D	3	5290	PIK3CA	CTGAGTCAGTATAAGTATATA	SI02622207	Hs_PIK3CA_5
Farfsing No.1	D	4	10644	IGF2BP2	CAGCGAAAGGATGGTCATCAT	SI04138820	Hs_IGF2BP2_3
Farfsing No.1	D	5	64333	ARHGAP9	TTGGGTGGTGTTAACGGGTAA	SI00302596	Hs_ARHGAP9_2
Farfsing No.1	D	6	5916	RARG	AAGAGCTGGACGGAGGCTAAA	SI04025595	Hs_RARG_6
Farfsing No.1	D	7	5036	PA2G4	CCCACTCCCTTCCAACAACAA	SI00085344	Hs_PA2G4_2
Farfsing No.1	D	8	140465	MYL6B	CAGCAACGGCTGCATCAACTA	SI00646240	Hs_MLC1SA_4
Farfsing No.1	D	9	51320	MEX3C	TAGGCTAAAGTTGTTAGTAAA	SI00703675	Hs_RKHD2_1
Farfsing No.1	D	10	8932	MBD2	AAGATGATGCCTAGTAAATTA	SI02663787	Hs_MBD2_8
Farfsing No.1	D	11	3832	KIF11	ACGGAGGAGATAGAACGTTTA	SI02653693	Hs_KIF11_6
Farfsing No.1	D	12	3832	KIF11	ACGGAGGAGATAGAACGTTTA	SI02653693	Hs_KIF11_6
Farfsing No.1	E	1	55689	YEATS2	GCGGATAGATATCATACATAA	SI00764421	Hs_YEATS2_3
Farfsing No.1	E	2	285386	TPRG1	AAGGATCAGCCTGACAATCGA	SI04167688	Hs_FAM79B_2
Farfsing No.1	E	3	26996	GPR160	CAACTTTAAGATATCAACCTA	SI00105315	Hs_GPR160_1
Farfsing No.1	E	4	5918	RARRES1	CCGCGCGTGGATTAATCCAAA	SI00045290	Hs_RARRES1_1
Farfsing No.1	E	5	1649	DDIT3	AAGGAAGTGTATCTTCATACA	SI00059528	Hs_DDIT3_1
Farfsing No.1	E	6	92979	MARCH-9	CTGCGGTTATACAATCTTGCA	SI04141872	Hs_MARCH9_1
Farfsing No.1	E	7	10220	GDF11	AAGGTGATGTTCACAAAGGTA	SI00081515	Hs_GDF11_2
Farfsing No.1	E	8	4234	METTL1	CAGAATATGCCTACGTGCTAA	SI00076118	Hs_METTL1_1
Farfsing No.1	E	9	6925	TCF4	CACAGCTGTTTGGTCTAGAAA	SI00048958	Hs_TCF4_3
Farfsing No.1	E	10	55205	ZNF532	CCAGATATGGTCGATCCTAAA	SI00775733	Hs_ZNF532_3
Farfsing No.1	E	11	596	BCL2	TCCATTATAAGCTGTCGCAGA	SI00299397	Hs_BCL2_9
Farfsing No.1	E	12	1847	DUSP5	CGCGACCCACCTACACTACAA	SI03194282	Hs_DUSP5_9
Farfsing No.1	F	1	86	ACTL6A	AAAGCTTTAACTGGCTCTATA	SI02779987	Hs_ACTL6A_5
Farfsing No.1	F	2	590	BCHE	CGGGTTGAAAGAGTTATTGTA	SI00000917	Hs_BCHE_2
Farfsing No.1	F	3	2119	ETV5	CAGGATCTCAGTCAACTTCAA	SI03019394	Hs_ETV5_5
Farfsing No.1	F	4	11213	IRAK3	CACATTCGAATCGGTATATTA	SI02224278	Hs_IRAK3_5
Farfsing No.1	F	5	114785	MBD6	TTCCACTGTAGTGATGCCTTA	SI04147864	Hs_MBD6_6
Farfsing No.1	F	6	6778	STAT6	ACGGATAGGCAGGAACATACA	SI02662905	Hs_STAT6_5
Farfsing No.1	F	7	91523	FAM113B	AGGGACGAGATCTAGAATCAA	SI00633934	Hs_MGC16044_2
Farfsing No.1	F	8	196403	DTX3	TCAGATACAGTTCTCCCTTAA	SI00374626	Hs_DTX3_4
Farfsing No.1	F	9	4677	NARS	ATGCGTATCTTTGATAGTGAA	SI00655179	Hs_NARS_1
Farfsing No.1	F	10	8792	TNFRSF11A	ACCCGCTAGGTGGTTAATTTA	SI00056616	Hs_TNFRSF11A_1
Farfsing No.1	F	11	1847	DUSP5	CGCGACCCACCTACACTACAA	SI03194282	Hs_DUSP5_9
Farfsing No.1	G	1	5984	RFC4	CAGAAGTCTATTATCACAGAA	SI02665726	Hs_RFC4_7
Farfsing No.1	G	2	10051	SMC4	CAGCGTTTAATAGAGCAAGAA	SI04324873	Hs_SMC4_3
Farfsing No.1	G	3	1857	DVL3	CTCCTGGTTACTTCATCACAA	SI02781387	Hs_DVL3_6
Farfsing No.1	G	4	54407	SLC38A2	CTCATCAGGCATAATGTCTAA	SI02777845	Hs_SLC38A2_6
Farfsing No.1	G	5	1019	CDK4	AAGGTAACCCTGGTGTTTGAG	SI00299803	Hs_CDK4_6
Farfsing No.1	G	6	7786	MAP3K12	CTGGAATAGCAAACCACGAAA	SI00087185	Hs_MAP3K12_1
Farfsing No.1	G	7	25840	METTL7A	CTGGCTTTCAGAATTAACATA	SI00102921	Hs_DKFZP586A0522_1
Farfsing No.1	G	8	1606	DGKA	CACGACCAGTGTGCCATGAAA	SI00605206	Hs_DGKA_6
Farfsing No.1	G	9	9352	TXNL1	AACTCAAGCTCTGGAACTGAC	SI00302064	Hs_TXNL1_5
Farfsing No.1	G	10	5055	SERPINB2	CAGAAGGGTAGTTATCCTGAT	SI00039753	Hs_SERPINB2_2
Farfsing No.1	H	1	9718	ECE2	CAAGGGCGCGAGTATGACAAA	SI03054639	Hs_ECE2_5
Farfsing No.1	H	2	84984	C3orf34	CCAGAGCTGCTGAACAATTAA	SI00632947	Hs_MGC14126_1
Farfsing No.1	H	3	84859	LRCH3	CTGGATCAGATTGACTACATA	SI00623308	Hs_LRCH3_4
Farfsing No.1	H	4	3223	HOXC6	ACCGTCAGTGTTCCTATCCAA	SI00440874	Hs_HOXC6_3
Farfsing No.1	H	5	121268	RHEBL1	CTCCAGTGGCCTGGATGTCAA	SI04142341	Hs_RHEBL1_6
Farfsing No.1	H	6	1017	CDK2	CAGGTTATATCCAATAGTAGA	SI00605360	Hs_CDK2_8
Farfsing No.1	H	7	10102	TSFM	CAGACCGAGAATGCATGGGTA	SI03167402	Hs_TSFM_5
Farfsing No.1	H	8	10376	TUBA1B	TCCATCATATCTCAAAGTAAA	SI00084308	Hs_K-ALPHA-1_1
Farfsing No.1	H	9	10892	MALT1	TAGATAGAGGTTAAGAATCAA	SI00091896	Hs_MALT1_1
Farfsing No.1	H	10	9306	SOCS6	TAGAATCGTGAATTGACATAA	SI00061383	Hs_SOCS6_3
Farfsing No.1	H	12			AACTTACGCTGAGTACTTCGA	1022073	Unspecific_LuciferaseGL3_1
Farfsing No.3	A	1	5217	PFN2	CCGGGAAGGTTTCTTTACCAA	SI00040670	Hs_PFN2_1
Farfsing No.3	A	2	8975	USP13	CACTACGAGCAACGAATAATA	SI03061968	Hs_USP13_5
Farfsing No.3	A	3	116832	RPL39L	TCGGAGTCTCAGAGACACCAA	SI00706545	Hs_RPL39L_3
Farfsing No.3	A	4	5062	PAK2	AAGAGACTGCTCCTCCCGTTA	SI00301084	Hs_PAK2_7
Farfsing No.3	A	5	10411	RAPGEF3	AACTCGGTGAAGCGAGAATTA	SI03126928	Hs_RAPGEF3_5
Farfsing No.3	A	6	3695	ITGB7	ACGGTCGTGCTCAGAGTGAGA	SI03041815	Hs_ITGB7_5
Farfsing No.3	A	7	91419	XRCC6BP1	TGGAAGGATCCCACATAACAA	SI04358704	Hs_XRCC6BP1_3
Farfsing No.3	A	8	29127	RACGAP1	CAGGTGGATGTAGAGATCAAA	SI00101178	Hs_RACGAP1_3
Farfsing No.3	A	9	115106	CCDC5	CGCAGGTTGCTGCGTGGTTAA	SI04776919	Hs_CCDC5_12
Farfsing No.3	A	10	596	BCL2	AACCGGGAGATAGTGATGAAG	SI00299418	Hs_BCL2_12
Farfsing No.3	A	11	284273	ZADH2	ACCCGTAGGTACCGTCCTTAA	SI00159558	Hs_ZADH2_2
Farfsing No.3	A	12			AACTTACGCTGAGTACTTCGA	1022073	Unspecific_LuciferaseGL3_1
Farfsing No.3	B	1	55214	LEPREL1	TACTATCGAGTTGGTGAGTAT	SI04244849	Hs_LEPREL1_6
Farfsing No.3	B	2	23043	TNIK	CACCTATGGCCGGATAACTAA	SI02794463	Hs_TNIK_7
Farfsing No.3	B	3	27074	LAMP3	CACCTCGGAGATACTTCAACA	SI04153226	Hs_LAMP3_5
Farfsing No.3	B	4	1894	ECT2	ATGACGCATATTAATGAGGAT	SI03049249	Hs_ECT2_6
Farfsing No.3	B	5	10728	PTGES3	CGGAGAGAAGTCGACTCCCTA	SI03085740	Hs_PTGES3_3
Farfsing No.3	B	6	8914	TIMELESS	CACCTGAATACTGTTCCTCGA	SI04142194	Hs_TIMELESS_6
Farfsing No.3	B	7	121355	GTSF1	GCCGTATGTTCTGCCATGGAA	SI04353069	Hs_FAM112B_3

Plate Name	Row	Col	Entrez Gene Id	NCBI gene symbol	siRNA Target Sequence 5´→3´	Product ID	Product Name
Farfsing No.3	B	8	83729	INHBE	TGGCTTATACTTTCTTAATAA	SI02646392	Hs_INHBE_5
Farfsing No.3	B	9	9063	PIAS2	TCCGCCTTCATTAACAGACTA	SI04338215	Hs_PIAS2_6
Farfsing No.3	B	10	9525	VPS4B	AGCGATATATGAACGGCATAA	SI03144463	Hs_VPS4B_6
Farfsing No.3	B	11	5347	PLK1	CCGGATCAAGAAGAATGAATA	SI02223837	Hs_PLK1_6
Farfsing No.3	B	12	5347	PLK1	CCGGATCAAGAAGAATGAATA	SI02223837	Hs_PLK1_6
Farfsing No.3	C	1	152137	CCDC50	CGGCGCGTCACTGAGCACAAA	SI04272254	Hs_CCDC50_2
Farfsing No.3	C	2	131583	FAM43A	CCCGCTAGTGCCGCTGCGCAA	SI04154794	Hs_FAM43A_6
Farfsing No.3	C	3	347	APOD	GCCTGCCAAGCTGGAAGTTAA	SI04173750	Hs_APOD_7
Farfsing No.3	C	4	5276	SERPINI2	AAGAGGTTTCCTTATCTCATA	SI00085827	Hs_SERPINI2_4
Farfsing No.3	C	5	23306	TMEM194A	TAGGTAGTGGTCAGTTATCTT	SI04309242	Hs_KIAA0286_7
Farfsing No.3	C	6	6601	SMARCC2	GAAGTCCTTGGTGCAGAATAA	SI04135383	Hs_SMARCC2_6
Farfsing No.3	C	7	25895	FAM119B	CAGTGAGGTGCCTGCTTACAA	SI04300646	Hs_FAM119B_3
Farfsing No.3	C	8	2735	GLI1	CTCGGGCACCATCCATTTCTA	SI02634835	Hs_GLI1_5
Farfsing No.3	C	9	51124	IER3IP1	CAGCGTAAATATTAGCCCACA	SI04209009	Hs_IER3IP1_7
Farfsing No.3	C	10	5596	MAPK4	CACAGAGGACCTCGTGCTCAA	SI00042483	Hs_MAPK4_2
Farfsing No.3	C	11	595	CCND1	AAGGCCAGTATGATTTATAAA	SI00147812	Hs_CCND1_1
Farfsing No.3	C	12	595	CCND1	AAGGCCAGTATGATTTATAAA	SI00147812	Hs_CCND1_1
Farfsing No.3	D	1	401105	FLJ42393	CGCAGTGGGTGAAGTATTGTA	SI04773692	Hs_FLJ42393_6
Farfsing No.3	D	2	131408	FAM131A	AACGGGCACAAGCATTCTATA	SI00635320	Hs_MGC21688_4
Farfsing No.3	D	3	5290	PIK3CA	ATGGCTGAATTATGATATATA	SI00085834	Hs_PIK3CA_1
Farfsing No.3	D	4	10644	IGF2BP2	TCCGCTAGCCAAGAACCTATA	SI03232481	Hs_IGF2BP2_2
Farfsing No.3	D	5	64333	ARHGAP9	CTGGACGCTGCTTCTACATAA	SI04228987	Hs_ARHGAP9_5
Farfsing No.3	D	6	5916	RARG	TCCTGTTTCGCCGGACTTGAA	SI04025616	Hs_RARG_9
Farfsing No.3	D	7	5036	PA2G4	TCCCACCAGCATTTCGGTAAA	SI02636865	Hs_PA2G4_5
Farfsing No.3	D	8	140465	MYL6B	CAAGAAGGATGTTCCCGTGAA	SI04266696	Hs_MYL6B_3
Farfsing No.3	D	9	51320	MEX3C	AGGAAACTATATAGAGCTCAA	SI00703696	Hs_RKHD2_4
Farfsing No.3	D	10	8932	MBD2	CAAGTGGTAAGAAGTTCAGAA	SI03054996	Hs_MBD2_9
Farfsing No.3	D	11	3832	KIF11	CTCGGGAAGCTGGAAATATAA	SI03019793	Hs_KIF11_8
Farfsing No.3	D	12	3832	KIF11	CTCGGGAAGCTGGAAATATAA	SI03019793	Hs_KIF11_8
Farfsing No.3	E	1	55689	YEATS2	CTGGCACTAAACTCTACCTAA	SI04211956	Hs_YEATS2_6
Farfsing No.3	E	2	285386	TPRG1	AAGACTAGATAAAGTCGATAT	SI04145323	Hs_FAM79B_1
Farfsing No.3	E	3	26996	GPR160	CACATCTGCCTATTTACTCAA	SI04901022	Hs_GPR160_8
Farfsing No.3	E	4	5918	RARRES1	CGCGGCGCTTCACTTCTTCAA	SI03085229	Hs_RARRES1_9
Farfsing No.3	E	5	1649	DDIT3	ACGGCTCAAGCAGGAAATCGA	SI03041633	Hs_DDIT3_5
Farfsing No.3	E	6	92979	09-Mar	CAGCACTCCGAGGTATCTAAA	SI04245101	Hs_MARCH9_3
Farfsing No.3	E	7	10220	GDF11	CCTGCAGATCTTGCGACTAAA	SI03083388	Hs_GDF11_5
Farfsing No.3	E	8	4234	METTL1	CACGTGGATTTGGTAGAGAAA	SI00076139	Hs_METTL1_4
Farfsing No.3	E	9	6925	TCF4	GACGACAAGAAGGATATCAAA	SI03101805	Hs_TCF4_5
Farfsing No.3	E	10	55205	ZNF532	CAGCGTTATCGTCAAGAATGT	SI04215701	Hs_ZNF532_8
Farfsing No.3	E	11	596	BCL2	AACCGGGAGATAGTGATGAAG	SI00299418	Hs_BCL2_12
Farfsing No.3	E	12	1847	DUSP5	CTGCATGGCTTACCTTATGAA	SI04228700	Hs_DUSP5_13
Farfsing No.3	F	1	86	ACTL6A	ACCTTACGTTTCATAGCTTTA	SI04433933	Hs_ACTL6A_9
Farfsing No.3	F	2	590	BCHE	TTGCAGAGAATCGGAAATCAA	SI00000910	Hs_BCHE_1
Farfsing No.3	F	3	2119	ETV5	CCCGATTATACTTTGACGACA	SI03184657	Hs_ETV5_6
Farfsing No.3	F	4	11213	IRAK3	AAGTATGTAGACCAAGGTAAA	SI00095417	Hs_IRAK3_2
Farfsing No.3	F	5	114785	MBD6	CAGCCTCAATGCTCCCTCATA	SI04184691	Hs_MBD6_8
Farfsing No.3	F	6	6778	STAT6	AACCAAGACAACAATGCCAAA	SI00048468	Hs_STAT6_4
Farfsing No.3	F	7	91523	FAM113B	CACCCGCGTGTACTCCGATTA	SI03161508	Hs_FAM113B_1
Farfsing No.3	F	8	196403	DTX3	AAGGGTATCACAGATGACTGA	SI03036089	Hs_DTX3_6
Farfsing No.3	F	9	4677	NARS	TTGGGCTTGGAACGATTCTTA	SI04323907	Hs_NARS_7
Farfsing No.3	F	10	8792	TNFRSF11A	TTGGATAGCTGGAATGAAGAA	SI03024812	Hs_TNFRSF11A_6
Farfsing No.3	F	11	1847	DUSP5	CTGCATGGCTTACCTTATGAA	SI04228700	Hs_DUSP5_13
Farfsing No.3	G	1	5984	RFC4	AGGGAATAGCTTATCTTGTTA	SI00045682	Hs_RFC4_1
Farfsing No.3	G	2	10051	SMC4	TACCATCGTAGAAATCAATAA	SI04137714	Hs_SMC4_1
Farfsing No.3	G	3	1857	DVL3	CAGCATATCATATCCATTTCA	SI00063469	Hs_DVL3_2
Farfsing No.3	G	4	54407	SLC38A2	CAACGTAGAATTACTTGTTTA	SI00123480	Hs_SLC38A2_2
Farfsing No.3	G	5	1019	CDK4	AAGGTAATCCGGAGTGAGCAA	SI00604744	Hs_CDK4_7
Farfsing No.3	G	6	7786	MAP3K12	CAGGGAGCACTATGAAAGGAA	SI02637187	Hs_MAP3K12_5
Farfsing No.3	G	7	25840	METTL7A	AAGCAATCTGTGAGTCTGTAA	SI00102935	Hs_DKFZP586A0522_3
Farfsing No.3	G	8	1606	DGKA	CCCATGCAAATTGACGGAGAA	SI00025662	Hs_DGKA_2
Farfsing No.3	G	9	9352	TXNL1	ATGAATGACTTCAAACGAGTA	SI03049137	Hs_TXNL1_8
Farfsing No.3	G	10	5055	SERPINB2	CTGGAAAGTGAAATAACCTAT	SI02628969	Hs_SERPINB2_6
Farfsing No.3	H	1	9718	ECE2	CAGACACTATGCCCAAGCCTA	SI00635852	Hs_MGC2408_4
Farfsing No.3	H	2	84984	C3orf34	ATGGAACAAATTCAACGGGAA	SI00632961	Hs_MGC14126_3
Farfsing No.3	H	3	84859	LRCH3	ACAGACGATCACCCTAGATAA	SI04288774	Hs_LRCH3_6
Farfsing No.3	H	4	3223	HOXC6	TGGGTCCGTTCTCGAATATTT	SI03239670	Hs_HOXC6_6
Farfsing No.3	H	5	121268	RHEBL1	AGGCGAGTTCTCGGAAGGCTA	SI04243498	Hs_RHEBL1_9
Farfsing No.3	H	6	1017	CDK2	AGGTGGTGGCGCTTAAGAAAA	SI00299775	Hs_CDK2_5
Farfsing No.3	H	7	10102	TSFM	ATGATGCATTGTCAGACCCTA	SI04348848	Hs_TSFM_7
Farfsing No.3	H	8	10376	TUBA1B	CCCGCCCTAGTGCGTTACTTA	SI02636627	Hs_K-ALPHA-1_5
Farfsing No.3	H	9	10892	MALT1	CTGGTAATCCAAGTAATGTTA	SI02638062	Hs_MALT1_5
Farfsing No.3	H	10	9306	SOCS6	CGGGTACAAATTGGCATAACA	SI00061376	Hs_SOCS6_2
Farfsing No.3	H	12			AACTTACGCTGAGTACTTCGA	1022073	Unspecific_LuciferaseGL3_1

Col=Column in which the siRNA is located in the 96-well plate.

Publications

Articles based on this thesis

Farfsing A, Engel F, Seiffert M, Hartmann E, Ott G, Rosenwald A, Stilgenbauer S, Döhner H, Boutros M, Lichter P, Pscherer A
'Gene knockdown studies identified CCDC50 as candidate gene in mantle cell lymphoma and chronic lymphocytic leukemia.' *In preparation*.

Posters and abstracts based on this thesis

Farfsing A, Engel F, Seiffert M, Hartmann E, Ott G, Rosenwald A, Stilgenbauer S, Döhner H, Boutros M, Lichter P, Pscherer A
'Identification of overexpressed genes and their pathogenic relevance in B-cell non-Hodgkin lymphoma applying RNAi tools'.
Keystone Symposia - RNAi, micro RNA and non-coding RNA, Whistler, British Columbia, Canada

Farfsing A, Engel F, Seiffert M, Hartmann E, Ott G, Rosenwald A, Stilgenbauer S, Döhner H, Boutros M, Lichter P, Pscherer A
'Functional analysis of deregulated genes in B-cell non-Hodgkin lymphoma.'
14th International AEK Cancer Congress, Frankfurt am Main, Garmany

Farfsing A, Engel F, Seiffert M, Hartmann E, Ott G, Rosenwald A, Stilgenbauer S, Döhner H, Boutros M, Lichter P, Pscherer A
'Functional analysis of deregulated genes in human leukemic neoplasias by means of RNAi.'
Functional and Structural Genomics, DKFZ Heidelberg, Germany

Farfsing A, Engel F, Seiffert M, Hartmann E, Ott G, Rosenwald A, Stilgenbauer S, Döhner H, Boutros M, Lichter P, Pscherer A
'RMCE is a striking tool for antagonizing deregulated genes in B-cell non-Hodgkin lymphoma.'
Genomics and Cancer 2006, DKFZ Heidelberg, Germany

Acknowledgements

My deepest thanks go to Prof. Dr. Peter Lichter for the kind opportunity to perform my PhD in your laboratories. I very much appreciated our enriching discussions about the course and progress of this work, and your continuous support over the last 3½ years. Peter, your thoughtful supervision gave me throughout my PhD enduring motivation and eagerness.

I would like to thank Prof. Dr. Werner Buselmaier and Prof. Dr. Peter Lichter for the evaluation of this thesis work.

Furthermore, I would especially like to express my thanks to my supervisor Dr. Armin Pscherer. Thanks to your continuous and outstanding support, our weekly discussions, your excellent ideas and your endless input, this work achieved success. Thank you for your precious advices that reached even far beyond this PhD work.

Moreover, I appreciate the valuable cooperations with Prof. Dr. Michael Boutros for his expert knowledge on RNAi screens, with Prof. Dr. Hartmut Döhner and Prof. Dr. Stephan Stilgenbauer from the University hospital of Ulm for their kind collaboration in the field of CLL, with PD Dr. Andreas Rosenwald from the University of Würzburg, and Prof. Dr. Reiner Siebert from the University of Kiel for the fruitful collaboration in the field of MCL.

I would like to thank all members of the bioinformatics group for their excellent support in the evaluation of expression arrays. A special thanks goes to Felix Engel for your gainful collaboration and your throughout bioinformatic support during the evaluation of my chip experiments.

For great technical assistance, especially during my final year, I would like to thank Verena Gschwend for your highly qualified assistance during the RNAi screen and your great help with the functional assays.

In addition, I appreciated very much the cooperation and expertise of Martina Seiffert and Angela Schulz in the field of CLL, Bernhard Radlwimmer and Stefanie Hofmann for your support in array CGH, Dorothee Nickles for your help with the bioinformatic evaluation of the RNAi screen, Daniel Mertens and Martina Enz from the University hospital in Ulm together with Magdalena Schlotter and Michael Rogers for your great collaboration and joint technical support. Besides, deep thanks goes also to Antoneta Mincheva and to Frauke Devens for your kind introduction in generating metaphase cells and performing FISH.

For a wonderful working atmosphere, for lab support, for valuable discussions and for your friendship I would like to thank Josephine Bageritz, Hsing Chen Bai, Sebastian Barbus, Suzin Choi, Frauke Devens, Martina Enz, Laura Dittmann, Karin Pfleger, Aurelie Ernst, Verena Fleig, Violaine Goidts, Jan Gronych, Madeleine Groß, Verena Gschwend, Daniel Haag, Stefanie Heck, Stefanie Hofmann, Valentina Kovaleva, Charly Knöpfle, Margit MacLeod, Jan Meier, Sandra Müller, Susumu Nakata, Elena Orlova, Sabrina Pleier, Laura Puccio, Blanka Rebacz, Marc Remke, Karsten Richter, Michael Rogers, Melanie Ruppel, Petra Sander, Magdalena Schlotter, Petra Schroeter, Angela Schulz, Martina Seiffert, Leticia Serra, Maria Shahmoradgoli, Dominik Sturm, Verena Thewes, Cordula Tschuch and Andrea Wittmann.

For wonderful and enjoyable 'girl evenings' I would like to thank Aurelie Ernst, Suzin Choi, Frauke Devens, Violaine Goidts, Melanie Ruppel, Angela Schulz, Cordula Tschuch, and Leticia Serra. This was for sure a memorable and lovely time with all of you.

Moreover, I would like to thank Aurelie Ernst for the sportive motivation and our joint running sessions during the time of my PhD. Our sportive hours throughout the years gave me the motivation and balance for the daily lab routine.

My deepest gratitude and appreciation goes to my husband Jan and to my family. Thank you, Jan, for your caring motivation and wonderful inspirations, your sunshine in my life and your endlessly pleasant support in any kind of situation. I would like to express my appreciation to my parents, my sister Barbara, Martin, my grandmother, Wilfried and Sybille for your unconditional support and your tireless trust in me and my work. In addition, I would like to thank Stephanie, Frank, Anja, Katja and Kai for your throughout motivation. You all helped me in your specific manners to finish this dissertation successfully.